

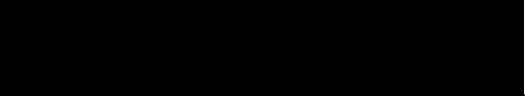
School of Medicine
Oregon Health & Science University

CERTIFICATE OF APPROVAL

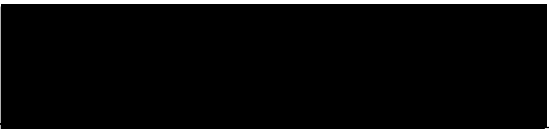
This is to certify that the Ph.D dissertation of

Gregory Kennard Scott

Has been approved


Gary Thomas / Mentor


John P Adelman / Committee Member


Gary A. Banker / Committee Member


Michael Forte / Committee Member


Show-Ling Shyng / Committee Member

Regulation of PACS-1-directed protein trafficking

By

Gregory Kennard, Scott

A Dissertation

Presented to the Neuroscience Graduate Program
and the Oregon Health & Science University
School of Medicine
in partial fulfillment of
the requirements for the degree of
Doctor of Philosophy

May 2006

Table of Contents

CHAPTER 1. INTRODUCTION	1
Overview.....	1
The biosynthetic and endocytic pathways	4
Organelle identity	7
<i>Phospholipids</i>	8
<i>The ARF and Rab GTPases</i>	9
<i>SNAREs</i>	13
Itinerant membrane proteins	14
Sorting motifs and adaptor proteins	18
<i>Tyrosine motifs, dileucine motifs and the adaptor proteins</i>	18
<i>Acidic-dileucine motifs and the GGAs</i>	21
<i>Acidic cluster motifs and PACS-1</i>	25
<i>Tip47 and the Retromer complex</i>	29
Protein kinase CK2.....	31
Conclusion	33
CHAPTER 2.....	35
The phosphorylation state of an autoregulatory domain controls PACS-1-directed protein traffic	
Gregory K. Scott, Feng Gu, Colin M. Crump, Laurel Thomas, Lei Wan, Yang Xiang and Gary Thomas.	
Published in the EMBO Journal , December 1, 2003, 22(23):6234-6244	
Introduction.....	37
Results	41
Discussion.....	49
Materials and Methods	55
Figure Legends.....	63
CHAPTER 3.....	74
A PACS-1, GGA3 and CK2 complex regulates CI-MPR trafficking	
Gregory K. Scott, Hao Fei, Laurel Thomas, Guruprasad R. Medigeshi and Gary Thomas.	
Submitted for publication	
Introduction.....	76
Results	77
Discussion.....	90
Materials and Methods	95
Figure Legends.....	101
CHAPTER 4. DISCUSSION	117

Summary	117
Implications for PACS-1 cargo binding.....	118
Implications for PACS-1 regulation	119
Implications for CK2 binding and activation	121
Implications for GGA binding.....	123
Implications for PACS-2.....	125
Implications for neuronal function	126
Conclusion.....	127
APPENDIX A. VZV REVIEW	148
Endocytosis of Varicella-Zoster Virus glycoproteins: virion envelopment and egress	
Charles Grose, Lucie Maresova, Guruprasad Medigeshe, Gregory K. Scott, and Gary Thomas.	
In Press with Horizon Press, Fall 2006	
Introduction	150
1. Glycoprotein gE.....	151
2. VZV Glycoprotein gI.....	153
3. VZV Glycoprotein B.....	154
4. VZV Glycoprotein H	157
5.0. Incorporation of endocytosed VZV glycoproteins into virion envelopes	159
6.0. Summary of trafficking pathways.....	162
Figure Legends	168
APPENDIX B. FURIN ACTIVATION.....	178
Identification of a pH sensor in the furin propeptide that regulates enzyme activation	
Sylvain F. Feliciangeli, Laurel Thomas, Gregory K. Scott, Ezhilkani Subbian, Chien Hui Hung, Sean S. Molloy, François Jean, Ujwal Shinde and Gary Thomas	
In press in The Journal of Biological Chemistry	
Abstract	179
Introduction	180
Experimental Procedures	183
Results.....	188
Discussion	196
Figure Legends	202
APPENDIX C. PRELIMINARY RESULTS	212

Acknowledgments

I am deeply indebted to my advisor, Dr. Gary Thomas, whose support, advice and scientific mentoring was essential for the development of this project and my training as a research scientist. I am also indebted to Laurel Thomas, who has contributed greatly to these studies, and has kept the lab running smoothly. Together, Gary and Laurel run a tight ship, and this dissertation reflects their hard work and determination to produce high quality research.

The Thomas Lab is a team environment and the work presented in this dissertation could not have been done without the help of others. I was especially lucky to work with Feng Gu and Hao Fei, who each contributed greatly to these studies. I am also indebted to the members of the Thomas Lab, past and present who have been great advisors, collaborators and friends. Several individuals worked hard to keep my graduate training successful and interesting. Many thanks to: Neal Alto, Joe Aslan, Rachel Dresbek, Chien-Hui Hung, Stefanie Kaech-Petrie, Tom O'Hare and Oleg Varlamov.

Finally, I extend special thanks to my parents, who have supported me through all levels of education, and to Laura Baraff, who has kept me sane through graduate school.

Abstract

The cation-independent mannose-6-phosphate receptor (CI-MPR) follows a highly regulated sorting itinerary to deliver hydrolases from the *trans*-Golgi network (TGN) to lysosomes. Cycling of CI-MPR between the TGN and early endosomes is mediated by GGA3, which directs TGN export, and PACS-1, which directs endosome-to-TGN retrieval. Despite executing opposing sorting steps, GGA3 and PACS-1 both utilize a CK2-phosphorylated acidic cluster trafficking motif to bind the CI-MPR. But how CK2 coordinates these opposing roles is unknown. This thesis shows that an acidic cluster on PACS-1, which is highly similar to acidic cluster sorting motifs on cargo molecules, acts as an autoregulatory domain that controls PACS-1-directed sorting. Biochemical studies show Ser₂₇₈ adjacent to the acidic cluster is phosphorylated by CK2 and dephosphorylated by PP2A. Similar to our findings for PACS-1, GGA3 binding to the phosphorylated CI-MPR is also controlled by the CK2 phosphorylation of an autoregulatory domain. However, whereas CK2 phosphorylation of the PACS-1 autoregulatory domain *promotes* cargo binding, CK2 phosphorylation of the GGA3 autoregulatory domain *inhibits* cargo binding. Experiments performed in this dissertation test the hypothesis that an intimate association of CK2 with these trafficking molecules coordinates their sorting activity. Accordingly, we found that PACS-1 links GGA3 to CK2, forming a multimeric complex required for CI-MPR sorting. PACS-1-bound CK2 stimulates GGA3 phosphorylation, releasing GGA3 from CI-MPR and early endosomes. Bound CK2 also phosphorylates PACS-1Ser₂₇₈, promoting binding of PACS-1 to CI-MPR to retrieve the receptor to the TGN. These results identify a CK2-controlled phosphorylation cascade regulating hydrolase trafficking and sorting of itinerant proteins in the TGN/endosomal system.

List of Figures

Chapter 1

Figure 1. Intracellular Transport Pathways	4
Figure 2. Examples of phosphoinositides and Rab and ARF GTPases that are localized to specific membranes within eukaryotic cells	8
Figure 3. Organelle identity specifies coat recruitment	10
Figure 4. Late secretory protein sorting	15
Figure 5. Schematic diagram of the APs	19
Figure 7. Model of GGA3 activation	21
Figure 6. Diagram of GGA3 showing domain organization and protein interactions	22
Figure 8. Schematic diagram of PACS-1 proteins	26
Figure 9. Ribbon diagram of the CK2 holoenzyme	31

Chapter 2

Figure 1. PACS-1 Ser ₂₇₈ is phosphorylated by CK2 and dephosphorylated by PP2A	68
Figure 2. Phosphorylation of PACS-1 Ser ₂₇₈ promotes PACS-1 binding to cargo proteins	69
Figure 3. Phosphorylated PACS-1 directs endosome-to-TGN transport	70
Figure 4. Expression of PACS-1 S ₂₇₈ A blocks HIV-1 Nef-mediated MHC-1 downregulation.	71
Figure 5. Expression of PACS-1 S ₂₇₈ A disrupts furin and CI-MPR localization	72
Figure 6. A working model of the CK2/PP2A regulation of PACS-1 sorting activity	73

Chapter 3

Figure 1. PACS-1 binds to GGA3	109
Figure 2. PACS-1 _{GGAmut} disrupts CI-MPR trafficking	110
Figure 3. PACS-1 is required for CI-MPR function	111
Figure 4. PACS-1 associates with CK2	112
Figure 5. PACS-1 binding to CK2 β activates CK2	113
Figure 6. PACS-1 _{CKmut} redistributes CI-MPR, furin and GGA3 and controls GGA3 phosphorylation	114
Figure 7. Working model of PACS-1/GGA3/CK2 controlled CI-MPR trafficking	115
Sup. Figure 1. siRNA depletion of PACS-1 does not effect CI-MPR half-life	116

Chapter 4

Figure 1. Model of PACS-1 function	118
------------------------------------	-----

Appendix A

Figure 1. Amino acid sequences of the cytosolic domains of VZV glycoproteins gE, gH, gI and gB	172
Figure 2. Endocytosis assay	173
Figure 3. Identification of biotinylated VZV glycoproteins on infected cells and purified virions	174
Figure 4. Endosomal trafficking of the VZV glycoproteins	175
Figure 5. Egress and exocytosis of virions from a cytosolic vacuole	176

Appendix B

Figure 1. Homology modeling of the furin propeptide	206
Figure 2. His ₆₉ controls the pH-sensitive furin propeptide cleavage and enzyme activation in vitro	207
Figure 3. The protonation state of His ₆₉ controls propeptide excision and enzyme activation in vivo	208
Figure 4. The protonation state of His ₆₉ affects the subcellular localization of furin	209
Figure 5. PACS-2 and COPI localize H69K:fur/f/ha to the ER	210

Appendix C

Figure 1. PACS-1 forms an oligomer in cells	212
Figure 2. PACS-1 binds to PI3P	212

List of Tables

Chapter 1

Table 1. List of published PACS-1 cargo proteins. 28

Appendix A

Table 1. Endocytosis motifs in herpesvirus gH homologs. 177

Appendix B

Table 1. Furin cleavage of peptidyl substrates 211

List of Abbreviations

ANTH	AP180 NH2-terminal Homology Domain
AP	Adaptor Protein or Assembly Polypeptide
Arf	ADP-ribosylation Factor
ARR	Atropin Related Region
BAR	Bin/Amphiphysin/Rvs
CCV	Clathrin-Coated Vesicle
CD-MPR	Cation-dependent Mannose-6-phosphate Receptor
CI-MPR	Cation-independent Mannose-6-phosphate Receptor
CK1	Protein Kinase CK1
CK2	Protein Kinase CK2
COP	Coatomer Protein
CPD	Carboxypeptidase D
CTR	C-Terminal Region
DRB	5,6-dichlorobenzimidazole
EE	Early Endosome
EEA1	Early Endosome Antigen 1
ENTH	Epsin NH2-terminal Homology Domain
ER	Endoplasmic Reticulum
FBR	Furin Binding Region
GAE	γ -Adaptin Ear Domain
GAP	GTPase-activating Protein
GAT	GGA and TOM Domain
GEF	Guanine Nucleotide Exchange Factor
GFP	Green Fluorescent Protein
HCMV	Human Cytomegalovirus
HIV	Human Immunodeficiency Virus
Hrs	Hepatocyte-growth-factor-receptor Substrate
LDLR	Low Density Lipoprotein Receptor
LE	Late Endosome
MHC-I	Major Histocompatibility Complex-1
MR	Middle Region
MVB	Multi-vesicular Body
Nef	Negative Factor
PACS-1	Phosphofurin Acidic Cluster Sorting Protein-1
PACS-2	Phosphofurin Acidic Cluster Sorting Protein-2
PI3K	Phosphatidylinositol-(3)-kinase
PKA	Protein Kinase A
PKD-2	Polycystin-2
PP2A	Protein Phosphatase 2A
PtdIns	Phosphatidylinositol
PX	Phox Homology Domain
SNARE	Soluble NSF-attachment Protein Receptor

SNX1	Sorting Nexin 1
SNX2	Sorting Nexin 2
TBB	4,5,6,7-tetrabromo-2-azabenzimidazole
Tf	Transferrin Receptor
TGN	<i>trans</i> -Golgi Network
TIP47	Tail-interacting Protein of 47 kD
TOM	Target of Myo1B
VAMP4	Vesicle Associated Membrane Protein 4
VHS	Vps26, Hrs, Stam Domain
Vps26	Vacuolar Protein Sorting 26
VSV	Vesicular Stomatitis Virus
HPS	Hermansky-Pudlak syndrome
BACE	β -secretase

CHAPTER 1. INTRODUCTION

Overview

The central hypothesis of this dissertation is that protein kinase CK2 (CK2) controls a phosphorylation cascade that regulates the function of phosphofurin acidic cluster sorting protein (PACS)-1 and Golgi-localized, γ -ear-containing, ARF-binding protein (GGA)-3, and thus, trafficking of certain itinerant membrane proteins in the *trans*-Golgi network (TGN)/endosomal system. Itinerant membrane proteins utilize cytosolic sorting motifs, which interact with components of the cellular protein trafficking apparatus, to segregate into nascent vesicles bound for target organelles. PACS-1 and GGA3 bind to acidic cluster and acidic-dileucine sorting motifs, respectively, both of which overlap on the cytosolic domain of the cation-independent mannose-6-phosphate receptor (CI-MPR). Cycling of CI-MPR between the TGN and early endosomes is mediated by GGA3, which directs TGN export, and PACS-1, which directs endosome-to-TGN retrieval. However, information pertaining to the regulation of PACS-1, and how PACS-1 and GGA3 utilize an overlapping motif on the CI-MPR, was hitherto unknown. Experiments performed to address this hypothesis evaluate if CK2 phosphorylation of a potential autoregulatory domain on PACS-1 controls PACS-1-directed trafficking events, if CK2 directly associates with PACS-1 to control phosphorylation of the PACS-1 autoregulatory domain, and if the PACS-1/CK2 complex controls the sorting activity of GGA3.

This chapter provides an introduction to vesicular trafficking through the TGN and endosomal systems. I discuss how subcellular localization of itinerant membrane proteins is directed, paying special attention to the sorting proteins PACS-1 and GGA3. Finally, I

also include a description of protein kinase CK2, a kinase that has manifold roles in the regulation of protein trafficking.

Studies in Chapter 2 describe the identification of an autoregulatory domain that controls the ability of PACS-1 to bind to acidic cluster motifs. Inspection of the PACS-1 protein sequence reveals residues—S₂₇₈EEEE— that are similar to acidic cluster sorting motifs on itinerant membrane proteins and which constitute a consensus CK2 phosphorylation site. With the help of other Thomas lab members, I used biochemical-, cell-free- and cellular-methods to establish that PACS-1 is a phosphoprotein, that Ser₂₇₈ is phosphorylated by CK2, and that this cluster of acidic residues act as an autoregulatory domain for PACS-1 function. CK2 phosphorylation of Ser₂₇₈ within the PACS-1 acidic cluster or substitution of Ser₂₇₈ → Asp increased the interaction between PACS-1 and cargo, whereas a Ser₂₇₈ → Ala substitution decreased this interaction. Moreover, the Ser₂₇₈ → Ala substitution, which does not bind to cargo proteins, yields an interfering PACS-1 molecule that selectively blocks retrieval of PACS-1-regulated cargo molecules to the TGN. These results suggest that coordinated signaling events regulate protein transport within the TGN/endosomal system through the phosphorylation state of both cargo and the sorting machinery.

Studies in Chapter 3 describe a PACS-1, GGA3, and CK2 complex, which regulates trafficking of itinerant membrane proteins that contain acidic cluster and acidic-dileucine sorting motifs. With the help of other Thomas Lab members, I used cellular- and biochemical- methods to show that PACS-1 interacts directly with the regulatory subunit

of CK2. This interaction stimulates CK2 activity and controls phosphorylation of the PACS-1 autoregulatory domain. While this work was ongoing, two key observations came to light: 1) we discovered that PACS-1 directly interacts with the cytosolic sorting protein GGA3, and 2) GGA3's sorting activity was reported to be controlled by the CK2 phosphorylation of an autoregulatory domain (Doray et al., 2002b; Ghosh and Kornfeld, 2003a). However, CK2 control of GGA3 is directly opposite that of PACS-1: while CK2 phosphorylation of the PACS-1 autoregulatory domain *promotes* cargo binding, CK2 phosphorylation of the GGA3 autoregulatory domain *inhibits* cargo binding. Therefore, we used cellular- and biochemical-methods to show PACS-1 recruits CK2 to phosphorylate both PACS-1 and GGA3, thereby inactivating GGA3 and activating PACS-1, thus causing PACS-1 to bind CI-MPR and direct its retrieval to the TGN. These findings demonstrate a regulatory “switch” controlled by CK2 phosphorylation, which dictates anterograde and retrograde transport of the CI-MPR in the TGN/endosomal system.

In Chapter 4, I discuss the findings presented in Chapters 2 and 3, present a model that integrates these findings in the context of other published results and my preliminary data regarding PACS-1 function (presented in Appendix C), and suggest future experiments. Additionally, Appendix A includes a review entitled “Endocytosis of varicella-Zoster Virus glycoproteins: virion envelopment and egress” and Appendix B includes a study describing the autocatalytic activation of the furin endoprotease that I co-authored. Taken together, studies completed for this dissertation demonstrate a novel regulatory mechanism for protein sorting in the TGN/endosomal system.

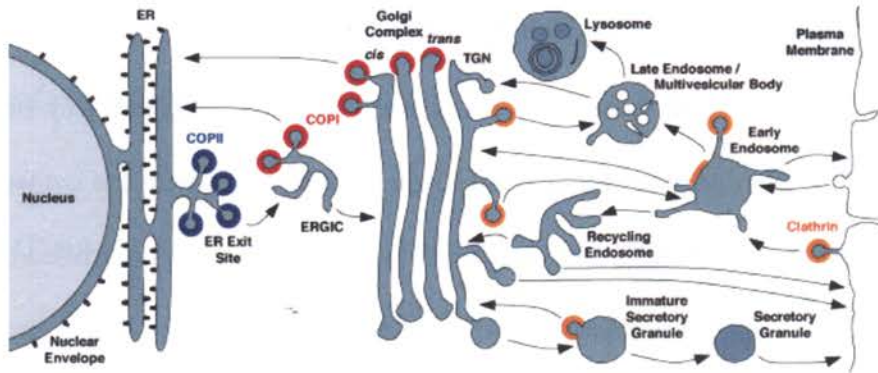


Figure 1. Intracellular Transport Pathways. Schematic diagram of the compartments of the secretory, lysosomal/vacuolar, and endocytic pathways. Transport steps are indicated by arrows. Colors indicate the known or presumed locations of COPII (blue), COPI (red), and clathrin (orange). Additional coats or coat-like complexes exist but are not represented in this figure. From Bonifacino and Glick, 2004.

The biosynthetic and endocytic pathways

Eukaryotic cells evolved a system of membrane-bound organelles essential for homeostasis, which control cellular functions such as production of membrane proteins, protein secretion, nutrient uptake, degradation of membrane and internalized proteins, and energy production (Behnia et al., 2005). Efficient transport of protein and lipid between organelles is essential for these cellular processes to take place and occurs via vesicular transport or organelle maturation. These processes are intrinsically linked—as vesicles bud from a membrane compartment the organelle “matures”. Vesicular transport can be loosely divided into four basic steps: budding, transport, docking, and fusion. Efficient and correct completion of these steps requires a wide array of cytosolic and membrane factors, including GTPases, phosphoinositides, motor proteins, coat proteins, adaptor complexes, protein and lipid kinases and phosphatases, and PACS-1, the main subject of this thesis (Bonifacino and Glick, 2004; Gu et al., 2001).

The organelles, cytosolic factors, and modification steps, that allow vesicular trafficking govern the mechanics of the endocytic and biosynthetic pathways, connecting the plasma

membrane to the endoplasmic reticulum (ER; Figure 1; Bonifacino and Glick, 2004; Palade, 1975). Membrane and luminal proteins are synthesized at the ER and, once folded, travel to the Golgi compartment (Kleizen and Braakman, 2004; Mancias and Goldberg, 2005). From the Golgi, proteins move on to the *trans*-Golgi network (TGN). Strategically located at the boundary of the biosynthetic and endocytic pathways, the TGN acts as a sorting station for membrane proteins and lipids moving through the biosynthetic pathway by segregating them into nascent vesicles bound for specific organelles including the endosomes, lysosomes and plasma membrane (Griffiths et al., 1985; Gu et al., 2001). The TGN also receives molecules internalized from the cell surface via the endocytic pathway. From the cell surface, these molecules are transported via clathrin-coated vesicles to the early endosomes, where initial sorting occurs (Anderson et al., 1977). A plethora of reports has illuminated the many possible trafficking itineraries an internalized molecule may follow. From the early endosomes, molecules can return to the cell surface via tubular recycling endosomes (van Dam et al., 2002), travel farther along the endocytic pathway to multivesicular late endosomes and ultimately to the lysosomes for degradation, or internalized proteins can travel directly to the TGN. These trafficking steps are thought to occur by vesicular transport from the cell surface to the early endosome and then by a process of compartment maturation to the lysosomes (Rink et al., 2005; Stoorvogel et al., 1991). Endosome maturation involves the vesicular recycling of cellular proteins either back to the cell surface, or to the TGN, thus escaping degradation in the lysosomes. Therefore, the TGN/endosomal system can be considered a network of membrane bound compartments constantly fluctuating in time, and not a collection of static individual organelles.

The endocytic and biosynthetic pathways are essential for homeostasis, but they also compose a cellular Achilles heel: infectious viruses use these systems to enter and replicate within the cell. For example, Herpes-viruses are proposed to use an “envelopment/de-envelopment/re-envelopment” pathway for virion assembly (Jones and Grose, 1988). The viral DNA-containing capsid assembles in the nucleus, buds across the inner nuclear membrane and fuses with the outer nuclear membrane (envelopment/de-envelopment), then obtains its final membrane envelope by budding into the TGN or endosomal compartments (re-envelopment). Virion-containing vacuoles form from the TGN and endosomes then travel toward and fuse with the plasma membrane, releasing infectious virus. In addition, several viruses use the endocytic pathway to downregulate the cell surface receptors that signal a viral infection (Marsh and Pelchen-Matthews, 2000; Marsh and Helenius, 2006). For instance, the human immunodeficiency virus (HIV)-1 down regulates the major histocompatibility complex (MHC-I; Schwartz et al., 1996), thereby “evading” the immune system (Collins et al., 1998). These viruses take advantage of the cell’s trafficking machinery, tricking the cells vesicular coats to form vesicles that allow entry into and control of the cell.

Vesicle coats were first observed by electron microscopy (EM) at the cell and internal membranes of mosquito oocytes and termed “bristle-coated pits” (Roth and Porter, 1964). This bristle-coat forms a lattice that induces membrane curvature at sites of endocytosis leading to formation of coated vesicles that are 50-150 nm in diameter (Kanaseki and Kadota, 1969; Keen and Willingham, 1979). The coat protein was purified from pig brain

in 1975 and called “clathrin” to indicate the lattice-like structure it forms (Pearse, 1976). Clathrin coated vesicles (CCVs) are found in all eukaryotic cells and tissue (Roth, 2006). Of particular interest for this dissertation, CCVs control biogenesis of dense core granules in neuroendocrine cells (Tooze and Tooze, 1986) and mediate protein transport between the TGN and endosomes in all cells (Friend and Farquhar, 1967). Initially, clathrin was thought to control all vesicular traffic. However, studies of the budding yeast *Saccharomyces cerevisiae* (Novick et al., 1980), and the use of a cell-free assay to measure intra-Golgi transport (Balch et al., 1984), soon led to the identification of COPI and COPII: clathrin-independent vesicle coats of the early secretory pathway (Barlowe et al., 1994; Waters et al., 1991). The COPI and COPII complexes form vesicles at the *cis*-Golgi and ER, respectively, to direct transport between these organelles. COPI may also direct clathrin independent transport within the endosomes (Whitney et al., 1995). A prominent focus in the field of intracellular transport is to determine how assembly of these coat proteins occurs at specific “donor” sites and how selection of “cargo” molecules to be included in the budding vesicle is determined.

Organelle identity

Each organelle has a unique membrane signature that enables cytosolic coat proteins to correctly identify donor membrane sites and initiate vesicle budding, and for docking and fusion of vesicles with acceptor membranes. This signature consists of a combination of several factors, including derivatives of phosphatidylinositol (PtdIns), GTPases and soluble NSF-attachment Protein Receptors (SNAREs), as well as the effector proteins that regulate these molecules. These factors compose an organelle “map” that the cellular

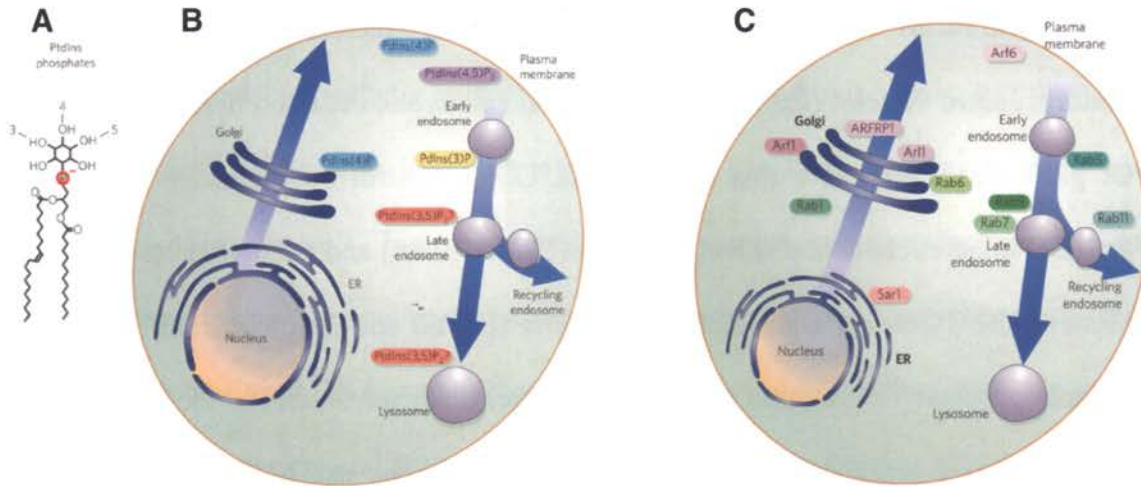


Figure 2. Examples of phosphoinositides and Rab and ARF GTPases that are localized to specific membranes within eukaryotic cells. (A) Phosphoinositides are generated by phosphorylation of phosphatidylinositol (PtdIns) on the 3, 4 or 5 positions of the inositol ring. All seven possible combinations of phosphorylation occur *in vivo*. (B) A schematic illustration of the major sites of intracellular accumulation of the well-characterized phosphoinositides. (C) ARF family GTPases are shown in purple, and Rabs in green. Some, such as ARF1, are found in multiple locations (in this case throughout the Golgi stack), but most are restricted to only one organelle. The examples shown are the best-characterized and ubiquitous cases, but there are many more GTPases, especially Rabs, that are less well characterized or are found in specialized or polarized cells. From Behnia and Munro, 2005.

trafficking machinery uses to identify target membranes (see Figure 2; Behnia and Munro, 2005).

Phosphoinositides

Different phospholipids recruit effector proteins to the cytosolic leaflet of specific organelle membranes (Haucke, 2005). Most notable for the purposes of this introduction are the derivatives of phosphatidylinositol (PtdIns), found on the cytosolic leaflets of the TGN (phosphatidylinositol-4-phosphate (PtdIns(4)P)), cell surface (phosphatidylinositol-4,5-phosphate (PtdIns(4,5)P₂)), as well as early (phosphatidylinositol-3-phosphate (PtdIns(3)P)) and late (phosphatidylinositol-3,5-phosphate (PtdIns(3,5)P₂)) endosomes. The presence of these phosphoinositides on cytosolic membranes is regulated by phosphatidylinositol kinases and phosphatases, creating a short-lived signal to recruit

peripheral membrane proteins and vesicular coats. Many peripheral membrane proteins contain modular domains, which bind specific phospholipids. These domains include FYVE domains and PHOX homology (PX) domains, which bind to PtdIns(3)P (Burd and Emr, 1998, Cheever et al., 2001); pleckstrin homology (PH) domains, which bind to PtdIns(4)P (Harlan et al., 1994); and AP180 NH₂-terminal homology (ANTH) and Epsin NH₂-terminal homology (ENTH) domains, which bind to PtdIns(4,5)P (Itoh et al., 2001; Ford et al., 2001). Phosphoinositides are also required for the recruitment of adaptor proteins to organelle membranes (see Figure 3 and discussed below). However, the cellular distribution of coat and adaptor proteins is more restricted than the distribution of phosphoinositides, indicating that other factors must also play a role.

The ARF and Rab GTPases

In addition to phosphoinositides, the ADP-ribosylation factor (ARF) and Rab (for Ras genes from rat brain; Touchot et al., 1987) GTPases act to recruit proteins involved with vesicular trafficking to organelle membranes (Behnia and Munro, 2005). As I discuss below, GTPases alternately bind guanosine diphosphate (GDP) and guanosine triphosphate (GTP) and, as the name implies, hydrolyze GTP to GDP. These two GTPase families cycle between GTP- and GDP-bound states as they bind and unbind membranes. In the GTP-bound state, they adopt a conformation that interacts with the cytosolic leaflet of cellular organelles and effector proteins, whereas in the GDP-bound conformation, they adopt an alternate conformation and are cytosolic. GTP loading of ARF and Rab GTPases is activated by guanine nucleotide exchange factors (GEFs), and GTP hydrolysis is activated by GTPase-activating proteins (GAPs). Though they contain many

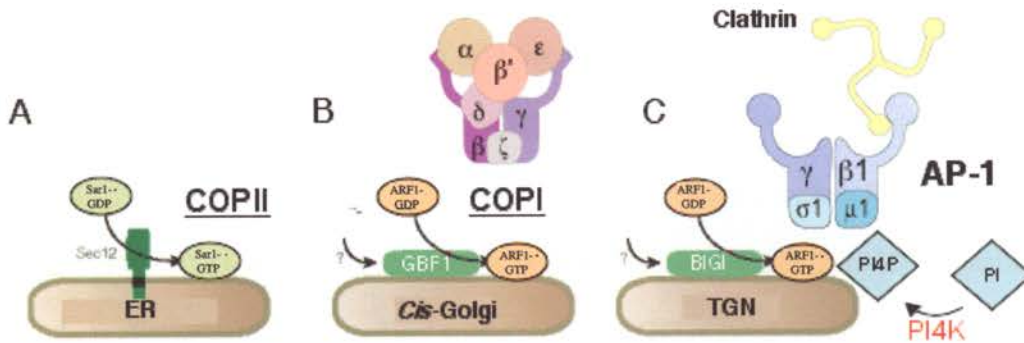


Figure 3. Organelle identity specifies coat recruitment. (A) Sar1 is recruited to ER membranes by SEC12, which is a GEF that is also an integral ER membrane protein. Sar1 in turn recruits the COPII coat. (B) At the *cis*-Golgi ARF1 is recruited by GBF1, which is an ARF1 GEF. ARF1 then recruits the COPI coat. (C) At the TGN, ARF1 is recruited by BIG1 or BIG2 (not shown), which are both ARF1 GEFs that recruit the AP-1/clathrin coat. However, recruitment of AP-1 also requires PtdIns(4)P, which is synthesized from PtdIns by Golgi resident isoforms of phosphatidylinositol-4-kinase (PI4K; Wang et al., 2003). From G. Thomas.

similarities, ARFs and Rabs also have important differences that contribute to organelle identity.

ARF1 is the prototypical member of the ARF family, which includes ARF1-6, Sar1 and several ARF-like GTPases (Behnia and Munro, 2005). ARF1 recruits the COPI coat as well as clathrin adaptors and GGAs to Golgi membranes to form vesicles bound for ER and endosomal membranes (Puertallano, 2001b; Serafini et al., 1991; Stamnes and Rothman, 1993). Sar1 recruits the COPII coat to ER membranes to form vesicles bound for the *cis*-Golgi (Barlowe et al., 1994). ARF6 is localized to the cell membrane (Cavenagh et al., 1996), where it may (Paleotti et al., 2005), or may not (Radhakrishna and Donaldson, 1997), initiate AP-2/clathrin-dependent endocytosis (this function is not entirely understood). The roles of ARF2-ARF5 are poorly defined, though some reports suggest ARF3 mediates intra-Golgi transport (Volpicelli-Daley et al., 2005). The N-terminus of ARFs contains a myristoyl group and an amphipathic helix that reversibly binds to target membranes. The myristoyl group inserts into membranes, but the ARF is

not stabilized until the N-terminal amphipathic helix also interacts with the membrane—a process that requires GEF activation (Goldberg, 1998). In the cytosol, the N-terminal amphipathic helix binds to a hydrophobic pocket on ARF–GDP, preventing membrane insertion. The GDP/GTP switch causes a conformational change that displaces the N-terminal helix out of its pocket and onto the membrane, allowing effector recruitment and vesicle formation. After formation of the vesicle, GAPs stimulate the ARF to hydrolyze GTP, resulting in a conformational change that triggers coat dissociation before vesicle fusion (Randazzo and Kahn, 1994; Serafini et al., 1991).

ARF GEFs, which are localized to specific membrane compartments, direct ARF recruitment to target organelles (Figure 3). For example, Sar1 is recruited to the ER by SEC12, an integral ER membrane protein that functions as a Sar1 GEF (Barlowe and Schekman, 1993), whereas ARF1 is recruited to the *cis*-Golgi by GBF1 (Kawamoto et al., 2002), or to the TGN by BIGI and BIGII (Yamaji et al., 2000). The importance of GEFs for controlling ARF localization, and thus regulation of membrane protein trafficking, is illustrated by the microbial-based inhibitor of Sec7-like ARF GEFs, Brefeldin A. Sec7 is a yeast ARF, whose mammalian homologs include GBF1, but not Sar1. Treatment of mammalian cells with BrefeldinA causes a massive disruption of protein trafficking through the secretory pathway, leading to redistribution of Golgi proteins into the ER (Lippincott-Schwartz et al., 1989). Paradoxically, this is due to an inhibition of Golgi-to-ER trafficking, by blocking COPI recruitment to the *cis*-Golgi and intermediate compartment (Donaldson et al., 1992; Helms and Rothman, 1992). While the exact mechanism for the redistribution of Golgi proteins to the ER remains unknown,

one possible explanation is that blocking COPI recruitment to the *cis*-Golgi disrupts the membrane organization of the golgi, leading to abhorrant tubulogenesis and unorganized fusion of the Golgi with the ER (Nebenfuhr et al., 2002). These complex interactions allow the ARFs to generate signaling microdomains on different organelles, or in the case of ARF1, the same organelle.

While ARFs function to recruit coat proteins to donor membranes, Rabs are thought to mediate specificity of vesicular fusion with target membranes (Zerial and McBride, 2001). The Rabs constitute a family of over 60 small GTPases of the Ras superfamily that, like ARFs, cycle on and off organelle membranes to recruit proteins that effect vesicular trafficking (Pfeffer and Aivazian, 2004). For example, Rab1, Rab2 and Rab6 function at the level of the ER and Golgi to regulate trafficking through these compartments (Martinez et al., 1994; Plutner et al., 1991; Tisdale et al., 1992). Several Rabs function at endosomal membranes, including Rab5, which is localized to early endosomal membranes and effects vesicular transport between the cell surface and early endosomes (Gorvel et al., 1991; Simonsen et al., 1998); Rab11, which is found at the TGN and recycling endosomes and regulates sorting between these compartments (Wilcke et al., 2000); Rab4, which is found at early and recycling endosomes (Van Der Sluijs et al., 1991), and functions for transport through these compartments (van der Sluijs et al., 1992); and Rab7 and Rab9, which both mark the late endosome and function for early to late endosomal and late endosome to TGN trafficking, respectively (Feng et al., 1995; Lombardi et al., 1993). A system of Rab effectors mediates targeting of Rabs to distinct organelles (Pfeffer and Aivazian, 2004). In the cytosol, GTP dissociation

inhibitor (GDI) binds to and prevents two C-terminal phrenyl groups on the Rab from inserting into target membrane (Matsui et al., 1990). GDI displacement factor (GDF), found on the Rab target membrane, catalyzes transfer of the Rab phrenyl groups from GDI to organelle membranes (Dirac-Svejstrup, 1997). Like ARFs, targeting of Rabs to distinct organelles can be mediated by GEF localization (Horiuchi, 1997). For instance, overexpression of Rabaptin 5, which recruits the Rab5 GEF, Rabex5, to early endosomal membranes, concentrates Rab5 on early endosomes (Horiuchi et al., 1997). Thus, Rabs contribute to specifying vesicle-target membrane fusion.

ARFs and Rabs function with phosphoinositides to direct trafficking events. For instance, early endosome antigen protein 1 (EEA1; commonly used as a marker for the early endosome) requires both the presence of PtdIns(3)P and the GTPase Rab5, to localize to the early endosome and regulate homotypic membrane fusion (Christoforidis, 1999; Simonsen et al., 1998). In addition, the adaptor protein AP-1, uses an ARF1-GTP and PtdIns(4)P combination to recruit clathrin to TGN membranes (Wang et al., 2003). Together, ARFs, Rabs, and phospholipids serve as a “coincidence” detection system: peripheral proteins recognize target membrane by the short-lived presence of an activated GTPase-phospholipid combination.

SNAREs

After a vesicle sheds its coat, it must find and fuse with the appropriate compartment, a process that requires a complex of N-ethyl-malaimide sensitive factor (NSF), soluble NSF-Attachment Protein (SNAP) and two SNAREs: one found on the vesicle (v-

SNARE) and one found on the target membranes (t-SNARE; Zerial and McBride, 2001). SNARES are localized to specific donor and target membranes and help mediate specificity of fusion (Pfeffer and Aivazian, 2004). SNARES and SNAPs form a four-helix bundle to drive hetero- and homo-typic membrane fusion (Nichols et al., 1997; Sutton et al., 1998; Weber et al., 1998), after which NSF, an ATPase, hydrolyzes ATP to disassociate the SNARE complex (Sollner et al., 1993). A v-SNARE will only bind to its cognate t-SNARE, thereby controlling downstream target destination (McNew et al., 2000). SNAREs function with Rabs to direct membrane fusion: an incoming vesicle docks with the donor membrane when it encounters a Rab, and fuses when cognate SNARE proteins interact (Pfeffer and Aivazian, 2004). Requiring multiple signals to identify donor and target membranes add an additional layer of specificity and control over the path of itinerant membrane proteins through the TGN/endosomal system.

Itinerant membrane proteins

Membrane proteins within the endocytic and biosynthetic pathways traverse various membrane-bound compartments depending on the protein and its function. For example, transferrin receptors constitutively recycle between the plasma membrane and recycling endosomes via early endosomes (van Dam et al., 2002), whereas growth factor receptors, such as the epidermal growth factor receptor (EGFR), are segregated into the sorting compartment of early endosomes and are delivered via the late endosome/ multivesicular body (MVB) pathway to lysosomes where they are degraded (Gruenberg and Stenmark, 2004; Raiborg et al., 2003). Similarly, low-density lipoprotein receptors (LDLRs) are endocytosed from the cell surface, travel to Rab5-positive early endosomes via clathrin-

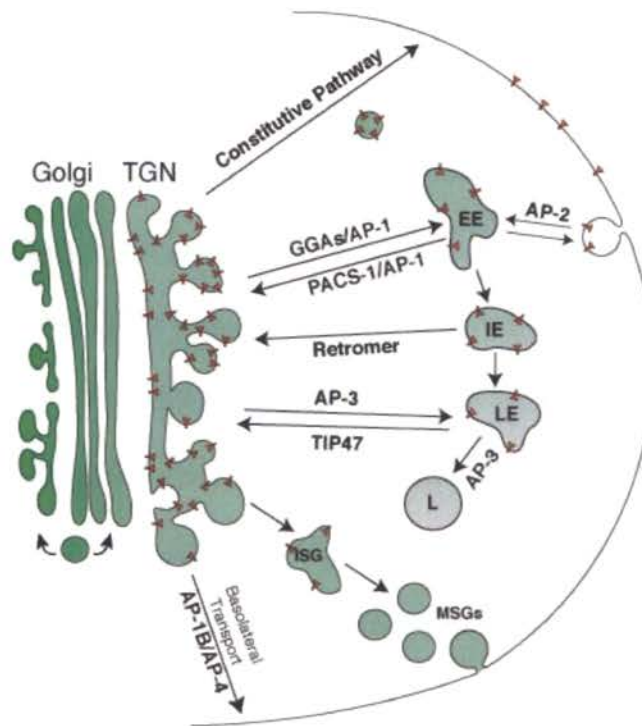


Figure 4. Late secretory protein sorting. Depicted are the organelles of the late secretory pathway, and the adapter and coat proteins that mediate protein sorting between these compartments. As an example, the sorting pathways of the CI-MPR (red triangles) are illustrated, though many other itinerant membrane proteins use these sorting pathways and adapter complexes. The cytosolic tail of the CI-MPR contains several sorting motifs that interact with adaptor proteins to direct sorting between organelles. These motifs include tyrosine and dileucine motifs that bind to AP1-4, an acidic-dileucine motif that interacts with the GGAs and acidic cluster motif that binds to PACS-1. The CI-MPR follows several late secretory trafficking pathways: anterograde transport from the TGN to early endosomes (EE) requires the GGAs and AP-1, retrograde transport from endosomes to the TGN may occur from early endosomes via PACS-1 and AP-1, intermediate endosomes (IE) via the retromer complex, or from late endosomes (LE) via TIP47. The CI-MPR is retrieved from the endosomes to the TGN before reaching the lysosome (L). In addition, the CI-MPR is retrieved from immature secretory granules (ISG) to the TGN during maturation of mature secretory granules (MSGs), a transport step that requires GGA3 and AP-1. CI-MPR transport from the cell surface to early endosomes requires AP-2.

coated vesicles, and then to Rab7 positive late endosomes using a vesicular-free maturation process (Rink et al., 2005). In addition, several itinerant membrane proteins recycle between the TGN, early and late endosomes to perform biological functions. The steady-state localization of the cation-dependent (CD)- and CI-MPRs and the furin endoprotease is at the TGN; however, like other itinerant membrane proteins, these molecules cycle between the TGN, cell surface, immature secretory granules and endosomes (Figure 4; Griffiths et al., 1988; Molloy et al., 1999). Furin must traverse the

low pH of late secretory compartments before becoming autocatalytically activated to cleave at doublets or clusters of basic amino acids within inactive precursors to form peptide hormones and bioactive proteins (Molloy et al., 1992). The MPRs sort newly synthesized lysosomal hydrolases, such as Cathepsin D, to lysosomes before being recycled to the TGN (Ghosh et al., 2003a; Griffiths et al., 1988). Lysosomal hydrolases, such as Cathepsin D, are synthesized at the ER and then travel to the Golgi compartment, where they acquire a mannose-6-phosphate ligand. This modification requires a phosphotransferase and a diesterase (Reitman and Kornfeld, 1981; Waheed et al., 1981). Once hydrolases reach the TGN, the mannose-6-phosphate receptor binds the modified hydrolase (Sly and Fischer, 1982), concentrating the hydrolase into clathrin-coated vesicles which bud from the TGN and travel to the early endosomes. The hydrolase/receptor complex travels through the maturing endosomes until the hydrolase releases from the receptor in the lower pH of the late endosome, and the receptor is recycled back to the TGN (Griffiths et al., 1988). Disruption of this lysosomal hydrolase sorting pathway causes lysosomal storage disorders. For example, mutations in the phosphotransferase gene that prevent modification of hydrolases in the Golgi result in inclusion (I)-cell disease, so named because the lysosomes become so swollen that they form “inclusions” that can be seen by phase microscopy of fibroblasts taken from patients (Tondeur et al., 1971). Patients with I-cell disease exhibit buildup of lipids in the lysosome and suffer numerous defects, including mental retardation. The observation that I-cell fibroblasts were able to internalize and use lysosomal enzymes produced by normal cells, whereas normal or other lysosomal disease fibroblasts were incapable of

internalizing lysosomal enzymes secreted by the I-cell fibroblasts, led to the identification of mannose-6-phosphate and the MPR (Hickman and Neufeld, 1972).

Despite the immense body of literature produced to explain sorting of itinerant membrane proteins in the endosomal system, the exact trafficking itinerary for many of these molecules remains controversial. For instance, the trafficking itinerary proposed for furin and the MPRs is different depending on cell system and reagents used for study (Hirst et al., 1998; Lin et al., 2004; Mallet and Maxfield, 1999; Molloy et al., 1998). Why would a membrane protein use multiple sorting itineraries to move through the late secretory system? Possibly itinerant membrane proteins traverse various endosomal paths depending on the presence or absence of ligand molecules, or, in the case of CI-MPR, the type of ligand. The CI-MPR directs trafficking of hydrolases from the TGN to the lysosome, but also functions as a receptor for insulin-like growth factor 2 (IGF2) at the cell surface, undergoing clathrin-mediated endocytosis from the cell surface and traveling to a pre-lysosomal compartment (Oka et al., 1985; Oka and Czech, 1986)—a function that may involve receptor dimerization (Byrd et al., 2000). Enzymes such as furin, have known functions in different organelles, and may require different sorting itineraries to reach different endosomal compartments. Additionally, many investigations into the trafficking of itinerant membrane trafficking utilize chimeric reporter constructs containing the cytosolic component of the receptor fused to the transmembrane and luminal domains of CD4 or Tac proteins, which may or may not reflect the full-length molecule's trafficking itinerary (Mallet and Maxfield, 1999; Lin et al., 2004). However, a broad research consensus concludes that these complex trafficking events rely upon

canonical sorting motifs within the cytosolic domains of itinerant membrane proteins. These sorting signals act as "address tags," which are recognized by components of the vesicular trafficking machinery that direct sorting to specific subcellular compartments (Bonifacino and Traub, 2003).

Sorting motifs and adaptor proteins

The presence of sorting signals on the cytosolic domain of membrane proteins was first identified on the low-density-lipoprotein receptor (LDLR) in a series of classical studies by the Brown and Goldstein laboratory. These studies identified the LDLR as essential for internalization of LDL by clathrin-mediated endocytosis from the cell membrane (Anderson et al., 1977; Brown and Goldstein, 1975) and led to the discovery that a tyrosine residue on the cytosolic domain of the LDLR was required for incorporation into CCVs and internalization of the protein from the cell surface (Davis et al., 1987; Lehrman et al., 1985a; Lehrman et al., 1985b). This seminal work led to the characterization of several sorting motifs, which are found on the cytosolic domain of membrane proteins. Below I introduce tyrosine, dileucine, acidic-dileucine and acidic cluster-based motifs, as well as the trafficking machinery that recognizes them.

Tyrosine motifs, dileucine motifs and the adaptor proteins

The best characterized of the sorting motifs are the tyrosine- (YXX ϕ , where ϕ is a bulky hydrophobic residue) and dileucine- ([D/E]xxxL[L/I]) based motifs. The function of tyrosine- and dileucine-based signals arises from the interaction of these motifs with the heterotetrameric adaptor complexes (APs) AP-1, AP-2, AP-3 and AP-4. Originally

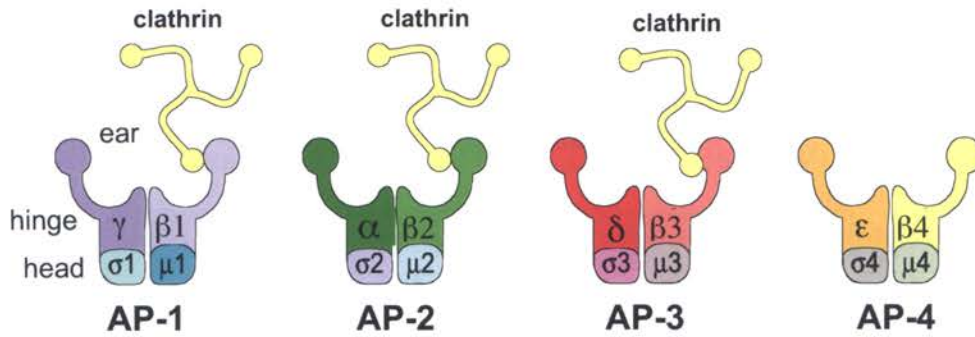


Figure 5. Schematic diagram of the APs. Adaptor complexes are composed of the four indicated subunits. The μ 1-4 subunits bind to tyrosine-based motifs, and the β 1-3 subunits bind to dileucine motifs. The β subunits of AP-1-3 bind to clathrin, but it is not known if AP-4 binds clathrin.

identified as assembly polypeptides (also APs), which could induce *in vitro* formation of clathrin coats (Zaremba and Keen, 1983), adaptor complexes connect clathrin to sorting signals in the cytosolic domains of several membrane proteins, including the CI- and CD-MPRs and furin, thereby promoting their concentration into clathrin-coated pits (Robinson, 2004). Adaptor complex-induced formation of vesicles from clathrin-coated pits requires membrane fission, which is mediated by the GTPase dynamin at the plasma membrane and a dynamin homologue, dynamin 2, at the TGN and endosomes (Cao et al., 2000; van Dam and Stoorvogel, 2002a).

All the adaptor complexes are highly homologous, and are composed of four subunits, which form a “mickey mouse”-like structure, with a core domain and two appendage or “ear” domains connected to the core domain by two unstructured hinge regions (Figure 5; Heuser and Keen, 1988; Collins et al., 2002). The core domains bind to ARF-GTP, phosphoinositides and cargo proteins; the hinge regions contain a clathrin-box sequence and bind to clathrin and the appendage domains bind to accessory proteins. AP-1 (subunits: γ , β 1, μ 1 and σ 1), which is localized mainly at the TGN, mediates sorting of

membrane proteins in both anterograde and retrograde pathways between the TGN and endosomes. This complex binds to phosphatidylinositol-4-phosphate (PtdIns(4)P) on the Golgi membrane (Wang et al., 2003), and mutations that disrupt this interaction block AP-1 localization at the TGN (Heldwein et al., 2004). AP-1B (subunits: γ , $\beta 1$, $\mu 1B$ and $\sigma 1$), an epithelial-cell-specific isoform of AP-1, directs transport to the basolateral surface from the TGN and endosomes (Anderson et al., 2005; Fèolsch et al., 1999). AP-2 (subunits: α , $\beta 2$, $\mu 2$ and $\sigma 2$), which is localized to the plasma membrane, plays a prominent role in clathrin-mediated endocytosis of cell-surface-receptors. This complex binds to phosphatidylinositol-4,5-phosphate (PtdIns(4,5)P; Rohde et al., 2002), which is concentrated on the inner leaflet of the cell membrane. AP-3 (subunits: δ , $\beta 3$, $\mu 3$ and $\sigma 3$) is localized to the TGN and endosomes and mediates sorting of membrane proteins to the lysosomes and melanosomes (Peden et al., 2004). Mutations of the β subunit of AP-3 lead to Hermansky-Pudlak syndrome (HPS), a rare disorder characterized by defective lysosomal organelles, including melanosomes, which leads to albinism in some HPS patients (Dell'Angelica et al., 1999). AP-4 (subunits: ϵ , $\beta 4$, $\mu 4$ and $\sigma 4$), which is localized to the TGN and endosomes, mediates the sorting of membrane proteins to basolateral membrane in polarized cells (Simmen et al., 2002). The AP-1, AP-2 and AP-3 complexes bind directly to clathrin via a clathrin box sequence on their β subunits (Dell'Angelica et al., 1998; Gallusser and Kirchhausen, 1993), whereas the $\beta 1-3$ and $\mu 1-4$ subunits bind to [D/E]XXXL[L/I] and Yxx ϕ motifs in the cytosolic domain of the cargo proteins, respectively (Hirst et al., 1999; Ohno et al., 1995; Ohno et al., 1998; Rapoport et al., 1998). Whether or not the $\beta 4$ subunit binds to clathrin or dileucine motifs remains unclear. The σ subunit is predicted to play a structural role by stabilizing the tetrameric

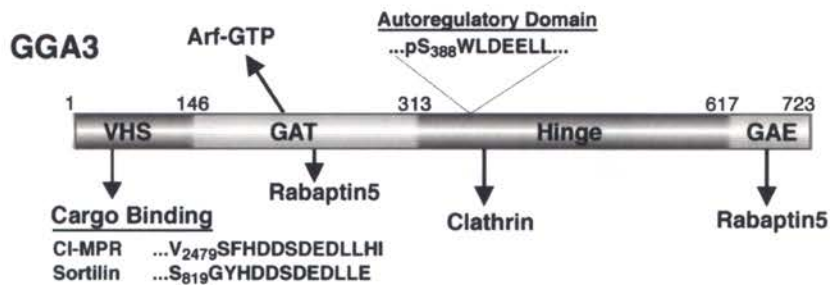


Figure 6. Diagram of GGA3 showing domain organization and protein interactions. The VHS (Vps27, Hrs, Stam) domain binds to cargo proteins, the GAT (GGA and TOM) domain binds to ARF-GTP and Rabaptin5, the hinge segment binds to clathrin and contains the autoregulatory acidic-dileucine motif and Ser₃₈₈, and the GAE (γ -adaptin ear) domain also binds to Rabaptin5, as well as several other accessory proteins. The domain organization of GGA1 and GGA2 is highly similar to that of GGA3.

complex (Collins et al., 2002a). The crystal structures of the AP-1 and AP-2 core domains suggest these molecules occupy active and inactive states. In the inactive state, the tyrosine-binding module of the μ subunit is masked, and must be exposed, possibly by a phosphorylation event that results in a conformational change (Ghosh and Kornfeld, 2003b), before the adaptor complex can bind cargo. Together these adaptor complexes and coat proteins orchestrate intracellular transport of many membrane proteins in the TGN/endosomal system.

Acidic-dileucine motifs and the GGAs

Acidic-dileucine motifs (D/ExxLL) are found on the cytosolic domains of several itinerant membrane proteins, including the CI- and CD-MPRs, sortilin, β -secretase (BACE), vesicle associated membrane protein 4 (VAMP4) and sorting protein related receptor (SorLA), which all cycle between the TGN and endosomes. The function of these motifs arises from an interaction with the GGA proteins 1-3 (Figure 6; Doray et al., 2002 Kakhlon et al., 2006; Nielsen et al., 2001; Wahle et al., 2005; Zhu et al., 2001).

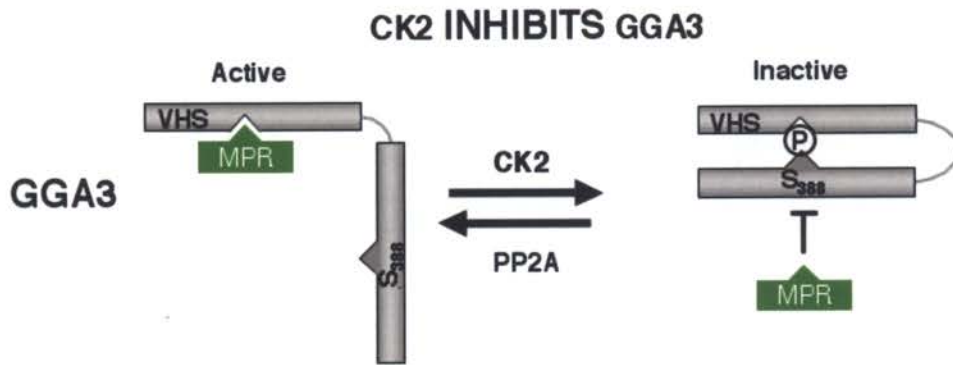


Figure 7. Model of GGA3 activation. CK2 phosphorylation of Ser₃₈₈ inhibits GGA3 binding to the CI-MPR. When Ser₃₈₈ is not phosphorylated, the CI-MPR can interact with the cargo-binding VHS domain. However, upon CK2 phosphorylation of Ser₃₈₈, the autoinhibitory acidic-dileucine motif in the hinge region of GGA3 binds to the VHS domain, precluding cargo binding. PP2A dephosphorylation of Ser₃₈₈ reverses the process. GGA1, but not GGA2, undergoes the same regulatory mechanism (Doray et al., 2002b).

GGAs are monomeric clathrin adaptors that bind to membranes in an ARF-GTP-dependent manner and function to sort the CI-MPR into clathrin-coated vesicles at the TGN, thus activating anterograde trafficking to early endosomes (Puertollano et al., 2001b). Phosphorylation of serine residues within the CI-MPR and sortilin acidic-dileucine motifs enhances GGA binding (Kato et al., 2002), though this is not true for phosphorylation of the CD-MPR (Stockli et al., 2004). In addition, GGA1 and 3 binding to the CI-MPR is regulated by CK2 phosphorylation of an autoregulatory domain (Doray et al., 2002b). Phosphorylation of Ser₃₅₅ or Ser₃₈₈ within the GGA1 or GGA3 autoregulatory domains, respectively, inhibits binding to the CI-MPR, whereas dephosphorylation by PP2A activates binding to the CI-MPR. Thus CK2 and PP2A control the cargo binding ability of the GGAs.

The structures of all three GGAs are similar; they contain the VHS, GAT and GAE structured domains, as well as, one unstructured “hinge” between the latter two domains (Figure 6; Miller et al., 2003; Misra et al., 2002; Suer et al., 2003). The VHS (Vps26

(Vacuolar protein sorting 26), Hrs (Hepatocyte-growth-factor-receptor substrate) and STAM (signal-transducing adaptor molecule)) domain binds to acidic dileucine motifs on the cytosolic domains of cargo proteins and is named for its homology to these other proteins involved in endocytic trafficking. The GAT (GGA and TOM (target of Myo1B)) domain is found in all three GGAs and is homologous to TOM. The GAT domain binds to Rabaptin5 (Mattera et al., 2003) and to the GTP-, but not GDP-bound forms of ARF1 and ARF3—the latter interaction is required for GGAs to bind membranes, localization of GGAs to the TGN, and correct sorting of lysosomal hydrolases (Dell'Angelica et al., 2000; Puertollano et al., 2001b). The GGA hinge regions bind to clathrin (Puertollano et al., 2001b), and the GGA1 and GGA3 hinges contains the above-mentioned autoregulatory acidic-dileucine motif. The GAE (γ -adaptin ear) domain carries limited homology with the AP-1- γ subunit ear domain, and interacts with several accessory proteins including Rabaptin-5 (the GGA-rabaptin5 interaction is bipartite) and enthoproin/EpsinR (Saint-Pol et al., 2004). EpsinR binds to PtdIns(4)P at the TGN (Hirst et al., 2003), which may help to specify GGA binding to TGN membranes. The discovery of several GAE binding proteins allowed identification of a GAE binding motif (DFGX ϕ , where X is any amino acid and ϕ is a bulky hydrophobic residue; Nogi et al., 2002), which was confirmed by the crystallization of Rabaptin5 with the GAE domain (Miller et al., 2003).

While the GGAs were originally proposed to direct sorting exclusively at the TGN (Boman et al., 2000; Dell'Angelica et al., 2000; Hirst et al., 2000; Poussu et al., 2000; Takatsu et al., 2000), newer evidence suggests GGAs play a significant role in the

endosomal sorting of the CI-MPR (Puertollano and Bonifacino, 2004; Mattera et al., 2003) and β -secretase (Wahle et al., 2005), as well as removal of VAMP4 from immature secretory granules (Kakhlon et al., 2006). In particular, GGA3 is suspected to function at multiple membrane compartments. GGA3 associates with early endosomes and immature secretory granules when overexpressed (Kakhlon et al., 2006; Puertollano and Bonifacino, 2004), and endogenous GGA3 can be detected on the early endosome by electron microscopy (Ghosh et al., 2003b). GGA3 depletion by siRNA causes accumulation of the CI-MPR and internalized epidermal growth factor (EGF) within early endosomes (Puertollano and Bonifacino, 2004) and accumulation of VAMP4 in mature secretory granules (Kakhlon et al., 2006). Further supporting the endosomal role of GGAs, Mattera and coworkers reported the interaction of all three GGAs with the Rab4/5 effector Rabaptin5 (Mattera et al., 2003). Rabaptin5 stabilizes Rab5-GTP and recruits the Rab5 GEF Rabex5 to early endosome membranes, thereby leading to endosome fusion. The authors proposed that vesicles or tubules leaving the TGN use the GGA-Rabaptin5 interaction to fuse with early endosomes. While endogenous GGA1 is normally detected only at the TGN, they showed that overexpression of Rabaptin 5 causes endogenous GGA1 and CI-MPR to redistribute from the TGN to enlarged early endosome membranes. In addition, they found that Rabaptin5 precludes GGA3 binding to clathrin—preventing GGA3 from initiating vesicular transport of the endosomal CI-MPR. Together, these findings suggest that a small population of GGA3 leaves the TGN on vesicles or tubules destined for the early endosomes, and remains with the CI-MPR until retrograde transport of the receptor is initiated, an event inhibited by overexpression of Rabaptin5. Alternatively, multiple pools of GGA3 may function for both anterograde

and retrograde CI-MPR transport: one pool travels on vesicle bound for the endosomes and interacts with Rabaptin5 for endosome fusion, and another pool is recruited to the early endosomes by Rabaptin5 and is required for a sorting step that occurs before the CI-MPR can initiate retrograde transport to the TGN. In Chapter 3, I present evidence that PACS-1 and GGA3 form a complex to regulate endosome-to-TGN sorting of the CI-MPR.

Acidic cluster motifs and PACS-1

Frequently, acidic-dileucine motifs are found near sorting motifs represented by clusters of acidic residues, which often contain serine or threonine residues that can be phosphorylated by CK2 or, less frequently, protein kinase CK1 (CK1; Bonifacino and Traub, 2003; Gu et al., 2001; Thomas 2002). Membrane proteins that contain acidic sorting motifs include processing enzymes such as furin (Jones et al., 1995), protein convertase 6B (PC6B; Xiang et al., 2000) and carboxypeptidase D (CPD; Kalinina et al., 2002); receptors such as the CI- and CD-MPRs (Chen et al., 1997); transporters such as vesicular monoamine transporter 2 (VMAT2; Waites et al., 2001); SNAREs, including VAMP-4 (Zeng et al., 2003); a number of pathogen-derived molecules, including the envelope glycoproteins of many herpes viruses such as varicella-zoster virus gE (VZV-gE; Alconada et al., 1999) and human cytomegalovirus gB (HCMV gB; Norais et al., 1996), as well as human immunodeficiency virus type 1 (HIV-1) negative factor (Nef; Piguet et al., 2000). Perhaps the best studied of these acidic cluster motifs is the one present in the cytosolic domain of furin (Thomas 2002). The phosphorylation state of a serine residue within the furin acidic cluster controls in large part the dynamic sorting

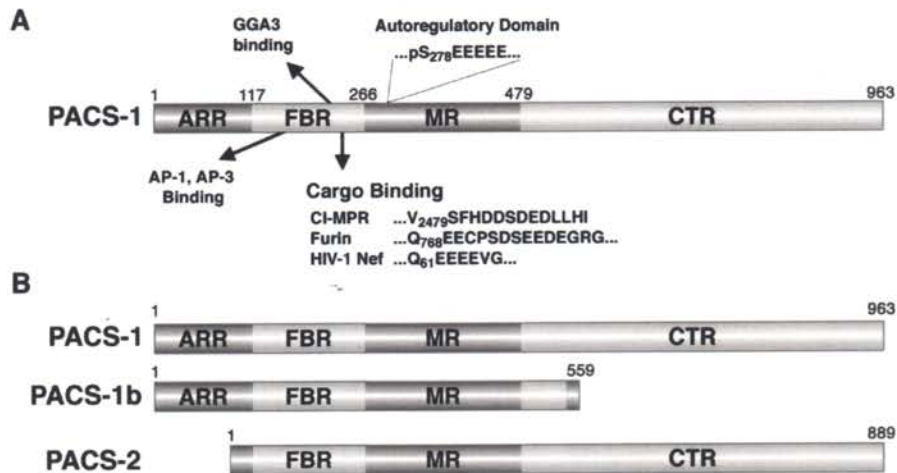


Figure 8. Schematic diagram of PACS-1 proteins. (A) Diagram of PACS-1 showing the atropin-1-related region (ARR), cargo binding region (FBR), which interacts with cargo, AP-1/AP-3 adaptor complexes and GGA3 (Crump et al., 2001a; Wan et al., 1998; and described in Chapter 3), the middle region (MR), which contains the autoregulatory acidic cluster and Ser₂₇₈ (described in Chapter 2), and the C-terminal region (CTR). (B) Diagram of human PACS proteins. PACS-1 and PACS-1b are splice variants and are 100% identical except for a short C-terminal region. PACS-2 protein is encoded from a separate gene to PACS-1, and is 54% identical to PACS-1. The cargo-binding (FBR) regions of PACS-1 and PACS-2 proteins are 81% identical at the amino acid level.

itinerary of the endoprotease, including the localization of furin to the TGN (Jones et al., 1995), recycling of furin from early endosomes to the cell surface (Molloy et al., 1998) and, in neuroendocrine cells, removal of furin from immature secretory granules (Dittie et al., 1997). By contrast, dephosphorylation of the furin acidic cluster by specific isoforms of protein phosphatase 2A (PP2A) allows transport of furin from sorting/recycling endosomes to the TGN (Molloy et al., 1998), apparently via a late endosome (Mallet and Maxfield, 1999) intermediate. Thus, the coordinated activities of CK2 and PP2A control the complex, acidic cluster-mediated trafficking of furin.

Acidic cluster motifs derive their function by interacting with the members of the PACS family of proteins: PACS-1a, PACS-1b and PACS-2 (see Figure 4). The Thomas lab identified PACS-1a (hereafter PACS-1), through its preferential interaction with the

PACS-1 cargo proteins

Protein	Acidic cluster sequence	Other sorting motifs
Proteases		
Furin ^a	... Q ₇₆₈ EECPDSEEDDEGRG...	Y ^b
PC6B ^c	... D ₁₈₃₀ RDYDEDDDD...	Y ^c
CPD ^d	... S ₁₃₅₉ HEFQDETDTTEEET	
Receptors		
CI-MPR ^a	... H ₂₄₈₉ DDSDEDLLHI	Y ^c , LL ^f , AC-LL ^g
Snares		
VAMP4 ^j	... E ₂₇ DDSDEEED...	LL ^k
Viral Proteins		
HCMV gB ^l	... L ₈₉₇ KDSDEEENV...	
VZV gE ^a	... F ₅₉₀ EDSESTDTEEF...	Y ^m
HIV-1 Nef ⁿ	... Q ₆₁ EEEEVG...	LL ^o
Channels		
PKD-2 ^p	... D ₈₁₀ DSEEDDDDEDS...	
Nephrocystin ^q	... E ₁₁₆ EEEESESEDSGSGG...	
TRPV4 ^p	... L THKKRLTDEEFREP...	
CLC-7 ^p	... S KKVSWSGRDRDDEE...	
Transporters		
VMAT-2 ^r	... E ₅₉₃ DEESES...	

Table 1. List of published PACS-1 cargo proteins. Reported PACS-1 cargo proteins are shown with their acidic cluster motifs. Serine or threonine residues phosphorylated by CK2 and important for PACS-1 binding are shown in bold. Additional tyrosine (Y), dileucine (LL) or acidic-dileucine (AC-LL) sorting motifs are indicated. The references for these findings are: ^aWan et al., 1998, ^bVoorhees et al., 1995, ^cXiang et al., 2000, ^dKalinina et al., 2002b, ^eLobel et al., 1989, ^fChen et al., 1997a, ^gPuertollano et al., 2001a, ^hNielsen et al., 2001, ⁱVAMP4, Hinners et al., 2003, ^jZeng et al., 2003, ^kCrump et al., 2003, ^lOlson and Grose, 1997, ^mPiguet et al., 2000, ⁿGreenberg et al., 1998, ^oKottgen et al., 2005, ^pSchermer et al., 2005, ^qWaites et al., 2001.

phosphorylated acidic cluster on the cytosolic domain of furin (Molloy et al., 1998). PACS-1 connects furin to the cytosolic coat protein AP-1, and is required for the correct subcellular localization of furin to the TGN (Crump et al., 2001). PACS-1 also binds to acidic clusters within the cytosolic domains of several other cellular proteins (see Table 1). Interfering mutant-, siRNA- and antisense- based studies have shown that PACS-1 is required for the TGN localization of these molecules from an endosome compartment. PACS-1 binding to HIV-1 Nef is required for the ability of this viral protein to

downregulate cell-surface major histocompatibility class-I (MHC-I) complexes (Blagoveshchenskaya et al., 2002; Piguet et al., 2000). Depletion of PACS-1 using an antisense strategy disrupts the ability of Nef to downregulate MHC-I, a function that can be rescued by PACS-1b (Piguet et al., 2000). PACS-1 is divided into four regions (see Figure 8): the Atropin-1-related region (ARR), which bears homology to the nuclear protein Atropin-1; the cargo binding region (FBR), which interacts with cargo and AP-1/AP-3 adaptor complexes (Crump et al., 2001; Wan et al., 1998); the middle region (MR), which contains an acidic cluster, -S₂₇₈EEEE-, that is similar to the acidic cluster sorting motifs on many membrane cargo proteins that bind to the PACS-1 FBR; and the C-terminal region (CTR). This thesis examines how the predicted domains of PACS-1 function to regulate PACS-1 FBR binding to cargo proteins.

Like PACS-1, PACS-2 binds to acidic cluster motifs on the cytosolic domains of itinerant cargo proteins (Simmen et al., 2005). However, PACS-2 connects cargo proteins to COPI and functions in Golgi-to-ER transport (Kottgen et al., 2005). For example, the subcellular localization and function of the ER-localized TRP channel polycystin-2 (PKD-2) is regulated by the phosphorylation state of an acidic cluster in the carboxy-terminal domain, which binds to PACS-1 and PACS-2 (Kottgen et al., 2005). The normal steady-state localization of polycystin-2 is at the ER. However, blocking binding to PACS-2 mislocalizes polycystin-2 to the TGN, and blocking the binding to both PACS-1 and PACS-2 mis-localizes polycystin-2 to the plasma membrane, demonstrating that the PACS family members can cooperate to control protein sorting. In addition, PACS-2 is required for efficient apoptosis and ER homeostasis (Simmen et al., 2005). Together,

the PACS family members link protein trafficking to control of cellular homeostasis and disease.

Tip47 and the Retromer complex

In addition, two other sorting molecules are relevant for this thesis: TIP47 and the Retromer complex. Similar to PACS-1, TIP47 and the Retromer complex also direct retrograde transport of CI-MPR from endosomes to the TGN (Diaz and Pfeffer, 1998; Seaman et al., 1998). The retromer complex was first identified in yeast (Seaman et al., 1998), and is now known to localize to tubular-vesicular profiles emanating from either early endosomes or from intermediates in the maturation of early endosomes to late endosomes in mammalian cells (Arighi et al., 2004). Retromer consists of five subunits: vacuolar protein sorting (Vps)-35, Vps29, Vps26, SNX1 and SNX2. From endosomal compartments, Vps35 binds to an unknown motif on the CI-MPR, mediating recycling of CI-MPR to the TGN (Arighi et al., 2004; Seaman, 2004). Recruitment of retromer to endosomal membranes requires SNX1 and 2, which each contain a PX domain that binds PtdIns(3)P (Cozier et al., 2002), and a BAR domain, which senses membrane curvature (Peter et al., 2004). SNX1 forms multimers, which, in combination with the BAR domain, may cause membrane curvature and tubulation (Carlton et al., 2004). Like retromer, TIP47 also directs transport of MPRs from endosomes to the TGN. TIP47 links a diaromatic amino acid motif in the cytosolic domain of the CI- and CD-MPRs (FW) and HIV-gp160 (YW) to the late endosome localized GTPase Rab9, thus concentrating these molecules at the late endosomes and mediating TGN transport (Blot et al., 2003; Carroll et al., 2001; Diaz and Pfeffer, 1998). Depletion of TIP47 results in a reduction of

CI-MPR half-life, presumably because the receptor fails to recycle to the TGN and gets destroyed in lysosomes (Diaz and Pfeffer, 1998). Also, expression of a TIP47 interfering mutant blocks gp160 transport to the TGN and reduces HIV virion production (Blot et al., 2003). Despite these findings, the role of TIP47 for endosomal transport is quite controversial. Several reports found that TIP47 functions in the storage of intracellular lipid droplets (Miura et al., 2002; Wolins et al., 2001; Wolins et al., 2005), and the structure of TIP47 was solved bound to a neutral lipid droplet (Hickenbottom et al., 2004). Some have suggested TIP47 may not effect CI-MPR function, based on a report showing that siRNA depletion of TIP47 has no effect on CI-MPR transport (Medigeshi and Schu, 2003). However, a negative result does not prove TIP47 has no function in endosome-to-TGN transport—most likely, TIP47 functions in both roles. The TIP47 structure shows this molecule curved around a lipid droplet (Hickenbottom et al., 2004), raising the intriguing possibility that TIP47 somehow senses the curvature of a budding vesicle. Together, TIP47 and Retromer function to recycle the MPRs to the TGN from later endosomal compartments.

The complicated nature of sorting motifs and protein trafficking is illustrated by the presence of multiple sorting motifs on the cytosolic domain of the CI-MPR, which binds to adaptor proteins, GGAs, PACS-1, TIP47 and the retromer complex. This has produced confusion in the literature regarding which sorting molecule is responsible for which trafficking itinerary, and has led some to discount the individual importance of these sorting proteins. Most likely, the cell utilizes different sorting motifs depending on which sorting step needs to occur. Perhaps localized differences in membrane identity direct

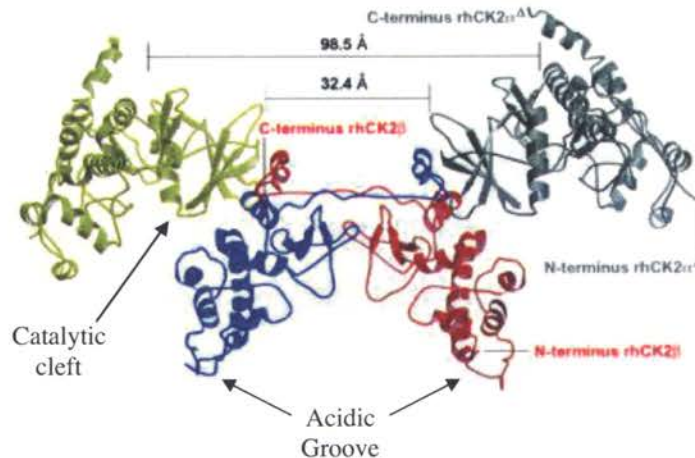


Figure 9. Ribbon diagram of the CK2 holoenzyme. The regulatory β subunits (blue and red) interact with each other and with both catalytic α subunits (yellow and grey). The catalytic core and the acidic groove of the regulatory subunit are indicated. One theory of CK2 activation is that basic compounds such as polyamines, or proteins with clusters of basic residues, such as FGF-2 interact with the acidic groove of the regulatory subunit, causing a conformational change that increases the enzymatic activity of the catalytic subunit. In Chapter 3, I describe a cluster of basic residues on PACS-1 that is required to bind and activate CK2. The ribbon diagram is from Niefind et al., 2001.

different sorting proteins to the CI-MPR to direct transport. Alternatively, phosphorylation can control which sorting proteins can bind to an itinerant protein. For instance, phosphorylation of Ser₂₄₈₄ on the CI-MPR cytosolic domain enhances binding to GGAs or PACS-1 (Kato et al., 2002 and Chapter 3) and CK2 phosphorylation of serine residues within the GGA3 and PACS-1 autoregulatory domains controls their ability to bind to cargo proteins (Doray et al., 2002 and Chapter 2). A central player in these phosphorylation events is protein kinase CK2.

Protein kinase CK2

Acidic and acidic-dileucine motifs often contain a serine or threonine residue that can be phosphorylated by protein kinase CK2 (CK2). CK2 is a ubiquitous protein kinase with more than 300 putative polypeptide substrates and is a heterotetramer composed of two catalytic subunits ($\alpha\alpha$, $\alpha\alpha'$, or $\alpha'\alpha'$) and two regulatory β subunits (Pinna, 2002). The

regulatory β subunits form a dimer that interacts with the catalytic core of the α subunits to direct phosphorylation of the consensus sequence [S/T]_{xx}[D/E/pS/pT] with an average of 5 acidic residues surrounding the substrate S/T (Chantalat et al., 1999; Meggio and Pinna, 2003; Niefind et al., 2001). The importance of CK2 is illustrated by disruption of the catalytic α' subunit gene in mice, which leads to aberrant spermatogenesis (Xu et al., 1999), and disruption of the regulatory β subunit gene, which leads to embryonic lethality (Buchou et al., 2003). In yeast, disruption of the genes encoding the two catalytic subunits is lethal (Padmanabha et al., 1990). Serine or threonine residues that are phosphorylated by CK2 are often dephosphorylated by protein phosphatase 2A, a ubiquitous phosphatase found in all cells (Sontag, 2001). The dynamic interplay between CK2 and PP2A is evidenced by the observation that these enzymes can form a complex in cells (Heriche et al., 1997). Unfortunately, whether or not the activity of CK2 and PP2A is controlled by upstream regulators remains unknown. Additionally, comparative studies to determine the relative expression of these two enzymes in different tissues are lacking. Regardless, CK2 and PP2A function as master regulators of protein traffic in the TGN/endosomal system by controlling the phosphorylation of cargo proteins, as well as the activity of the trafficking machinery.

Despite being the first kinase activity observed (Burnett and Kennedy, 1954), the regulation of CK2 has long remained enigmatic. No known CK2 stimulator produces a huge increase in kinase activity. However, binding of polyamines or substrate proteins to an acidic groove on the regulatory β subunit increases kinase activity 3-fold (Leroy et al., 1997). For instance, FGF-2 binding to CK2 β stimulates kinase activity for nucleolin (Bonnet et al., 1996), and correlates with an enhancement of DNA synthesis (Skjerpen et

al., 2002). Together with the CK2 holoenzyme crystal structure, biochemical data suggests polyamine binding to the β subunit results in a conformational change in the catalytic core that increases enzyme activity (Leroy et al., 1997; Niefind et al., 2001). These increases in kinase activity are small, but may be significant when coupled with targeting of the kinase to substrate proteins. In Chapter 3, I present evidence supporting this hypothesis, showing that PACS-1 binds directly to the regulatory subunit of CK2, stimulates CK2 activity, and that this interaction is required for the phosphorylation of PACS-1 itself, as well as PACS-1 binding partners.

Conclusion

While the importance of PACS-1 for localizing acidic cluster containing membrane cargo to the TGN is well established, no information pertaining to the regulation of its sorting activity has been reported. For many cargo molecules, including furin, CI-MPR, VMAT2 and VZV-gE, phosphorylation of specific residues within their acidic clusters enhances binding to PACS-1 (Waites et al., 2001; Wan et al., 1998), whereas others, including PC6B and HIV-1 Nef, contain non-phosphorylatable acidic clusters (Piguet et al., 2000; Xiang et al., 2000). Together, these results suggest that binding of PACS-1 to cargo acidic clusters may be regulated by more than just the phosphorylation state of the cargo protein. Interestingly, PACS-1 itself contains an acidic cluster with a potential CK2 phosphorylation site (...S₂₇₈EEEE...). The striking similarity between the acidic cluster in PACS-1 to acidic clusters found on PACS-1 cargo molecules such as furin raises the possibility that the PACS-1 acidic cluster may control PACS-1 sorting activity by interacting with the PACS-1 cargo binding region (FBR) and thereby preventing the

interaction of PACS-1 with cargo proteins. In addition, the overlapping nature of the acidic- and acidic-dileucine-trafficking motifs suggests that the sorting activity of PACS and GGA sorting proteins may be coordinated—and may explain the differences observed regarding the trafficking itineraries of furin, which binds PACS-1 but not GGAs and CI-MPR, which binds both PACS-1 and GGAs (Lin et al., 2004; Mallet and Maxfield, 1999). The requirement of CK2 phosphorylation of cargo proteins for binding to PACS and GGAs, as well as for the known and potential regulation of GGA and PACS-1 function, respectively, raised the possibility that this kinase might associate with these sorting molecules to control PACS-1 and GGA directed protein sorting. This thesis explores the hypothesis that protein kinase CK2 controls a phosphorylation cascade that regulates the function of PACS-1 and GGA3, and thus, trafficking of certain itinerant membrane proteins in the *trans*-Golgi network (TGN)/endosomal system.

CHAPTER 2

The phosphorylation state of an autoregulatory domain controls PACS-1-directed protein traffic

Gregory K. Scott, Feng Gu¹, Colin M. Crump², Laurel Thomas, Lei Wan, Yang Xiang³ and Gary Thomas⁴

Vollum Institute, L-474, 3181 SW Sam Jackson Park Road, Portland, Oregon 97239 USA; ¹McGill Cancer Center, McGill University, 3655, Promenade Sir William Osler, Montreal, Quebec, H3G 1Y6, Canada; ²Division of Virology, Department of Pathology, University of Cambridge, Tennis Court Road, Cambridge CB2 1QP, UK; ³Department of Molecular and Cellular Physiology, Stanford Medical Center, Palo Alto, California 94305 USA

G. K. Scott and F. Gu contributed equally to this work

⁴Corresponding author

Tel: (503) 494-6955

Fax: (503) 494-1218

e-mail: thomasg@ohsu.edu

Published in: The EMBO Journal, December 1, 2003, Volume 22, p. 6234-44

In this chapter I performed the experiments in Figures 1B, 1F, 2B, 2D and 4. F. Gu and L. Thomas performed the cell free transport assay (Figure 3), C. Crump performed the phospho-amino acid analysis (Figure 1D), L. Wan performed the ³²P labeling of GST-MR (Figure 1C), and F Gu performed all other experiments (Figures 1E, 2A, 2C, 5C and 5B). I also participated by writing the manuscript and responding to the referees comments with G. Thomas.

Abstract

PACS-1 is a cytosolic sorting protein that directs the localization of membrane proteins in the *trans*-Golgi network (TGN)/endosomal system. PACS-1 connects the clathrin adaptor AP-1 to acidic cluster sorting motifs contained in the cytosolic domain of cargo proteins such as furin, the cation-independent mannose-6-phosphate receptor and in viral proteins such as HIV-1 Nef. Here we show that an acidic cluster on PACS-1, which is highly similar to acidic cluster sorting motifs on cargo molecules, acts as an autoregulatory domain that controls PACS-1-directed sorting. Biochemical studies show Ser₂₇₈ adjacent to the acidic cluster is phosphorylated by CK2 and dephosphorylated by PP2A. Phosphorylation of Ser₂₇₈ by CK2 or mutation of Ser₂₇₈ → Asp increased the interaction between PACS-1 and cargo, whereas a Ser₂₇₈ → Ala substitution decreased this interaction. Moreover, the Ser₂₇₈ → Ala mutation yields an interfering mutant PACS-1 molecule that selectively blocks retrieval of PACS-1-regulated cargo molecules to the TGN. These results suggest that coordinated signaling events regulate transport within the TGN/endosomal system through the phosphorylation state of both cargo and the sorting machinery.

Key Words: autoregulatory domain /CK2/Nef /PACS-1 /phosphorylation

Introduction

The control of homeostasis and disease requires that cellular or pathogen proteins are correctly modified and targeted to specific cellular compartments. Many of these modification and targeting steps rely on the communication between the dynamic and highly regulated network of late secretory pathway organelles that comprise the *trans*-Golgi network (TGN)/endosomal system (Gruenberg, 2001). In addition to housing several biochemical reactions, the TGN orchestrates the routing of proteins to lysosomes, secretory granules, and, in polarized cells, to the apical and basolateral surfaces. The TGN also receives molecules internalized from the cell surface via a series of complex and highly dynamic endosomal compartments. Precisely how the TGN/endosomal system controls the sorting and localization of proteins is incompletely understood, but numerous studies show the requirement for the orchestrated interaction of many cellular factors including various small molecules, lipids, cytosolic and membrane proteins and components of the cytoskeleton (Gu et al., 2001).

The localization of many membrane proteins within the TGN/endosomal system relies upon specific sorting motifs contained within the cytosolic domain of these proteins (Bonifacino and Traub, 2003). One of these motifs is represented by clusters of acidic residues, often containing serine or threonine residues that can be phosphorylated by casein kinase 2 (CK2) or, less frequently, casein kinase 1 (CK1, for reviews, see (Bonifacino and Traub, 2003; Gu et al., 2001; Thomas 2002). Membrane proteins that contain acidic sorting motifs include processing enzymes such as furin (Jones et al., 1995), PC6B (Xiang et al., 2000) and carboxypeptidase D (CPD, Kalinina et al., 2002);

receptors such as the cation-independent mannose-6-phosphate receptor (CI-MPR, Chen et al., 1997); transporters such as VMAT2 (Waites et al., 2001); SNAREs including VAMP-4 (Zeng et al., 2003); a number of pathogen molecules including the envelope glycoproteins of many herpesviruses such as varicella-zoster virus gE (VZV-gE, Alconada et al., 1999) and human cytomegalovirus gB (HCMV gB, Norais et al., 1996), as well as human immunodeficiency virus type 1 (HIV-1) Nef (Piguet et al., 2000). Perhaps the best studied of these acidic cluster motifs is the one present in the cytosolic domain of furin (Thomas, 2002b). The phosphorylation state of the furin acidic cluster controls in large part the dynamic sorting itinerary of the endoprotease including the localization of furin to the TGN (Jones et al., 1995), recycling of furin from early endosomes to the cell surface (Molloy et al., 1998) and, in neuroendocrine cells, removal of furin from immature secretory granules (Dittie et al., 1997). By contrast, dephosphorylation of the furin acidic cluster by specific isoforms of protein phosphatase 2A (PP2A) allows transport of furin from sorting/recycling endosomes to the TGN (Molloy et al., 1998), apparently via a late endosome intermediate (Mallet and Maxfield, 1999). Thus, the coordinated activities of CK2 and PP2A control the complex, acidic cluster-mediated trafficking of furin.

The phosphorylated furin acidic cluster binds to the sorting protein PACS-1 (phosphofurin acidic cluster sorting protein-1), which is a sorting connector that links furin to the AP-1 clathrin adaptor and is required for localizing furin to the TGN (Crump et al., 2001; Wan et al., 1998). PACS-1 is not exclusively dedicated to the localization of furin, as it is also required for the TGN localization of a number of membrane proteins

that contain acidic cluster sorting motifs. These include cellular proteins, such as CI-MPR (Wan et al., 1998), PC6B (Xiang et al., 2000), and VMAT2 (Waites et al., 2001) as well as several viral proteins including HCMV gB (Crump et al., 2003) and HIV-1 Nef (Piguet et al., 2000). PACS-1 binding to HIV-1 Nef is required for the ability of this viral protein to downregulate cell-surface major histocompatibility class-I (MHC-I) complexes (Blagoveshchenskaya et al., 2002; Piguet et al., 2000).

While the importance of PACS-1 for localizing acidic cluster containing membrane cargo to the TGN is well established, no information pertaining to the regulation of its sorting activity has been reported. For many cargo molecules including furin, CI-MPR, VMAT2 and VZV-gE, phosphorylation of specific residues within their acidic clusters enhances binding to PACS-1 (Waites et al., 2001; Wan et al., 1998), whereas others including PC6B and HIV-1 Nef contain non-phosphorylatable acidic clusters (Piguet et al., 2000; Xiang et al., 2000). Together, these results suggest that binding of PACS-1 to cargo acidic clusters may be regulated by more than just the phosphorylation state of the cargo protein. Interestingly, PACS-1 itself contains an acidic cluster with a potential CK2 phosphorylation site, ..S₂₇₈EEEE.., located C-terminal to the cargo-binding domain (named the FBR, see Fig. 1A). The striking similarity between the acidic clusters in PACS-1 to those in cargo molecules such as furin raises the possibility that the PACS-1 acidic cluster may control PACS-1 sorting activity.

In this report we show that the PACS-1 acidic cluster acts as an autoregulatory domain for PACS-1-directed protein trafficking and is itself a target of CK2 phosphorylation and

PP2A dephosphorylation. We demonstrate that the PACS-1 acidic cluster associates with the cargo-binding region of PACS-1 in a phosphorylation dependent manner. Using biochemical, cellular- and cell-free studies, we show that the phosphorylation state of the PACS-1 acidic cluster regulates the ability of PACS-1 to bind to and sort cargo proteins to the TGN. Disruption of PACS-1 phosphorylation by a Ser₂₇₈ → Ala substitution results in an interfering mutant that inhibits PACS-1-directed endosome-to-TGN sorting. These results provide new insight into how a coordinated signaling mechanism controlling the phosphorylation of both the cargo and a sorting connector can regulate TGN/endosomal sorting.

Results

Inspection of the PACS-1 protein sequence reveals an acidic cluster, -S₂₇₈EEEE-, C-terminal to the cargo-binding region (FBR, residues 117-266) that is similar to the acidic cluster sorting motifs on many membrane cargo proteins that bind to the PACS-1 FBR (Fig. 1A). Interestingly, the serine residue within the PACS-1 acidic cluster forms a consensus sequence for CK2 phosphorylation. To determine if Ser₂₇₈ is a major site of phosphorylation in PACS-1, cells expressing wild type PACS-1 or PACS-1 with a Ser₂₇₈ → Ala substitution (PACS-1 S₂₇₈A) were incubated with ³²P_i and the immunoprecipitated PACS-1 proteins were resolved by SDS PAGE. Quantification of the incorporated radioactivity showed that PACS-1 S₂₇₈A contained 50% less ³²P than wild type PACS-1, indicating that Ser₂₇₈ is a major PACS-1 phosphorylation site *in vivo* (Fig. 1B).

Next we conducted a series of *in vitro* studies to characterize the reversible phosphorylation of PACS-1 at Ser₂₇₈. First, we showed that Ser₂₇₈ could be phosphorylated by CK2 (Fig. 1C). GST-PACS-1₂₄₀₋₄₇₉ (GST-MR, which contains the PACS-1 acidic cluster) or GST-MRS₂₇₈A was incubated with purified CK2 and [γ -³²P]ATP. GST-MRS₂₇₈A incorporated significantly less ³²P than did GST-MR, suggesting that Ser₂₇₈ within the PACS-1 acidic cluster is a substrate for CK2. Moreover, neither protein kinase A nor protein kinase C could phosphorylate GST-MR despite their ability to efficiently phosphorylate a control substrate (data not shown). Second, to unequivocally identify Ser₂₇₈ as a CK2 phosphorylation site, we conducted phosphoamino acid analysis on GST-MRS₂₇₈T following CK2 phosphorylation (Fig. 1D). The Ser₂₇₈ → Thr substitution was chosen because GST-MR lacks a phosphorylatable threonine

residue. Thus, the formation of pThr in GST-MRS₂₇₈T following incubation with CK2 must be due to phosphorylation at residue 278 and not to steric inhibition of phosphorylation at some other Ser/Thr residue. Replicate samples of GST-MR, GST-MRS₂₇₈A and GST-MRS₂₇₈T were incubated with recombinant CK2 and [γ -³²P]ATP. Phosphoamino acid analysis of GST-MR and GST-MRS₂₇₈A showed a prominent signal of only pSer. By contrast, analysis of GST-MRS₂₇₈T revealed pThr in addition to pSer. These data strongly indicate that Ser₂₇₈ is a major CK2 phosphorylation site in PACS-1. Third, because many cargo acidic cluster motifs that require CK2 phosphorylation for binding to PACS-1 are dephosphorylated by PP2A (Molloy et al., 1998; Varlamov et al., 2001), we investigated whether PP2A can similarly dephosphorylate the CK2-phosphorylated GST-MR (Fig. 1E). Consistent with a potential role for PP2A at this step, [³²P]-GST-MR was efficiently dephosphorylated by PP2A and this reaction was blocked by okadaic acid, a PP2A specific inhibitor. By contrast, protein phosphatase 1, PP1, failed to dephosphorylate [³²P]-GST-MR despite its ability to efficiently dephosphorylate a control substrate (data not shown), suggesting a role for PP2A as the PACS-1 Ser₂₇₈ phosphatase.

We conducted metabolic labeling studies to determine whether endogenous PACS-1 is phosphorylated *in vivo*. Cells were incubated with ³²P_i and endogenous PACS-1 was immunoprecipitated with affinity purified anti-PACS-1 antibodies but not with an IgG control (Fig. 1F). In agreement with our *in vitro* studies, incubation of the cells with okadaic acid increased the amount of ³²P incorporated into PACS-1 by two-fold. By contrast, and in agreement with the analysis of PACS-1 S₂₇₈A (Fig. 1B), incubation of the

cells with the CK2 inhibitor DRB decreased the amount of ^{32}P incorporated into endogenous PACS-1 by to approximately 50% relative to control conditions. Together with our *in vitro* studies, these data strongly implicate CK2 and PP2A as the enzymes that control the phosphorylation state of PACS-1 Ser₂₇₈.

The reversible phosphorylation of Ser₂₇₈ raised the possibility that, similar to PACS-1 cargo proteins, the PACS-1 acidic cluster may interact with the PACS-1 FBR. To test this possibility, non-phosphorylated or CK2-phosphorylated GST-MR was incubated with Trx-PACS-1FBR and captured using glutathione agarose (Fig. 2A). We found that GST-PACS-1MR indeed bound to Trx-PACS-1FBR. Surprisingly, however, whereas phosphorylation of most PACS-1 cargo proteins enhanced binding to the PACS-1 FBR, the phosphorylation of GST-PACS-1MR by CK2 diminished binding to Trx-PACS-1FBR. To test whether this reduced binding was due specifically to phosphorylation of Ser₂₇₈, we measured the binding of the PACS-1 FBR to GST-MR constructs containing either a Ser₂₇₈ → Ala or a Ser₂₇₈ → Asp substitution. Consistent with the results using CK2-phosphorylated molecules, GST-MRS₂₇₈A exhibited stronger binding to Trx-PACS-1FBR than the GST-MRS₂₇₈D.

We performed competitive binding assays to test whether GST-MR, which contains the PACS-1 acidic cluster, competes with cargo protein acidic clusters for binding to the PACS-1 FBR (Fig. 2B). GST-PACS-1MR was pre-incubated with Trx-PACS-1 FBR and then mixed with increasing concentrations of Trx-furinS_{773,775}D, which contains the CK2 phosphomimic furin cytosolic domain that binds to the PACS-1 FBR (Crump et al.,

2001) or Trx alone. GST-PACS-1 MR was captured using glutathione agarose and bound Trx-PACS-1 FBR was detected by western blot. Using this assay, we found that Trx-furinS_{773,775}D competed in a dose-dependent manner with GST-MR for binding to the PACS-1 FBR whereas Trx alone had no effect. Together, the data in figures 2A and 2B indicate that binding of the PACS-1MR to the PACS-1 FBR precludes cargo binding to PACS-1.

To examine the importance of Ser₂₇₈ phosphorylation in the context of full-length PACS-1, we tested the ability of PACS-1S₂₇₈A or PACS-1S₂₇₈D to bind to the PACS-1 cargo protein HIV-1 Nef (Fig. 2C). We previously showed that the Nef acidic cluster, EEEE₆₅, is required for binding to PACS-1 and for PACS-1 dependent sorting of HIV-1 Nef reporter proteins to the TGN (Blagoveshchenskaya et al., 2002; Piguet et al., 2000). Because the Nef acidic cluster cannot be phosphorylated by CK2, only CK2 phosphorylation of the putative PACS-1 autoregulatory domain may regulate Nef-PACS-1 binding. Cells expressing PACS-1, PACS-1S₂₇₈A, or PACS-1S₂₇₈D were harvested and incubated with GST-Nef. Quantification of proteins binding to HIV-1 Nef showed that the S₂₇₈D substitution enhanced PACS-1 binding to GST-Nef by more than 50% whereas the S₂₇₈A substitution inhibited PACS-1 binding to GST-Nef by nearly 80%. Thus, the ability of PACS-1 to bind cargo is regulated by the phosphorylation state of t Ser₂₇₈.

The Ser₂₇₈ → Ala/Asp substitutions could potentially inhibit the interaction of PACS-1 with AP-1 due to some indirect structural deformation. To test this possibility, PACS-1 proteins were immunoprecipitated from cells expressing PACS-1, PACS-1 S₂₇₈A, PACS-

1 S₂₇₈D, or PACS-1Admut, which contains an alanine substitution of E₁₆₈TELQLTF₁₇₅ within the PACS-1 FBR that blocks binding to AP-1 but not cargo (Crump et al., 2001). Co-immunoprecipitation analysis showed that each PACS-1 construct, except PACS-1Admut, associated with AP-1 (Fig. 2D). Together, the data in figure 2 show that phosphorylation at Ser₂₇₈ terminates the autoinhibitory domain to the cargo binding domain, thereby promoting binding of PACS-1 to cargo proteins.

The inhibitory effect of the Ser₂₇₈ → Ala substitution on the ability of PACS-1 to bind cargo proteins suggested that expression of PACS-1S₂₇₈A in cells might interfere with PACS-1 dependent sorting. Therefore, we examined the effect of PACS-1S₂₇₈A and PACS-1S₂₇₈D on the TGN sorting of the HIV-1 Nef reporter construct 44Nef (Fig. 3A). 44Nef is a chimera composed of the CD4 extracellular and transmembrane domains fused to cytosolic HIV-1 Nef. Using this construct, CD4 antibody uptake assays showed that co-expression of the reporter with either PACS-1 or PACS-1S₂₇₈D had no effect on the efficient delivery of internalized 44Nef to the TGN. By contrast, co-expression of PACS-1S₂₇₈A blocked the sorting of internalized 44Nef to the TGN and caused the reporter to be mislocalized to a dispersed, punctate endosomal population. The interfering effect of PACS-1S₂₇₈A on the sorting of 44Nef to the TGN was indistinguishable from the missorting of 44NefAla, which contains an EEEE₆₅ → AAAA₆₅ substitution that cannot bind to PACS-1 (Piguet et al., 2000).

Next, we used a cell-free assay to unequivocally establish the role of PACS-1, and in particular the phosphorylation state of Ser₂₇₈, in endosome-to-TGN sorting (Fig. 3B). This

assay utilizes the activity of a resident TGN- tyrosylprotein sulfotransferase that sulfates Tyr residues in the luminal domain of cargo proteins to demonstrate sorting to the TGN. A 44Nef mutant, 44Nef-Y, was constructed containing the cholecystinin tyrosine O-sulfation motif within the CD4 luminal domain. Cells expressing 44Nef-Y were treated with cycloheximide to block protein synthesis and promote accumulation of the nascently synthesized 44Nef-Y in late secretory pathway compartments. The membrane fraction from these cells was incubated with the unlabeled sulfate donor PAPS (3'-phosphoadenosine 5'-phosphosulfate) to quench any 44Nef-Y present at the TGN but not in endosomal compartments, which lack the sulfotransferase. The quenched membrane preparation was then incubated with cytosol from control C6 cells, AS19 PACS-1 antisense cells, or AS19 cells expressing PACS-1, PACS-1S₂₇₈D or PACS-1S₂₇₈A. Each sample was incubated with an ATP regenerating system in the presence of [³⁵S]-PAPS to promote endosome-to-TGN transport. Using this assay, we found that addition of cytosol from control cells (C6) but not cytosol from PACS-1 antisense cells (AS19), which contain reduced levels of PACS-1, supported endosome-to-TGN transport as measured by an increase in [³⁵S]-labeled 44Nef-Y. By contrast, cytosol from AS19 cells replete with PACS-1 rescued the endosome-to-TGN transport of 44Nef-Y demonstrating the importance of PACS-1 in the retrieval of membrane cargo from endosomes to the TGN. Next, we analyzed the PACS-1 phosphorylation state mutants and found that only PACS-1S₂₇₈D but not PACS-1S₂₇₈A rescued the endosome to TGN sorting of 44Nef-Y, supporting a role for the phosphorylation of Ser₂₇₈ as a key regulator of PACS-1 sorting activity. We suspect that the less efficient rescue of 44Nef-Y sorting by PACS-1S₂₇₈D compared to PACS-1 may reflect a requirement for the temporal regulation of PACS-1

phosphorylation in directing protein sorting. Nonetheless, these results demonstrate that PACS-1 directs the endosome-to-TGN transport and that its sorting activity is regulated by the phosphorylation state of Ser₂₇₈.

The immunofluorescence and *in vitro* transport studies showed that phosphorylation of PACS-1 controls the endosome-to-TGN transport of the 44Nef reporter and suggested that PACS-1S₂₇₈A may act as an interfering mutant to selectively block the sorting of PACS-1 cargo proteins. To test this possibility we first examined the effect of PACS-1S₂₇₈D and PACS-1 S₂₇₈A on the ability of HIV-1 Nef to downregulate MHC-I molecules (Fig. 4). Cells expressing HIV-1 Nef alone or together with either PACS-1 or PACS-1S₂₇₈D caused the redistribution of cell surface MHC-I to the TGN whereas co-expression of PACS-1S₂₇₈A blocked MHC-I downregulation. Second, we determined whether PACS-1S₂₇₈A could affect the TGN localization of CI-MPR and furin (Fig. 5A). Expression of PACS-1 or PACS-1S₂₇₈D in A7 cells had no effect on the paranuclear localization of either endogenous CI-MPR or co-expressed Flag-tagged furin (fur/f) both of which overlapped with the staining pattern of TGN46. By contrast, expression of PACS-1S₂₇₈A caused both CI-MPR and fur/f to redistribute to an endosomal population that no longer overlapped with TGN46. Finally, to establish that PACS-1S₂₇₈A selectively blocked the sorting of PACS-1 cargo, we examined the effects of PACS-1S₂₇₈A and PACS-1S₂₇₈D on the distribution of several secretory compartment markers (Fig. 5B). In addition to their lack of effect on the localization of TGN46, which does not require PACS-1 to localize to the TGN, we found that neither PACS-1 mutant affected the localization of AP-1 or markers for early endosomes (internalized transferrin), late

endosomes (LBPA) or the Golgi cisternae (mannosidase II). Together, these analyses show that the sorting activity of PACS-1 is controlled by the phosphorylation state of an autoregulatory domain and that interference with this autoregulatory mechanism specifically blocks PACS-1-directed protein traffic in the TGN/endosomal system.

Discussion

In this study, we have identified a biochemical mechanism that controls the sorting activity of PACS-1. We discovered that the phosphorylation state of an autoregulatory domain within PACS-1 controls binding of this sorting connector to cargo proteins. CK2 phosphorylation of Ser₂₇₈ within this autoregulatory domain weakens the interaction between the PACS-1 FBR and the PACS-1 autoregulatory domain (Figs. 1 and 2), thereby enhancing binding to cargo (Fig. 2). These interactions are competitive, such that the unphosphorylated PACS-1 autoregulatory domain precludes binding of cargo proteins to the PACS-1 FBR (Fig. 2). Moreover, immunofluorescence and cell-free transport studies showed that both PACS-1 and the phosphomimic PACS-1 mutant, PACS-1S₂₇₈D, support endosome-to-TGN sorting of cargo (Fig. 3). By contrast, the non-phosphorylatable PACS-1 mutant, PACS-1S₂₇₈A, fails to support this sorting step and in cellular studies disrupts both the TGN localization of PACS-1 cargo and Nef-mediated downregulation of MHC-I (Figs. 4 and 5). Together, our results demonstrate that the sorting capacity of PACS-1 is regulated by the phosphorylation state of an autoregulatory domain, revealing a fundamental mechanism used to control the regulation of protein traffic in the TGN/endosomal system.

The control of PACS-1 function by the coordinated activities of CK2 and PP2A is highly reminiscent to the role of these two enzymes in controlling the trafficking of furin. The phosphorylation state of furin's cytosolic acidic cluster sorting motif, which mediates binding to PACS-1, controls the trafficking itinerary of the endoprotease (Molloy et al., 1999; Thomas 2002). However, whereas CK2 phosphorylation of acidic cluster sorting

motifs within the furin cytosolic domain or other cargo proteins including CI-MPR, VZV gE and VMAT-2 increases their binding to the PACS-1 FBR, CK2 phosphorylation of Ser₂₇₈ within the PACS-1 acidic cluster weakens the binding of these residues to the PACS-1 FBR (Waites et al., 2001; Wan et al., 1998 and Fig. 2). These opposite effects of CK2 phosphorylation on binding of the PACS-1 FBR to the PACS-1 autoregulatory domain versus membrane cargo acidic clusters suggests a simple model whereby CK2 phosphorylation promotes protein sorting by both activating PACS-1 and increasing the affinity of PACS-1 for phosphorylated membrane cargo proteins. But how CK2 phosphorylation of acidic cluster motifs within membrane cargo and PACS-1 influence in a completely opposite manner the binding of these various acidic motifs to the PACS-1 FBR remains unknown. Moreover, acidic cluster binding to the PACS-1 FBR may be more complex than a simple phosphorylation switch as the non-phosphorylatable Nef and PC6B acidic clusters bind to PACS-1 (Piguet et al., 2000; Xiang et al., 2000). Together, these studies suggest that, unlike that shown for many phosphopeptide binding modules including the 14-3-3 and forkhead modules (Durocher et al., 2000; Muslin et al., 1996), the PACS-1 FBR may not contact the phosphoamino acids directly but may instead recognize other acidic cluster determinants that would be masked or unmasked by the phosphorylation of embedded Ser/Thr residues. Perhaps phosphorylation of cargo proteins increases the affinity of cargo for the PACS-1 FBR whereas phosphorylation of the PACS-1 autoregulatory domain triggers a conformational change that unmasks the FBR to promote cargo binding (Figure 6). Alternatively, subtle structural differences between the phosphorylated PACS-1 acidic cluster and the phosphorylated acidic clusters

on furin or CI-MPR may result in a different set of contacts between these motifs and the cargo binding residues within the FBR.

Blocking phosphorylation at Ser₂₇₈ in PACS-1 has a profound effect on the trafficking of PACS-1 cargo. For example, the PACS-1S₂₇₈A mutant blocked the HIV-1 Nef-mediated downregulation of cell-surface MHC-I molecules to the *trans*-Golgi network (Figure 4) and caused the mislocalization of furin and MPR from the TGN to dispersed endosomal compartments (Fig. 5A). The lack of a measurable effect of PACS-1S₂₇₈A on markers for the TGN and Golgi cisternae, as well as for early and late endosomal compartments (Fig. 5B), further demonstrated the selectivity of this interfering mutant for disrupting the trafficking and localization of membrane proteins that are sorted by PACS-1. The selective disruption in protein traffic caused by PACS-1S₂₇₈A is very similar to that observed in cells lacking either PACS-1 (Wan et al., 1998) or the AP-1A adaptor (Meyer et al., 2000), as well as in cells expressing PACS-1Admut (Crump et al., 2001). Because PACS-1 forms a ternary complex with AP-1 and cargo proteins (Crump et al., 2001), the similar sorting defect caused by both PACS-1 S₂₇₈A and PACS-1Admut reflects the selective inhibition of the two arms of this protein complex. Moreover, as the PACS-1 S₂₇₈A mutation has no measurable effect on PACS-1 binding either to AP-1 (Fig. 2D) or to cellular membranes (data not shown), a simple explanation for how PACS-1S₂₇₈A acts as an interfering mutant may be that it competes with endogenous PACS-1 for membrane recruitment and adaptor complexes but fails to bind to cargo.

To directly test the ability of PACS-1 to control endosome-to-TGN sorting, we used an *in vitro* re-sulfation assay that quantitatively measures the sorting of tyrosine-phosphorylatable reporter proteins to the TGN (Itin et al., 1997). We found that cytosol from control cells, but not from PACS-1 antisense cells, supports endosome-to-TGN transport of a tyrosine-sulfatable Nef reporter, 44Nef-Y (Fig. 3). In addition, PACS-1 antisense cytosol replete with either PACS-1 or containing PACS-1S₂₇₈D restored endosome-to-TGN transport of 44Nef-Y whereas cytosol containing PACS-1S₂₇₈A could not. These data combined with the immunofluorescence studies demonstrate the importance of PACS-1, and in particular the phosphorylation state of Ser₂₇₈, for directing the endosome-to-TGN sorting of membrane cargo proteins. The requirement for PACS-1 to direct endosome-to-TGN transport is in agreement with earlier cell-free assays demonstrating that the phosphorylation state of the furin and CPD acidic clusters, which bind to PACS-1, have no effect on TGN budding or retention (Kalinina et al., 2002; Wan et al., 1998). However, the transport assay does not show whether PACS-1 mediates retrieval specifically from early endosomes, late endosomes, or both. Previous studies showed that 44Nef reporter mutants unable to bind to PACS-1 accumulate in an acidified late endosome-like compartment (Piguet et al., 2000) whereas AP-1, a PACS-1 effector, is required for retrieval of membrane cargo from early endosomes to the TGN (Meyer et al., 2000). Because PACS-1 is required for multiple sorting steps including endosome-to-TGN sorting, retrieval of furin from immature secretory granules, and for recycling of phosphorylated furin from endosomes to the cell surface (Thomas 2002), it is possible that PACS-1 participates in the retrieval of membrane proteins from multiple post-TGN compartments.

Whereas the diverse roles of autoregulatory domains in regulating processes ranging from protease activation to signal transduction is well established (Anderson et al., 2002; Pufall and Graves, 2002), the roles of autoregulatory domains in regulating the activities of trafficking proteins are only now beginning to emerge. Recent reports describe autoregulatory domains in the GGA1 and GGA3 adaptors, which direct anterograde sorting from the TGN to endosomes (Doray et al., 2002; Ghosh and Kornfeld, 2003a). Similar to PACS-1, autoinhibition of GGA1 is controlled by the CK2-catalyzed phosphorylation of a serine residue (Ser₃₅₅) within a cluster of acidic residues but, interestingly, in an opposite manner to that of PACS-1. Whereas CK2 phosphorylation of the PACS-1 autoregulatory domain promotes cargo binding (Fig. 2), CK2 phosphorylation of the GGA1 autoregulatory domain inhibits cargo binding (Doray et al., 2002). Perhaps CK2 phosphorylation promotes endosome-to-TGN sorting by simultaneously activating PACS-1 and inhibiting GGA1. Conversely, activation of PP2A would drive movement from the TGN to endosomes by simultaneously activating GGA1 and inhibiting PACS-1. Indeed, our findings that inhibition of either CK2 or PP2A decreased or increased, respectively, the phosphorylation of endogenous PACS-1 (Fig. 2), suggests that a balance in the activities of these two enzymes controls PACS-1 sorting activity. Whether GGAs and PACS-1 intimately participate in controlling protein localization is currently being investigated. Together these findings provide new insight into how the localization of membrane cargo molecules is controlled by the CK2 and PP2A-mediated activities of PACS-1 and GGAs. Elucidating the signaling pathways that

control these phosphorylation events will be an important step for understanding trafficking in the TGN/endosomal system.

Materials and Methods

Cell lines

BSC-40 epithelial cells, A7 melanoma cells, AS19 PACS-1 antisense cells and control C6 cells containing empty vector were cultured as previously described (Wan et al., 1998).

DNA constructs

pGEX3X-MR (containing PACS-1 residues 257 to 449) and pET32-PACS-1 FBR (containing PACS-1 residues 117 to 256) expressing GST- and His/thioredoxin (Trx)-fusion proteins were previously described (Crump et al., 2001). PACS-1 point mutants were generated by standard PCR methods and subcloned into pGEX3x to produce pGEX-PACS-1MRS278A, pGEX-PACS-1MRS278D and pGEX-PACS-1MRS278T. pGEX-Nef and pCMX44Nef NotI were obtained from D. Trono (Piguet et al., 1998 ; Piguet et al., 2000). pGEX3X-CK2 α was obtained from D. Litchfield.

Recombinant virus

Vaccinia virus (VV) and adenovirus (AV) were constructed using standard methods (Blagoveshchenskaya et al., 2002). VV recombinants expressing human HA-tagged PACS-1 and FLAG-tagged furin were previously described (Crump et al., 2001 ; Molloy et al., 1994). VV recombinants expressing HA-tagged PACS-1S₂₇₈A and PACS-1S₂₇₈D were made by replacing the mutation from pGEX-PACS-1MR plasmid into pZVneo:PACS-1ha. The AV expressing 44Nef sequence was constructed by subcloning 44Nef from pCMX44Nef NotI into pAdtet7. 44Nef-Y was generated by inserting the

cholecystokinin tyrosyl sulfation motif (SAEDYEYPS) after Lys₂₆ of 44Nef in pAdtet44Nef.

Protein purification

pGEX or pET32a-Trx vectors encoding the various PACS-1 proteins were transformed in to BL21 (DE3) pLysS (Novagen). GST fusion proteins were purified using glutathione agarose (Sigma) following the manufacturers protocol. Thioredoxin (Trx) fusion proteins were purified using Ni-NTA-agarose following the manufacturers protocol (Qiagen).

Metabolic labeling and immunoprecipiations

To label recombinant PACS-1, BSC-40 cells were infected with VV expressing HA-tagged PACS-1 or PACS-1S₂₇₈A (m.o.i. = 10) for 4 hours, washed and incubated with phosphate free media for 1 hr. 0.5 mCi/ml [³²P_i] sodium orthophosphate (NEN NEX053C) was then added for 3 hrs. The labeled cells were washed with PBS, lysed with 500 µl mRIPA (1%NP40, 1% sodium deoxycholate, 150 mM NaCl, 50 mM Tris pH 8.0) plus 1 mM CaCl₂, 50 mM NaF, 80 mM β-glycerol phosphate and 0.1 µM orthovanadate. HA-tagged PACS-1 proteins were immunoprecipitated with mAb HA.11 (Berkeley Antibody Co.), separated by SDS-PAGE and analyzed by autoradiography. To label endogenous PACS-1, A7 cells were grown to confluency, incubated with phosphate free media for 2 hours, then labeled with 0.6 mCi/ml [³²P_i] sodium orthophosphate (NEN NEX053C) for 2 hr in the absence or presence of either 100 µM 5,6-dichlorobenzimidazole riboside (DRB) or 20 nM okadaic acid (OA). The cells were lysed with PBS plus 1% NP-40 containing protease inhibitors (Complete, Sigma). PACS-1 was

immunoprecipitated overnight using affinity purified rabbit anti PACS-1 antibody 601 (antigen, PACS-1 KGSLGKDDTTSPME₄₃₃). The immunoprecipitates were washed, split into two, and each half separated by SDS-PAGE. One half was used for PACS-1 autoradiography and the other for control western blot with mAb anti-PACS-1 (BD Transduction Labs). Co-immunoprecipitation of PACS-1 constructs with AP-1 were performed as previously described (Crump et al., 2001).

***In vitro* phosphorylation/ dephosphorylation**

1 μ g purified GST-PACS-1MR was incubated with 0.02 μ l purified bovine CK2 in 50 μ l reaction buffer (50 mM Tris pH 7.5, 140 mM KCl, 10 mM MnCl₂ and 100 μ M ATP) and 10 μ Ci [γ -³²P]ATP. The reaction mixture was incubated for 1 hour at 30°C, separated by SDS-PAGE and analyzed by autoradiography. For the dephosphorylation assays, Sf9 extract containing over-expressed PP2A holoenzyme (A, C and B α subunits) was prepared as described (Molloy et al., 1998). Five μ g CK2 phosphorylated GST-PACS-1MR were incubated for 30 minutes at 37°C with 5 μ l PP2A extract and in assay buffer (25 mM Tris pH 7.4, 0.2 mM MnCl₂, 0.2 mg/ml BSA and 1 mM DTT) in the presence or absence of 10 nM okadaic acid (Calbiochem). GST-PACS-1 MR proteins were separated by SDS-PAGE and analyzed by autoradiography.

Phosphoamino acid analysis

CK2 phosphorylated GST-MR, GST-MRS₂₇₈A and GST-MRS₂₇₈T were prepared as above except that recombinant CK2 α was used. ³²P-labeled proteins were separated by SDS-PAGE and either dried and exposed to X-ray film to observe protein

phosphorylation or transferred to PVDF membranes. The protein bands were excised, hydrolyzed in 6N HCl and analyzed by two-dimensional thin layer chromatography as previously described (Jones et al., 1995). Radioactive samples were visualized by phosphorimage analysis.

GST protein binding assays

One μg of GST, GST-MR, GST-MRS₂₇₈A, GST-MRS₂₇₈D or their CK2 phosphorylated forms was incubated with 1 μg of Trx-PACS-1FBR in 200 μl GST binding buffer (10 mM Tris pH 7.5, 200 mM NaCl, 1% NP40) at room temperature for 1 hr. Proteins bound to glutathione agarose were washed with GST-binding buffer and analyzed by western blot using anti-Trx mAb 46-0436 (Invitrogen). Furin competition assays were conducted as above with the addition of indicated amounts of Trx-furinS_{773,775}D or Trx alone to the binding reaction for one hr after a one hr pre-incubation. For the GST-Nef binding experiments, A7 cells were infected with VV expressing PACS-1, PACS-1S₂₇₈A or PACS-1S₂₇₈D (m.o.i. = 5) for 16 hours and lysed with GST-binding buffer. 2 μg of GST-Nef were incubated with this lysate. Bound epitope-tagged PACS-1 molecules were analyzed by western blot using the anti-HA mAb HA.11.

Immunofluorescence microscopy

Furin, MPR, TGN46, AP-1, mannosidase II, LBPA, and transferrin uptake– A7 cells grown to 80% confluency and infected with recombinant VV expressing either PACS-1, PACS-1S₂₇₈A or PACS-1S₂₇₈D alone (m.o.i. = 10), or co-infected with VV:fur/f expressing Flag-tagged furin (m.o.i. = 3) with each of the PACS-1 expressing VV

recombinants (m.o.i. =7, total m.o.i. = 10). Cells were fixed with 4% paraformaldehyde and processed for immunofluorescence as previously described (Blagoveshchenskaya et al., 2002; Crump et al., 2001). Primary antibodies to the FLAG tag (mAb M1, Kodak, 1:300), TGN46 (Serotech, 1:30), CI-MPR (from B. Hoflack, 1:200), AP-1 (mAb 100/3, Sigma, 1:50), LBPA (mAb 6C4, from J. Gruenberg, 1:10) mannosidase II (from K. Moremen, 1:200) were used to localize antigens. Iron-loaded rhodamine-transferrin (Molecular Probes) was used as described (Crump et al., 2001). Following incubation with fluorescently labeled secondary antisera, all images were captured using a 63x oil immersion objective on a Leica DM-RB microscope and processed with the Scion Image 1.62 program.

MHC-I and TGN-46– A7 cells grown to 80% confluency were infected with VV:WT, VV expressing HIV-1 Nef (m.o.i. = 10) or co-infected with VV expressing HIV-1 Nef (m.o.i. = 3) and either PACS-1, PACS-1S₂₇₈A or PACS-1S₂₇₈D (m.o.i. = 7, m.o.i. = 10 total) for 5 hr. Cells were then processed for immunofluorescence. Primary antibodies to MHC-I (mAb w6/32; 1:100) and TGN-46 (Serotech, 1:30) were incubated at 4 C overnight followed by incubation with fluorescently labeled species-specific secondary antibodies (Southern Biotech).

CD4 antibody uptake– A7 cells were infected with AV expressing 44Nef, or 44NefAla proteins for 24 hr (m.o.i. = 5) then infected with VV expressing PACS-1, PACS-1S₂₇₈A and PACS-1S₂₇₈D (m.o.i. = 10) for an additional 4 hr. The CD4 mAb Ab-2 (Labvision) was added to the media for 1 hr uptake and the cells were then washed and incubated in

the absence of antibody for an additional 30 min. The cells were fixed with 4% paraformaldehyde, permeabilized with Triton-X100 and stained with sheep anti-TGN46 (Serotech) followed by secondary mouse-FITC and sheep-TxRd antibodies.

***In vitro* transport assay**

The endosome-to-TGN transport assay is based on a previously published method but with several modifications (Itin et al., 1997). *Membrane preparation*– A7 cells were cultured in sulfate-free media (Sigma) for 24 hr, infected with AV expressing 44Nef-Y (m.o.i. = 2) for 16 hr, and then treated with 20 µg/ml cycloheximide for 4 hr. The cells were washed twice with cold PBS, scraped into PBS, pelleted and resuspended in 4 ml homogenization buffer (HB; 8.5 % sucrose (w/v) in 3 mM imidazole) containing protease inhibitors (Boehringer Mannheim). The cells were passed repeatedly (~10 times) through a 22g needle, post-nuclear supernatant (PNS) was collected, and sedimented over a 50% sucrose cushion (Beckman TLS 55, 45k rpm, 20 min). 500 µl of resuspended membranes were diluted to 2 ml H₂O, adjusted to 12.5 mM Hepes pH 7.0, 1 mM DTT, 1.5 mM MgOAc, 60 mM KCl and supplemented with 60 µl ATP regenerating system (100 mM ATP (pH 7.0), 800 mM creatine phosphate, 4 mg/ml creatine kinase), and 10 µl of 5 mM cold PAPS, followed by incubation for 15 min at RT. Membranes were then diluted to 4 ml of HB, re-sedimented on a 50% sucrose cushion and stored at -70°C.

Cytosol preparation– C6 control and AS19 PACS-1 antisense cells were grown to confluency and infected with VV expressing PACS-1, PACS-1 S₂₇₈A or PACS-1 S₂₇₈D (m.o.i = 5) for 24 hr. The cells were washed, sedimented and resuspended in 1 ml of

cytosol buffer (100 mM KCl, 8.5% sucrose w/v, 1 mM MgCl₂, 20 mM Hepes (pH 7.4)). The resuspended cells were passed through a 22g needle and the post-nuclear supernatant was clarified (Beckman TLA100.3, 45k rpm, 30 min). The cytosol layer (lower) was collected and stored at -70°C.

In vitro re-sulfation assay– A 200 µl reaction containing cytosol (1mg/ml), donor membrane, an ATP regenerating system and ³⁵S-PAPS (NEN, 20uCi/assay) was incubated at 37°C for one hr. The membranes were solubilized in IP buffer (20 mM Tris pH 7.4, 200mM NaCl, 1% NP40) and the 44Nef-Y- chimera was immunoprecipitated with anti CD4 mAb Ab-4 (Calbiochem) at 4°C. Immune complexes were collected with protein G sepharose, separated by SDS-PAGE, analyzed by autoradiography for ³⁵S incorporation and western blotted for 44Nef-Y protein load.

Acknowledgments

We thank D. Litchfield (University of Western Ontario), J. Gruenberg (University of Geneva), B. Hoflack (Pasteur Institute), K. Moremen (University of Georgia), S. Pfeffer (Stanford University) and D. Trono (University of Geneva) for their generous gifts of reagents and advice. We thank A. Blagoveshchenskaya (Vollum Institute) for the affinity purified PACS-1 antiserum, D. Brickey (Vollum Institute) for help with phosphoamino acid analysis and members of the Thomas lab for helpful discussions. This work was supported by NIH grants DK37274, AI49793 and AI48585. C.M.C. is funded by a Prize Traveling Research Fellowship from the Wellcome Trust. F.G. is funded by the Human Frontiers of Science Program.

Figure Legends

Figure 1. PACS-1 Ser₂₇₈ is phosphorylated by CK2 and dephosphorylated by PP2A.

(A) Schematic diagram of PACS-1 showing the atrophin related region (ARR), the furin binding region (FBR) which interacts with cargo molecules and AP-1/AP-3 adaptor complexes, the middle region (MR) which contains the autoregulatory acidic cluster and Ser₂₇₈, and the C-terminal region (CTR). The acidic cluster in the PACS-1 MR as well as acidic cluster sequences contained in membrane cargo molecules, which bind to the PACS-1 FBR, are indicated. (B) *In vivo* phosphorylation of expressed PACS-1. BSC40 cells infected with VV recombinants expressing either epitope (HA)-tagged PACS-1 or PACS-1 S₂₇₈A were labeled with ³²P_i, and the immunoprecipitated PACS-1 proteins were separated by SDS-PAGE and analyzed by autoradiography (upper panel). A western blot using the anti-HA mAb HA.11 shows equal expression and loading of the two proteins (lower panel). (C) *In vitro* CK2 phosphorylation of GST-MR. GST-MR or GST-MRS₂₇₈A was incubated with CK2 and [γ -³²P]ATP, separated by SDS-PAGE and analyzed by autoradiography. (D) PACS-1 MR is phosphorylated at amino acid 278. GST-MR or GST-MRS₂₇₈T was phosphorylated by CK2 with [γ -³²P]ATP, separated by SDS-PAGE, transferred to PVDF, acid hydrolyzed, and subjected to 2D thin layer chromatography. The position of phosphoserine (pS), phosphothreonine (pT) and phosphotyrosine (pY) standards are shown. (E) PP2A dephosphorylates GST-PACS-1 MR. *In vitro* CK2 phosphorylated ³²P-GST-MR was incubated without (control) or with recombinant PP2A in the presence or absence of 10 nM okadaic acid (OA), separated by SDS-PAGE and analyzed by autoradiography. (F) CK2 and PP2A regulate phosphorylation of endogenous PACS-1 *in vivo*. A7 cells were labeled with ³²P_i, treated

or not with either 100 μ M DRB or 20 nM OA, and endogenous PACS-1 was immunoprecipitated, separated by SDS-PAGE and analyzed by autoradiography. All autoradiography was quantified using NIH image 1.61 software. 32 P incorporation was normalized to PACS-1 protein loading and presented relative to control PACS-1 phosphorylation. Bar graphs represent the mean \pm SE of at least three separate experiments.

Figure 2. Phosphorylation of PACS-1 Ser₂₇₈ promotes PACS-1 binding to cargo proteins. (A) Phosphorylation of PACS-1 Ser₂₇₈ inhibits PACS-1 MR binding to the PACS-1 FBR. GST-MR, GST-MRS₂₇₈A, GST-MRS₂₇₈D, or CK2-phosphorylated GST-MR were incubated with Trx-PACS-1FBR and captured using glutathione agarose. Bound Trx-PACS-1FBR was analyzed by western blot (upper panel). Incomplete phosphorylation of GST-MR may explain the slightly greater binding of Trx-PACS-1FBR to CK2 phosphorylated GST-MR compared with GST-MRS₂₇₈D. (B) The PACS-1 MR acidic cluster competes with cargo proteins for binding to the PACS-1 FBR. GST-capture assays were performed as in (A), with the addition of varying concentrations of Trx-furinS_{773,775}D (Trx-furin S \rightarrow D) or Trx alone to the binding reaction. (C) Ser₂₇₈ regulates binding to cargo proteins. Epitope-(HA)-tagged PACS-1, PACS-1S₂₇₈A and PACS-1S₂₇₈D were expressed in replicate plates of A7 cells using VV recombinants. Cell lysates were incubated with GST-Nef and GST-Nef was captured using glutathione agarose. PACS-1 proteins bound to GST-Nef were analyzed by western blot using the anti-HA mAb HA.11 (top panel). GST-Nef input and expression of PACS-1 proteins is shown (lower panels). (D) Mutation of PACS-1 Ser₂₇₈ does not effect binding to AP-1.

Epitope-(HA)-tagged PACS-1, PACS-1_{S278A}, PACS-1_{S278D} or PACS-1Admut were expressed in A7 cells and immunoprecipitated with mAb HA.11. Precipitated proteins were separated by SDS-PAGE and analyzed by western blot using mAb 100/3 (AP-1) or mAb PACS-1. All data were quantified as described in the legend to Figure 1.

Figure 3. Phosphorylated PACS-1 directs endosome-to-TGN transport. (A) PACS-1_{S278A} expression disrupts the TGN localization of 44Nef. A7 cells were infected with recombinant virus expressing 44Nef as well as PACS-1, PACS-1_{S278A} or PACS-1_{S278D}. Localization of 44Nef was determined by CD4 antibody uptake. The cells were fixed, permeabilized and co-stained with the TGN marker anti-TGN46 followed by fluorescent secondary antisera. As a control, a mutant Nef reporter, 44NefAla, which does not bind PACS-1, was also expressed. (B) PACS-1 directs endosome-to-TGN sorting in a cell free assay. A7 cells were infected with AV expressing 44Nef-Y after which membranes from these cells were harvested and quenched with cold PAPS. The quenched membranes were incubated in the absence (background, bkg) or presence of cytosol from C6, (control), AS19 (PACS-1 antisense) or from AS19 cells expressing PACS-1 (AS19+PACS-1), PACS-1_{S278A} (AS19+_{S278A}) or PACS-1_{S278D} (AS19 +_{S278D}) and with the sulfate donor ³⁵S-PAPS. 44Nef-Y was immunoprecipitated and ³⁵S incorporation was determined by autoradiography, and protein load by western blot. ³⁵S incorporation was quantified using NIH image 1.61 software, normalized for protein load and presented relative to 44Nef-Y labeling with AS19 cytosol. Bar graph represents the mean ± SE of three separate experiments.

Figure 4. Expression of PACS-1 S₂₇₈A blocks HIV-1 Nef-mediated MHC-1 downregulation. A7 cells were infected with VV:WT or co-infected with VV recombinants expressing Nef and either PACS-1, PACS-1S₂₇₈A or PACS-1S₂₇₈D. Cells were fixed, permeabilized and incubated with anti MHC-I and anti-TGN46 followed by fluorescently labeled secondary antisera. The expression of PACS-1 alone has no effect on MHC-I localization (Blagoveshchenskaya et al., 2002 and data not shown). In many experiments PACS-1S₂₇₈D causes cargo proteins to show a more compact TGN staining pattern than that observed with controls, indicating this PACS-1 mutant is constitutively active.

Figure 5. Expression of PACS-1 S₂₇₈A disrupts furin and CI-MPR localization. (A) A7 cells were co-infected with VV co-expressing flag-tagged furin (fur/f) and PACS-1, PACS-1S₂₇₈A or PACS-1S₂₇₈D. The cells were fixed, permeabilized and incubated with anti-TGN46 and either M1 (fur/flag) or anti-CI-MPR followed by fluorescently labeled secondary antisera. **(B)** A7 cells infected with VV expressing PACS-1, PACS-1S₂₇₈A or PACS-1S₂₇₈D were fixed, permeabilized and stained with anti- γ -adaplin, anti-LBPA, anti-mannosidase II. A replicate plate of cells was incubated with rhodamine-transferrin prior to fixation.

Figure 6. A working model of the CK2/PP2A regulation of PACS-1 sorting activity. In the Ser₂₇₈ nonphosphorylated state, the PACS-1MR is bound to the PACS-1 FBR, thereby preventing cargo binding. This conformation is mimicked by PACS-1S₂₇₈A. CK2 phosphorylation of Ser₂₇₈ disrupts the PACS-1 MR-FBR interaction and permits binding

of cargo molecules to the FBR. This conformation is mimicked by PACS-1S₂₇₈D. In addition, CK2 phosphorylation of cargo proteins increases their affinity for activated PACS-1 and thus their association with AP-1 (Crump et al., 2001; Teuchert et al., 1999). Inactivation of PACS-1 sorting activity is achieved by PP2A-catalyzed dephosphorylation of Ser₂₇₈, which promotes binding of the PACS-1 MR and FBR regions. Whether the MR and FBR domains interact intramolecularly as depicted or intermolecularly remains to be determined.

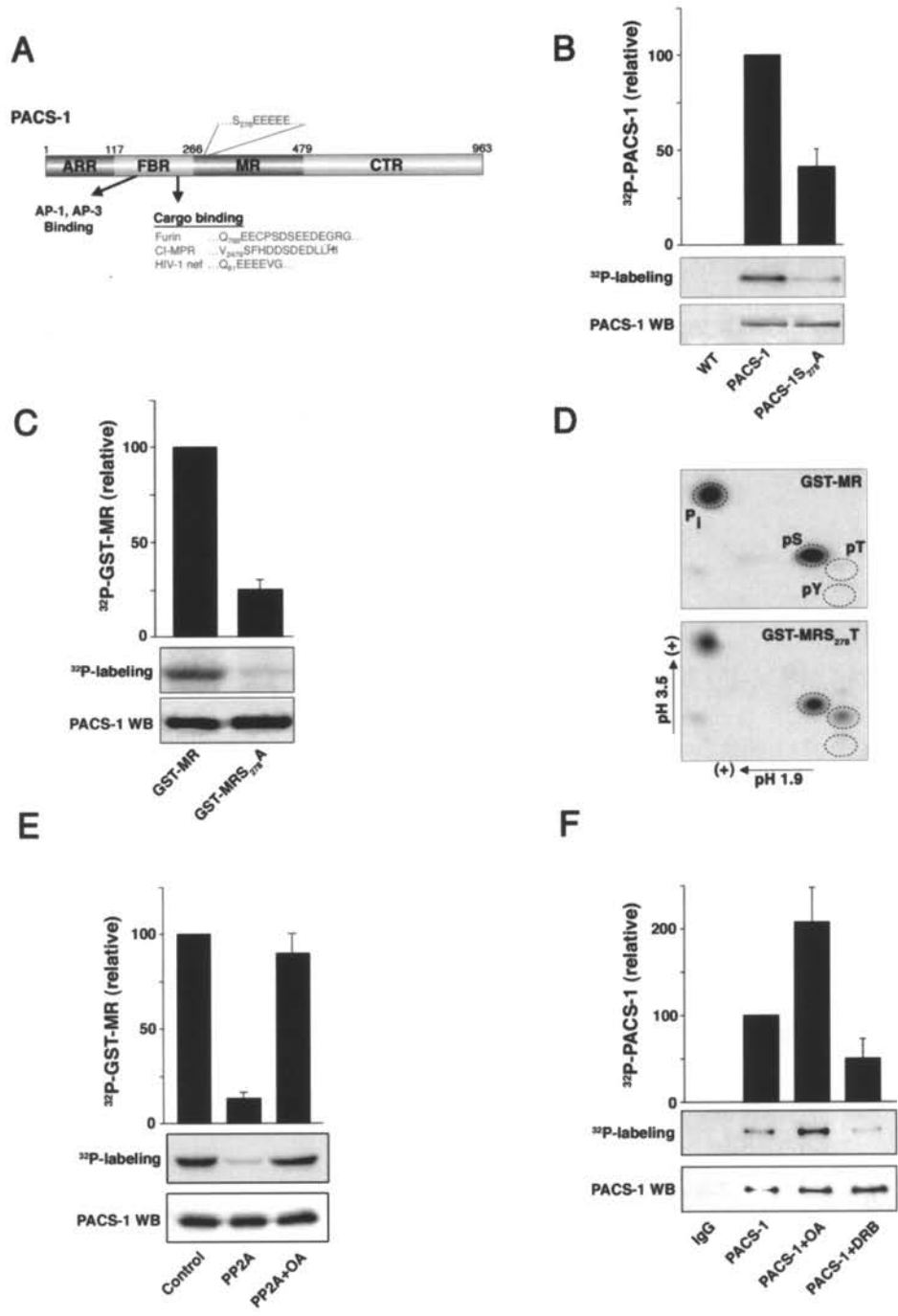


Figure 1

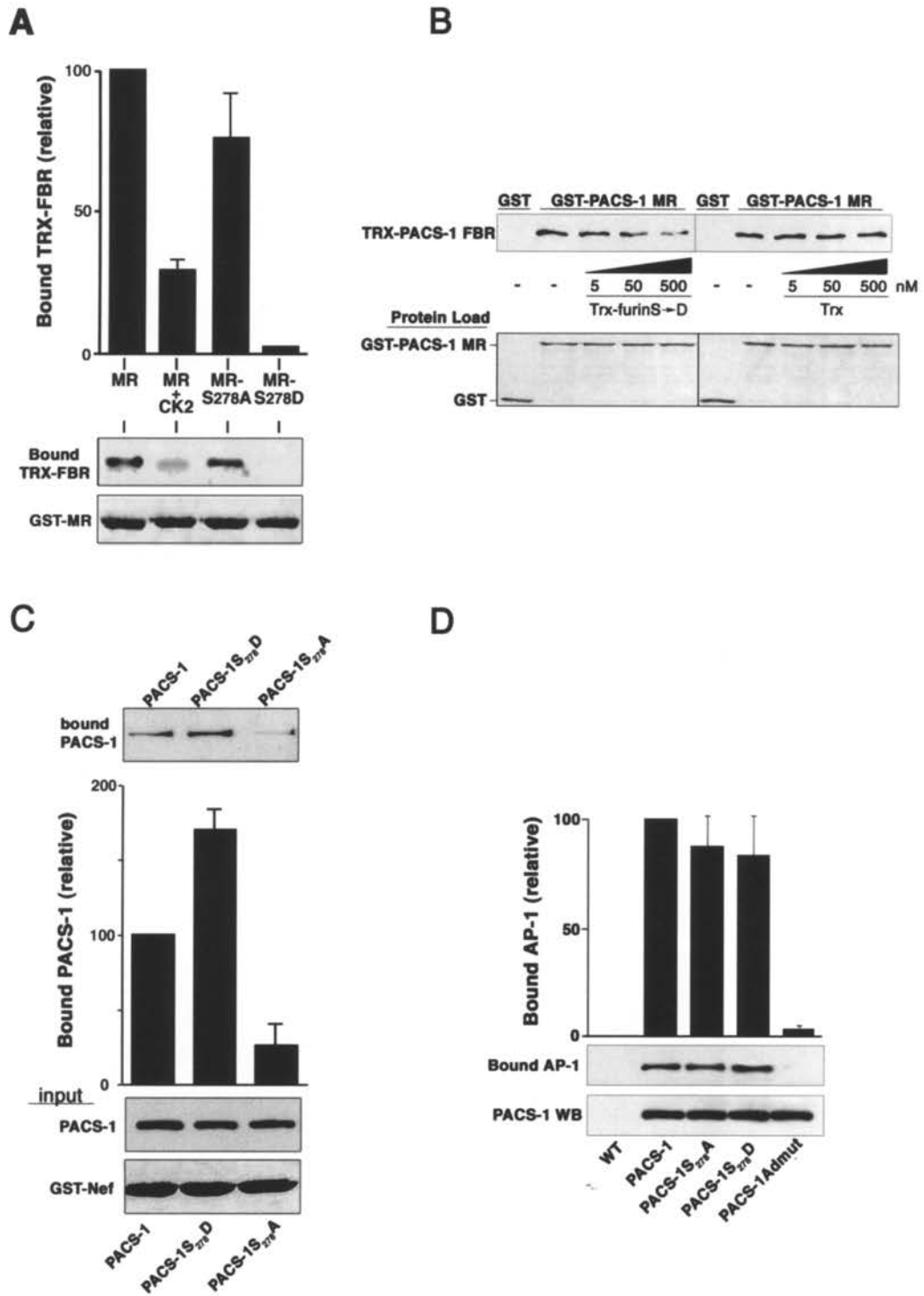


Figure 2

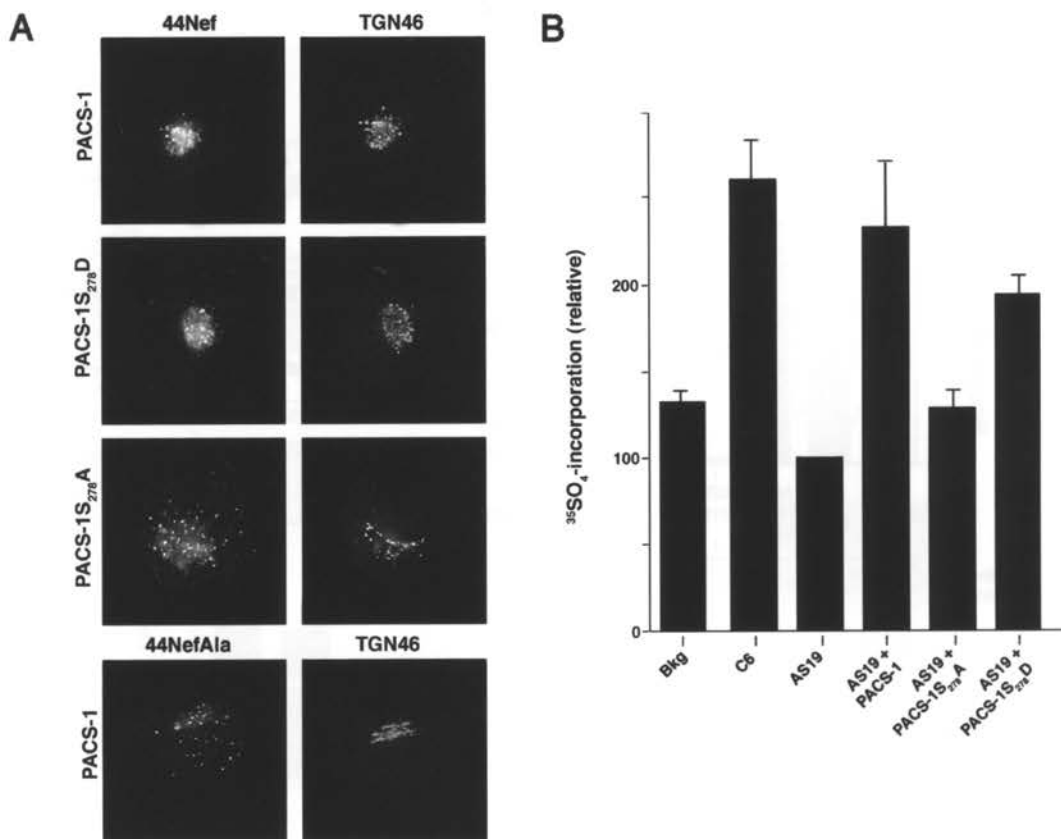


Figure 3

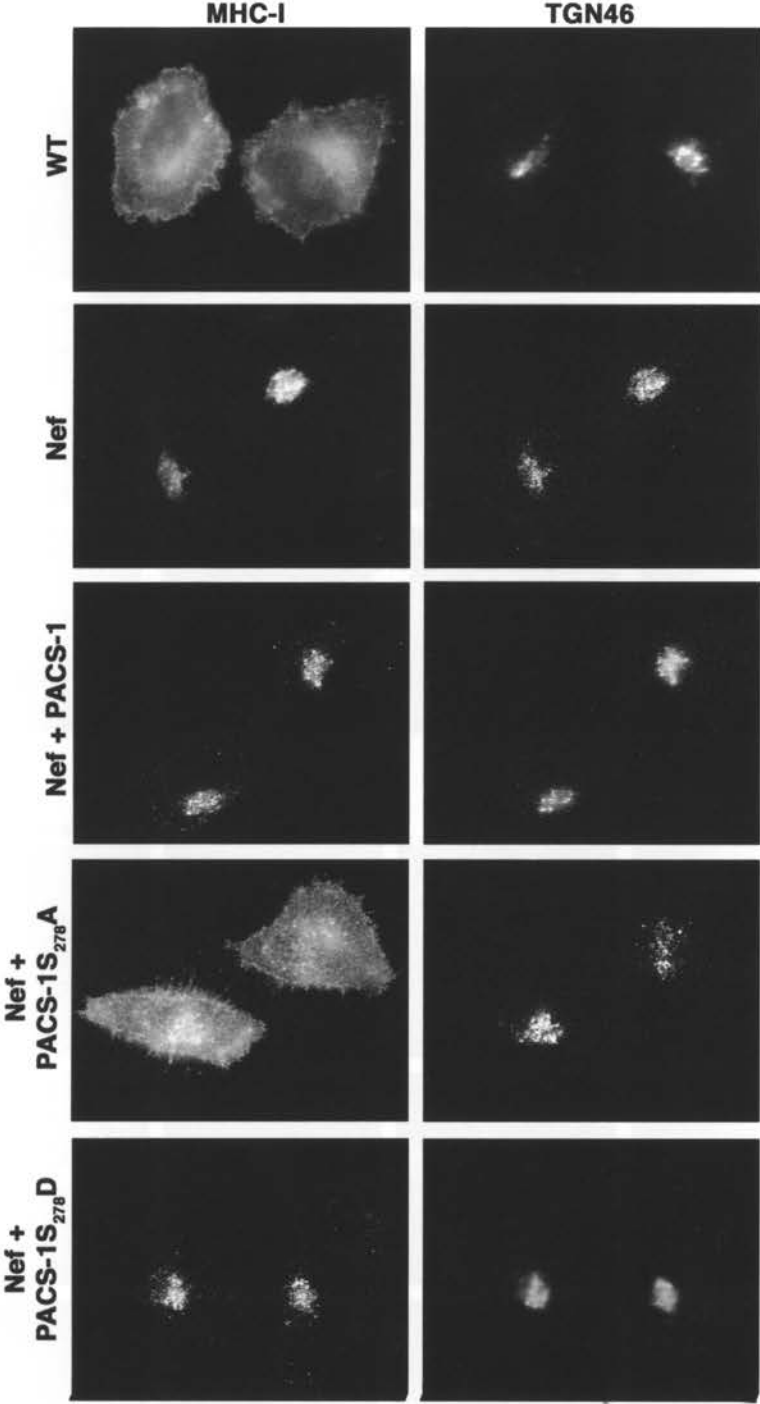


Figure 4

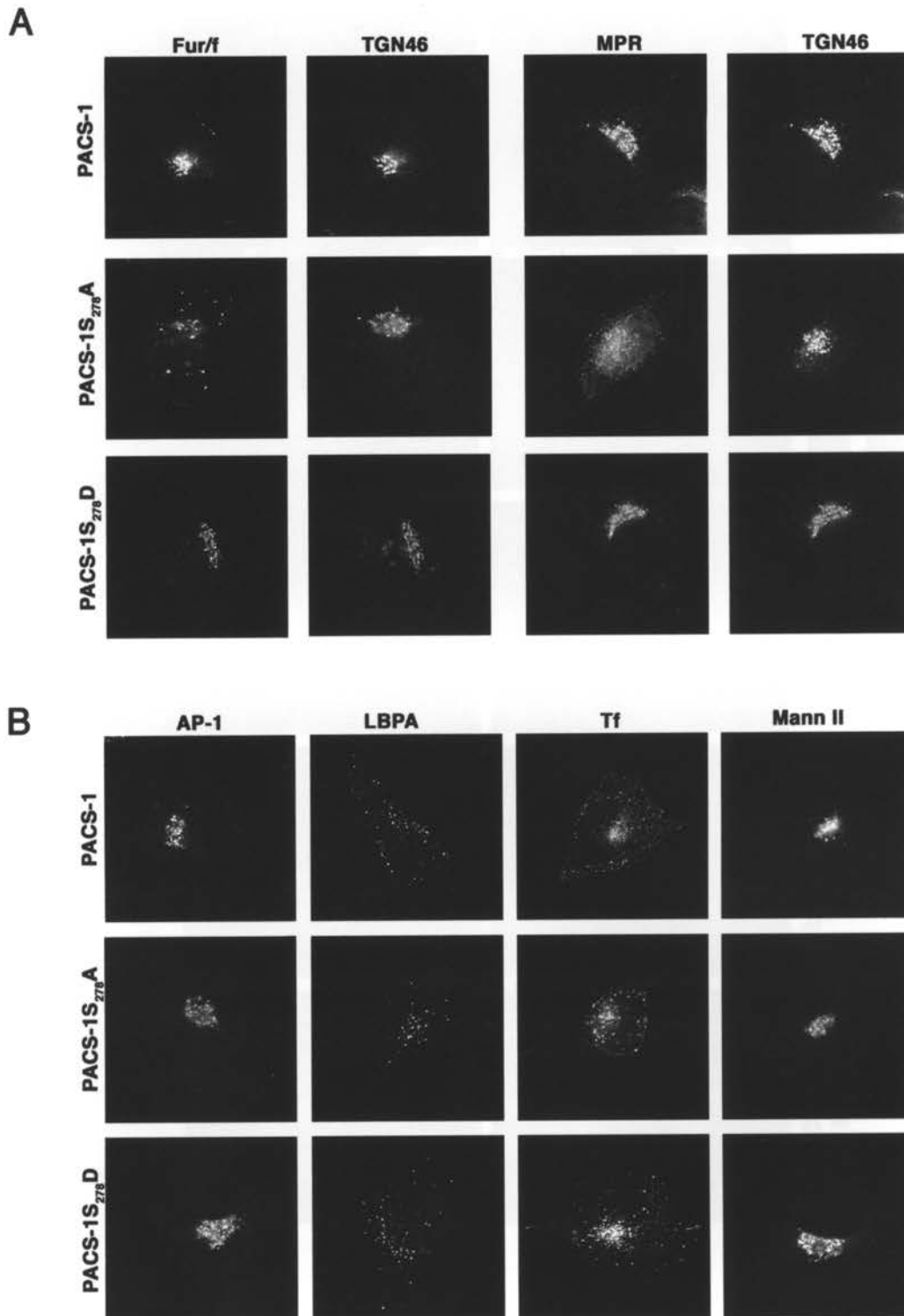


Figure 5

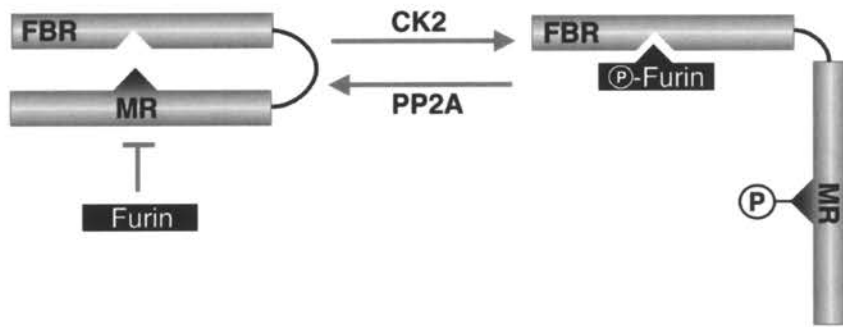


Figure 6

CHAPTER 3

A PACS-1, GGA3 AND CK2 COMPLEX REGULATES CI-MPR TRAFFICKING

GREGORY K. SCOTT, HAO FEI¹, LAUREL THOMAS, GURUPRASAD R. MEDIGESHI² AND GARY THOMAS³

Vollum Institute, L-474, 3181 SW Sam Jackson Park Road, Portland, Oregon 97239 USA

Current Address: ¹Department of Psychiatry and Biobehavioral Sciences, UCLA, Los Angeles, California 90095. ²Department of Molecular Microbiology and Immunology, OHSU, Portland, Oregon.

³Corresponding author
Tel: (503) 494-6955
Fax: (503) 494-1218
e-mail: thomasg@ohsu.edu

Submitted for publication

In this chapter, Hao Fei performed experiments in Figures 1D, 1E, 1F; Guruprasad Medigeshi performed experiments in Figures 3D and 3E; I performed experiments in Figures 1C, 1H, 4, 5, 6d and 6E. Hao Fei and I performed experiments in Figure 1G. Laurel Thomas and I performed experiments in Figures 2, 6A and 6B.

Abstract

The cation-independent mannose-6-phosphate receptor (CI-MPR) follows a highly regulated sorting itinerary to deliver hydrolases from the *trans*-Golgi network (TGN) to lysosomes. Cycling of CI-MPR between the TGN and early endosomes is mediated by GGA3, which directs TGN export, and PACS-1, which directs endosome-to-TGN retrieval. Despite executing opposing sorting steps, GGA3 and PACS-1 bind to an overlapping CI-MPR trafficking motif and their sorting activity is controlled by the CK2 phosphorylation of their respective autoregulatory domains. But how CK2 coordinates these opposing roles is unknown. We report a CK2-activated phosphorylation cascade controlling PACS-1- and GGA3-mediated CI-MPR sorting. PACS-1 links GGA3 to CK2, forming a multimeric complex required for CI-MPR sorting. PACS-1-bound CK2 stimulates GGA3 phosphorylation, releasing GGA3 from CI-MPR and early endosomes. Bound CK2 also phosphorylates PACS-1Ser₂₇₈, promoting binding of PACS-1 to CI-MPR to retrieve the receptor to the TGN. Our results identify a CK2-controlled cascade regulating hydrolase trafficking and sorting of itinerant proteins in the TGN/endosomal system.

Key Words: PACS-1/GGA3/CK2/CI-MPR/endosome

Introduction

The localization and trafficking of itinerant membrane cargo proteins within the *trans*-Golgi network (TGN)/endosomal system relies upon canonical sorting motifs within their cytosolic domains, which are recognized by components of the vesicular trafficking machinery (Robinson, 2004). These motifs include tyrosine (YXX ϕ) and dileucine ([D/E]xxxL[L/I]) based signals, which bind to the heterotetrameric adaptors (APs), acidic-dileucine (DxxLL) based motifs, which bind to GGAs and acidic cluster based motifs, which bind to PACS proteins. The cytosolic domain of one membrane protein, the cation-independent mannose-6-phosphate receptor (CI-MPR), requires motifs that bind to each of these three groups of sorting molecules to localize to the TGN and to efficiently sort cathepsin D to lysosomes (Chen et al., 1997a; Ghosh et al., 2003b; Meyer et al., 2000; Puertollano et al., 2001b; Wan et al., 1998). The GGAs sort the CI-MPR into clathrin-coated vesicles at the TGN and may also mediate CI-MPR trafficking between endosomal compartments (Doray et al., 2002c; Mattera et al., 2003; Puertollano and Bonifacino, 2004). By contrast, PACS-1 and AP-1, which mediate endosome-to-TGN retrieval, are required to localize CI-MPR to the TGN (Crump et al., 2001; Meyer et al., 2000; Wan et al., 1998). In addition, other sorting molecules including TIP47, Retromer, and EpsinR also function in the endosome-to-TGN retrieval of CI-MPR (Arighi et al., 2004; Diaz and Pfeffer, 1998; Saint-Pol et al., 2004; Seaman, 2004), supporting the highly regulated and complex trafficking pathway followed by this multifunctional receptor.

We identified PACS-1 through its binding to the protein kinase CK2 (CK2) phosphorylated acidic cluster (...EECPpSDpSEEDE...) on the furin cytosolic domain (Fig. 1A and (Wan et al., 1998). The 140 amino acid PACS-1 cargo binding region (FBR, Fig. 1A) contains an 8-amino acid segment ETELQLTF₁₇₅ that binds AP-1, and is required for correct subcellular localization of furin and CI-MPR to the TGN (Crump et al., 2001). PACS-1 also binds to acidic cluster motifs on several additional itinerant cellular proteins (Thomas 2002), including proprotein convertase 6B (Xiang et al., 2000), polycystin-2 (Köttgen et al., 2005) and VAMP4 (Hinners et al., 2003), as well as the viral proteins HCMV gB (Crump et al., 2003) and HIV-1 Nef (Piguet et al., 2000). Studies using interfering mutant-, siRNA- and antisense-based methods show PACS-1 is required for the TGN localization of each of these proteins, suggesting a broad role for PACS-1 in cellular homeostasis and disease.

Similar to furin, binding of PACS-1 to the CI-MPR cytosolic domain (CI-MPR_{CD}) requires the CK2 phosphorylatable acidic cluster ...DDpSDEDLLHI, located at the CI-MPR_{CD} C-terminus (Wan et al., 1998). Interestingly, the three GGA family members (1-3) also bind to this phosphorylated motif on the CI-MPR_{CD} but require the dileucine motif for binding, which furin lacks (Puertollano et al., 2001a). The GGAs contain three principal domains including the VHS domain, which binds to cargo proteins, the GAT domain, which binds to ARF1, a hinge segment, which binds clathrin and contains an autoregulatory acidic-dileucine motif (GGA1 and 3 only), and the GAE domain, which binds to several accessory proteins (Fig. 1B and Bonifacino, 2004). Through these interactions, the GGAs function as monomeric clathrin adaptors that link itinerant cargo

directly to clathrin (Puertollano et al., 2001b). However, why GGAs and PACS-1 share overlapping binding sites on the CI-MPR_{CD} is not known.

The functional similarities shared by PACS-1 and GGAs extend to regulation of their cargo binding. The sorting activity of PACS-1 is regulated by the CK2- and PP2A-controlled phosphorylation of an autoregulatory domain (Scott et al., 2003). Phosphorylation of PACS-1Ser₂₇₈ within the PACS-1 autoregulatory domain activates cargo binding and is required for the endosome-to-TGN transport of furin, CI-MPR and HIV-1 Nef. Similar to PACS-1, GGA1 and GGA3 binding to cargo proteins is regulated by CK2 phosphorylation of an autoregulatory domain within the GGA1 and GGA3 hinge segment (Doray et al., 2002b; Ghosh and Kornfeld, 2003a). Phosphorylation of GGA1Ser₃₅₅ (which corresponds to GGA3Ser₃₈₈, see Fig. 1B) within the GGA1 autoregulatory domain inhibits binding to CI-MPR. Therefore, CK2 phosphorylation of the PACS-1 autoregulatory domain *promotes* cargo binding (Scott et al., 2003), whereas CK2 phosphorylation of GGA1 or 3 autoregulatory domains *inhibits* cargo binding (Doray et al., 2002b).

CK2 is a ubiquitous protein kinase with more than 300 putative polypeptide substrates and is a heterotetramer composed of two catalytic subunits ($\alpha\alpha$, $\alpha\alpha'$, or $\alpha'\alpha'$) and two regulatory β subunits (Meggio and Pinna, 2003). The regulation of this basally active kinase has long remained enigmatic, though the binding of the regulatory β subunit to polyamines or substrate proteins can increase kinase activity 3-fold (Litchfield, 2003). The requirement for CK2 phosphorylation for the regulation of PACS-1, GGA1 and

GGA3 action led us to determine how this kinase may control the PACS-1 and GGA3-mediated trafficking of CI-MPR. We report that PACS-1 binds to GGA3 and recruits CK2, forming a multimeric complex, which regulates PACS-1/GGA3-mediated sorting of CI-MPR between the TGN and early endosomes. Together our results describe a novel cellular mechanism for the phospho-regulation of membrane protein traffic through the TGN/endosomal system.

Results

PACS-1 binds to GGA3

Despite regulating opposing CI-MPR trafficking steps, PACS-1 and GGAs share several biochemical functions. These include binding to the CI-MPR_{CD} at a C-terminal acidic cluster and the regulation of their binding to membrane cargo by the CK2 phosphorylation of an autoregulatory domain (Doray et al., 2002b ;Puertollano et al., 2001a; Scott et al., 2003; Wan et al., 1998). These common properties led us to ask if GGA3 and PACS-1 associate *in vivo*. Accordingly, we immunoprecipitated PACS-1 from rat brain cytosol (RBC) and found that GGA3 co-precipitated with PACS-1 (Fig. 1C). To determine if PACS-1 bound directly to GGA3 and to identify the GGA3 binding region of PACS-1, we used glutathione-S-transferase (GST)-tagged PACS-1 fusion proteins corresponding to predicted domains of PACS-1 (Fig. 1A) to capture Thioredoxin (Trx)-tagged GGA3_{VHS+GAT} (Fig. 1D). Only GST-PACS-1_{FBR}, which binds to cargo including CI-MPR_{CD}, was able to precipitate Trx-GGA3_{VHS+GAT}. Reciprocal mapping experiments using purified GST-GGA3 constructs (Fig. 1B) showed that the GGA3 VHS domain, which binds the CI-MPR_{CD}, was sufficient to bind Trx-PACS-1_{FBR} (Fig. 1E). These results demonstrate a direct interaction between PACS-1 and GGA3 through their cargo binding regions.

To further define the GGA3 binding site on the PACS-1 FBR, we took advantage of a PACS-1 homologue, PACS-2, an ER/mitochondria trafficking protein that does not bind to GGA3 (Simmen et al., 2005). Through the FBR, PACS-1 and PACS-2 are 75% identical and 83% homologous. Serial mutation of non-homologous amino acids was

used to identify residues in the PACS-1 FBR required for binding GGA3. Using this approach, we found that mutation of PACS-1 FBR residues K₂₄₉IY to the corresponding PACS-2 residues (W₁₇₁IA; hereafter PACS-1 FBR-GGAmut) disrupted GGA3 binding (Fig. 1F). Because the PACS-1 FBR also binds AP-1 and CI-MPR, we tested whether the K₂₄₉Y₂₅₁ → WA substitution interfered with binding to these molecules (Fig. 1G). Protein binding studies showed that the K₂₄₉Y₂₅₁ → WA substitution had no effect on GST-PACS-1_{FBR} binding to purified AP-1 or Trx-tagged CI-MPR_{CD}. Therefore, we introduced the K₂₄₉Y₂₅₁ → WA mutation into full-length PACS-1 (hereafter PACS-1_{GGAmut}), and compared the ability of hemagglutinin (HA)-tagged PACS-1 and HA-PACS-1_{GGAmut} to co-immunoprecipitate co-expressed myc-GGA3 (Fig. 1H). In agreement with our *in vitro* binding studies, we found that myc-GGA3 co-immunoprecipitated with HA-PACS-1, but not with HA-PACS-1_{GGAmut}. Thus, we identified a PACS-1 mutant that does not bind GGA3 and whose binding to cargo proteins or AP-1 is unaffected.

Blocking the PACS-1/GGA3 interaction disrupts CI-MPR and GGA3 localization

We expressed PACS-1_{GGAmut} in cells to determine if PACS-1 binding to GGA3 is required for the steady state localization of their mutual cargo protein: CI-MPR. In control cells or PACS-1-expressing cells, CI-MPR demonstrated a paranuclear staining pattern that overlapped with TGN46 (Fig. 2A). However, in PACS-1_{GGAmut}-expressing cells, CI-MPR showed a pronounced redistribution to an endosomal population that overlapped with the early endosomal marker EEA1. As a control, we asked whether PACS-1_{GGAmut} disrupted the localization of furin, which requires PACS-1 for endosome-to-TGN retrieval (Wan et al., 1998), but lacks the canonical D/ExxLL GGA-binding motif (Fig. 2B). We found that

expression of PACS-1 or PACS-1_{GGAmut} failed to affect the TGN localization of FLAG-furin, suggesting that PACS-1_{GGAmut} selectively disrupts the trafficking of itinerant cargo that depend on binding to both PACS-1 and GGAs. Because GGA3 distributes between the TGN and early endosomes (Puertollano and Bonifacino, 2004), we also examined the localization of GGA3 in PACS-1_{GGAmut}-expressing cells (Fig. 2C). We found that expression of PACS-1_{GGAmut}, but not PACS-1, caused a striking redistribution of GGA3 from a paranuclear localization to a dispersed endosome population that overlapped with the redistributed CI-MPR. In addition, we tested the effect of an interfering mutant PACS-1 molecule, PACS-1_{Admut}, which fails to bind AP-1 and redistributes the CI-MPR and furin from the TGN (Crump et al., 2001), on the localization of GGA3. We observed no effect of PACS-1_{Admut} expression on the localization of GGA3 (Fig. 2C), suggesting that the redistribution of GGA3 to endosomal compartments induced by PACS-1_{GGAmut} expression results from the inability of PACS-1_{GGAmut} to interact with GGA3. These findings suggest the PACS-1/GGA3 interaction is required for CI-MPR retrieval and for release of GGA3 from endosomal membranes.

PACS-1 is required for CI-MPR function

To better understand how PACS-1 and GGA3 might cooperate to direct trafficking of CI-MPR, we conducted protein-protein binding assays to define the PACS-1 binding site on the CI-MPR_{CD}. Previously, we found that truncation of the last ten amino acids (...DDpS₂₄₈₄DEDLLHI) of the CI-MPR_{CD}, which contain a CK2 phosphorylatable acidic cluster and constitutes a DxxLL GGA-binding motif, abolished binding to the FBR region of PACS-1 (Wan et al., 1998). We used a GST-pull down strategy to determine

which CI-MPR_{CD} residues mediate direct binding to the PACS-1 FBR. First, we sought to determine if, similar to the interaction of PACS-1 and furin (Wan et al., 1998), as well as the CI-MPR with GGA3 (Kato et al., 2002), phosphorylation of CI-MPR Ser₂₄₈₄ would enhance binding to the PACS-1 FBR (Fig. 3A). We tested the binding of Trx-PACS-1_{FBR} to GST-CI-MPR_{CD} phosphorylated by CK2 or to GST-CI-MPR_{CD} mutants containing a phosphomimic Ser₂₄₈₄→Asp or non-phosphorylatable Ser₂₄₈₄→Ala substitution. We found that both pre-incubation of GST-CI-MPR_{CD} with CK2 and the Ser₂₄₈₄→Asp substitution enhanced binding to Trx-PACS-1_{FBR}, indicating that like other PACS-1 cargo proteins, CK2 phosphorylation of Ser₂₄₈₄ within the CI-MPR acidic cluster enhanced binding to PACS-1. Next, we conducted an alanine scan of each of the acidic residues from Asp₂₄₈₂ to Asp₂₄₈₇ and found that alanine mutation of any of the acidic residues reduced binding to Trx-PACS-1_{FBR} (Fig. 3B). Finally, we found that Leu₂₄₈₈→Ala and Leu₂₄₈₉→Ala mutations had no effect on Trx-PACS-1_{FBR} binding whereas these mutations completely blocked Trx-GGA3_{VHS-GAT} binding, as previously reported (Fig. 3C and (Puertollano et al., 2001a). Thus, PACS-1 and GGA3 share overlapping but not identical CI-MPR binding sites.

The importance of CI-MPR Asp₂₄₈₅, which is required for GGA binding and sorting of lysosomal enzymes (Chen et al, 1997a; Puertollano et al., 2001a), for binding to PACS-1, as well as the requirement of PACS-1 for the TGN localization of CI-MPR (Simmen et al., 2005; Wan et al., 1998), led us to determine if PACS-1 is required for CI-MPR function. Therefore, we investigated the effect of PACS-1 depletion on the sorting of lysosomal enzymes by CI-MPR. The sorting and maturation of cathepsin D, a ligand of

CI-MPR, to lysosomes was followed in metabolically labeled cells. The intracellular (C) and extracellular (E) forms of cathepsin D were immunoprecipitated from both the cells and medium after pulse-chase in the presence of mannose-6-phosphate. We found that siRNA depletion of PACS-1 (Fig. 3D), which redistributes CI-MPR from the TGN (Simmen et al., 2005), caused an ~20% increase in secreted cathepsin D and a corresponding ~20% decrease in intracellular cathepsin D compared to control cells (Fig. 3E). As a positive control, and in agreement with previous studies (Meyer et al., 2000), we found that siRNA depletion of the μ 1A subunit of AP-1 caused ~50% of the newly synthesized procathepsin D to be released into the culture medium. Additionally, we observed no change in the half-life of CI-MPR in PACS-1-depleted cells (data not shown), indicating that this increased secretion of cathepsin D does not result from decreased CI-MPR stability.

PACS-1 binds to and activates CK2

The overlapping PACS-1 and GGA3 binding sites on CI-MPR, as well as the requirement for binding of PACS-1 to GGA3 to control the TGN localization of CI-MPR, suggested that the interaction between PACS-1, GGA3 and CI-MPR is tightly regulated. One clue to the underlying mechanism controlling the PACS-1/GGA3-dependent sorting of CI-MPR is the prominent role CK2 phosphorylation plays in the regulation of each protein (Doray et al., 2002b; Scott et al., 2003). Although earlier studies demonstrated that an AP-1-associated CK2 activity could phosphorylate GGA1 (Doray et al., 2002c), we speculated that a more direct association of CK2 with PACS-1 and GGA3 might afford greater signaling efficacy. Accordingly, we immunoprecipitated PACS-1 from RBC and

assayed the bound material for co-precipitating CK2 activity (Fig. 4A). We observed a ~14 fold increase in PACS-1-associated CK2 activity compared to the control, which was blocked by the CK2-specific inhibitor TBB, but not the PKA inhibitor PKI. To identify the region of PACS-1 that associates with CK2, we used GST-PACS-1 segments (see Fig. 1A) to capture CK2 α from RBC (Fig. 4B). Similar to our analysis of GGA3 binding (Fig. 1), we found that CK2 α was captured solely by GST-PACS-1_{FBR}. We more precisely identified PACS-1 FBR residues required for CK2 binding by testing a battery of GST-PACS-1_{FBR} truncations and substitutions for their ability to capture CK2 α from RBC (Fig. 4C). We found a 18-amino acid segment of the PACS-1 FBR between L₁₉₄ and A₂₁₂ was required to capture CK2 α (Fig. 4D). Next, we conducted an alanine scan of this PACS-1 segment and found that an R₁₉₆RKRY \rightarrow AAAAA substitution (hereafter called PACS-1_{FBR-CKmut}) blocked CK2 α association with GST-PACS-1_{FBR} whereas alanine substitution of adjacent 5-amino acid segments, including K₂₀₁NRTI \rightarrow AAAAA and L₂₀₆GYKT \rightarrow AAAAA, did not. As a control, we observed no difference between the binding of GST-PACS-1_{FBR} or GST-PACS-1_{FBR-CKmut} to purified AP-1, Trx-CI-MPR_{CD}, or Trx-GGA3_{VHS+GAT} (Fig. 4E). Thus, PACS-1 associates with CK2 *in vivo* and the PACS-1 FBR-CKmut substitution specifically blocks the CK2/PACS-1 interaction.

To determine which CK2 subunit associates with PACS-1, we conducted a yeast-two-hybrid analysis (Fig. 5A). We found that yeast expressing PACS-1 FBR and CK2 β , but not CK2 α or CK2 α' , supported growth under histidine selection. Moreover, co-transformation of PACS-1_{FBR-CKmut} with CK2 β failed to support cell growth, further indicating that PACS-1 R₁₉₆RKRY is required for the interaction between the PACS-1

FBR and CK2 β . To determine if the PACS-1 FBR binds directly to CK2 β we conducted a protein-protein binding assay, and found that Trx-CK2 β bound directly to GST-PACS-1_{FBR} but not GST-PACS-1_{FBR-CKmut} (Fig. 5B). Finally, to confirm the effect of the CKmut substitution in the context of full-length PACS-1, we expressed full-length HA-PACS-1 or HA-PACS-1_{CKmut} in cells, immunoprecipitated the PACS-1 proteins and examined co-precipitating endogenous CK2 α and β by western blot (Fig. 5C). In agreement with the *in vitro* protein capture studies, we found that HA-PACS-1, but not HA-PACS-1_{CKmut}, co-precipitated CK2.

One characteristic property of CK2 is the 3-fold activation observed upon binding of polycationic molecules or proteins containing clusters of basic amino acids to a patch of acidic residues in the regulatory β subunit (Bonnet et al., 1996; Leroy et al., 1997). As the R₁₉₆RKRY cluster of basic amino acids in the PACS-1 FBR is required for binding to CK2 β , we tested the effect of PACS-1 on CK2 activity levels using an *in vitro* kinase assay. Purified bovine CK2 holoenzyme was pre-incubated with increasing concentrations of GST, GST-PACS-1_{FBR} or GST-PACS-1_{FBR-CKmut}, and CK2 activity was scored as incorporation of ³²P into a peptide substrate (Fig. 5D). GST-PACS-1_{FBR} stimulated CK2 activity ~2.5 fold, whereas GST or GST-PACS-1_{FBR-CKmut} had a lesser (~0.5 fold) effect on CK2 activity. Thus, PACS-1 FBR binding stimulates the activity of the CK2 holoenzyme.

We previously determined that CK2 phosphorylation of Ser₂₇₈ within the PACS-1 autoregulatory domain activates cargo binding and accounts for ~50% of the incorporated

phosphate on PACS-1 (Scott et al., 2003). Thus, our finding that PACS-1 bound and activated CK2 suggested that this interaction may be critical for regulating the phosphorylation state of PACS-1. To test this possibility, we metabolically labeled replicate plates of cells expressing full-length HA-PACS-1, HA-PACS-1_{CKmut} or HA-PACS-1_{S278A} with ³²P_i, and quantified the amount of radiolabel incorporated into each protein (Fig. 5E). We observed ~40% less ³²P incorporation into HA-PACS-1_{CKmut} compared to HA-PACS-1, whereas HA-PACS-1_{S278A} exhibited ~60% less ³²P incorporation compared to HA-PACS-1. This indicated that the PACS-1/CK2 interaction is required for efficient PACS-1 phosphorylation, but does not reduce PACS-1 phosphorylation to the level observed by Ser₂₇₈→Ala substitution. Therefore, to gauge whether the CKmut substitution affects PACS-1 Ser₂₇₈ phosphorylation, we examined the ³²P incorporation into a PACS-1_{S278A/CKmut} double mutant. We predicted that if CK2 that is bound to PACS-1 phosphorylates only Ser₂₇₈, then PACS-1_{S278A/CKmut} would exhibit equal ³²P incorporation compared to PACS-1_{S278A}. Conversely, if CK2 bound to PACS-1 primarily phosphorylates residues other than Ser₂₇₈, then PACS-1_{S278A/CKmut} would incorporate less ³²P than PACS-1_{S278A}. We observed no difference between the ³²P incorporation of HA-PACS-1_{S278A} and HA-PACS-1_{S278A/CKmut}, suggesting that CK2 binding to PACS-1 is required for efficient phosphorylation of Ser₂₇₈ and thus the ability of PACS-1 to bind cargo.

PACS-1-bound CK2 inactivates GGA3 to retrieve CI-MPR to the TGN

The inhibitory effects of the CKmut substitution suggested that PACS-1_{CKmut} may interfere with the PACS-1-dependent sorting of membrane cargo. To test this possibility,

we expressed PACS-1_{CKmut} in cells and determined any effect on the TGN localization of CI-MPR and furin. Similar to PACS-1_{GGAmut}, PACS-1_{CKmut} caused CI-MPR to redistribute to an EEA1-positive compartment (Fig. 6A). We also found that PACS-1_{CKmut} caused furin to redistribute from the TGN, suggesting that PACS-1 binding to CK2 is required for the sorting of all PACS-1 cargo (Fig. 6B). To determine whether PACS-1_{CKmut} blocked PACS-1-dependent trafficking solely because this mutant cannot bind CK2 to phosphorylate Ser₂₇₈, we expressed a double mutant, PACS-1_{S278D/CKmut} in cells (Fig. 6A). We previously showed that the phosphomimic construct PACS-1_{S278D} had no effect on PACS-1-dependent sorting when expressed in cells, and could rescue the disruption of endosome-to-TGN trafficking caused by depletion of PACS-1 in a cell-free assay (Scott et al., 2003). Therefore, based on our determination that CK2 bound to PACS-1 is required for efficient phosphorylation of Ser₂₇₈ (Fig. 5), we predicted that the PACS-1_{S278D/CKmut} double mutant would override the disruption of CI-MPR localization caused by PACS-1_{CKmut}. Accordingly, we found that expression of PACS-1_{S278D/CKmut} had no effect on the localization of CI-MPR (Fig. 6A). Together, these results suggest that PACS-1 recruits CK2 and activates the kinase to promote cargo binding by phosphorylating Ser₂₇₈ in the PACS-1 autoregulatory domain.

The ability of PACS-1_{CKmut} and PACS-1_{GGAmut} to redistribute CI-MPR to EEA1-positive endosomes suggested that, as for PACS-1_{GGAmut}, PACS-1_{CKmut} might disrupt the steady-state localization of GGA3. Accordingly, we found that PACS-1_{CKmut} caused GGA3 to redistribute with CI-MPR to an endosome population (Fig. 6C). Because CK2 phosphorylation of GGA3 blocks cargo binding (Doray et al., 2002b), we next asked

whether the ability of PACS-1 to bind GGA3 may affect the efficiency of GGA3 phosphorylation by CK2. Therefore, we metabolically labeled cells expressing HA-PACS-1 or HA-PACS-1_{CKmut} with $^{32}\text{P}_i$ and quantified the amount of immunoprecipitated, ^{32}P -labeled, endogenous GGA3 (Fig. 6D). We found that HA-PACS-1 expression increased the amount of ^{32}P -GGA3 whereas expression of HA-PACS-1_{CKmut} reduced by ~45% the amount of ^{32}P -GGA3. These results suggest that PACS-1 recruits CK2 to GGA3, enabling CK2 to phosphorylate and inactivate the binding of GGA3 to CI-MPR. To further test this possibility, we determined whether PACS-1 could form a ternary complex with GGA3 and CK2 β *in vitro* and found that GST-GGA3_{VHS+GAT} could capture Trx-CK2 β only in the presence of Trx-PACS-1_{FBR} (Fig. 6E). Together, our results suggest PACS-1 recruits CK2 to phosphorylate both PACS-1 and GGA3, thereby inactivating GGA3 and activating PACS-1, thus causing PACS-1 to bind CI-MPR and direct its retrieval to the TGN.

Discussion

The results presented here show that PACS-1, GGA3 and CK2 form a multimeric complex to regulate the endosomal sorting and TGN retrieval of CI-MPR. We found that PACS-1 FBR binds directly to the cargo-binding VHS domain of GGA3 (Fig. 1). Substitution of PACS-1 residues K₂₄₉Y₂₅₁ (PACS-1_{GGAmut}) blocked binding of PACS-1 to GGA3, but had no effect on adaptor, cargo protein or CK2 binding (Fig. 1). Likewise, mutation of the R₁₉₆RKRY basic amino acid cluster (PACS-1_{CKmut}), blocked binding of PACS-1 to CK2 β , but did not affect cargo, adaptor or GGA3 binding (Figs. 4 and 5). Expression of PACS-1_{GGAmut} or PACS-1_{CKmut} caused the redistribution of the CI-MPR and GGA3 from the TGN to an early endosomal compartment (Figs. 2 and 6). However, only PACS-1_{CKmut} disrupted TGN localization of furin (Fig. 6), suggesting that the interaction of PACS-1 with GGA3 is specifically required for the trafficking of a subset of cargo proteins that bind to both PACS-1 and GGAs. Furthermore, binding of PACS-1 to CK2 β stimulated CK2 activity (Fig. 5), and was required for the phosphorylation of both PACS-1_{Ser278} and GGA3, which forms a ternary complex with PACS-1 and CK2 β (Figs. 5 and 6). Considering the known requirement for CK2 phosphorylation to regulate cargo binding of PACS-1 and GGA3 (Doray et al., 2002b; Scott et al., 2003), one interpretation of these findings is that PACS-1 directs CK2 to GGA3 to initiate the retrieval of CI-MPR from endosomes to the TGN as depicted in the model shown in Figure 7.

Previously, we and others reported that CI-MPR requires an acidic cluster/PACS-1 dependent retrieval step to localize to the TGN (Wan et al., 1998), and function for lysosomal enzyme sorting (Chen et al., 1997a). Here we refine the CI-MPR residues

required for PACS-1 binding to include phosphorylation of Ser₂₄₈₄ as well as the presence of surrounding acidic residues, but not LL₂₄₈₉ required for GGA3 binding (Fig. 3 and (Puertollano et al., 2001a). Thus, PACS-1 and GGA3 bind to overlapping but distinct motifs on the CI-MPR. In addition, siRNA depletion of PACS-1 disrupted maturation and lysosomal delivery of cathepsin D, but had no effect on CI-MPR stability. These results differ from those observed with depletion of the retromer subunit Vps26 (Arighi et al., 2004) or TIP47 (Diaz and Pfeffer, 1998), molecules that function in retrieving CI-MPR from Hrs-coated maturing endosomal intermediates or late endosomes, respectively, to the TGN and whose depletion results in a dramatic reduction of CI-MPR half-life. This suggests that PACS-1 functions upstream of or in a separate pathway from retromer and TIP47 for sorting CI-MPR. Interestingly, the cytosolic domain of sortilin, which also sorts lysosomal cargo, binds to GGAs (Lefrancois et al., 2003; Nielsen et al., 2001) and PACS-1 (our unpublished data), and contains a cluster of acidic residues nearly identical to that found on the CI-MPR. Thus, the mechanism described here for control of CI-MPR trafficking may be common to other acidic-dileucine containing receptors. Possibly, the interaction of PACS-1 with CK2 and GGA3 prolongs movement of CI-MPR through endosomes, representing a timing mechanism to aid ligand uncoupling before retrieval of the receptor to the TGN. Alternatively, PACS-1 and GGA3 may combine to retrieve non-ligated CI-MPR to the TGN whereas ligated receptor would continue to the prelysosomal compartment to release cargo to lysosomes and then be retrieved to the TGN by a retromer- or TIP47-based pathway. The association of PACS-1 and GGA3 with non-ligated receptor in early endosomes may explain why depletion of PACS-1 or AP-1 has no effect on CI-MPR stability whereas disruption of retromer or TIP47 decreases the CI-

MPR half-life (Arighi et al., 2004; Diaz and Pfeffer, 1998; Meyer et al., 2000; Seaman, 2004).

Our observation that the R₁₉₆RKRY polybasic segment is required for PACS-1 to bind and activate CK2 *in vitro* and *in vivo* (Figs. 4 and 5) provides a mechanism for localizing this kinase to phosphorylate regulatory sites on PACS-1 and GGA3. In particular, our demonstration that blocking CK2 β binding to PACS-1 prevented activation of the CK2 holoenzyme, caused a 40% decrease in PACS-1 phosphorylation (Fig. 5), and disrupted the TGN localization of CI-MPR, furin and GGA3 (Fig. 6), suggests that localization of CK2 to PACS-1 is required for activation of PACS-1 cargo binding. Exactly how PACS-1 stimulates CK2 activity remains unknown, but may occur in a similar way as spermine or FGF-2, which are proposed to bind the acidic groove of CK2 β , causing a conformational change in the CK2 holoenzyme that correlates with an increase in CK2 activity (Bonnet et al., 1996; Leroy et al., 1997; Leroy et al., 1995). Additionally, our finding that PACS-1, GGA3 and CK2 β form a ternary complex *in vitro* (Fig. 6), and that expression of PACS-1_{CKmut} disrupted the phosphorylation and localization of GGA3 suggests that CK2 controls GGA3 phosphorylation through an interaction with PACS-1.

The redistribution of CI-MPR we observed with expression of PACS-1_{GGAmut} or PACS-1_{CKmut} (Fig. 6) is similar to our findings in cells lacking PACS-1 (Simmen et al., 2005; Wan et al., 1998), or expressing interfering mutant PACS-1 molecules that cannot bind cargo or AP-1 (Crump et al., 2001; Scott et al., 2003), and further support the role of PACS-1 in the endosome-to-TGN retrieval step of acidic cluster containing cargo

proteins as determined using a cell-free assay (Scott et al., 2003). Notably, the redistributed steady-state concentration of CI-MPR and GGA3 from the TGN to an EEA1-positive compartment we observed with expression of PACS-1_{GGAmut} or PACS-1_{CKmut} is reminiscent of that observed with overexpression of Rabaptin5, which shifts the localization of endogenous GGA1 and CI-MPR to enlarged early endosomes (Mattera et al., 2003). However, expression of PACS-1_{Admut}, which does not bind AP-1, caused the redistribution of the CI-MPR from the TGN (Crump et al., 2001), but had no effect on GGA3 localization (Fig. 2), suggesting a temporal ordering of molecular interactions such that PACS-1 is required downstream of GGA3 in the endosomal sorting of CI-MPR and also recruits AP-1 to retrieve this itinerant receptor to the TGN (see Fig. 7). These results suggest that PACS-1 must bind GGA3 for GGA3 to release from an early endosome compartment and that PACS-1 does not utilize GGA3 as a clathrin adaptor, rather AP-1 or -3 must also be present (Crump et al., 2001). We do not know how the block of PACS-1 binding to GGA3 traps GGA3 in this endosomal compartment, but it is possible that PACS-1 is required to receive the CI-MPR from GGA3 before GGA3 can release from this compartment, or perhaps PACS-1 affects the ability of GGA3 to interact with the early endosomal membrane, possibly by directing CK2 phosphorylation.

Several reports have now identified phosphorylation sites on the GGAs (Doray et al., 2002b; Kametaka et al., 2005; McKay and Kahn, 2004), including two CK2 sites thought to regulate GGA3 function: Ser₃₅₅ of GGA1 (which corresponds to Ser₃₈₈ in GGA3) and Ser₃₇₂ of GGA3. Phosphorylation of GGA1 Ser₃₅₅ promotes an intramolecular interaction of the GGA DxxLL autoregulatory domain with the cargo binding VHS domain (Doray

et al., 2002b), resulting in a conformational change that correlates with an inhibition of CI-MPR binding (Ghosh and Kornfeld, 2003a). CK2 phosphorylation of GGA3 Ser₃₇₂ is required for EGF stimulated phosphorylation of GGA3 Ser₃₆₈ by an unidentified kinase, which causes a conformational change in GGA3 that correlates with reduced association with membranes (Kametaka et al., 2005). Our finding that expression of PACS-1 interfering mutants that cannot bind GGA3 or CK2, respectively, shifted the steady state distribution of GGA3 with CI-MPR from the TGN to an EEA1-positive compartment (Figs. 2 and 6) may represent the manifold effect of phosphorylation of GGA3 Ser₂₇₂ and Ser₃₈₈ on binding to cargo and membranes. Whether phosphorylation of PACS-1 at sites in addition to Ser₂₇₈ control cargo and membrane association warrant further investigation. Nonetheless, our results suggest that a CK2-initiated phosphorylation cascade controls a novel cellular mechanism for regulating the dynamic movement of membrane protein traffic through the TGN/endosomal system.

Materials and methods

Cell lines and recombinant virus

A7 cells were cultured as previously described (Wan et al., 1998b). Viral recombinants were constructed using standard methods (Blagoveshchenskaya et al., 2002). Vaccinia virus (VV) recombinants expressing human HA-PACS-1, HA-PACS-1_{Admut}, and HA-PACS-1_{S278A} were previously described (Crump et al., 2001; Scott et al., 2003). VV recombinants expressing HA-PACS-1_{CKmut} and HA-PACS-1_{GGAmut} were made by replacing the mutation from pGEX-PACS-1_{FBR-CKmut} or pGEX-PACS-1_{FBR-GGAmut} plasmid into pZVneo PACS-1ha. VV recombinants expressing HA-PACS-1_{S278A/CKmut}, and HA-PACS-1_{S278D/CKmut} were made by subcloning the S_{278A} or S_{278D} mutations into pZVneo HA-PACS-1_{CKmut}. Adenovirus (AV) recombinants expressing human HA-PACS-1, HA-PACS-1_{GGAmut} or myc-GGA3 (long form) were previously described (Blagoveshchenskaya et al., 2002) or subcloned into pADtet7 HA-PACS-1 from pGEX-PACS-1_{FBR-GGAmut} or pCR3.1 GGA3 and constructed using standard methods (Blagoveshchenskaya et al., 2002).

DNA constructs

pGEX3x plasmids expressing PACS-1 segments ARR, FBR, MR, and CTR, the PACS-1 *FBR truncations* $\Delta 1$, $\Delta 2$, $\Delta 4$, $\Delta 5$, $\Delta 6$, and pET32-PACS-1_{FBR} expressing His/thioredoxin (Trx)-fusion proteins were previously described (Crump et al., 2001). PACS-1 FBR mutants $\Delta 3$, K₂₀₁5A, L₂₀₆5A, GGAmut and CKmut, GST-CI-MPR_{CD} mutants and pVP16 PACS-1_{FBR-CKmut} were generated by standard PCR methods and subcloned into pGEX3x or pVP16. pET32-CK2 β was constructed by subcloning CK2 β from pGEX3x-CK2 β .

pGEX3x-CK2 β , pGBT9-CK2 α , pGBT9-CK2 α' and pGBT9-CK2 β were provided by D. Litchfield. PCR3.1GGA3 as well as pGEX constructs expressing the VHS, VHS+GAT, and Hinge+GAE domains of GGA3 were provided by J. Bonifacino. pET32-GGA3_{VHS+GAT} was subcloned from pGEX3xGGA3_{VHS+GAT} using standard techniques. pVP16-PACS-1_{FBR} and pGEX3xCI-MPR_{CD} were previously described (Wan et al., 1998).

Yeast-two-hybrid

HF7c yeast were transformed with pVP16-PACS-1_{FBR} as well as pGBT9-CK2 α , pGBT9-CK2 α' or pGBT9-CK2 β then grown on media lacking histidine supplemented with 1 mM 3-aminotriazole according to standard methods (Clontech).

Protein purification

pGEX or pET32-Trx vectors were transformed into BL21 (DE3) pLysS cells (Novagen). GST- or Trx-fusion proteins were purified using glutathione sepharose (Amersham-Pharmacia) or Ni-NTA-agarose (Qiagen), respectively, according to the manufacturer's protocol. Purified porcine AP-1 was provided by S. Tooze. Native CK2 was purified from bovine testicles as described (Litchfield et al., 1990).

Metabolic labeling

A7 cells were infected with VV expressing HA-tagged PACS-1 proteins (m.o.i. =3) for 16 hours, washed and incubated with phosphate-free media for 1 hr after which 0.5 mCi/ml ³²P_i (NEN) was added for 2 hrs. The labeled cells were washed with PBS and lysed in labeling buffer (PBS with 1% TX-100, 50 mM NaF, 80 mM β -glycerol

phosphate and 0.1 μ M orthovanadate). HA-PACS-1 proteins were immunoprecipitated with mAb HA.11 (Covance), separated by SDS-PAGE and analyzed by autoradiography. To label endogenous GGA3, A7 cells were infected with VV expressing HA-PACS-1 proteins (m.o.i. =10) for 4 hr, processed as above, and endogenous GGA3 was immunoprecipitated from the cell lysate using mAb GGA3 (BD #612311), separated by SDS-PAGE and GGA3 phosphorylation determined by autoradiography.

Co-immunoprecipitation

Endogenous PACS-1 was immunoprecipitated using affinity purified rabbit PACS-1 antibody 701 from RBC prepared as described (Simmen et al., 2005). The immunoprecipitates were analyzed by western blot with mAb GGA3 (BD). For *co-immunoprecipitation of expressed proteins*, HA-PACS-1 was immunoprecipitated with mAb HA.11 (Covance), and co-immunoprecipitating proteins analyzed by western blot with anti-myc mAb 9E10 (Santa Cruz), anti-CK2 β mAb (Abcam), or anti-CK2 α (Upstate).

Cathepsin sorting

A7 cells were treated twice with siRNAs specific for PACS-1 (CUCAGUGGUCAUCGCUGUG), μ 1A (AAGGCAUCAAGUAUCGGAAGA) or a control siRNA as described (Simmen et al., 2005). Protein expression was determined by western blot using anti-PACS-1, anti- μ 1A Adaptin (provided by L. Traub), and anti-tubulin (Sigma). Cathepsin D pulse-chase analysis was performed as described (Meyer et al., 2000). Briefly, siRNA treated cells were labeled with 35 S-Met/Cys (NEN) for 0.5 hr,

then chased with fresh medium containing excess methionine and 10 mM M6P for 4 hr. Cathepsin D was immunoprecipitated from the media and cell extract using anti-cathepsin D (DAKO), separated by SDS-PAGE and detected by fluorography.

Kinase assays

Endogenous PACS-1 was immunoprecipitated from RBC using affinity purified rabbit anti-PACS-1 701, washed twice with PBS and once with kinase buffer (20 mM MOPS, pH 7.2, 25 mM β -glycerol phosphate, 5mM EGTA, 1mM sodium orthovanadate and 1mM DTT). Kinase assays were performed with 200 μ M CK2 substrate (RRRDDDSDDD), 100 μ M ATP, 15 mM $MgCl_2$ and 5 μ Ci γ - ^{32}P -ATP in the absence or presence of 40 nM 4,5,6,7-tetrabromo-2-azabenzimidazole (TBB; provided by L. Pinna) or 400 nM PKI (Upstate). Reactions were incubated for 10 min at 30°C, stopped with trichloroacetic acid, spotted on to P81 paper, washed with 0.75 % phosphoric acid, and counted. Kinase assays to determine the activation level of CK2 were performed as above using 40 ng native bovine CK2 and increasing amounts of GST, GST-PACS-1_{FBR} or GST-PACS-1_{FBR-CKmut}.

GST protein binding assays

Lysate interactions. 3 μ g of each purified PACS-1 fragment was incubated with 500 μ l RBC for 2 hr at 4°C, followed by incubation with glutathione agarose for 30 min. Glutathione beads were pelleted, washed with *In vitro* binding buffer (25 mM HEPES pH 7.2, 250 mM KCl, 2.5 mM MgOAc) +100mM NaCl and analyzed by western blot with anti-CK2 α (Upstate).

Direct interactions. 1 μ g of Trx-CK2 β or Trx-CI-MPR_{CD} was incubated with 3 μ g of GST, GST-PACS-1_{FBR}, GST-PACS-1_{FBR-GGAmut} or GST-PACS-1_{FBR-CKmut} in GST-binding buffer (20mM Tris pH 7.5, 200 mM NaCl, 1% NP40) for 2 hr at RT, followed by incubation with glutathione agarose for 30 min. Glutathione beads were pelleted, washed twice with GST-binding buffer, once with mRIPA and analyzed by western blot with mAb anti-Trx antibody (Invitrogen). GST-PACS-1 pulldown of purified AP-1 was performed as described (Crump et al., 2001).

Ternary complex. 3 μ g GST-GGA3_{VHS+GAT} was preincubated with 3 μ g Trx-PACS-1_{FBR} for 2 hr at RT, followed by the addition of 3 μ g Trx-CK2 β for 2 hr at RT, then glutathione agarose for 30 min. Glutathione beads were pelleted by centrifugation, washed with GST-binding buffer, and analyzed by western blotting with anti-Trx mAb.

Immunofluorescence microscopy

A7 cells grown to 80% confluency were infected with VV expressing PACS-1, PACS-1_{GGAmut}, PACS-1_{CKmut}, PACS-1_{Admut} or PACS-1_{S278D/CKmut} (m.o.i. = 10) or transfected with pCDNA FLAG-furin. Cells were fixed and processed for immunofluorescence as previously described (Crump et al., 2001). Primary antibodies to the CI-MPR (S. Pfeiffer, 1:2), GGA3 (BD, 1:50), EEA1 (BD, 1:100), FLAG tag (mAb M1, Kodak, 1:300) and TGN46 (Abcam, 1:100) were used to localize antigens. Following incubation with species- and subtype-specific fluorescently labeled secondary antisera (Molecular Probes), images were captured using a 60x oil immersion objective on an Olympus Fluo-

View FV300 confocal laser scanning microscope and processed with the NIH Image J program or a 63x oil immersion objective on a Leica DM-RB microscope and processed with the scion image 1.62 program. CI-MPR, Flag-furin and GGA3 redistribution was quantified morphometrically by comparing the staining area and pixel intensity of these molecules for each construct/marker pair (n = 25), relative to the corresponding TGN stain (TGN46), according to the following formula: $(\text{Mean pixel intensity})_O \cdot \text{Area}_O / (\text{Mean pixel intensity})_T \cdot \text{Area}_T$, where O= outside the TGN and T= whole cell. Background was set to the spurious signal intensity observed in the nuclear area. Quantification of immunofluorescence images was done using NIH Image J. Values for each morphometric analysis are provided in the respective figure legend.

Acknowledgments

We thank Q. Justmann for preliminary experiments and members of the Thomas lab, J. Bonifacino and S. Kaech Petrie (CROET Imaging Center) for helpful discussions. We thank J. Bonifacino, D. Litchfield , S. Tooze, S. Pfeffer, L. Pinna and L. Traub for reagents. The authors declare no financial conflict of interest with the described work. This work was supported by NIH grants AI49793 and DK37274 (to GT).

Figure Legends

Figure 1. PACS-1 binds to GGA3. (A) Diagram of PACS-1 showing the atropin-1-related region (ARR), cargo binding region (FBR), which interacts with cargo and AP-1/AP-3 adaptor complexes (Crump et al., 2001; Wan et al., 19998), the middle region (MR), which contains the autoregulatory acidic cluster and Ser₂₇₈ (Scott et al., 2003), and the C-terminal region (CTR) as well as GST-PACS-1 fusion proteins and PACS-1 cargo. (B) Diagram of GGA3 showing the VHS (Vps27, Hrs, Stam) domain, which binds to cargo proteins, the GAT (GGA and TOM) domain, which binds to ARF1, the hinge segment, which contains the autoregulatory acidic-dileucine motif and Ser₃₈₈, and the GAE (γ -adaplin ear) domain (Bonifacino, 2004a) as well as GST-GGA3 fusion proteins and cargo. (C) Endogenous PACS-1 was immunoprecipitated from RBC (lower panel) using anti-PACS-1 or control IgG and co-precipitating GGA3 analyzed by 8% SDS-PAGE and western blot (upper panel). The immunoprecipitated PACS-1 is shown by western blot (bottom panel). ~0.1% of the GGA3 input co-precipitated with PACS-1. The GGA3 doublet may represent differential phosphorylation or the GGA3 long and short isoforms (Dell'Angelica et al., 2000). (D-G) The indicated GST-fusion proteins were incubated with the indicated Trx-fusion proteins or with purified AP-1, isolated with glutathione sepharose and analyzed by western blot using anti-Trx or anti- γ -adaplin antibody (upper panels). Input of each GST-protein is also shown (lower panel). The Trx-PACS-1_{FBR} band is shifted lower in (E) because Trx-PACS-1_{FBR} migrates at the same size as GST-GGA3_{VHS}. GST-GGA3_{VHS-GAT} captured ~1% of Trx-PACS-1_{FBR} input, and GST-PACS-1_{FBR} captured ~1%, 0.5% and 1% of the Trx-GGA3_{VHS-GAT}, γ -adaplin and Trx-CI-MPR_{CD} input, respectively. (H) A7 cells infected with wild type (WT) adenovirus (AV)

or AV expressing Myc-GGA3, Myc-GGA3 and HA-PACS-1, or Myc-GGA3 and HA-PACS-1_{GGAmut} were harvested and HA-tagged proteins immunoprecipitated and co-precipitating myc-GGA analyzed by western blot (upper panel). Lower panels show myc-GGA3 and HA-PACS-1 expression.

Figure 2. PACS-1_{GGAmut} disrupts CI-MPR trafficking. (A) A7 cells infected with WT vaccinia virus (VV) or VV recombinants expressing PACS-1 or PACS-1_{GGAmut} were stained with antibodies to detect CI-MPR, TGN46 or EEA1 as indicated. Inset: colocalization of CI-MPR (green) and EEA1 (red) from the boxed area. CI-MPR staining outside the TGN area increased from $11\pm 5\%$ and $9\pm 7\%$ in the WT and PACS-1 expressing cells, respectively, to $40\pm 10\%$ for PACS-1_{GGAmut} expressing cells. (B) A7 cells expressing FLAG-furin were treated as in (A) and stained with anti-FLAG and anti-TGN46. (C) A7 cells infected with VV:WT or with VV expressing PACS-1, PACS-1_{Admut} or PACS-1_{GGAmut} and then co-stained with anti-GGA3 and anti-TGN46 or anti-CI-MPR. Inset: Colocalization of GGA3 (green) and CI-MPR (red) from the boxed area. GGA3 staining outside the TGN area increased from $11\pm 6\%$, $8\pm 4\%$ and $9\pm 5\%$ in the WT, PACS-1 and PACS-1_{Admut} expressing cells, respectively, to $38\pm 7\%$ for PACS-1_{GGAmut} expressing cells. Scale Bars = 20 μm .

Figure 3. PACS-1 is required for CI-MPR function. (A-C) GST, GST-CI-MPR_{CD} pre-incubated or not with CK2, or GST-CI-MPR_{CD} containing the indicated mutations was incubated with Trx-PACS-1_{FBR} or Trx-GGA3_{VHS+GAT}, isolated with glutathione sepharose and analyzed by western blot using anti-Trx (upper panels). Input of each GST-protein is

shown (lower panel). GST-CI-MPR_{CD} pulled down ~1% of the Trx-PACS-1_{FBR}. **(D)** A7 cells were treated with scrambled (scr.), PACS-1 or AP-1 μ 1A subunit siRNAs and cell lysates analyzed by western blot using anti-PACS-1, anti- μ 1A or anti-tubulin. **(E)** A7 cells were treated with the indicated siRNA and Cathepsin D pulse chase experiments performed. Extracellular (E) and intracellular (C) fractions were immunoprecipitated with anti-cathepsin D and analyzed by fluorography. Precursor (P), intermediate (I) and mature (M) forms of cathepsin D are shown (lower panel). The graph shows the % of total cathepsin D forms (precursor + intermediate + mature) in cell extracts or secreted into the culture medium. Error bars represent mean and SD of three independent experiments.

Figure 4. PACS-1 associates with CK2. **(A)** RBC was incubated with affinity purified anti-PACS-1 or control IgG to immunoprecipitate endogenous PACS-1 and co-precipitating CK2 activity was measured with an *in vitro* kinase assay in the absence or presence of 40 μ M TBB (CK2 inhibitor) or 400 μ M PKI (PKA inhibitor). Error bars represent mean and SD of three independent experiments. **(B-D)** GST-fusion proteins containing the indicated domains, truncations, or alanine substitutions of PACS-1 (see Fig. 1A and panel D) were incubated with RBC, captured with glutathione sepharose and analyzed by western blot using anti-CK2 α (panel B and D, upper panel). Input of each GST-protein is also shown (panel B and D, lower panel). GST-PACS-1_{FBR} captured ~3% of the input CK2 α . Relative to GST-PACS-1_{FBR}, the interaction of CK2 with GST- Δ 2 and GST- Δ 6 was reduced 60% and 75%, respectively (n=3). **(E)** GST, GST-PACS-1_{FBR} or GST-PACS-1_{FBR-CKmut} was incubated with Trx-GGA3_{VHS+GAT}, Trx-CI-MPR_{CD} or purified

AP-1, captured with glutathione sepharose and analyzed by western blot using anti-Trx or anti- γ -Adaptin antibody (upper panels). Input of each GST-protein is shown (lower panel).

Figure 5. PACS-1 binding to CK2 β activates CK2. (A) Yeast transformed with the indicated Gal4 activation and DNA binding domain (Gal4ad and Gal4bd) constructs were screened for growth on His⁺ and His⁻ media. (B) GST, GST-PACS-1_{FBR} or GST-PACS-1_{FBR-CKmut} was incubated with Trx-CK2 β , isolated with glutathione sepharose and analyzed by western blot using anti-Trx (upper panel). Input of each GST-protein is shown (lower panel). GST-PACS-1_{FBR} captured 2.5% of the input Trx-CK2 β . (C) A7 cells infected with VV:WT or VV expressing HA-PACS-1 or HA-PACS-1_{CKmut} were lysed, immunoprecipitated with HA antibody and any co-immunoprecipitating CK2 α and CK2 β detected by western blot using subunit-specific antisera (upper panels). HA-PACS-1 expression is shown (bottom panel). ~0.5% of the endogenous CK2 α and CK2 β co-precipitated with expressed HA-PACS-1, respectively. (D) *In vitro* CK2 holoenzyme activity assayed in the absence or presence of purified GST, GST-PACS-1_{FBR} or GST-PACS-1_{FBR-CKmut}. Activity is normalized to a parallel sample assayed in the absence of added protein. Error bars represent mean and SD of three independent experiments. (E) A7 cells were infected with VV:WT or VV expressing HA-PACS-1, HA-PACS-1_{CKmut}, HA-PACS-1_{S278A} or HA-PACS-1_{S278A/CKmut} and metabolically labeled with ³²P_i. HA-proteins were immunoprecipitated with mAb HA.11, resolved by SDS-PAGE and analyzed by autoradiography (upper panel). HA-PACS-1 expression is shown (bottom panel). Error bars represent mean and SD of three independent experiments.

Figure 6. PACS-1_{CKmut} redistributes CI-MPR, furin and GGA3 and controls GGA3 phosphorylation. (A) A7 cells infected with VV expressing PACS-1_{CKmut} or PACS-1_{CKmut/S278D}, then stained with anti-CI-MPR, anti-TGN46 or anti-EEA1. Inset: colocalization of CI-MPR (green) and EEA1 (red). CI-MPR staining outside the TGN area was 13±6% and 10±5% in the WT and PACS-1 expressing cells (Fig. 2A), respectively, compared with 39±9% for PACS-1_{CKmut} expressing cells and 11±7% in PACS-1_{CKmut/S278D} expressing cells. (B) A7 cells transfected with FLAG-furin, infected with VV expressing PACS-1_{CKmut} and stained with anti-FLAG and anti-TGN46. FLAG-furin staining outside the TGN area increased from 9±6% and 11±4% in the WT and PACS-1 expressing cells (Fig. 2B), respectively, to 36±5% in PACS-1_{CKmut} expressing cells. (C) A7 cells infected with VV expressing PACS-1_{CKmut} then stained with anti-GGA3 and anti-TGN46 or anti-CI-MPR. Inset: Colocalization of GGA3 (green) and CI-MPR (red). GGA3 staining outside the TGN area increased from 11±6 % and 8±4 % in the WT and PACS-1 expressing cells (Fig. 2), respectively, to 36±5% in PACS-1_{CKmut} expressing cells. Scale Bars = 20 μm. (D) A7 cells were infected with WT:VV or VV expressing HA-PACS-1 or HA-PACS-1_{CKmut}, metabolically labeled with ³²P_i, and endogenous GGA3 was immunoprecipitated and analyzed by 12% SDS-PAGE and autoradiography. Error bars represent mean and SD of three independent experiments normalized to the PACS-1 sample. (E) GST-GGA3_{VHS+GAT} or GST alone was incubated with Trx-CK2β or Trx-PACS-1_{FBR} or both, isolated with glutathione sepharose and analyzed with anti-Trx mAb (upper panel). Input of each fusion protein is shown (lower panel). ~0.1% of the Trx-

CK2 β input was captured in the GST-GGA3_{VHS-GAT}/Trx-PACS-1_{FBR}/CK2 β ternary complex.

Figure 7. Working model of PACS-1/GGA3/CK2 controlled CI-MPR trafficking.

CI-MPR is phosphorylated upon TGN exit (Mésesse and Hoflack, 1993), promoting binding to GGA3 which traffics with CI-MPR to endosomes (Puertollano et al., 2001a). PACS-1 is recruited to the early endosomal CI-MPR/GGA3 complex by the binding of the PACS-1 FBR to the GGA VHS domain (Figs. 1 and 2). PACS-1 then recruits and activates CK2 (Figs. 4 and 5), which catalyzes a phosphorylation cascade to regulate retrieval of CI-MPR from the early endosome. The bound CK2 phosphorylates the GGA3 autoregulatory domain at Ser₃₈₈ to release GGA3 from CI-MPR. CK2 may also phosphorylate GGA3 at additional sites to promote release of GGA3 from the early endosome membrane (Figs. 2 and 6 and (Kametaka et al., 2005). CK2 bound to the PACS-1 FBR then phosphorylates Ser₂₇₈ on the PACS-1 autoregulatory domain to promote binding of PACS-1 to the CI-MPR_{CD} (Figs. 3 and 6). Whether CK2 that is bound to PACS-1 controls phosphorylation of the CI-MPR or other cargo molecules is not known. PACS-1 bound to CI-MPR then recruits AP-1 to recycle CI-MPR to the TGN. This model only depicts the switch in CI-MPR trafficking at the endosome that is regulated by the interaction between PACS-1, GGA3 and CK2 and does not depict sorting molecules that contribute to other CI-MPR sorting steps.

Supplementary Figure 1. siRNA depletion of PACS-1 does not effect CI-MPR half-life. (A) A7 cells were treated with the indicated siRNAs for 72 hours and analyzed by

western blot. **(B)** A7 cells were treated with scrambled (Scr), vps26, or PACS-1 siRNAs for 72 hours, then treated with 20 $\mu\text{g/ml}$ cyclohexamide for the indicated time points. After cyclohexamide treatment, the cells were scraped into 0.5 ml boiling SDS buffer, separated by SDS-PAGE and western blotted with anti-CI-MPR and tubulin antibodies.

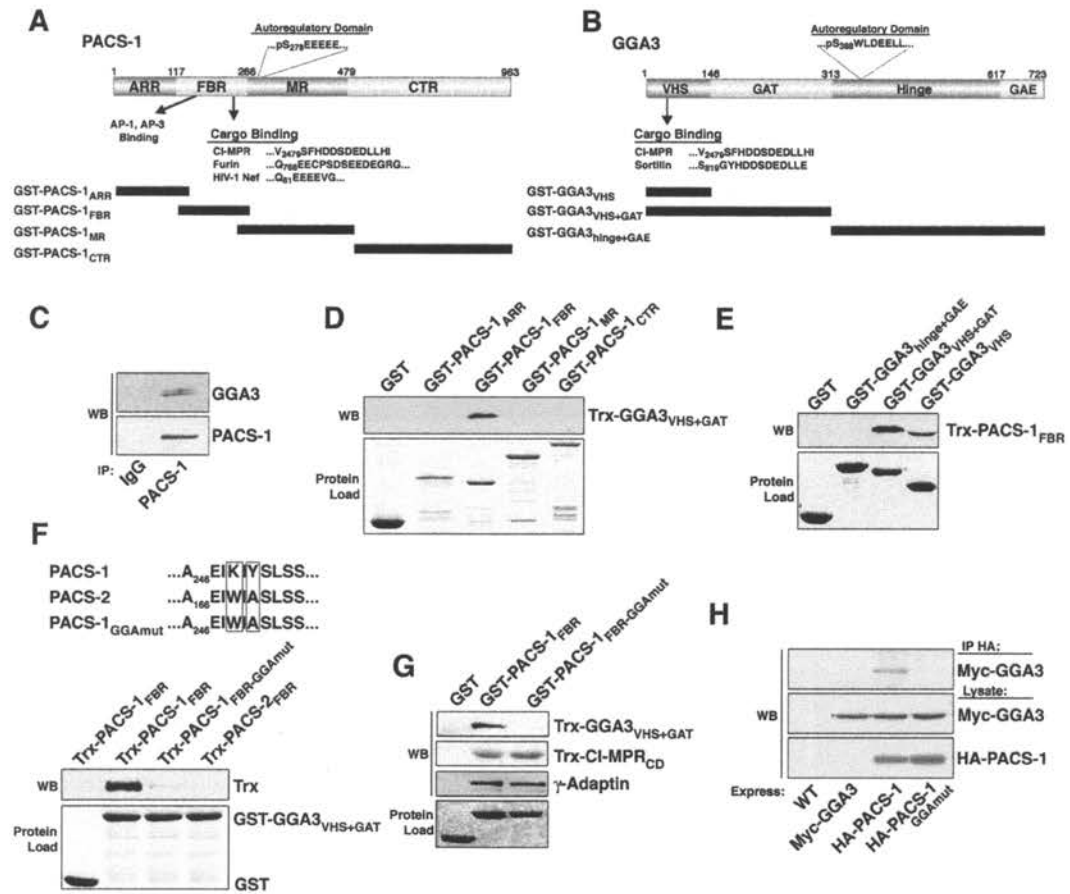


Figure 1

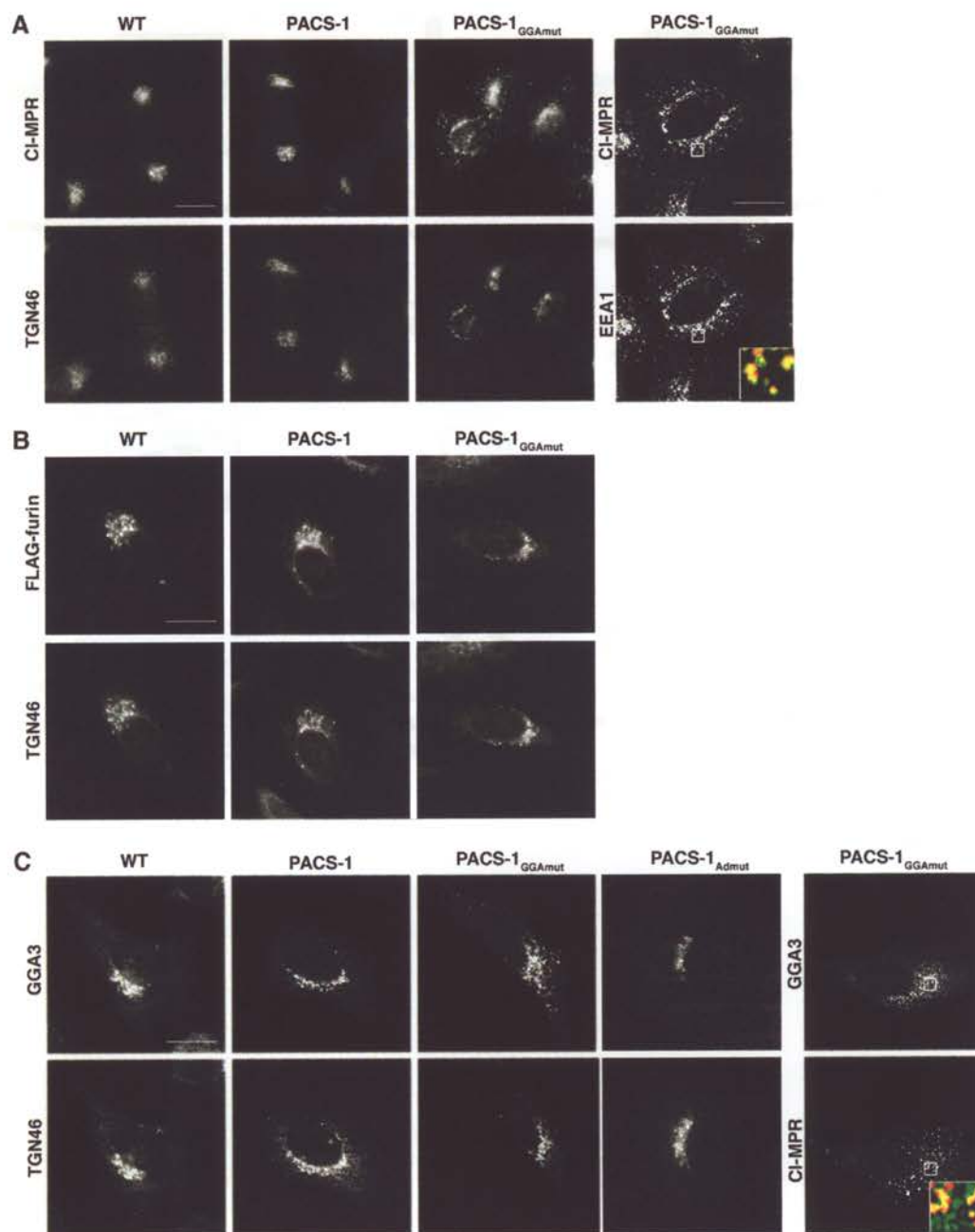


Figure 2

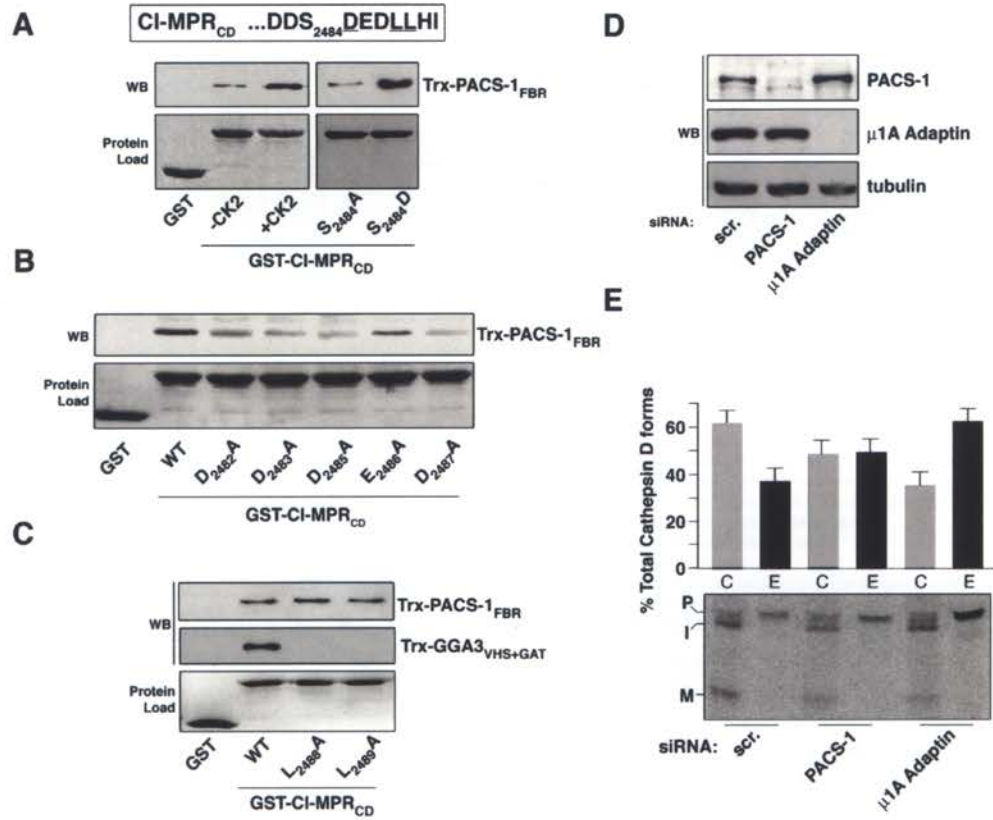


Figure 3

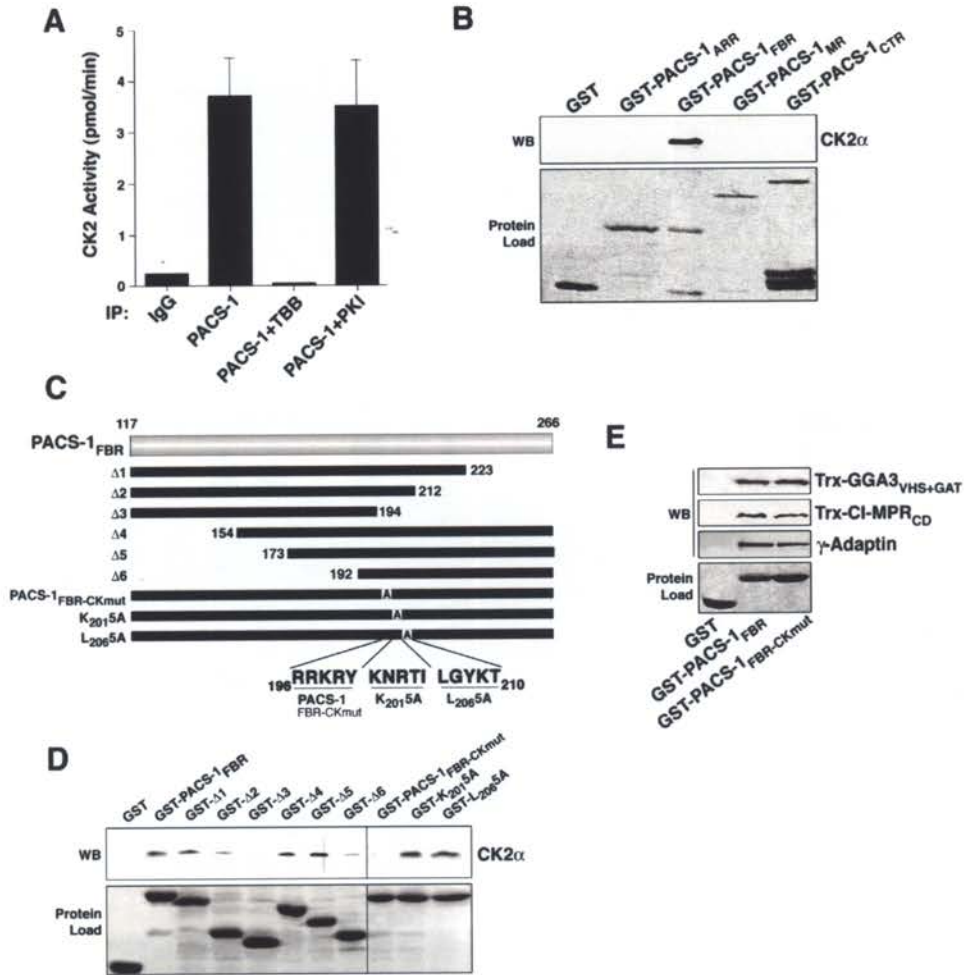


Figure 4

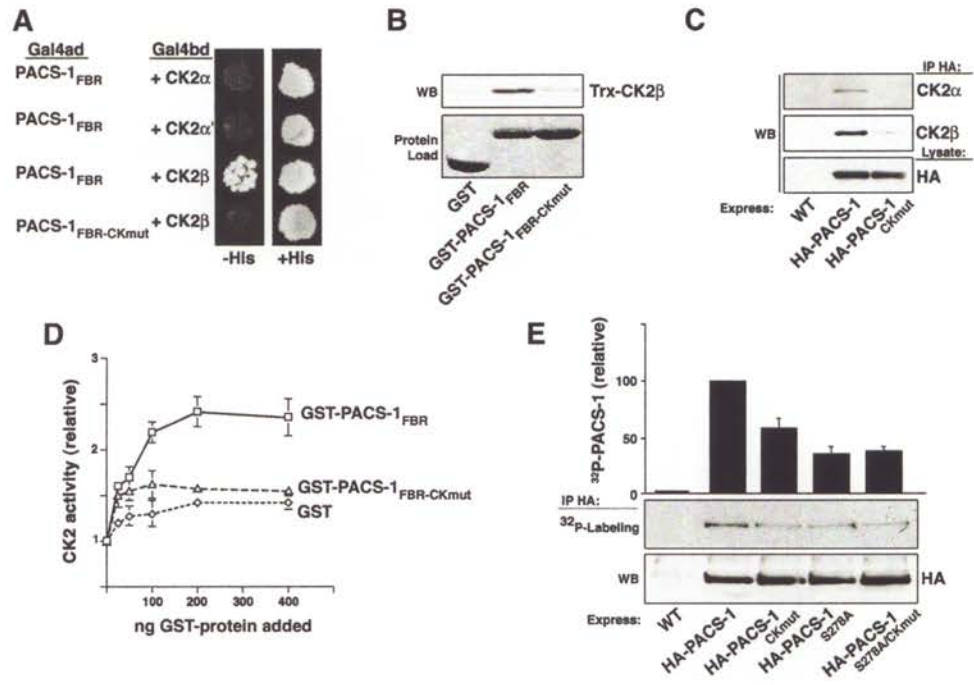


Figure 5

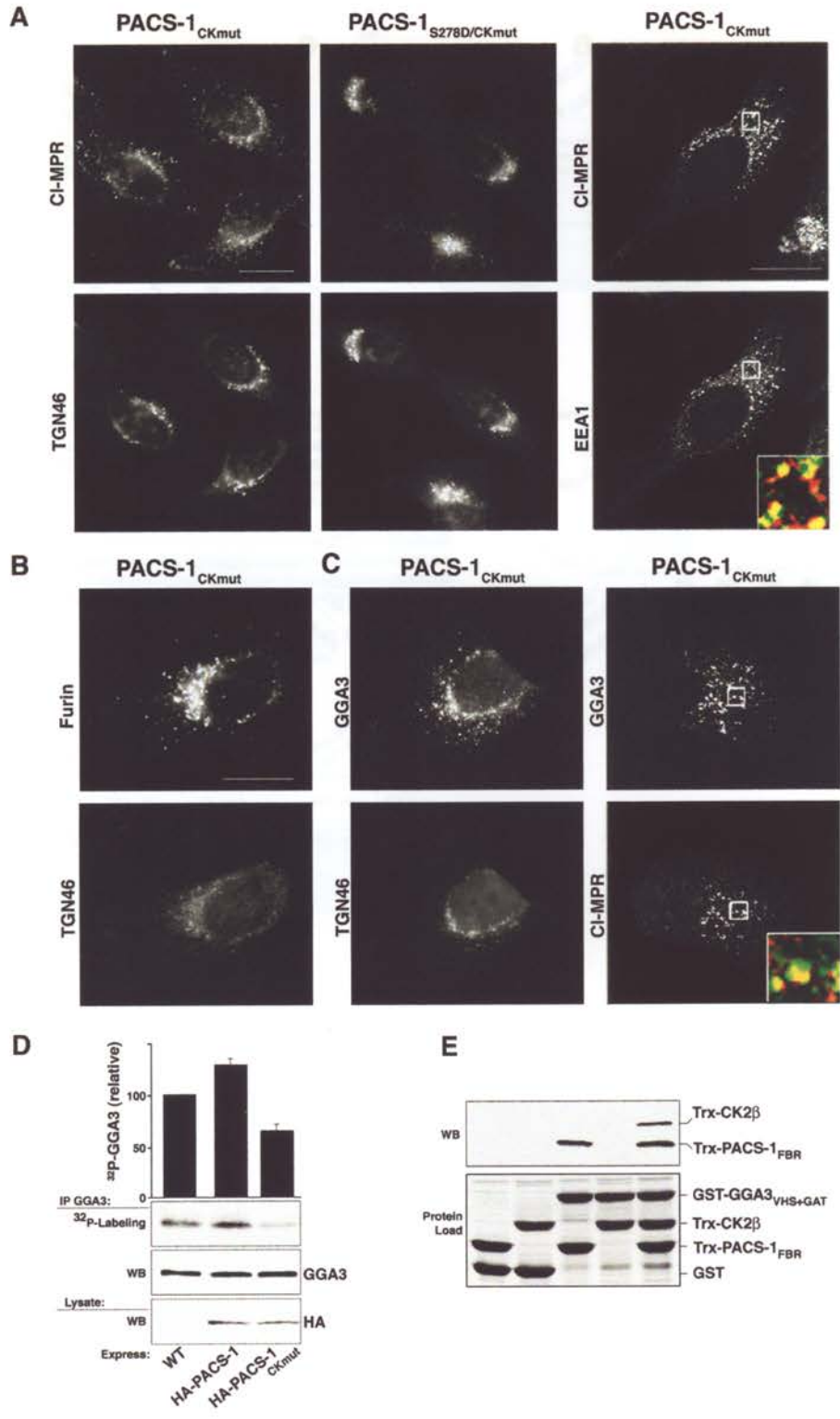


Figure 6

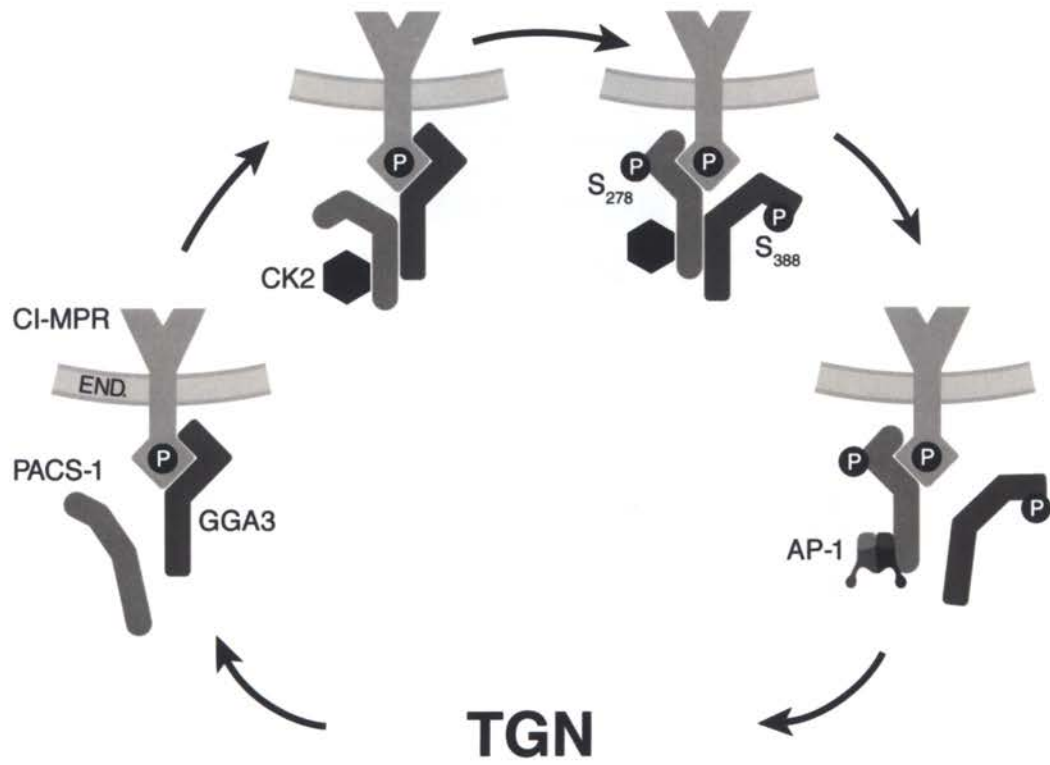
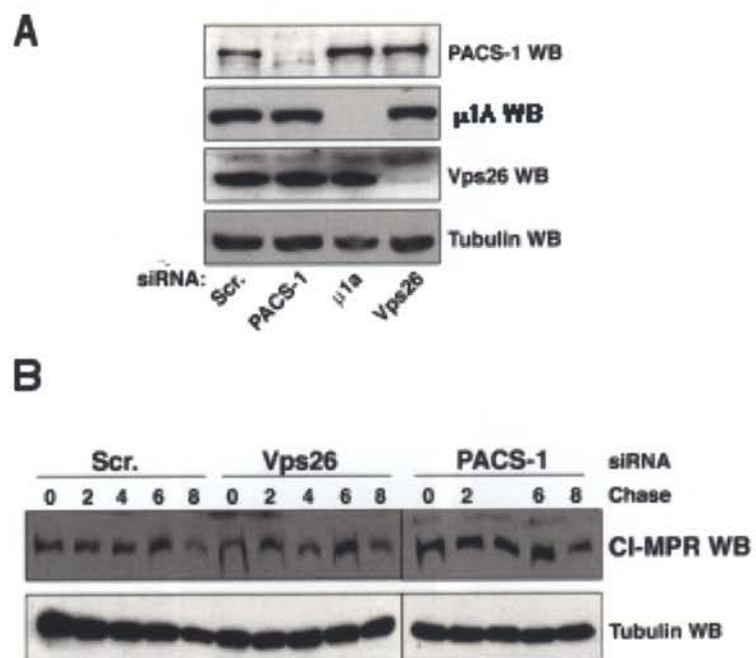


Figure 7



Supplementary Figure 1

CHAPTER 4. DISCUSSION

Summary

The results presented in this dissertation show that PACS-1, GGA3, and CK2 form a multimeric complex to regulate the endosomal sorting and TGN retrieval of cargo proteins with acidic- and acidic-dileucine trafficking motifs. We discovered that the PACS-1 FBR binds directly to both GGA3 and CK2. CK2 binds to PACS-1 FBR to control the phosphorylation state of Ser₂₇₈ within an autoregulatory domain on PACS-1, and to control the phosphorylation of GGA3. Blocking this phosphorylation or blocking the PACS-1/CK2 interaction interfered with the endosome-to-TGN retrieval of acidic cluster containing proteins, whereas blocking the PACS-1/GGA3 interaction only interfered with the endosome-to-TGN transport of proteins that contain both acidic cluster and acidic-dileucine motifs. These results suggest that the interaction of PACS-1 with GGA3 is specifically required for the trafficking of a subset of cargo proteins that bind to both PACS-1 and GGAs. Considering the known requirement for CK2 phosphorylation to regulate cargo binding of GGA3 (Doray et al., 2002b), one interpretation of these findings is that PACS-1 directs CK2 to GGA3 to initiate a phosphorylation “switch” that activates PACS-1 and inactivates GGA3, thereby driving retrieval of CI-MPR from endosomes to the TGN (Figure 1). Taken together, this work has broad implications on our understanding of PACS-1 function and allows the proposal of several new areas of investigation.

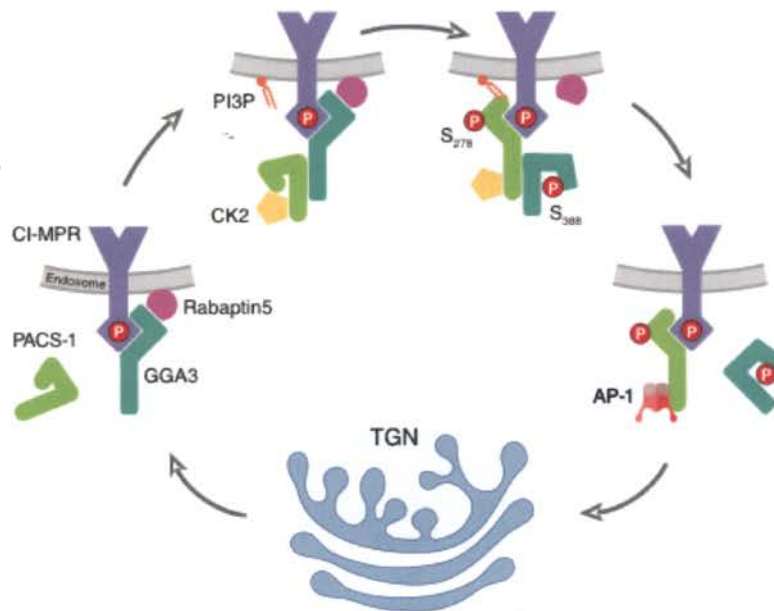


Figure 1. Working model of PACS-1/GGA3/CK2 controlled CI-MPR trafficking. CI-MPR is phosphorylated upon TGN exit (Mésesse and Hoflack, 1993), promoting binding to GGA3 which traffics with CI-MPR to endosomes (Puertollano et al, 2001a). GGA3 is inactivated for endosome-to-TGN retrieval of the CI-MPR because an interaction with Rabaptin5 blocks GGA3 binding to clathrin (Mattera et al., 2003). PACS-1 is recruited to the early endosomal CI-MPR/GGA3 complex by the binding of the PACS-1 FBR to the GGA VHS domain and by an interaction with PtdIns(3)P (PI3P) on early endosomal membranes (discussed in Chapter 4 and Appendix C). PACS-1 then recruits and activates CK2, which catalyzes a phosphorylation cascade to regulate retrieval of CI-MPR from the early endosome. The bound CK2 phosphorylates the GGA3 autoregulatory domain at Ser₃₈₈ to release GGA3 from CI-MPR. CK2 may also phosphorylate GGA3 at additional sites to promote release of GGA3 from the early endosome membrane (Kametaka et al., 2005). CK2 bound to the PACS-1 FBR then phosphorylates Ser₂₇₈ on the PACS-1 autoregulatory domain to promote binding of PACS-1 to the CI-MPR_{CD}. Whether CK2 that is bound to PACS-1 controls phosphorylation of the CI-MPR or other cargo molecules is not known. PACS-1 bound to CI-MPR then recruits AP-1 to recycle CI-MPR to the TGN.

Implications for future studies:

Implications for PACS-1 cargo binding

The studies presented here show that phosphorylation of PACS-1 Ser₂₇₈ is required for retrieval of furin, CI-MPR and HIV-1 Nef to the TGN from an endosomal compartment.

Additionally, the interaction of PACS-1 with CK2 is required for TGN retrieval of furin and CI-MPR, whereas the interaction of PACS-1 with GGA3 is required for endosome-

to-TGN retrieval of CI-MPR, but not furin. However, there are many other PACS-1 cargo proteins (see Chapter 1, Table 1) for which the importance of these interactions remains unknown. Of particular interest are membrane proteins that contain both acidic cluster and acidic-dileucine motifs, such as sortilin and β -secretase (BACE), which both bind to GGAs (Nielsen et al., 2001; Wahle et al., 2005) and contain potential PACS-1-binding acidic clusters. Future studies of PACS-1 regulation could ascertain if expression in cells of the interfering PACS-1 molecules developed for this dissertation—PACS-1_{S278A}, PACS-1_{CKmut} and PACS-1_{GGAmut}—affect the endosome-to-TGN retrieval of these proteins.

Implications for PACS-1 regulation

Whereas CK2 phosphorylation of acidic cluster sorting motifs within the furin cytosolic domain or other cargo proteins, including CI-MPR, VZV gE and VMAT-2, increases their binding to the PACS-1 FBR, CK2 phosphorylation of Ser₂₇₈ within the PACS-1 acidic cluster weakens the binding of these residues to the PACS-1 FBR (Waites et al., 2001; Wan et al., 1998 and Chapter 2, Figure 2). How CK2 phosphorylation of acidic cluster motifs within membrane cargo and PACS-1 influence in a completely opposite manner the binding of these various acidic motifs to the PACS-1 FBR remains unknown. Moreover, acidic cluster binding to the PACS-1 FBR may be more complex than a simple phosphorylation switch, as the non-phosphorylatable Nef and PC6B acidic clusters bind to PACS-1 (Piguet et al., 2000; Xiang et al., 2000). Together, these studies suggest there may be two acidic-cluster-binding modules on PACS-1: one for phosphorylated acidic clusters, and one for unphosphorylated acidic clusters. The residues surrounding cargo acidic clusters may dictate which binding module of PACS-1

is utilized, and the PACS-1 autoregulatory domain would block binding to both modules. Alternatively, the PACS-1 FBR may not contact the phosphoamino acids directly but may instead recognize other acidic cluster determinants that would be masked or unmasked by the phosphorylation of embedded Ser/Thr residues. Perhaps phosphorylation of cargo proteins increases the affinity of cargo for the PACS-1 FBR whereas phosphorylation of the PACS-1 autoregulatory domain triggers a conformational change that unmask the FBR to promote cargo binding. These possibilities could be investigated using limited proteolysis of PACS-1/cargo complexes to determine if phosphorylated acidic clusters bind a different region of the PACS-1 FBR than non-phosphorylated acidic clusters. More informative studies will come from the structural determination of the PACS-1 FBR with phosphorylated and non-phosphorylated acidic clusters.

Despite our identification of the PACS-1 autoregulatory domain, we do not yet know if autoregulation of PACS-1 is an intra- or inter-molecular event. The FBR and MR regions of PACS-1 directly interact *in vitro* in a phosphorylation-dependent manner, and my preliminary evidence (Appendix C, Figure 1) shows that PACS-1 molecules can form a complex *in vivo*. These results indicate that the regulation of PACS-1 binding to cargo proteins may indeed be an inter-molecular event, and that the formation of an oligomeric PACS-1 complex may be required to regulate the PACS-1 directed TGN localization of itinerant membrane proteins. I hypothesize that inactive PACS-1 is an oligomer in cells and that CK2 phosphorylation of Ser₂₇₈ induces a transition to a monomeric state—a process required for activation of PACS-1 and targeting of PACS-1 cargo proteins to the

TGN. Experiments to test this hypothesis should determine the oligomeric state of PACS-1 *in vitro* and *in vivo*, and the role of Ser₂₇₈ in formation of the PACS-1 oligomer. Gel filtration and laser light scattering (LLS) of purified full-length PACS-1 would reveal if the PACS-1 oligomer forms from a direct interaction, and, if so, the size of the PACS-1 complex compared to known markers, the ratio of oligomeric states, and the true size and molecular weight of the eluted protein. Using these methods, testing the oligomeric state of full-length PACS-1 containing a Ser₂₇₈→Ala or Ser₂₇₈→Asp substitution would determine if Ser₂₇₈ is critical for PACS-1 oligomerization *in vitro*. In addition, repeating my preliminary findings with full-length PACS-1 proteins containing these substitutions, would determine if Ser₂₇₈ is required for oligomerization *in vivo*. It is possible that phosphorylation of PACS-1 will have no detectable effect on the ability of PACS-1 to form oligomers. This would indicate that oligomerization of PACS-1 is probably not important for the regulation of cargo binding, but instead may be critical to concentrating cargo proteins into nascent vesicles.

Implications for CK2 binding and activation

Our observation that the R₁₉₆RKRY polybasic segment is required for PACS-1 to bind and activate CK2 *in vitro* and *in vivo* (Chapter 3, Figures 4 and 5) provides a mechanism for localizing this kinase to phosphorylate regulatory sites on PACS-1 and GGA3. Furthermore, our metabolic labeling studies (Chapter 3; Figure 6) showed that PACS-1_{S278A/CKmut} exhibited equal ³²P incorporation compared to PACS-1_{S278A}, providing evidence that CK2 that is bound to PACS-1 phosphorylates Ser₂₇₈. However, we have not yet determined which residues on GGA3 are affected by the PACS-1/CK2 interaction. There

are two consensus CK2 sites on GGA3 thought to regulate GGA3 function: Ser₃₇₂ and Ser₃₈₈. CK2 phosphorylation of GGA3 Ser₃₇₂ is required for EGF-stimulated phosphorylation of GGA3 Ser₃₆₈ by an unidentified kinase, which causes a conformational change in GGA3 that correlates with reduced association with membranes (Kametaka et al., 2005). GGA3 Ser₃₈₈ lies within the GGA3 autoregulatory domain, and CK2 phosphorylation of this residue induces a conformational change that correlates with an inhibition of CI-MPR binding (Doray et al., 2002b; Ghosh and Kornfeld, 2003a). One method to determine if phosphorylation of these residues is controlled by PACS-1/CK2 is to construct phospho-specific antibodies to these two sites and use them for western blotting of cell lysate made from cells expressing HA-PACS-1 or HA-PACS-1_{CKmut}. Alternatively, these studies could be done by quantitative phospho-analysis using mass spectrometry of immunoprecipitated endogenous GGA3 from cells expressing HA-PACS-1 or HA-PACS-1_{CKmut}.

In addition to interacting with CK2 α , several reports have shown that CK2 β can interact with and modulate the activity of a number of other protein kinases, including A-Raf (Boldyreff and Issinger, 1997), c-Mos (Chen et al., 1997b), the Src family tyrosine kinase Lyn (Lehner et al., 2004), p90^{sk} (ribosome S6 kinase; Kusk et al., 1999), check point kinase (Chk)-1 (Guerra et al., 2003) and Chk2 (Bjrling-Poulsen et al., 2005). These kinases have functions ranging from control of cell-cycle progression (Chk1, Chk2 and c-Mos; Matsuoka et al., 1998; Mutter et al., 1988; Walworth et al., 1993) to cell proliferation (A-Raf; Metz et al., 1995) to viral pathogenesis (Lyn; Tomkowicz et al., 2006), raising the possibility that PACS-1 anchored CK2 β may serve other functions

besides regulation of endosomal trafficking, or that PACS-1 may localize these other kinases to sites of endosomal function. An interaction between PACS-1 and these other kinases could be investigated by expressing full length HA-PACS-1 or HA-PACS-1_{CKmut} in cells, immunoprecipitating the HA-proteins and western blotting for these kinases. Additional experiments would involve direct protein-protein binding studies to show that CK2 β is required for the interaction, such as formation of a PACS-1/CK2 β /kinase ternary complex. Any finding that a CK2 β binding protein uses this interaction to recruit more than one kinase would be completely novel, and could shed light on PACS-1 and CK2 β biology.

Implications for GGA binding

A number of sorting proteins are known to direct endosome-to-TGN retrieval of the CI-MPR, leading one to ask why the PACS-1/GGA3 complex is required for this sorting step. One possibility involves Rabaptin5. Mattera and coworkers showed that when Rabaptin5 bound to GGA3, binding of GGA3 to clathrin was reduced—thereby preventing GGA3 from initiating vesicular transport of the endosomal CI-MPR (Mattera et al., 2003). PACS-1 could replace GGA3, and bring AP-1/clathrin to the endosomal CI-MPR to direct TGN retrieval. This additional sorting step may represent a timing mechanism to prevent immediate retrieval of the CI-MPR before hydrolase disassociation. Alternatively, perhaps the binding requirements on the cytosolic domain of the CI-MPR differ depending on the ligand-bound state of the receptor, determining the need for a PACS-1/GGA3 directed sorting event, or a sorting event directed by another molecule. This theory could be tested using reporter constructs that contain the CI-MPR cytosolic

and transmembrane domains fused to GFP. The endosomal path of the reporter could be followed using GFP, which would mimic the non-ligated state of the receptor, or by using an anti-GFP antibody, which would mimic the ligated-state of the receptor.

Our finding that PACS-1 binds to GGA3 may represent a mechanism for recruiting PACS-1 to early endosomal membranes. However, my preliminary evidence indicates that an interaction of PACS-1 with PtdIns(3)P may also play a role (Appendix C, Figure 2). PtdIns(3)P is concentrated on early endosomal membranes and interacts with PX and FYVE domains. But, PACS-1 does not contain either of these predicted domains, or any other known phospholipid binding module. Therefore, future studies to determine if PACS-1 is recruited to endosomal membranes by an interaction with PtdIns(3)P must first map the PtdIns(3)P binding site on PACS-1 and then create a mutant PACS-1 that does not bind PtdIns(3)P. This mutant could be used to determine if PtdIns(3)P is required for the subcellular localization of PACS-1, and for PACS-1 dependent sorting steps. An alternative strategy is to determine if siRNA depletion of PI3K, the kinase that catalyzes PtdIns(3)P production, affects the localization of PACS-1. PACS-1 may also be recruited to membranes through an interaction with an activated GTPase on the endosomal membrane. Perhaps the “coincidence” detection system for PACS-1 differs depending on the particular cargo protein: for cargoes that have acidic-dileucine motifs such as the CI-MPR, PACS-1 could be recruited by the acidic cluster/acidic-dileucine motif, PtdIns(3)P and GGA3, whereas for cargo that only have acidic cluster motifs, such as furin or HIV-1 Nef PACS-1 would be recruited by the acidic cluster motif and PtdIns(3)P.

Implications for PACS-2

The similarities in PACS-2 amino acid sequence compared to PACS-1, especially in the FBR and MR regions, indicate that, like PACS-1, PACS-2 may also be regulated by CK2 phosphorylation of an autoregulatory domain. PACS-2 contains an acidic cluster in the MR region (...S₁₉₉EEEYE...) that is similar to the PACS-1 autoregulatory domain and also to acidic clusters in known PACS-2 cargo proteins. In addition, the basic cluster of amino acids on PACS-1 (...R₁₉₆RKR...) that is required for CK2 binding is also present on PACS-2. Preliminary data from metabolically labeled cells indicates that PACS-2 is a phosphoprotein, and yeast-two-hybrid analysis indicates that the PACS-2 FBR and CK2 β interact (unpublished results). However, CK2 does not co-immunoprecipitate with expressed full-length HA-PACS-2 (unpublished results), indicating that PACS-2 may interact with CK2, but that this interaction is regulated differently than for PACS-1 or is a weaker interaction that can be detected in yeast, but not by co-immunoprecipitation from mammalian cells. These preliminary results suggest that PACS-2 Ser₁₉₉ may be phosphorylated by CK2 to act as an autoregulatory domain for PACS-2 cargo binding. Future studies should determine if Ser₁₉₉ of PACS-2 is required for PACS-2 phosphorylation, if phosphorylation of PACS-2 Ser₁₉₉ affects binding of the PACS-2 autoregulatory domain with the PACS-2 cargo binding region, and if CK2 binding to PACS-2 is required for phosphorylation of this, or other PACS-2 residues. These studies could address whether the phosphorylation state of the PACS-2 acidic cluster regulates the ability of PACS-2 to interact with and control the ER localization of PKD-2. Interestingly, the PACS-2 acidic cluster contains a tyrosine residue, Tyr₂₀₃, that is

predicted to be phosphorylated by Src family kinases (Scansite), suggesting that phosphorylation of Tyr₂₀₃ increases the ability of CK2 to phosphorylate Ser₁₉₉, and adding an extra layer of regulation to PACS-2 function.

Implications for neuronal function

PACS-1 is highly expressed in neuronal tissue (Simmen et al., 2005), and several PACS-1 cargo proteins have known functions in neurons. For instance, VAMP-4 is a snare protein that binds to PACS-1 and may be important for the maturation and homotypic fusion of immature secretory granules within neuroendocrine cells (Hinnert et al., 2003). Additionally, our studies of the interplay between PACS-1, GGA3 and CK2 to control the sorting of the CI-MPR, as well as our finding that PACS-1 depletion increases secretion of the lysosomal hydrolase Cathepsin D from cultured cell lines, indicates that PACS-1 is an essential cellular component for directing hydrolases to the lysosome. In neurons, correct sorting of lysosomal hydrolases is critical, as evidenced by manifestation of severe neuronal defects in patients suffering from lysosomal storage disorders, such as I-Cell and Tay-Sachs disease, which are congenital disorders stemming from a reduction in hydrolase activity. I-cell disease is characterized by enhanced secretion of hydrolases into extracellular fluids, swelling of lysosomes and severe neuronal defects (Wiesmann et al., 1971). Patients with I-cell disease exhibit buildup of lipids in the lysosome due to disrupted trafficking of hydrolases and suffer numerous defects, including mental retardation. Patients with Tay-Sachs disease develop inclusion bodies filled with GM2-ganglioside in the peripheral and central nervous systems, due to defects in the gene encoding the lysosomal hydrolase beta-hexosaminidase A (Abe et al., 1985), resulting in

deterioration of mental and physical abilities, severe brain damage, enlargement of the head, convulsions, blindness, deafness, and, finally, death. Based on our findings that PACS-1 is required for sorting of hydrolases, it is possible that targeted disruption of the PACS-1 gene in mice may yield increased hydrolase secretion into the extracellular space, a defect similar to that observed in patients with I-cell or Tay-Sachs disease.

Conclusion

Studies performed for this dissertation used biochemical-, cellular-, and cell-free-methods to investigate how trafficking of membrane proteins in the TGN and endosomal systems is regulated. By investigating how regulation of PACS-1 affects endosomes-to-TGN retrieval of membrane proteins, these studies shed light on the molecular interactions required for efficient transport within the secretory system. However, the long-term goal is to identify and understand all of the molecular interactions with sorting signals on the cytosolic tails of membrane proteins required for directed transport in the secretory system.

References

- Abe, T, Ogawa, K, Fuziwara, H, Urayama, K and Nagashima, K. (1985) Spinal ganglia and peripheral nerves from a patient with Tay-Sachs disease. Morphological and ganglioside studies. *Acta Neuropathol (Berl)*, **66(3)**.
- Alconada, A, Bauer, U, Baudoux, L, Piette, J and Hoflack, B. (1998) Intracellular transport of the glycoproteins gE and gI of the varicella-zoster virus. gE accelerates the maturation of gI and determines its accumulation in the trans-Golgi network. *J Biol Chem*, Vol. 273, pp. 13430-13436.
- Alconada, A, Bauer, U and Hoflack, B. (1996) A tyrosine-based motif and a casein kinase II phosphorylation site regulate the intracellular trafficking of the varicella-zoster virus glycoprotein I, a protein localized in the trans-Golgi network. *Embo J*, Vol. 15, pp. 6096-6110.
- Alconada, A, Bauer, U, Sodeik, B and Hoflack, B. (1999) Intracellular traffic of herpes simplex virus glycoprotein gE: characterization of the sorting signals required for its trans-Golgi network localization. *J Virol*, Vol. 73, pp. 377-387.
- Anderson, E, Maday, S, Sfakianos, J, Hull, M, Winckler, B, Sheff, D, Fèolsch, H and Mellman, I. (2005) Transcytosis of NgCAM in epithelial cells reflects differential signal recognition on the endocytic and secretory pathways. *J Cell Biol*, **170(4)**, 595-605.
- Anderson, ED, Molloy, SS, Jean, F, Fei, H, Shimamura, S and Thomas, G. (2002) The ordered and compartment-specific autoproteolytic removal of the furin intramolecular chaperone is required for enzyme activation. *J Biol Chem*, **277**, 12879-12890.
- Anderson, ED, Thomas, L, Hayflick, JS and Thomas, G. (1993) Inhibition of HIV-1 gp160-dependent membrane fusion by a furin-directed alpha 1-antitrypsin variant. *J Biol Chem*, **268**, 24887-24891.
- Anderson, ED, VanSlyke, JK, Thulin, CD, Jean, F and Thomas, G. (1997) Activation of the furin endoprotease is a multiple-step process: requirements for acidification and internal propeptide cleavage. *Embo J*, **16**, 1508-1518.
- Anderson, RG, Brown, MS and Goldstein, JL. (1977) Role of the coated endocytic vesicle in the uptake of receptor-bound low density lipoprotein in human fibroblasts. *Cell*, **10(3)**, 351-364.
- Arighi, CN, Hartnell, LM, Aguilar, RC, Haft, CR and Bonifacino, JS. (2004) Role of the mammalian retromer in sorting of the cation-independent mannose 6-phosphate receptor. *J Cell Biol*, **165**, 123-133.
- Balch, WE, Dunphy, WG, Braell, WA and Rothman, JE. (1984) Reconstitution of the transport of protein between successive compartments of the Golgi measured by the coupled incorporation of N-acetylglucosamine. *Cell*, **39(2) Pt 1**, 405-416.
- Barlowe, C, Orci, L, Yeung, T, Hosobuchi, M, Hamamoto, S, Salama, N, Rexach, MF, Ravazzola, M, Amherdt, M and Schekman, R. (1994) COPII: a membrane coat formed by Sec proteins that drive vesicle budding from the endoplasmic reticulum. *Cell*, **77(6)**, 895-907.
- Barlowe, C and Schekman, R. (1993) SEC12 encodes a guanine-nucleotide-exchange factor essential for transport vesicle budding from the ER. *Nature*, **365(6444)**, 347-349.

- Baukrowitz, T, Tucker, SJ, Schulte, U, Benndorf, K, Ruppertsberg, JP and Fakler, B. (1999) Inward rectification in KATP channels: a pH switch in the pore. *Embo J*, **18**, 847-853.
- Behnia, R and Munro, S. (2005) Organelle identity and the signposts for membrane traffic. *Nature*, **438(7068)**, 597-604.
- Beitia Ortiz de Zarate, I, Kaelin, K and Rozenberg, F. (2004) Effects of mutations in the cytoplasmic domain of herpes simplex virus type 1 glycoprotein B on intracellular transport and infectivity. *J Virol*, Vol. 78, pp. 1540-1551.
- Bergeron, E, Basak, A, Decroly, E and Seidah, NG. (2003) Processing of alpha4 integrin by the proprotein convertases: histidine at position P6 regulates cleavage. *Biochem J*, **373**, 475-484.
- Bhattacharjya, S, Xu, P, Xiang, H, Chretien, M, Seidah, NG and Ni, F. (2001) pH-induced conformational transitions of a molten-globule-like state of the inhibitory prodomain of furin: implications for zymogen activation. *Protein Sci*, **10**, 934-942.
- Bissonnette, L, Charest, G, Longpre, JM, Lavigne, P and Leduc, R. (2004) Identification of furin pro-region determinants involved in folding and activation. *Biochem J*, **379**, 757-763.
- Bjerring-Poulsen, M, Siehler, S, Wiesmüller, L, Meek, D, Niefind, K and Issinger, OG. (2005) The 'regulatory' beta-subunit of protein kinase CK2 negatively influences p53-mediated allosteric effects on Chk2 activation. *Oncogene*, **24**, 6194-6200.
- Blagoveshchenskaya, AD, Thomas, L, Feliciangeli, SF, Hung, CH and Thomas, G. (2002) HIV-1 Nef downregulates MHC-I by a PACS-1- and PI3K-regulated ARF6 endocytic pathway. *Cell*, **111**, 853-866.
- Blot, G, Janvier, K, Le Panse, S, Benarous, R and Berlioz-Torrent, C. (2003) Targeting of the human immunodeficiency virus type 1 envelope to the trans-Golgi network through binding to TIP47 is required for env incorporation into virions and infectivity. *J Virol*, **77(12)**, 6931-6945.
- Boldyreff, B and Issinger, OG. (1997) A-Raf kinase is a new interacting partner of protein kinase CK2 beta subunit. *FEBS lett*, **403**, 197-199.
- Boll, W, Ohno, H, Songyang, Z, Rapoport, I, Cantley, LC, Bonifacino, JS and Kirchhausen, T. (1996) Sequence requirements for the recognition of tyrosine-based endocytic signals by clathrin AP-2 complexes. *Embo J*, Vol. 15, pp. 5789-5795.
- Boman, AL, Zhang, C, Zhu, X and Kahn, RA. (2000) A family of ADP-ribosylation factor effectors that can alter membrane transport through the trans-Golgi. *Mol Biol Cell*, **11**, 1241-1255.
- Bonifacino, JS. (2004a) The GGA proteins: adaptors on the move. *Nat Rev Mol Cell Biol*, **5**, 23-32.
- Bonifacino, JS and Dell'Angelica, EC. (1999) Molecular bases for the recognition of tyrosine-based sorting signals. *J Cell Biol*, Vol. 145, pp. 923-926.
- Bonifacino, JS and Glick, BS. (2004) The mechanisms of vesicle budding and fusion. *Cell*, Vol. 116, pp. 153-166.
- Bonifacino, JS and Traub, LM. (2003) Signals for sorting of transmembrane proteins to endosomes and lysosomes. *Annu Rev Biochem*, **72**, 395-447.

- Bonnet, H, Filhol, O, Truchet, I, Brethenou, P, Cochet, C, Amalric, F and Bouche, G. (1996) Fibroblast growth factor-2 binds to the regulatory beta subunit of CK2 and directly stimulates CK2 activity toward nucleolin. *J Biol Chem*, **271**, 24781-24787.
- Brideau, AD, Eldridge, MG and Enquist, LW. (2000a) Directional transneuronal infection by pseudorabies virus is dependent on an acidic internalization motif in the Us9 cytoplasmic tail. *J Virol*, Vol. 74, pp. 4549-4561.
- Brideau, AD, Enquist, LW and Tirabassi, RS. (2000b) The role of virion membrane protein endocytosis in the herpesvirus life cycle. *J Clin Virol*, Vol. 17, pp. 69-82.
- Brown, MS and Goldstein, JL. (1975) Regulation of the activity of the low density lipoprotein receptor in human fibroblasts. *Cell*, **6(3)**, 307-316.
- Buchou, T, Vernet, M, Blond, O, Jensen, HH, Pointu, H, Olsen, BB, Cochet, C, Issinger, OG and Boldyreff, B. (2003) Disruption of the regulatory beta subunit of protein kinase CK2 in mice leads to a cell-autonomous defect and early embryonic lethality. *Mol Cell Biol*, **23**, 908-915.
- Burd, CG and Emr, SD. (1998) Phosphatidylinositol(3)-phosphate signaling mediated by specific binding to RING FYVE domains. *Mol Cell*, **2(1)**, 157-162.
- Burnett, G and Kennedy, EP. (1954) The enzymatic phosphorylation of proteins. *J Biol Chem*, **211(2)**, 969-980.
- Byrd, JC, Park, JH, Schaffer, BS, Garmroudi, F and MacDonald, RG. (2000) Dimerization of the insulin-like growth factor II/mannose 6-phosphate receptor. *J Biol Chem*, **275(25)**, 18647-18656.
- Cai, WH, Gu, B and Person, S. (1988) Role of glycoprotein B of herpes simplex virus type 1 in viral entry and cell fusion. *J Virol*, Vol. 62, pp. 2596-2604.
- Cao, H, Thompson, HM, Krueger, EW and McNiven, MA. (2000) Disruption of Golgi structure and function in mammalian cells expressing a mutant dynamin. *J Cell Sci*, **113**, 1993-2002.
- Card, JP, Rinaman, L, Lynn, RB, Lee, BH, Meade, RP, Miselis, RR and Enquist, LW. (1993) Pseudorabies virus infection of the rat central nervous system: ultrastructural characterization of viral replication, transport, and pathogenesis. *J Neurosci*, Vol. 13, pp. 2515-2539.
- Carlton, J, Bujny, M, Peter, BJ, Oorschot, VM, Rutherford, A, Mellor, H, Klumperman, J, McMahon, HT and Cullen, PJ. (2004) Sorting nexin-1 mediates tubular endosome-to-TGN transport through coincidence sensing of high-curvature membranes and 3-phosphoinositides. *Curr Biol*, **14(20)**, 1791-1800.
- Carroll, KS, Hanna, J, Simon, I, Krise, J, Barbero, P and Pfeffer, SR. (2001) Role of Rab9 GTPase in facilitating receptor recruitment by TIP47. *Science*, **292(5520)**, 1373-1376.
- Cavenagh, MM, Whitney, JA, Carroll, K, Zhang, C, Boman, AL, Rosenwald, AG, Mellman, I and Kahn, RA. (1996) Intracellular distribution of ARF proteins in mammalian cells. ARF6 is uniquely localized to the plasma membrane. *J Biol Chem*, **271(36)**, 21767-21774.
- Chantalat, L, Leroy, D, Filhol, O, Nueda, A, Benitez, MJ, Chambaz, EM, Cochet, C and Dideberg, O. (1999) Crystal structure of the human protein kinase CK2 regulatory subunit reveals its zinc finger-mediated dimerization. *EMBO J*, **18**, 2930-2940.

- Cheever, ML, Sato, TK, de Beer, T, Kutateladze, TG, Emr, SD and Overduin, M. (2001) Phox domain interaction with PtdIns(3)P targets the Vam7 t-SNARE to vacuole membranes. *Nat Cell Biol*, **3**(7), 613-618.
- Chen, HJ, Yuan, J and Lobel, P. (1997a) Systematic mutational analysis of the cation-independent mannose 6-phosphate/insulin-like growth factor II receptor cytoplasmic domain. An acidic cluster containing a key aspartate is important for function in lysosomal enzyme sorting. *J Biol Chem*, **272**, 7003-7012.
- Chen, M, Li, D, Krebs, EG and Cooper, JA. (1997b) The casein kinase II beta subunit binds to Mos and inhibits Mos activity. *Mol Cell Biol*, **17**, 1904-1912.
- Christoforidis S, McBride HM, Burgoyne RD, Zerial M. (1999) The Rab5 effector EEA1 is a core component of endosome docking. *Nature*, **397**(6720), 621-5.
- Collins, BM, McCoy, AJ, Kent, HM, Evans, PR and Owen, DJ. (2002) Molecular architecture and functional model of the endocytic AP2 complex. *Cell*, **109**(4), 523-535.
- Collins, KL, Chen, BK, Kalams, SA, Walker, BD and Baltimore, D. (1998) HIV-1 Nef protein protects infected primary cells against killing by cytotoxic T lymphocytes. *Nature*, **391**(6665), 397-401.
- Comellas-Bigler, M, Maskos, K, Huber, R, Oyama, H, Oda, K and Bode, W. (2004) 1.2 A crystal structure of the serine carboxyl proteinase pro-kumamolisin; structure of an intact pro-subtilase. *Structure*, **12**, 1313-1323.
- Cozier, GE, Carlton, J, McGregor, AH, Gleeson, PA, Teasdale, RD, Mellor, H and Cullen, PJ. (2002) The phox homology (PX) domain-dependent, 3-phosphoinositide-mediated association of sorting nexin-1 with an early sorting endosomal compartment is required for its ability to regulate epidermal growth factor receptor degradation. *J Biol Chem*, **277**(50), 48730-48736.
- Crump, CM, Hung, CH, Thomas, L, Wan, L and Thomas, G. (2003) Role of PACS-1 in trafficking of human cytomegalovirus glycoprotein B and virus production. *J Virol*, **77**, 11105-11113.
- Crump, CM, Xiang, Y, Thomas, L, Gu, F, Austin, C, Tooze, SA and Thomas, G. (2001) PACS-1 binding to adaptors is required for acidic cluster motif-mediated protein traffic. *Embo J*, **20**, 2191-2201.
- Davis, CG, van Driel, IR, Russell, DW, Brown, MS and Goldstein, JL. (1987) The low density lipoprotein receptor. Identification of amino acids in cytoplasmic domain required for rapid endocytosis. *J Biol Chem*, **262**(9), 4075-4082.
- Davison, AJ and Scott, JE. (1986) The complete DNA sequence of varicella-zoster virus. *J Gen Virol*, Vol. 67, pp. 1759-1816.
- Degnin, C, Jean, F, Thomas, G and Christian, JL. (2004) Cleavages within the prodomain direct intracellular trafficking and degradation of mature bone morphogenetic protein-4. *Mol Biol Cell*, **15**, 5012-5020.
- Dell'Angelica, EC, Klumperman, J, Stoorvogel, W and Bonifacino, JS. (1998) Association of the AP-3 adaptor complex with clathrin. *Science*, **280**(5362), 431-434.
- Dell'Angelica, EC, Puertollano, R, Mullins, C, Aguilar, RC, Vargas, JD, Hartnell, LM and Bonifacino, JS. (2000) GGAs: a family of ADP ribosylation factor-binding proteins related to adaptors and associated with the Golgi complex. *J Cell Biol*, **149**, 81-94.

- Dell'Angelica, EC, Shotelersuk, V, Aguilar, RC, Gahl, WA, Bonifacino, JS and Cell, B. (1999) Altered trafficking of lysosomal proteins in Hermansky-Pudlak syndrome due to mutations in the beta 3A subunit of the AP-3 adaptor. *Mol Cell*, **3**(1), 11-21.
- Diaz, E and Pfeffer, SR. (1998) TIP47: a cargo selection device for mannose 6-phosphate receptor trafficking. *Cell*, Vol. 93, pp. 433-443.
- Dirac-Svejstrup AB, Sumizawa T, Pfeffer SR. (1997) Identification of a GDI displacement factor that releases endosomal Rab GTPases from Rab-GDI. *EMBO J*, **16**(3), 465-72.
- Dittie, AS, Thomas, L, Thomas, G and Tooze, SA. (1997) Interaction of furin in immature secretory granules from neuroendocrine cells with the AP-1 adaptor complex is modulated by casein kinase II phosphorylation. *Embo J*, **16**, 4859-4870.
- Donaldson, JG, Finazzi, D and Klausner, RD. (1992) Brefeldin A inhibits Golgi membrane-catalysed exchange of guanine nucleotide onto ARF protein. *Nature*, **360**(6402), 350-352.
- Doray, B, Bruns, K, Ghosh, P and Kornfeld, S. (2002a) Interaction of the cation-dependent mannose 6-phosphate receptor with GGA proteins. *J Biol Chem*, Vol. 277, pp. 18477-18482.
- Doray, B, Bruns, K, Ghosh, P and Kornfeld, SA. (2002b) Autoinhibition of the ligand-binding site of GGA1/3 VHS domains by an internal acidic cluster-dileucine motif. *Proc Natl Acad Sci USA*, **99**, 8072-8077.
- Doray, B, Ghosh, P, Griffith, J, Geuze, HJ and Kornfeld, S. (2002c) Cooperation of GGAs and AP-1 in packaging MPRs at the trans-Golgi network. *Science*, **297**, 1700-1703.
- Dorner, AJ, Wasley, LC, Raney, P, Haugejorden, S, Green, M and Kaufman, RJ. (1990) The stress response in Chinese hamster ovary cells. Regulation of ERp72 and protein disulfide isomerase expression and secretion. *J Biol Chem*, **265**, 22029-22034.
- Durocher, D, Taylor, IA, Sarbassova, D, Haire, LF, Westcott, SL, Jackson, SP, Smerdon, SJ and Yaffe, MB. (2000) The molecular basis of FHA domain:phosphopeptide binding specificity and implications for phospho-dependent signaling mechanisms. *Mol Cell*, **6**, 1169-1182.
- Duus, KM and Grose, C. (1996) Multiple regulatory effects of varicella-zoster virus (VZV) gL on trafficking patterns and fusogenic properties of VZV gH. *J Virol*, Vol. 70, pp. 8961-8971.
- Duus, KM, Hatfield, C and Grose, C. (1995) Cell surface expression and fusion by the varicella-zoster virus gH:gL glycoprotein complex: analysis by laser scanning confocal microscopy. *Virology*, Vol. 210, pp. 429-440.
- Edson, CM, Hosler, BA, Respass, RA, Waters, DJ and Thorley-Lawson, DA. (1985) Cross-reactivity between herpes simplex virus glycoprotein B and a 63,000-dalton varicella-zoster virus envelope glycoprotein. *J Virol*, Vol. 56, pp. 333-336.
- Elliott, G and O'Hare, P. (1999) Live-cell analysis of a green fluorescent protein-tagged herpes simplex virus infection. *J Virol*, Vol. 73, pp. 4110-4119.
- Favoreel, HW, Van Minnebruggen, G, Nauwynck, HJ, Enquist, LW and Pensaert, MB. (2002) A tyrosine-based motif in the cytoplasmic tail of pseudorabies virus

- glycoprotein B is important for both antibody-induced internalization of viral glycoproteins and efficient cell-to-cell spread. *J Virol*, Vol. 76, pp. 6845-6851.
- Feng, Y, Press, B and Wandinger-Ness, A. (1995) Rab 7: an important regulator of late endocytic membrane traffic. *J Cell Biol*, **131(6) Pt 1**, 1435-1452.
- Fèolsch, H, Ohno, H, Bonifacino, JS and Mellman, I. (1999) A novel clathrin adaptor complex mediates basolateral targeting in polarized epithelial cells. *Cell*, **99(2)**, 189-198.
- Fish, KN, Soderberg-Naucler, C and Nelson, JA. (1998) Steady-state plasma membrane expression of human cytomegalovirus gB is determined by the phosphorylation state of Ser900. *J Virol*, Vol. 72, pp. 6657-6664.
- Ford, MG, Pearse, BM, Higgins, MK, Vallis, Y, Owen, DJ, Gibson, A, Hopkins, CR, Evans, PR and McMahon, HT. (2001) Simultaneous binding of PtdIns(4,5)P₂ and clathrin by AP180 in the nucleation of clathrin lattices on membranes. *Science*, **291(5506)**, 1051-1055.
- Forghani, B, Ni, L and Grose, C. (1994) Neutralization epitope of the varicella-zoster virus gH:gL glycoprotein complex. *Virology*, Vol. 199, pp. 458-462.
- Friend DS, Farquhar MG. (1967) Functions of coated vesicles during protein absorption in the rat vas deferens. *J Cell Biol*, **35(2)**, 357-76.
- Gallusser, A and Kirchhausen, T. (1993) The beta 1 and beta 2 subunits of the AP complexes are the clathrin coat assembly components. *Embo J*, **12(13)**, 5237-5244.
- Gershon, AA, Sherman, DL, Zhu, Z, Gabel, CA, Ambron, RT and Gershon, MD. (1994) Intracellular transport of newly synthesized varicella-zoster virus: final envelopment in the trans-Golgi network. *J Virol*, Vol. 68, pp. 6372-6390.
- Ghosh, P, Dahms, NM and Kornfeld, S. (2003a) Mannose 6-phosphate receptors: new twists in the tale. *Nat Rev Mol Cell Biol*, Vol. 4, pp. 202-212.
- Ghosh, P, Griffith, J, Geuze, HJ and Kornfeld, S. (2003b) Mammalian GGAs act together to sort mannose 6-phosphate receptors. *J Cell Biol*, **163**, 755-766.
- Ghosh, P and Kornfeld, S. (2003a) Phosphorylation-induced conformational changes regulate GGAs 1 and 3 function at the trans-Golgi network. *J Biol Chem*, **278**, 14543-14549.
- Ghosh P, Kornfeld S. (2003b) AP-1 binding to sorting signals and release from clathrin-coated vesicles is regulated by phosphorylation. *J Cell Biol.*, **160(5)**, 699-708.
- Goldberg, J. (1998) Structural basis for activation of ARF GTPase: mechanisms of guanine nucleotide exchange and GTP-myristoyl switching. *Cell*, **95(2)**, 237-248.
- Gonzalez-Noriega A, Grubb JH, Talkad V, Sly WS. (1980) Chloroquine inhibits lysosomal enzyme pinocytosis and enhances lysosomal enzyme secretion by impairing receptor recycling. *J Cell Biol*, **85(3)**, 839-52.
- Gorvel, JP, Chavier, P, Zerial, M and Gruenberg, J. (1991) rab5 controls early endosome fusion in vitro. *Cell*, **64(5)**, 915-925.
- Greenberg, M, DeTulleo, L, Rapoport, I, Skowronski, J and Kirchhausen, T. (1998) A dileucine motif in HIV-1 Nef is essential for sorting into clathrin-coated pits and for downregulation of CD4. *Curr Biol*, **8(22)**, 1239-1242.
- Griffiths, G, Hoflack, B, Simons, K, Mellman, I and Kornfeld, S. (1988) The mannose 6-phosphate receptor and the biogenesis of lysosomes. *Cell*, **52**, 329-341.

- Griffiths, G, Pfeiffer, S, Simons, K and Matlin, K. (1985) Exit of newly synthesized membrane proteins from the trans cisterna of the Golgi complex to the plasma membrane. *J Cell Biol*, **101**(3), 949-964.
- Grose, C. (1990) Glycoproteins encoded by varicella-zoster virus: biosynthesis, phosphorylation, and intracellular trafficking. *Annu Rev Microbiol*, Vol. 44, pp. 59-80.
- Grose, C. (2002) The predominant varicella-zoster virus gE and gI glycoprotein complex. In Holzenburg, A.a.B., E. (ed.), *Structure-Function Relationships of Human Pathogenic Viruses*. Kluwer Academic Press, New York, N.Y., pp. 195-223.
- Grose, C, Jackson, W and Traugh, JA. (1989) Phosphorylation of varicella-zoster virus glycoprotein gpI by mammalian casein kinase II and casein kinase I. *J Virol*, Vol. 63, pp. 3912-3918.
- Grose, C, Perrotta, DM, Brunell, PA and Smith, GC. (1979) Cell-free varicella-zoster virus in cultured human melanoma cells. *J Gen Virol*, Vol. 43, pp. 15-27.
- Gruenberg, J. (2001) The endocytic pathway: a mosaic of domains. *Nat Rev Mol Cell Biol*, **2**, 721-730.
- Gruenberg, J. (2003) Lipids in endocytic membrane transport and sorting. *Curr Opin Cell Biol*, Vol. 15, pp. 382-388.
- Gruenberg, J and Stenmark, H. (2004) The biogenesis of multivesicular endosomes. *Nat Rev Mol Cell Biol*, **5**(4), 317-323.
- Gu, F, Crump, CM and Thomas, G. (2001) Trans-Golgi network sorting. *Cell Mol Life Sci*, **58**, 1067-1084.
- Guerra, B, Issinger, OG and Wang, JY. (2003) Modulation of human checkpoint kinase Chk1 by the regulatory beta-subunit of protein kinase CK2. *Oncogene*, **22**, 4933-4942.
- Harlan, JE, Hajduk, PJ, Yoon, HS and Fesik, SW. (1994) Pleckstrin homology domains bind to phosphatidylinositol-4,5-bisphosphate. *Nature*, **371**(6493), 168-170.
- Haucke, V. (2005) Phosphoinositide regulation of clathrin-mediated endocytosis. *Biochem Soc Trans*, **33**(Pt 6), 1285-1289.
- Heineman, TC and Hall, SL. (2001) VZV gB endocytosis and Golgi localization are mediated by YXXphi motifs in its cytoplasmic domain. *Virology*, Vol. 285, pp. 42-49.
- Heineman, TC and Hall, SL. (2002) Role of the varicella-zoster virus gB cytoplasmic domain in gB transport and viral egress. *J Virol*, Vol. 76, pp. 591-599.
- Heineman, TC, Krudwig, N and Hall, SL. (2000) Cytoplasmic domain signal sequences that mediate transport of varicella-zoster virus gB from the endoplasmic reticulum to the Golgi. *J Virol*, Vol. 74, pp. 9421-9430.
- Heldwein, EE, Macia, E, Wang, J, Yin, HL, Kirchhausen, T and Harrison, SC. (2004) Crystal structure of the clathrin adaptor protein 1 core. *Proc Natl Acad Sci U S A*, **101**(39), 14108-14113.
- Helms, JB and Rothman, JE. (1992) Inhibition by brefeldin A of a Golgi membrane enzyme that catalyses exchange of guanine nucleotide bound to ARF. *Nature*, **360**(6402), 352-354.
- Henrich, S, Cameron, A, Bourenkov, GP, Kiefersauer, R, Huber, R, Lindberg, I, Bode, W and Than, ME. (2003) The crystal structure of the proprotein processing proteinase furin explains its stringent specificity. *Nat Struct Biol*, **10**, 520-526.

- Heriche, JK, Lebrin, F, Rabilloud, T, Leroy, D, Chambaz, EM and Goldberg, Y. (1997) Regulation of protein phosphatase 2A by direct interaction with casein kinase 2alpha. *Science*, **276**(5314), 952-955.
- Heuser, JE and Keen, J. (1988) Deep-etch visualization of proteins involved in clathrin assembly. *J Cell Biol*, **107**(3), 877-886.
- Hickenbottom, SJ, Kimmel, AR, Londos, C and Hurley, JH. (2004) Structure of a lipid droplet protein; the PAT family member TIP47. *Structure (Cambridge, Mass. : 2001)*, **12**(7), 1199-1207.
- Hickman S, Neufeld EF. (1972) A hypothesis for I-cell disease: defective hydrolases that do not enter lysosomes. *Biochem Biophys Res Commun*. **49**(4):992-9
- Hinners, I, Wendler, F, Fei, H, Thomas, L, Thomas, G and Tooze, SA. (2003) AP-1 recruitment to VAMP4 is modulated by phosphorylation-dependent binding of PACS-1. *EMBO Rep*, **4**, 1182-1189.
- Hirst, J, Bright, NA, Rous, B and Robinson, MS. (1999) Characterization of a fourth adaptor-related protein complex. *Mol Biol Cell*, **10**(8), 2787-2802.
- Hirst, J, Futter, CE and Hopkins, CR. (1998) The kinetics of mannose 6-phosphate receptor trafficking in the endocytic pathway in HEp-2 cells: the receptor enters and rapidly leaves multivesicular endosomes without accumulating in a prelysosomal compartment. *Mol Biol Cell*, **9**(4), 809-816.
- Hirst, J, Lui, WW, Bright, NA, Totty, N, Seaman, MN and Robinson, MS. (2000) A family of proteins with gamma-adaptin and VHS domains that facilitate trafficking between the trans-Golgi network and the vacuole/lysosome. *J Cell Biol*, **149**, 67-80.
- Hirst, J, Motley, A, Harasaki, K, Peak Chew, SY and Robinson, MS. (2003) EpsinR: an ENTH domain-containing protein that interacts with AP-1. *Mol Biol Cell*, **14**(2), 625-641.
- Horiuchi, H, Lippâe, R, McBride, HM, Rubino, M, Woodman, P, Stenmark, H, Rybin, V, Wilm, M, Ashman, K, Mann, M and Zerial, M. (1997) A novel Rab5 GDP/GTP exchange factor complexed to Rabaptin-5 links nucleotide exchange to effector recruitment and function. *Cell*, **90**(6), 1149-1159.
- Inouye M, Fu X, Shinde U. (2001) Substrate-induced activation of a trapped IMC-mediated protein folding intermediate. *Nat Struct Biol*. 2001, (4), 321-5.
- Itin, C, Rancano, C, Nakajima, Y and Pfeffer, SR. (1997) A novel assay reveals a role for soluble N-ethylmaleimide-sensitive fusion attachment protein in mannose 6-phosphate receptor transport from endosomes to the trans Golgi network. *J Biol Chem*, **272**, 27737-27744.
- Itoh, T, Koshihara, S, Kigawa, T, Kikuchi, A, Yokoyama, S and Takenawa, T. (2001) Role of the ENTH domain in phosphatidylinositol-4,5-bisphosphate binding and endocytosis. *Science*, **291**(5506), 1047-1051.
- Jain, SC, Shinde, U, Li, Y, Inouye, M and Berman, HM. (1998) The crystal structure of an autoprocessed Ser221Cys-subtilisin E-propeptide complex at 2.0 Å resolution. *J Mol Biol*, **284**, 137-144.
- Jean, F, Stella, K, Thomas, L, Liu, G, Xiang, Y, Reason, AJ and Thomas, G. (1998) alpha1-Antitrypsin Portland, a bioengineered serpin highly selective for furin: application as an antipathogenic agent. *Proc Natl Acad Sci U S A*, **95**, 7293-7298.

- Jensen, FB. (2004) Red blood cell pH, the Bohr effect, and other oxygenation-linked phenomena in blood O₂ and CO₂ transport. *Acta Physiol Scand*, **182**, 215-227.
- Jones, BG, Thomas, L, Molloy, SS, Thulin, CD, Fry, MD, Walsh, KA and Thomas, G. (1995) Intracellular trafficking of furin is modulated by the phosphorylation state of a casein kinase II site in its cytoplasmic tail. *Embo J*, **14**, 5869-5883.
- Jones, F and Grose, C. (1988) Role of cytoplasmic vacuoles in varicella-zoster virus glycoprotein trafficking and virion envelopment. *J Virol*, Vol. 62, pp. 2701-2711.
- Kakhlon O, Sakya P, Larijani B, Watson R, Tooze SA. (2006) GGA function is required for maturation of neuroendocrine secretory granules. *EMBO J*, **25(8)**, 1590-602.
- Kalinina, E, Varlamov, O and Fricker, LD. (2002) Analysis of the carboxypeptidase D cytoplasmic domain: Implications in intracellular trafficking. *J Cell Biochem*, **85**, 101-111.
- Kametaka, S, Mattera, R and Bonifacino, JS. (2005) Epidermal growth factor-dependent phosphorylation of the GGA3 adaptor protein regulates its recruitment to membranes. *Mol Cell Biol*, **25**, 7988-8000.
- Kanaseki, T and Kadota, K. (1969) The "vesicle in a basket". A morphological study of the coated vesicle isolated from the nerve endings of the guinea pig brain, with special reference to the mechanism of membrane movements. *J Cell Biol*, **42(1)**, 202-220.
- Kato, Y, Misra, S, Puertollano, R, Hurley, JH and Bonifacino, JS. (2002) Phosphoregulation of sorting signal-VHS domain interactions by a direct electrostatic mechanism. *Nat Struct Biol*, **9**, 532-536.
- Kawamoto, K, Yoshida, Y, Tamaki, H, Torii, S, Shinotsuka, C, Yamashina, S and Nakayama, K. (2002) GBF1, a guanine nucleotide exchange factor for ADP-ribosylation factors, is localized to the cis-Golgi and involved in membrane association of the COPI coat. *Traffic*, **3(7)**, 483-495.
- Keen JH, Willingham MC, Pastan IH. (1979) Clathrin-coated vesicles: isolation, dissociation and factor-dependent reassociation of clathrin baskets. *Cell*, **16(2)**:303-12.
- Keller, PM, Davison, AJ, Lowe, RS, Bennett, CD and Ellis, RW. (1986) Identification and structure of the gene encoding gpII, a major glycoprotein of varicella-zoster virus. *Virology*, Vol. 152, pp. 181-191.
- Kenyon, TK, Cohen, JI and Grose, C. (2002) Phosphorylation by the varicella-zoster virus ORF47 protein serine kinase determines whether endocytosed viral gE traffics to the trans-Golgi network or recycles to the cell membrane. *J Virol*, Vol. 76, pp. 10980-10993.
- Kirchhausen, T. (1999) Adaptors for clathrin-mediated traffic. *Annu Rev Cell Dev Biol*, **15**, 705-732.
- Kleizen B, Braakman I. (2004) Protein folding and quality control in the endoplasmic reticulum. *Curr Opin Cell Biol*, **16(4)**, 343-9.
- Kottgen, M, Benzing, T, Simmen, T, Tauber, R, Buchholz, B, Feliciangeli, S, Huber, TB, Schermer, B, Kramer-Zucker, A, Hopker, K, Simmen, KC, Tschucke, CC, Sandford, R, Kim, E, Thomas, G and Walz, G. (2005) Trafficking of TRPP2 by PACS proteins represents a novel mechanism of ion channel regulation. *Embo J*, **24**, 705-716.

- Krantz, DE, Waites, C, Oorschot, V, Liu, Y, Wilson, RI, Tan, PK, Klumperman, J and Edwards, RH. (2000) A phosphorylation site regulates sorting of the vesicular acetylcholine transporter to dense core vesicles. *J Cell Biol*, **149**, 379-396.
- Krysan, DJ, Rockwell, NC and Fuller, RS. (1999) Quantitative characterization of furin specificity. Energetics of substrate discrimination using an internally consistent set of hexapeptidyl methylcoumarinamides. *J Biol Chem*, **274**, 23229-23234.
- Kusk, M, Ahmed, R, Thomsen, B, Bendixen, C, Issinger, OG and Boldyreff, B. (1999) Interactions of protein kinase CK2beta subunit within the holoenzyme and with other proteins. *Mol Cell Biochem*, **191**, 51-58.
- Lefrancois, S, Zeng, J, Hassan, AJ, Canuel, M and Morales, CR. (2003) The lysosomal trafficking of sphingolipid activator proteins (SAPs) is mediated by sortilin. *EMBO J*, **22**, 6430-6437.
- Lehner, B, Semple, JI, Brown, SE, Counsell, D, Campbell, RD and Sanderson, CM. (2004) Analysis of a high-throughput yeast two-hybrid system and its use to predict the function of intracellular proteins encoded within the human MHC class III region. *Genomics*, **83**, 153-167.
- Lehrman, MA, Goldstein, JL, Brown, MS, Russell, DW and Schneider, WJ. (1985a) Internalization-defective LDL receptors produced by genes with nonsense and frameshift mutations that truncate the cytoplasmic domain. *Cell*, **41(3)**, 735-743.
- Lehrman, MA, Schneider, WJ, Sèudhof, TC, Brown, MS, Goldstein, JL and Russell, DW. (1985b) Mutation in LDL receptor: Alu-Alu recombination deletes exons encoding transmembrane and cytoplasmic domains. *Science*, **227(4683)**, 140-146.
- Leroy, D, Herichâe, JK, Filhol, O, Chambaz, EM and Cochet, C. (1997) Binding of polyamines to an autonomous domain of the regulatory subunit of protein kinase CK2 induces a conformational change in the holoenzyme. A proposed role for the kinase stimulation. *J Biol Chem*, **272**, 20820-20827.
- Leroy, D, Schmid, N, Behr, JP, Filhol, O, Pares, S, Garin, J, Bourgarit, JJ, Chambaz, EM and Cochet, C. (1995) Direct identification of a polyamine binding domain on the regulatory subunit of the protein kinase casein kinase 2 by photoaffinity labeling. *J Biol Chem*, **270**, 17400-17406.
- Lin, SX, Mallet, WG, Huang, AY and Maxfield, FR. (2004) Endocytosed cation-independent mannose 6-phosphate receptor traffics via the endocytic recycling compartment en route to the trans-Golgi network and a subpopulation of late endosomes. *Mol Biol Cell*, **15(2)**, 721-733.
- Lippincott-Schwartz, J, Yuan, LC, Bonifacino, JS and Klausner, RD. (1989) Rapid redistribution of Golgi proteins into the ER in cells treated with brefeldin A: evidence for membrane cycling from Golgi to ER. *Cell*, **56(5)**, 801-813.
- Litchfield, DW. (2003) Protein kinase CK2: structure, regulation and role in cellular decisions of life and death. *Biochem J*, **369**, 1-15.
- Litchfield, DW, Lozeman, FJ, Piening, C, Sommercorn, J, Takio, K, Walsh, KA and Krebs, EG. (1990) Subunit structure of casein kinase II from bovine testis. Demonstration that the alpha and alpha' subunits are distinct polypeptides. *J Biol Chem*, **265**, 7638-7644.
- Litwin, V, Jackson, W and Grose, C. (1992) Receptor properties of two varicella-zoster virus glycoproteins, gpI and gpIV, homologous to herpes simplex virus gE and gI. In *J Virol*, Vol. 66, pp. 3643-3651.

- Lobel, P, Fujimoto, K, Ye, RD, Griffiths, G and Kornfeld, S. (1989) Mutations in the cytoplasmic domain of the 275 kd mannose 6-phosphate receptor differentially alter lysosomal enzyme sorting and endocytosis. *Cell*, **57(5)**, 787-796.
- Lombardi, D, Soldati, T, Riederer, MA, Goda, Y, Zerial, M and Pfeffer, SR. (1993) Rab9 functions in transport between late endosomes and the trans Golgi network. *Embo J*, **12(2)**, 677-682.
- Mallard, F, Antony, C, Tenza, D, Salamero, J, Goud, B and Johannes, L. (1998) Direct pathway from early/recycling endosomes to the Golgi apparatus revealed through the study of shiga toxin B-fragment transport. *J Cell Biol*, Vol. 143, pp. 973-990.
- Mallard, F, Tang, BL, Galli, T, Tenza, D, Saint-Pol, A, Yue, X, Antony, C, Hong, W, Goud, B and Johannes, L. (2002) Early/recycling endosomes-to-TGN transport involves two SNARE complexes and a Rab6 isoform. *J Cell Biol*, Vol. 156, pp. 653-664.
- Mallet, WG and Maxfield, FR. (1999) Chimeric forms of furin and TGN38 are transported with the plasma membrane in the trans-Golgi network via distinct endosomal pathways. *J Cell Biol*, **146**, 345-359.
- Mallory, S, Sommer, M and Arvin, AM. (1997) Mutational analysis of the role of glycoprotein I in varicella-zoster virus replication and its effects on glycoprotein E conformation and trafficking. *J Virol*, Vol. 71, pp. 8279-8288.
- Mancias JD, Goldberg J. (2005) Exiting the endoplasmic reticulum. *Traffic*. 2005 **6(4)**, 278-85.
- Maresova, L, Pasiaka, T, Wagenaar, T, Jackson, W and Grose, C. (2003) Identification of the authentic varicella-zoster virus gB (gene 31) initiating methionine overlapping the 3' end of gene 30. *J Med Virol*, Vol. 70 Suppl 1, pp. S64-70.
- Marsh, M and Helenius, A. (2006) Virus entry: open sesame. *Cell*, **124(4)**, 729-740.
- Marsh, M and Pelchen-Matthews, A. (2000) Endocytosis in viral replication. *Traffic*, **1(7)**, 525-532.
- Martinez, O, Schmidt, A, Salamãero, J, Hoflack, B, Roa, M and Goud, B. (1994) The small GTP-binding protein rab6 functions in intra-Golgi transport. *J Cell Biol*, **127(6) Pt 1**, 1575-1588.
- Matsui Y, Kikuchi A, Araki S, Hata Y, Kondo J, Teranishi Y, Takai Y. (1990) Molecular cloning and characterization of a novel type of regulatory protein (GDI) for smg p25A, a ras p21-like GTP-binding protein. *Mol Cell Biol*. **10(8)**, 4116-22.
- Matsuoka, S, Huang, M and Elledge, SJ. (1998) Linkage of ATM to cell cycle regulation by the Chk2 protein kinase. *Science*, **282(5395)**, 1893-1897.
- Mattera, R, Arighi, CN, Lodge, R, Zerial, M and Bonifacino, JS. (2003) Divalent interaction of the GGAs with the Rabaptin-5-Rabex-5 complex. *EMBO J*, **22**, 78-88.
- McKay, MM and Kahn, RA. (2004) Multiple phosphorylation events regulate the subcellular localization of GGA1. *Traffic*, **5**, 102-116.
- McNew JA, Parlati F, Fukuda R, Johnston RJ, Paz K, Paumet F, Sollner TH, Rothman JE. Compartmental specificity of cellular membrane fusion encoded in SNARE proteins. *Nature*, **407(6801)**, 153-9.
- Medigeshi, GR and Schu, P. (2003) Characterization of the in vitro retrograde transport of MPR46. *Traffic*, **4**, 802-811.

- Meggio, F and Pinna, LA. (2003) One-thousand-and-one substrates of protein kinase CK2? *FASEB J*, **17**, 349-368.
- Méresse, S and Hoflack, B. (1993) Phosphorylation of the cation-independent mannose 6-phosphate receptor is closely associated with its exit from the trans-Golgi network. *J Cell Biol*, **120**, 67-75.
- Metz, T, Harris, AW, Adams, JM and Walter. (1995) Absence of p53 allows direct immortalization of hematopoietic cells by the myc and raf oncogenes. *Cell*, **82(1)**, 29-36.
- Meyer, C, Zizioli, D, Lausmann, S, Eskelinen, EL, Hamann, J, Saftig, P, von Figura, K and Schu, P. (2000) mu1A-adaptin-deficient mice: lethality, loss of AP-1 binding and rerouting of mannose 6-phosphate receptors. *Embo J*, **19**, 2193-2203.
- Miller, GJ, Mattera, R, Bonifacino, JS and Hurley, JH. (2003) Recognition of accessory protein motifs by the gamma-adaptin ear domain of GGA3. *Nat Struct Biol*, **10(8)**, 599-606.
- Misra, S, Puertollano, R, Kato, Y, Bonifacino, JS and Hurley, JH. (2002) Structural basis for acidic-cluster-dileucine sorting-signal recognition by VHS domains. *Nature*, **415**, 933-937.
- Miura, S, Gan, JW, Brzostowski, J, Parisi, MJ, Schultz, CJ, Londos, C, Oliver, B and Kimmel, AR. (2002) Functional conservation for lipid storage droplet association among Perilipin, ADRP, and TIP47 (PAT)-related proteins in mammals, *Drosophila*, and *Dictyostelium*. *J Biol Chem*, **277(35)**, 32253-32257.
- Molloy, SS, Anderson, ED, Jean, F and Thomas, G. (1999) Bi-cycling the furin pathway: from TGN localization to pathogen activation and embryogenesis. *Trends Cell Biol*, **9**, 28-35.
- Molloy, SS, Bresnahan, PA, Leppla, SH, Klimpel, KR and Thomas, G. (1992) Human furin is a calcium-dependent serine endoprotease that recognizes the sequence Arg-X-X-Arg and efficiently cleaves anthrax toxin protective antigen. *J Biol Chem*, **267**, 16396-16402.
- Molloy, SS, Thomas, L, Kamibayashi, C, Mumby, MC and Thomas, G. (1998) Regulation of endosome sorting by a specific PP2A isoform. *J Cell Biol*, **142**, 1399-1411.
- Molloy, SS, Thomas, L, VanSlyke, JK, Stenberg, PE and Thomas, G. (1994) Intracellular trafficking and activation of the furin proprotein convertase: localization to the TGN and recycling from the cell surface. *Embo J*, **13**, 18-33.
- Montalvo, EA, Parmley, RT and Grose, C. (1985) Structural analysis of the varicella-zoster virus gp98-gp62 complex: posttranslational addition of N-linked and O-linked oligosaccharide moieties. *J Virol*, Vol. 53, pp. 761-770.
- Muslin, AJ, Tanner, JW, Allen, PM and Shaw, AS. (1996) Interaction of 14-3-3 with signaling proteins is mediated by the recognition of phosphoserine. *Cell*, **84**, 889-897.
- Mutter, GL, Grills, GS and Wolgemuth, DJ. (1988) Evidence for the involvement of the proto-oncogene *c-mos* in mammalian meiotic maturation and possibly very early embryogenesis. *Embo J*, **7(3)**, 683-689.
- Nebenfuhr A, Ritzenthaler C, Robinson DG. (2002) Brefeldin A: deciphering an enigmatic inhibitor of secretion. *Plant Physiol*. **130(3)**, 1102-8.

- Nichols, BJ, Ungermann, C, Pelham, HR, Wickner, WT and Haas, A. (1997) Homotypic vacuolar fusion mediated by t- and v-SNAREs. *Nature*, **387(6629)**, 199-202.
- Niefind, K, Guerra, B, Ermakowa, I and Issinger, OG. (2001) Crystal structure of human protein kinase CK2: insights into basic properties of the CK2 holoenzyme. *EMBO J*, **20**, 5320-5331.
- Nielsen, MS, Madsen, P, Christensen, EI, Nykjaer, A, Gliemann, J, Kasper, D, Pohlmann, R and Petersen, CM. (2001) The sortilin cytoplasmic tail conveys Golgi-endosome transport and binds the VHS domain of the GGA2 sorting protein. *EMBO J*, **20**, 2180-2190.
- Nogi, T, Shiba, Y, Kawasaki, M, Shiba, T, Matsugaki, N, Igarashi, N, Suzuki, M, Kato, R, Takatsu, H, Nakayama, K and Wakatsuki, S. (2002) Structural basis for the accessory protein recruitment by the gamma-adaptin ear domain. *Nat Struct Biol*, **9(7)**, 527-531.
- Norais, N, Hall, JA, Gross, L, Tang, D, Kaur, S, Chamberlain, SH, Burke, RL and Marcus, F. (1996) Evidence for a phosphorylation site in cytomegalovirus glycoprotein gB. *J Virol*, Vol. 70, pp. 5716-5719.
- Novick, P, Field, C and Schekman, R. (1980) Identification of 23 complementation groups required for post-translational events in the yeast secretory pathway. *Cell*, **21(1)**, 205-215.
- Ohno, H, Aguilar, RC, Yeh, D, Taura, D, Saito, T and Bonifacino, JS. (1998) The medium subunits of adaptor complexes recognize distinct but overlapping sets of tyrosine-based sorting signals. *J Biol Chem*, **273(40)**, 25915-25921.
- Ohno, H, Stewart, J, Fournier, MC, Bosshart, H, Rhee, I, Miyatake, S, Saito, T, Gallusser, A, Kirchhausen, T and Bonifacino, JS. (1995) Interaction of tyrosine-based sorting signals with clathrin-associated proteins. *Science*, **269(5232)**, 1872-1875.
- Oka, Y and Czech, MP. (1986) The type II insulin-like growth factor receptor is internalized and recycles in the absence of ligand. *J Biol Chem*, **261(20)**, 9090-9093.
- Oka, Y, Rozek, LM and Czech, MP. (1985) Direct demonstration of rapid insulin-like growth factor II Receptor internalization and recycling in rat adipocytes. Insulin stimulates 125I-insulin-like growth factor II degradation by modulating the IGF-II receptor recycling process. *J Biol Chem*, **260(16)**, 9435-9442.
- Olson, JK and Grose, C. (1997) Endocytosis and recycling of varicella-zoster virus Fc receptor glycoprotein gE: internalization mediated by a YXXL motif in the cytoplasmic tail. *J Virol*, Vol. 71, pp. 4042-4054.
- Olson, JK and Grose, C. (1998) Complex formation facilitates endocytosis of the varicella-zoster virus gE:gI Fc receptor. *J Virol*, Vol. 72, pp. 1542-1551.
- Padmanabha, R, Chen-Wu, JL, Hanna, DE and Glover, CV. (1990) Isolation, sequencing, and disruption of the yeast CKA2 gene: casein kinase II is essential for viability in *Saccharomyces cerevisiae*. *Mol Cell Biol*, **10(8)**, 4089-4099.
- Palade, G. (1975) Intracellular aspects of the process of protein synthesis. *Science*, **189(4200)**, 347-358.
- Paleotti, O, Macia, E, Luton, F, Klein, S, Partisani, M, Chardin, P, Kirchhausen, T and Franco, M. (2005) The small G-protein ARF6GTP recruits the AP-2 adaptor complex to membranes. *J Biol Chem*, **280(22)**, 21661-21666.

- Pasieka, TJ, Maresova, L and Grose, C. (2003) A functional YNKI motif in the short cytoplasmic tail of varicella-zoster virus glycoprotein gH mediates clathrin-dependent and antibody-independent endocytosis. *J Virol*, Vol. 77, pp. 4191-4204.
- Pasieka, TJ, Maresova, L, Shiraki, K and Grose, C. (2004) Regulation of Varicella-Zoster Virus-Induced Cell-to-Cell Fusion by the Endocytosis-Competent Glycoproteins gH and gE. *J Virol*, Vol. 78, pp. 2884-2896.
- Pearse, BM. (1975). coated vesicles from pig brain: purification and biochemical characterization. *J Mol Bio*. **97**, 93-98
- Peden, AA, Oorschot, V, Hesser, BA, Austin, CD, Scheller, RH and Klumperman, J. (2004) Localization of the AP-3 adaptor complex defines a novel endosomal exit site for lysosomal membrane proteins. *J Cell Biol*, **164**(7), 1065-1076.
- Peter, BJ, Kent, HM, Mills, IG, Vallis, Y, Butler, PJ, Evans, PR and McMahon, HT. (2004) BAR domains as sensors of membrane curvature: the amphiphysin BAR structure. *Science*, **303**(5657), 495-499.
- Pfeffer, S and Aivazian, D. (2004) Targeting Rab GTPases to distinct membrane compartments. *Nat Rev Mol Cell Biol*, **5**(11), 886-896.
- Piguet, V, Chen, YL, Mangasarian, A, Foti, M, Carpentier, JL and Trono, D. (1998) Mechanism of Nef-induced CD4 endocytosis: Nef connects CD4 with the mu chain of adaptor complexes. *Embo J*, **17**, 2472-2481.
- Piguet, V, Wan, L, Borel, C, Mangasarian, A, Demaurex, N, Thomas, G and Trono, D. (2000) HIV-1 Nef protein binds to the cellular protein PACS-1 to downregulate class I major histocompatibility complexes. *Nat Cell Biol*, **2**, 163-167.
- Pinna, LA. (2002) Protein kinase CK2: a challenge to canons. *J Cell Sci*, **115**, 3873-3878.
- Plutner, H, Cox, AD, Pind, S, Khosravi-Far, R, Bourne, JR, Schwaninger, R, Der, CJ and Balch, WE. (1991) Rab1b regulates vesicular transport between the endoplasmic reticulum and successive Golgi compartments. *J Cell Biol*, **115**(1), 31-43.
- Poussu, A, Lohi, O and Lehto, VP. (2000) Vear, a novel Golgi-associated protein with VHS and gamma-adaptin "ear" domains. *J Biol Chem*, **275**, 7176-7183.
- Puertollano, R, Aguilar, RC, Gorshkova, I, Crouch, RJ and Bonifacino, JS. (2001a) Sorting of mannose 6-phosphate receptors mediated by the GGAs. *Science*, **292**, 1712-1716.
- Puertollano, R, Randazzo, PA, Presley, JF, Hartnell, LM and Bonifacino, JS. (2001b) The GGAs promote ARF-dependent recruitment of clathrin to the TGN. *Cell*, **105**, 93-102.
- Puertollano, R and Bonifacino, JS. (2004) Interactions of GGA3 with the ubiquitin sorting machinery. *Nat Cell Biol*, **6**, 244-251.
- Pufall, MA and Graves, BJ. (2002) Autoinhibitory Domains: Modular Effectors of Cellular Regulation. *Annu Rev Cell Dev Biol*.
- Radhakrishna, H and Donaldson, JG. (1997) ADP-ribosylation factor 6 regulates a novel plasma membrane recycling pathway. *J Cell Biol*, **139**(1), 49-61.
- Raiborg, C, Rusten, TE and Stenmark, H. (2003) Protein sorting into multivesicular endosomes. *Curr Opin Cell Biol*, **15**(4), 446-455.
- Randazzo PA, Kahn RA. (1994) GTP hydrolysis by ADP-ribosylation factor is dependent on both an ADP-ribosylation factor GTPase-activating protein and acid phospholipids. *J Biol Chem*, **269**(14), 10758-63.

- Rapoport, I, Chen, YC, Cupers, P, Shoelson, SE and Kirchhausen, T. (1998) Dileucine-based sorting signals bind to the beta chain of AP-1 at a site distinct and regulated differently from the tyrosine-based motif-binding site. *Embo J*, **17**(8), 2148-2155.
- Reitman ML, Kornfeld S. (1981) UDP-N-acetylglucosamine:glycoprotein N-acetylglucosamine-1-phosphotransferase. Proposed enzyme for the phosphorylation of the high mannose oligosaccharide units of lysosomal enzymes. *J Biol Chem*, **256**(9), 4275-81.
- Rhodes, CJ, Thorne, BA, Lincoln, B, Nielsen, E, Hutton, JC and Thomas, G. (1993) Processing of proopiomelanocortin by insulin secretory granule proinsulin processing endopeptidases. *J Biol Chem*, **268**, 4267-4275.
- Rink, J, Ghigo, E, Kalaidzidis, Y and Zerial, M. (2005) Rab conversion as a mechanism of progression from early to late endosomes. *Cell.*, **122**(5), 735-749.
- Robinson, MS. (2004) Adaptable adaptors for coated vesicles. *Trends Cell Biol*, **14**, 167-174.
- Rockwell, NC, Krysan, DJ, Komiyama, T and Fuller, RS. (2002) Precursor processing by kex2/furin proteases. *Chem Rev*, **102**, 4525-4548.
- Rockwell, NC and Thorner, JW. (2004) The kindest cuts of all: crystal structures of Kex2 and furin reveal secrets of precursor processing. *Trends Biochem Sci*, **29**, 80-87.
- Rohde, G, Wenzel, D and Haucke, V. (2002) A phosphatidylinositol (4,5)-bisphosphate binding site within mu2-adaptin regulates clathrin-mediated endocytosis. *J Cell Biol*, **158**(2), 209-214.
- Roth, MG. (2004) Phosphoinositides in constitutive membrane traffic. *Physiol Rev*, Vol. 84, pp. 699-730.
- Roth, TF and Porter, KR. (1964) Yolk Protein Uptake in the Oocyte of the Mosquito *Aedes Aegypti*. L. *J Cell Biol*, **20**, 313-332.
- Rotzschke, O, Lau, JM, Hofstatter, M, Falk, K and Strominger, JL. (2002) A pH-sensitive histidine residue as control element for ligand release from HLA-DR molecules. *Proc Natl Acad Sci U S A*, **99**, 16946-16950.
- Saint-Pol, A, Yâelamos, B, Amessou, M, Mills, IG, Dugast, M, Tenza, D, Schu, P, Antony, C, McMahon, HT, Lamaze, C and Johannes, L. (2004) Clathrin adaptor epsinR is required for retrograde sorting on early endosomal membranes. *Dev Cell*, **6**, 525-538.
- Sandvig, K and van Deurs, B. (2002) Transport of protein toxins into cells: pathways used by ricin, cholera toxin and Shiga toxin. *FEBS Lett*, Vol. 529, pp. 49-53.
- Santos, RA, Padilla, JA, Hatfield, C and Grose, C. (1998) Antigenic variation of varicella zoster virus Fc receptor gE: loss of a major B cell epitope in the ectodomain. *Virology*, Vol. 249, pp. 21-31.
- Schermer, B, Hèopker, K, Omran, H, Ghenoïu, C, Fliegau, M, Fekete, A, Horvath, J, Kèottgen, M, Hackl, M, Zschiedrich, S, Huber, TB, Kramer-Zucker, A, Zentgraf, H, Blaukat, A, Walz, G and Benzing, T. (2005) Phosphorylation by casein kinase 2 induces PACS-1 binding of nephrocystin and targeting to cilia. *Embo J*, **24**(24), 4415-4424.
- Schwartz, O, Marâechal, V, Le Gall, S, Lemonnier, F and Heard, JM. (1996) Endocytosis of major histocompatibility complex class I molecules is induced by the HIV-1 Nef protein. *Nat Med*, **2**(3), 338-342.

- Schwede, T, Kopp, J, Guex, N and Peitsch, MC. (2003) SWISS-MODEL: An automated protein homology-modeling server. *Nucleic Acids Res*, **31**, 3381-3385.
- Scott, GK, Gu, F, Crump, CM, Thomas, L, Wan, L, Xiang, Y and Thomas, G. (2003) The phosphorylation state of an autoregulatory domain controls PACS-1-directed protein traffic. *EMBO J*, **22**, 6234-6244.
- Seaman, MN. (2004) Cargo-selective endosomal sorting for retrieval to the Golgi requires retromer. *J Cell Biol*, **165**, 111-122.
- Seaman, MN, McCaffery, JM and Emr, SD. (1998) A membrane coat complex essential for endosome-to-Golgi retrograde transport in yeast. *J Cell Biol*, **142(3)**, 665-681.
- Serafini, T, Orci, L, Amherdt, M, Brunner, M, Kahn, RA and Rothman, JE. (1991) ADP-ribosylation factor is a subunit of the coat of Golgi-derived COP-coated vesicles: a novel role for a GTP-binding protein. *Cell*, **67(2)**, 239-253.
- Simmen, T, Aslan, JE, Blagoveshchenskaya, AD, Thomas, L, Wan, L, Xiang, Y, Feliciangeli, SF, Hung, CH, Crump, CM and Thomas, G. (2005) PACS-2 controls endoplasmic reticulum-mitochondria communication and Bid-mediated apoptosis. *EMBO J*, **24**, 717-729.
- Simmen, T, Hèoning, S, Icking, A, Tikkanen, R and Hunziker, W. (2002) AP-4 binds basolateral signals and participates in basolateral sorting in epithelial MDCK cells. *Nat Cell Biol*, **4(2)**, 154-159.
- Simonsen, A, Lippâe, R, Christoforidis, S, Gaullier, JM, Brech, A, Callaghan, J, Toh, BH, Murphy, C, Zerial, M and Stenmark, H. (1998) EEA1 links PI(3)K function to Rab5 regulation of endosome fusion. *Nature*, **394(6692)**, 494-498.
- Skjerpen, CS, Nilsen, T, Wesche, J and Olsnes, S. (2002) Binding of FGF-1 variants to protein kinase CK2 correlates with mitogenicity. *EMBO J*, **21**, 4058-4069.
- Sly, W. S., and Fischer, H. D. (1982). The phosphomannosyl recognition system for intracellular and intercellular transport of lysosomal enzymes. *J. Cell. Biochem*, **18**, 67-85.
- Sontag, E. (2001) Protein phosphatase 2A: the Trojan Horse of cellular signaling. *Cell Signal*, **13(1)**, 7-16.
- Stamnes MA, Rothman JE. (1993) The binding of AP-1 clathrin adaptor particles to Golgi membranes requires ADP-ribosylation factor, a small GTP-binding protein. *Cell*, **73(5)**, 999-1005.
- Steiner, DF. (1998) The proprotein convertases. *Curr Opin Chem Biol*, **2**, 31-39.
- Stockli, J, Hèoning, S and Rohrer, J. (2004) The acidic cluster of the CK2 site of the cation-dependent mannose 6-phosphate receptor (CD-MPR) but not its phosphorylation is required for GGA1 and AP-1 binding. *J Biol Chem*, **279(22)**, 23542-23549.
- Stoorvogel, W, Strous, GJ, Geuze, HJ, Oorschot, V and Schwartz, AL. (1991) Late endosomes derive from early endosomes by maturation. *Cell*, **65(3)**, 417-427.
- Subbian, E, Yabuta, Y and Shinde, UP. (2005) Folding pathway mediated by an intramolecular chaperone: intrinsically unstructured propeptide modulates stochastic activation of subtilisin. *J Mol Biol*, **347**, 367-383.
- Suer, S, Misra, S, Saidi, LF and Hurley, JH. (2003) Structure of the GAT domain of human GGA1: a syntaxin amino-terminal domain fold in an endosomal trafficking adaptor. *Proc Natl Acad Sci U S A*, **100(8)**, 4451-4456.

- Sutton, RB, Fasshauer, D, Jahn, R and Brunger, AT. (1998) Crystal structure of a SNARE complex involved in synaptic exocytosis at 2.4 Å resolution. *Nature*, **395**(6700), 347-353.
- Takatsu, H, Yoshino, K and Nakayama, K. (2000) Adaptor gamma ear homology domain conserved in gamma-adaptin and GGA proteins that interact with gamma-synergin. *BioChem Biophys Res Comm*, **271**, 719-725.
- Tangrea, MA, Alexander, P, Bryan, PN, Eisenstein, E, Toedt, J and Orban, J. (2001) Stability and global fold of the mouse prohormone convertase 1 pro-domain. *Biochemistry*, **40**, 5488-5495.
- Tangrea, MA, Bryan, PN, Sari, N and Orban, J. (2002) Solution structure of the prohormone convertase 1 pro-domain from *Mus musculus*. *J Mol Biol*, **320**, 801-812.
- Teuchert, M, Schafer, W, Berghofer, S, Hoflack, B, Klenk, HD and Garten, W. (1999) Sorting of furin at the trans-Golgi network. Interaction of the cytoplasmic tail sorting signals with AP-1 Golgi-specific assembly proteins. *J Biol Chem*, **274**, 8199-8207.
- Thomas, G. (2002) Furin at the cutting edge: from protein traffic to embryogenesis and disease. *Nat Rev Mol Cell Biol*, **3**, 753-766.
- Tirabassi, RS and Enquist, LW. (1998) Role of envelope protein gE endocytosis in the pseudorabies virus life cycle. *J Virol*, Vol. 72, pp. 4571-4579.
- Tisdale, EJ, Bourne, JR, Khosravi-Far, R, Der, CJ and Balch, WE. (1992) GTP-binding mutants of rab1 and rab2 are potent inhibitors of vesicular transport from the endoplasmic reticulum to the Golgi complex. *J Cell Biol*, **119**(4), 749-761.
- Tomkowicz, B, Lee, C, Ravyn, V, Cheung, R, Ptasznik, A and Collman, R. (2006) The Src kinase Lyn is required for CCR5 signaling in response to MIP-1{beta} and R5 HIV-1 gp120 in human macrophages. *Blood*, **in press**.
- Tooze, J, Hollinshead, M, Reis, B, Radsak, K and Kern, H. (1993) Progeny vaccinia and human cytomegalovirus particles utilize early endosomal cisternae for their envelopes. *Eur J Cell Biol*, Vol. 60, pp. 163-178.
- Tondeur M, Vamos-Hurwitz E, Cremer N, Loeb H. (1971) Mucopolysaccharidosis in a three months old infant. Clinical and ultrastructural studies. *Acta Paediatr Scand*, **60**(1), 98-101.
- Touchot N, Chardin P, and Tavitian A. (1987) Four Additional Members of the ras Gene Superfamily Isolated by an Oligonucleotide Strategy: Molecular Cloning of YPT-Related cDNAs from a Rat Brain Library. *PNAS* **84**, 8210-8214.
- Trowbridge, IS. (1991) Endocytosis and signals for internalization. *Curr Opin Cell Biol*, Vol. 3, pp. 634-641.
- van Dam, EM and Stoorvogel, W. (2002) Dynamin-dependent transferrin receptor recycling by endosome-derived clathrin-coated vesicles. *Molecular biology of the cell*, **13**(1), 169-182.
- van Dam, EM, Ten Broeke, T, Jansen, K, Spijkers, P and Stoorvogel, W. (2002) Endocytosed transferrin receptors recycle via distinct dynamin and phosphatidylinositol 3-kinase-dependent pathways. *The Journal of biological chemistry*, **277**(50), 48876-48883.
- van der Sluijs, P, Hull, M, Webster, P, Mãale, P, Goud, B and Mellman, I. (1992) The small GTP-binding protein rab4 controls an early sorting event on the endocytic pathway. *Cell*, **70**(5), 729-740.

- Van Der Sluijs, P, Hull, M, Zahraoui, A, Tavitian, A, Goud, B and Mellman, I. (1991) The small GTP-binding protein rab4 is associated with early endosomes. *Proc Natl Acad Sci U S A*, **88(14)**, 6313-6317.
- Varlamov, O, Kalinina, E, Che, FY and Fricker, LD. (2001) Protein phosphatase 2A binds to the cytoplasmic tail of carboxypeptidase D and regulates post-trans-Golgi network trafficking. *J Cell Sci*, **114**, 311-322.
- Volpicelli-Daley, LA, Li, Y, Zhang, CJ and Kahn, RA. (2005) Isoform-selective effects of the depletion of ADP-ribosylation factors 1-5 on membrane traffic. *Mol Biol Cell*, **16(10)**, 4495-4508.
- Voorhees, P, Deignan, E, van Donselaar, E, Humphrey, J, Marks, MS, Peters, PJ and Bonifacino, JS. (1995) An acidic sequence within the cytoplasmic domain of furin functions as a determinant of trans-Golgi network localization and internalization from the cell surface. *Embo J*, **14(20)**, 4961-4975.
- Waheed A, Hasilik A, von Figura K. (1981) Processing of the phosphorylated recognition marker in lysosomal enzymes. Characterization and partial purification of a microsomal alpha-N-acetylglucosaminyl phosphodiesterase. *J Biol Chem*, **256(11)**, 5717-21.
- Wahle, T, Prager, K, Raffler, N, Haass, C, Famulok, M and Walter, J. (2005) GGA proteins regulate retrograde transport of BACE1 from endosomes to the trans-Golgi network. *Mol Cell Neurosci*, **29**, 453-461.
- Waites, CL, Mehta, A, Tan, PK, Thomas, G, Edwards, RH and Krantz, DE. (2001) An acidic motif retains vesicular monoamine transporter 2 on large dense core vesicles. *J Cell Biol*, **152**, 1159-1168.
- Walworth, N, Davey, S and Beach, D. (1993) Fission yeast chk1 protein kinase links the rad checkpoint pathway to cdc2. *Nature*, **363(6427)**, 368-371.
- Wan, L, Molloy, SS, Thomas, L, Liu, G, Xiang, Y, Rybak, SL and Thomas, G. (1998) PACS-1 defines a novel gene family of cytosolic sorting proteins required for trans-Golgi network localization. *Cell*, **94**, 205-216.
- Wang, YJ, Wang, J, Sun, HQ, Martinez, M, Sun, YX, Macia, E, Kirchhausen, T, Albanesi, JP, Roth, MG and Yin, HL. (2003) Phosphatidylinositol 4 phosphate regulates targeting of clathrin adaptor AP-1 complexes to the Golgi. *Cell*, **114(3)**, 299-310.
- Wang, Z, Gershon, MD, Lungu, O, Panagiotidis, CA, Zhu, Z, Hao, Y and Gershon, AA. (1998) Intracellular transport of varicella-zoster glycoproteins. *J Infect Dis*, Vol. 178 Suppl 1, pp. S7-12.
- Wang, ZH, Gershon, MD, Lungu, O, Zhu, Z and Gershon, AA. (2000) Trafficking of varicella-zoster virus glycoprotein gI: T(338)-dependent retention in the trans-Golgi network, secretion, and mannose 6-phosphate-inhibitable uptake of the ectodomain. *J Virol*, Vol. 74, pp. 6600-6613.
- Wang, ZH, Gershon, MD, Lungu, O, Zhu, Z, Mallory, S, Arvin, AM and Gershon, AA. (2001) Essential role played by the C-terminal domain of glycoprotein I in envelopment of varicella-zoster virus in the trans-Golgi network: interactions of glycoproteins with tegument. *J Virol*, Vol. 75, pp. 323-340.
- Waters, MG, Serafini, T and Rothman, JE. (1991) 'Coatomer': a cytosolic protein complex containing subunits of non-clathrin-coated Golgi transport vesicles. *Nature*, **349(6306)**, 248-251.

- Weber, T, Zemelman, BV, McNew, JA, Westermann, B, Gmachl, M, Parlati, F, Söllner, TH and Rothman, JE. (1998) SNAREpins: minimal machinery for membrane fusion. *Cell*, **92**(6), 759-772.
- Whitney, JA, Gomez, M, Sheff, D, Kreis, TE and Mellman, I. (1995) Cytoplasmic coat proteins involved in endosome function. *Cell*, **83**(5), 703-713.
- Wiebe, CA, Dibattista, ER and Fliegel, L. (2001) Functional role of polar amino acid residues in Na⁺/H⁺ exchangers. *Biochem J*, **357**, 1-10.
- Wiesmann, U, Vassella, F and Herschkowitz, N. (1971) "I-cell" disease: leakage of lysosomal enzymes into extracellular fluids. *N Engl J Med*, **285**(19), 1090-1091.
- Wilcke, M, Johannes, L, Galli, T, Mayau, V, Goud, B and Salamero, J. (2000) Rab11 regulates the compartmentalization of early endosomes required for efficient transport from early endosomes to the trans-Golgi network. *J Cell Biol*, **151**(6), 1207-1220.
- Wolins, N, Bosshart, H, Kuster, H and Bonifacino, JS. (1997) Aggregation as a determinant of protein fate in post-Golgi compartments: role of the luminal domain of furin in lysosomal targeting. *J Cell Biol*, **139**, 1735-1745.
- Wolins, NE, Quaynor, BK, Skinner, JR, Schoenfish, MJ, Tzekov, A and Bickel, PE. (2005) S3-12, Adipophilin, and TIP47 package lipid in adipocytes. *J Biol Chem*, **280**(19), 19146-19155.
- Wolins, NE, Rubin, B and Brasaemle, DL. (2001) TIP47 associates with lipid droplets. *J Biol Chem*, **276**(7), 5101-5108.
- Xiang, Y, Molloy, SS, Thomas, L and Thomas, G. (2000) The PC6B cytoplasmic domain contains two acidic clusters that direct sorting to distinct trans-Golgi network/endosomal compartments. *Mol Biol Cell*, **11**, 1257-1273.
- Xu, X, Toselli, PA, Russell, LD and Seldin, DC. (1999) Globozoospermia in mice lacking the casein kinase II alpha' catalytic subunit. *Nat Genet*, **23**, 118-121.
- Yamaji, R, Adamik, R, Takeda, K, Togawa, A, Pacheco-Rodriguez, G, Ferrans, VJ, Moss, J and Vaughan, M. (2000) Identification and localization of two brefeldin A-inhibited guanine nucleotide-exchange proteins for ADP-ribosylation factors in a macromolecular complex. *Proc Natl Acad Sci U S A*, **97**(6), 2567-2572.
- Yamanaka, S, Johnson, MD, Grinberg, A, Westphal, H, Crawley, JN, Taniike, M, Suzuki, K and Proia, RL. (1994) Targeted disruption of the Hexa gene results in mice with biochemical and pathologic features of Tay-Sachs disease. *Proc Natl Acad Sci U S A*, **91**(21), 9975-9979.
- Zamyatnin, AA. (1984) Amino acid, peptide, and protein volume in solution. *Annu Rev Biophys Bioeng*, **13**, 145-165.
- Zaremba, S and Keen, JH. (1983) Assembly polypeptides from coated vesicles mediate reassembly of unique clathrin coats. *J Cell Biol*, **97**(5) Pt 1, 1339-1347.
- Zeng, Q, Tran, TT, Tan, HX and Hong, W. (2003) The cytoplasmic domain of Vamp4 and Vamp5 is responsible for their correct subcellular targeting: the N-terminal extension of VAMP4 contains a dominant autonomous targeting signal for the trans-Golgi network. *J Biol Chem*, **278**(25), 23046-23054.
- Zerial M, McBride H. (2001) Rab proteins as membrane organizers. *Nat Rev Mol Cell Biol*, **2**(2), 107-117.

- Zhou, A, Paquet, L and Mains, RE. (1995) Structural elements that direct specific processing of different mammalian subtilisin-like prohormone convertases. *J Biol Chem*, **270**, 21509-21516.
- Zhou, A, Webb, G, Zhu, X and Steiner, DF. (1999) Proteolytic processing in the secretory pathway. *J Biol Chem*, **274**, 20745-20748.
- Zhou, Y and Lindberg, I. (1993) Purification and characterization of the prohormone convertase PC1(PC3). *J Biol Chem*, **268**, 5615-5623.
- Zhu, Y, Doray, B, Poussu, A, Lehto, VP and Kornfeld, S. (2001) Binding of GGA2 to the lysosomal enzyme sorting motif of the mannose 6-phosphate receptor. *Science*, **292**, 1716-1718.

APPENDIX A

ENDOCYTOSIS OF VARICELLA-ZOSTER VIRUS GLYCOPROTEINS: VIRION ENVELOPMENT AND EGRESS

Charles Grose, Lucie Maresova, Guruprasad Medigeshe, Gregory K. Scott, and Gary Thomas.

Department of Pediatrics & Microbiology, University of Iowa, Iowa City, Iowa (CG, LM), and the Vollum Institute, Oregon Health Sciences University, Portland, Oregon (GM, GKS, GT)

Running title: Glycoprotein trafficking and egress of varicella virus
Title of Book: Alpha herpesviruses: Pathogenesis and Molecular Biology
Horizon Press, England.

Corresponding author:
Charles Grose
University of Iowa Hospital/2501 JCP
200 Hawkins Drive
Iowa City IA 52242
charles-grose@uiowa.edu

This Appendix is a chapter for a book on herpesviruses edited by R.Sandri-Goldin that will be published in the Fall of 2006 by Horizon press (UK). Guruprasad Medigeshe, Gary Thomas and myself wrote the section entitled “6.0. Summary of trafficking pathways” and contributed Figure 4.

Abstract

Endocytosis from the infected cell surface is a property of the four major glycoproteins of varicella-zoster virus (VZV), designated gE, gI, gB and gH. Each of these glycoproteins has a functional endocytosis motif in its cytosolic domain. Three have tyrosine based motifs, while gI has a dileucine motif. The YAGL motif of gE is located adjacent to an acidic cluster, which also contains serine and threonine residues variably phosphorylated by both a viral kinase (ORF 47 kinase) and casein kinase II. The acidic cluster interacts with a connector protein called proshphofurin acidic cluster sorting protein 1 (PACS-1) after clathrin mediated internalization. Although the function of endocytosis has been elusive, recent research suggests that the internalized VZV glycoproteins traffic to the site of virion assembly in the *trans*-Golgi network and are subsequently incorporated into the envelopes of nascent virions. In turn, the enveloped virions reside within vacuoles, which travel toward and fuse with the plasma membrane. A recombinant VZV genome containing a gE gene lacking only its endocytosis motif cannot replicate. Taken together, the above results indicate the importance of VZV glycoprotein endocytosis in the life cycle of this alpha herpesvirus.

Introduction

Endocytosis is an important process by which proteins are continually internalized within the cell through specific interactions at the plasma membrane. Cell surface receptors typically undergo endocytosis from the cell membrane through interactions with clathrin-coated pits and are often recycled through the endosomes back to the cell membrane. Both clustering in clathrin-coated pits and internalization of receptors have been shown to be dependent on internalization signals in the cytosolic domain, which have been defined as tyrosine motifs or dileucine motifs (Trowbridge, 1991). Endocytosis from the plasma membrane by a process similar to receptor-mediated endocytosis has now been demonstrated for numerous herpesvirus glycoproteins.

Varicella-zoster virus (VZV) has four major glycoproteins gE, gI, gH and gB. Their endocytosis motifs are highly conserved among all sequenced VZV strains (Davison and Scott, 1986; Grose, 1990; Grose et al., 2004). As discussed below, while the VZV glycoproteins share many characteristics with their alphaherpesvirus homologs, such as HSV and PRV, there are also unanticipated differences. One of these remarkable differences relates to trafficking pathways. In the case of VZV, glycoproteins internalized from the cell membrane are delivered to sites of assembly in the cytoplasm, where they are incorporated into nascent virions. In contrast, not all homologous glycoproteins from the closely related alpha herpesviruses appear to use the same pathways for transit to the site of assembly. For the above reasons, the subject of herpesviral glycoprotein endocytosis is reviewed. Also, the relationship of endocytosis to the deenvelopment–reenvelopment model of herpesvirus assembly and egress is discussed.

1. Glycoprotein gE

1.1 Endocytosis of VZV gE

Unlike other human herpesviruses, the predominant viral glycoprotein present on the envelope of the mature VZV virion is gE (Montalvo et al., 1985). VZV gE is a type I transmembrane protein of 623 amino acids. Of these, 544 residues are found in the ectodomain, 17 in the transmembrane domain, and 62 in the C-terminal cytosolic domain (Fig. 1; Grose, 1990). The gE protein traffics from the endoplasmic reticulum (ER) through the Golgi, where it is extensively processed, to the outer cell membrane. The extensive posttranslational modifications produce a mature gE glycoprotein of 98 kDa (Montalvo et al., 1985). Both the ectodomain and endodomain of gE have important functions. Based on the fact that a single point mutation in the VZV-MSP gE ectodomain changes VZV MSP egress pattern from a typical "viral highways" phenotype to a diffuse pattern similar to that observed in HSV infected cells (Santos et al., 1998), the ectodomain is critical for determining virus-cell interactions of the mature virion.

VZV gE was the first viral glycoprotein shown to undergo endocytosis in transfected cells (Olson and Grose, 1997). This process is mediated by a YAGL sequence (aa 582-585) located in the cytosolic domain of the protein (Fig. 1; Olson and Grose, 1997). This sequence fits the consensus tyrosine based endocytosis motif known to mediate endocytosis of numerous cellular transmembrane proteins (Bonifacino and Dell'Angelica, 1999). The tetrapeptide of the tyrosine-based motif is recognized by the alpha-2 subunit of AP-2, a clathrin-associated complex localized to the plasma membrane (Boll et al.,

1996). AP-2 facilitates the formation of clathrin-coated vesicles by acting as the adaptor between the membrane protein and clathrin. Endocytosis of gE was shown to be dependent on clathrin-coated vesicle formation within the cells. An example of the VZV endocytosis assay is shown in Fig. 2. In addition, colocalization studies showed that endocytosis of gE mimicked internalization of the transferrin receptor (Olson and Grose, 1997). Endocytic recycling of gE back to the plasma membrane post-endocytosis has been demonstrated, but there is also a pathway for gE to recycle to the *trans*-Golgi network (TGN) post-endocytosis (Alconada et al., 1996). TGN recycling is mediated by a cluster of acidic amino acids in the gE cytosolic domain (Fig.1; Grose et al., 1989). The acidic cluster of gE interacts with a connector protein, phosphofurin acidic cluster sorting protein 1 (PACS-1), and directs VZV gE from endosomes to the TGN, a proposed site of tegument assembly and virion envelopment (Crump et al., 2001b). Phosphorylation within this acidic cluster motif mediates PACS-1 interaction (Fish et al., 1998). VZV gE is phosphorylated on serine and threonine residues of its cytosolic domain (Grose et al., 1989).

In addition, differential phosphorylation of the serine and threonine residues adjacent to the gE acidic cluster by either the VZV ORF 47 protein serine kinase or the cellular casein kinase II targets endocytosed gE to either the TGN or cell surface, thereby increasing virus assembly or cell-to-cell spread, respectively (Kenyon et al., 2002). For example, in cells infected with a VZV ORF47-null mutant, internalized VZV gE recycles to the plasma membrane and causes an increased syncytial formation. Thus, endocytosis is also linked to the mechanisms of fusion in infected cells.

1.2 Endocytosis of alphaherpesvirus gE homologs

Similar to gE of VZV, pseudorabies virus (PrV) gE and herpes simplex type 1 (HSV-1) gE undergo endocytosis (Alconada et al., 1999). It has been demonstrated that PrV gE cytosolic domain is required for gE internalization from the plasma membrane (Tirabassi and Enquist, 1998). HSV-1 gE cycles between TGN and the cell surface. This TGN localization is determined by a tyrosine-based motif and an acidic stretch of amino acids in the gE cytosolic domain that are homologous to the VZV gE sites (Alconada et al., 1999). Given the high degree of conservation of the different C-terminal sorting signals in all of the alphaherpesvirus gE homologs, it would seem likely that these molecules traffic inside the cell following identical signal-mediated transport processes. Yet, studies described below will show that this assumption appears not to be true.

2. VZV Glycoprotein gI

2.1 Endocytosis of VZV gI

VZV gI is a type I transmembrane glycoprotein of 354 amino acids, 59 of which are cytosolic (Grose, 2002). Similar to gE, VZV gI also contains trafficking motifs in its cytosolic domain that mediate similar functions; however, the motifs are different (Fig. 1). While a YAGL tyrosine motif mediates gE endocytosis, a di-leucine motif ML at amino acids 328-329 mediates gI endocytosis (Olson and Grose, 1998). And instead of an acidic cluster for TGN targeting, gI has a threonine at position 338 that when mutated disrupts gI TGN targeting (Wang et al., 2000). VZV gE and gI form a complex in infected cells or when cotransfected. This non-covalent complex forms a biologically

active human Fc receptor (Litwin et al., 1992). Although gI can internalize in the absence of gE, complex formation between gE:gI increases the efficiency of gE:gI endocytosis over that of gE or gI alone (Olson and Grose, 1998). Complex formation between gE and gI is also able to direct internalization of a gE endocytosis deficient mutant, which suggests that the gI motif may be more efficient than that of gE (Olson and Grose, 1998). Further, this result suggests that VZV gI behaves as an accessory component by facilitating the endocytosis of the major constituent gE and thereby modulating the trafficking of the entire cell surface gE:gI complex. The fact that a VZV gI null mutant spreads very poorly in cell culture reinforces the importance of the VZV gE:gI complex (Mallory et al., 1997).

2.2 Endocytosis of alphaherpesvirus gI homologs

Complex formation and subsequent endocytosis between gE and gI and endocytosis as a complex has been shown not only in VZV, but also PrV and HSV. (Alconada et al., 1998). In contrast to VZV, however, the PrV gI protein cannot be internalized from the plasma membrane on its own. Thus, the PrV and VZV gI proteins seem to have functionally different roles in endocytosis, as the VZV gI protein increases the rate of internalization of the VZV gE protein, while the PrV gE protein directs endocytosis of the PrV gI protein.

3. VZV Glycoprotein B

3.1 Endocytosis of VZV gB

VZV gB is the second most abundant VZV glycoprotein and also the most conserved among the herpesvirus glycoproteins. VZV gB shares a higher degree of homology (49%) with gB of HSV-1 than that found between any other two VZV- HSV homologous glycoproteins (which range from 24 to 27%; Edson et al., 1985). The alphaherpesvirus gB homologs are required for virus replication, attachment to and penetration of the host membrane, and fusion (Cai et al., 1988). VZV gB is a type 1 membrane protein consisting of a large ectodomain, a hydrophobic transmembrane region, and a cytosolic domain (Davison and Scott, 1986). The mature 140 kDa form of gB is proteolytically cleaved into a disulfide linked heterodimer consisting of 66 and 68 kDa components (Keller et al., 1986). The length of the signal sequence has been recently corrected to include 71 amino acids, thereby giving gB a length of 931 amino acids (Maresova et al., 2003). Since the gB protein cytosolic domain is predicted to contain 125 amino acids, it has the longest cytosolic domain of any VZV encoded membrane protein (Fig. 1; Elliott and O'Hare, 1999). VZV gB accumulates in the Golgi of infected cells (Wang et al., 1998), and the cytosolic domain of gB contains specific sequences that are required for both its ER to Golgi transport and post-Golgi transport (Heineman and Hall, 2002).

The VZV gB protein contains three consensus internalization motifs within its cytosolic domain: two tyrosine (YMTL at aa 818-821 and YSRV at aa 857-860) and one di-leucine (LL at aa 841-842). The gB protein containing the mutation Y857 failed to be internalized, while gB mutated in Y818 was endocytosed but did not subsequently accumulate in the Golgi (Heineman and Hall, 2001). The LL motif within the cytosolic domain is not required for either VZV gB internalization or Golgi localization. Therefore

the membrane-distal YSRV motif is most responsible for gB endocytosis (Heineman and Hall, 2001). However, a VZV recombinant virus (VZV gB-36) that expresses a truncated form of gB lacking the C-terminal 36 amino acids of its cytosolic domain, despite lacking the YSRV endocytosis motif, is internalized from the plasma membrane but fails to localize to the Golgi (Heineman and Hall, 2002). Thus, when one of the internalization motifs is removed, the others may subsume some of the lost functions.

In addition to the post-Golgi transport signals, the cytosolic domain of VZV gB has been shown to contain specific ER-to-Golgi transport signals. The transmembrane domain proximal tyrosine motif (YMTL) is within a nine-amino acid region (YMTLVSAAE) required by a sequence-dependent mechanism for efficient ER-to-Golgi targeting of the gB protein (Heineman et al., 2000).

3.2 Endocytosis of alphaherpesvirus gB homologs

A similar triad of endocytosis motifs have been identified in HSV-1 and PRV gB. As for VZV gB, the homologous gB proteins contain two tyrosine motifs and one di-leucine based motif, arranged in a similar order in C-terminus. Endocytosis of HSV-1 gB depends principally on the membrane-distal YTQV motif, since either removal or disruption of this signal totally abolishes gB internalization from the cell surface to endosomes (Beitia Ortiz de Zarate et al., 2004). Analysis of the LL motif showed that its replacement did not hinder the process of gB endocytosis. However, the subsequent retrograde gB trafficking from early or recycling endosomes to the TGN was impaired while recycling from the endosomes to the plasma membrane was enhanced.

The PRV gB homolog is internalized from the cell surface and colocalizes precisely with the endocytosed PRV gE:gI complex (Tirabassi and Enquist, 1998). A mutated PrV gB form lacking the membrane-distal tyrosine and the di-leucine motifs remains primarily membrane associated because endocytosis is abolished (Tirabassi and Enquist, 1998). Furthermore, mutation of the one tyrosine Y902 residue in the tyrosine motif (YQRL) inhibits functioning of gB during antibody induced gB internalization in PRV infected monocytes (Favoreel et al., 2002). This same tyrosine mutation also diminishes efficient PrV cell-to-cell spread. However, mutating the dileucine motif in the gB domain has no effect on antibody triggered endocytosis but does promote an increased cell-to-cell spread phenotype with formation of larger syncytia, presumably through increased recycling of gB back to the cell surface (Favoreel et al., 2002).

4. VZV Glycoprotein H

4.1 Endocytosis of VZV gH

VZV gH is the third most abundant glycoprotein and the second most conserved. The gH glycoprotein of VZV is a major fusogen. Complete maturation of VZV gH in Golgi and its expression at the cell surface requires coexpression of gL (Forghani et al., 1994). When cotransfected with gE or gI, in the absence of gL, VZV gH is capable of exiting the ER in its immature form (Duus and Grose, 1996). However, unlike coexpression with gL, gH + gE or gH + gI does not result in complete gH maturation or subsequent syncytium formation. Within a transfection system, coexpression of VZV gH and gL is sufficient to mediate polykaryocytosis (Duus et al., 1995). While the requirement for gH and gL

association is conserved among herpesvirus gH homologues, HSV cell-to-cell fusion requires the quartet of gH, gL, gB and gD.

Like the three previously described VZV glycoproteins, VZV gH is internalized in infected cells. Further, when expressed alone with its chaperone gL in a transfected system, gH is capable of endocytosis independent of gE, gI, or gB. This observation was unexpected because all herpesvirus gH homologs have very short endodomains. Also, in the original sequencing, the cytosolic domain was assigned only 12 residues. Upon further inspection of the gH cytosolic domains of all alphaherpes viruses, however, a putative tyrosine-based YNKI endocytosis motif (aa 835-838) in proper context was discovered if the cytosolic domain was realigned to include 18 amino acids (Table 1). When the tyrosine was replaced with an alanine, endocytosis of gH was blocked. Thus, endocytosis of VZV glycoprotein gH is mediated by a tyrosine based YNKI motif in its short cytosolic domain (Fig. 1; Pasiëka et al., 2003).

4. 2. Endocytosis of alphaherpesvirus gH homologs.

Alignment analysis of the VZV gH cytosolic domain to other alphaherpes virus gH homologs revealed two important findings (Table 1). HSV-1 and 2 gE proteins lacked an endocytosis motif, while all other alphaherpesvirus gH homologs contained a potential motif. The VZV gH and simian varicella virus gH cytosolic domains were likely longer in length (18 amino acids) than predicted in the original sequence analyses (12 and 16 amino acids, respectively). The longer domains provide the proper context for a

functional endocytosis motif with at least 5 intervening amino acids between the transmembrane domain and the tyrosine residue.

5.0. Incorporation of endocytosed VZV glycoproteins into virion envelopes

Since endocytosis can target viral glycoproteins to the TGN, the proposed site of viral assembly, one attractive hypothesis is that endocytosis is a mechanism for delivering viral glycoproteins to the site of final envelopment (Brideau et al., 2000b). The deenvelopment-reenvelopment model for acquisition of the final viral envelope has been proposed for VZV (Jones and Grose, 1988). An analogous mechanism has been postulated to be involved in the envelopment of other herpesviruses (Card et al., 1993). The model predicts that capsids obtain a primary envelope as they pass through the inner nuclear membrane. As they exit the outer nuclear membrane, they undergo de-envelopment. Subsequently capsids released into the cytoplasm are enclosed by membranes of a post-Golgi compartment, such as the TGN. As previously reported, VZV apparently obtains its final envelope from these *trans*-Golgi network vesicles (Gershon et al., 1994). The glycoproteins of VZV are targeted to the TGN and, late in infection, all appear to become concentrated within this organelle (Olson and Grose, 1997). Thus, for the assembly of VZV a high degree of organization is required to localize all the viral envelope components to the final compartment. TGN sorting implies that TGN targeting signals must be present in the sequences of at least some VZV glycoproteins.

In a recently reported study, the role of viral glycoprotein endocytosis within the VZV life cycle was further assessed (Maresova et al., 2004). VZV differs from other

alphaherpesviruses in that gE is not only the major glycoprotein (as measured by percentage of total viral glycoprotein production in an infected cell) but also an essential protein for viral growth in cultured cells. Furthermore, the essential nature of the YAGL motif within gE itself was firmly documented by production of a recombinant VZV genome containing gE lacking its endocytosis motif but otherwise intact (Moffat et al., 2004). This mutated virus did not replicate. When other mutations were introduced into the gE cytosolic domain, the virus was able to replicate. Because of this remarkable demonstration of the apparent importance of endocytosis in the VZV life cycle, we subsequently analyzed the post-endocytosis trafficking pathways of glycoproteins in VZV infected cells. The methodology included biotinylation of cell surface glycoproteins followed by a glutathione cleavage assay. This assay measures the extent of endocytosis of a surface protein based on the proportion of a disulfide-linked biotinylated protein that becomes inaccessible to extracellular glutathione cleavage buffer added at the end of the endocytosis timepoint. Under the above conditions, viral glycoproteins are internalized efficiently during the first 24 hr after infection, but endocytosis is markedly decreased as infection advances over the next 24 hr time period.

To determine the extent to which VZV glycoproteins retrieved from the cell surface were incorporated into the virion particles, an uninfected monolayer was inoculated with infected cells (1:2 ratio) and incubated for 24 hr at 37C. After surface biotinylation with cleavable Sulfo-NHS-SS-biotin, the infected monolayer was incubated for an additional 5 hr to allow for endocytosis of the surface glycoproteins and their subsequent incorporation into virions (Fig. 3). After several washes, the infected monolayer was

harvested and sonically disrupted in order to break apart the infected cells. The released cell free virus was purified by ultracentrifugation in two sequential potassium-tartrate density gradients. The particulate virion band was removed and solubilized in a buffer for immunoprecipitation. Precipitations were performed with monoclonal antibodies specific for each of the four VZV glycoproteins. After the samples were separated by polyacrylamide gel electrophoresis, individual biotinylated glycoproteins were detected by Western blotting with Streptavidin-horse radish peroxidase staining (Fig. 3). The results demonstrated that the four glycoproteins retrieved from the cell surface were incorporated into virus particles isolated from infected cells by density gradient sedimentation (Fig. 3). Furthermore, additional glycoprotein complexes were present on the virion envelope, for example, the gE:gI complex and a higher molecular mass gE. Interestingly, the recently described gE:gH complex was also found in the virion envelope (Pasięka et al., 2004). This result supported a mechanism of gE:gH complex formation as a means by which gH was shuttled to the TGN after internalization.

To confirm and expand the above observations, the virions were also examined directly by transmission electron microscopy (TEM). To this end, an aliquot of the gradient-purified virion fraction was placed on a copper formvar grid and incubated at 24°C with ultra-small gold beads (0.8 nm) conjugated to anti-biotin antibody. Silver enhancement was performed in order to allow visualization of the ultra-small beads. In the next step, the sample was negatively stained with 1% ammonium molybdate and viewed by TEM. The biotin label was easily detected in the virion fraction (Maresova et al., 2004). When the particles with biotinylated glycoproteins on their envelope were counted, the

positively labeled virions represented approximately 27% of the total number of counted viral particles. This value corresponded to the percentage of intact enveloped virions expected after two successive gradient sedimentations, during which many particles lose their envelopes (Grose et al., 1979). When considered in this regard, the TEM visualization experiment indicated that a majority of enveloped virions were biotinylated. Thus, in the process of VZV assembly, endocytosis is one of the pathways by which viral glycoproteins are transported to the site of envelopment in the cytoplasm.

6.0. Summary of trafficking pathways

As is apparent from the previous sections, the replication and egress of viruses require that viral proteins be correctly modified and targeted to specific intracellular compartments. Many of these modification and targeting steps rely on the communication between the cell surface and a dynamic and highly regulated network of late secretory pathway organelles that comprise the TGN/ endosomal system. Strategically located at the boundary of the biosynthetic and endocytic pathways, the TGN acts as a sorting station for membrane proteins and lipids moving through the biosynthetic pathway by segregating them into nascent vesicles bound for specific target organelles including the endosomes, lysosomes and plasma membrane (Bonifacino and Glick, 2004; Gu et al., 2001b; Robinson, 2004b). In addition, the TGN receives molecules internalized from the cell surface via a series of complex and highly dynamic early/sorting and late endosomal compartments (Fig. 4).

Membrane proteins endocytosed from the cell surface may traverse various endosomal paths depending on the protein and its function. For example, transferrin receptors constitutively recycle between the plasma membrane and recycling endosomes via early endosomes (van Dam and Stoorvogel, 2002b), whereas growth factor receptors, such as the epidermal growth factor receptor (EGFR), are segregated into the sorting compartment of early endosomes and are delivered to lysosomes via the late endosome/multivesicular body (MVB) pathway for degradation (Gruenberg and Stenmark, 2004b; Raiborg et al., 2003). In addition, the two mannose 6-phosphate receptors (cation-dependent and cation-independent MPRs), recycle between the TGN, plasma membrane and endosomal compartments as they sort newly synthesized lysosomal hydrolases to lysosomes (Ghosh et al., 2003a). These complex protein trafficking events require the orchestrated interaction of lipid and protein components of the vesicular trafficking machinery, the cytoskeleton and multiple regulatory factors (Bonifacino and Traub, 2003b; Gruenberg, 2003; Roth, 2004).

The localization of many membrane proteins within the TGN/endosomal system relies upon canonical sorting motifs within their cytosolic domains, the best characterized of which are the tyrosine, dileucine and acidic cluster- based motifs. These sorting signals act as "address tags", which are recognized by components of the vesicular trafficking machinery that direct sorting to specific subcellular compartments (Bonifacino and Traub, 2003b). The four major VZV envelope glycoproteins have retained through evolution one or more types of these sorting signals, thus mimicking cellular membrane proteins to reach endosomes and the TGN. Together with the findings that gE and gI

may mediate the endocytosis of other VZV glycoproteins (Wang et al., 1998), these results strongly demonstrate the importance of sorting motifs for the trafficking of VZV glycoproteins to sites of virus assembly.

The function of tyrosine-based signals arises from the interaction of these motifs with the heterotetrameric adaptor complexes AP-1, AP-2, AP-3 and AP-4 (Robinson, 2004b). Adaptor complexes connect the vesicular coat protein clathrin to sorting signals in the cytosolic domains of membrane proteins thereby promoting their concentration into clathrin-coated pits (Fig. 4). AP-1 (subunits: γ , $\beta 1$, $\mu 1$ and $\sigma 1$), which is localized mainly at the TGN, mediates sorting of membrane proteins in both anterograde and retrograde pathways between the TGN and endosomes. AP-1B (subunits: γ , $\beta 1$, $\mu 1B$ and $\sigma 1$), an epithelial cell specific isoform of AP-1, directs transport to the basolateral surface from the TGN and endosomes. AP-2 (subunits: α , $\beta 2$, $\mu 2$ and $\sigma 2$), which is localized to the plasma membrane, plays a prominent role in clathrin-mediated endocytosis of cell surface receptors. AP-3 (subunits: δ , $\beta 3$, $\mu 3$ and $\sigma 3$) is localized to the TGN and endosomes and mediates sorting of membrane proteins to the lysosomes and melanosomes. AP-4 (subunits: ϵ , $\beta 4$, $\mu 4$ and $\sigma 4$), which is localized to the TGN and endosomes, mediates the sorting of membrane proteins to basolateral membrane in polarized cells. The $\gamma/\alpha/\delta$ subunits bind clathrin whereas the $\beta 1-4$ and $\mu 1-4$ subunits bind to [D/E]XXXL[L/I] and YXXL motifs in the cytosolic domain of the cargo proteins, respectively. The σ subunit is predicted to play a structural role by stabilizing the tetrameric complex. Adaptor complex induced formation of vesicles from clathrin-coated pits requires membrane fission, which is mediated by the GTPase dynamin at the plasma membrane and a

dynamamin homologue, dynamamin 2, at the TGN (Cao et al., 2000b). Together these adaptor complexes and coat proteins orchestrate intracellular transport of membrane proteins in the TGN/endosomal system (Collins et al., 2002b; Robinson, 2004b).

A number of cellular and viral membrane proteins containing acidic cluster sorting motifs have been identified including furin, a proprotein convertase that cleaves proteins in the secretory pathway (Thomas, 2002b), the MPRs (Ghosh et al., 2003a), as well as the herpesvirus glycoproteins VZV gE (Alconada et al., 1999), HCMV gB (Norais et al., 1996), HSV gB, gE (Alconada et al., 1999; Beitia Ortiz de Zarate et al., 2004) and the PrV glycoprotein Us9 (Brideau et al., 2000a). Acidic cluster motifs often contain a serine or threonine residue that can be phosphorylated by casein kinase II, a ubiquitous, heterotetrameric serine/ threonine kinase involved in a plethora of phosphorylation events including the regulation of protein sorting (Meggio and Pinna, 2003b). Phosphofurin acidic cluster sorting protein-1 (PACS-1) connects phosphorylated acidic cluster containing proteins to AP-1 and directs the delivery of membrane proteins from endosomes to the TGN (Fig. 4). This function of PACS-1 is required for the sorting of several integral membrane proteins such as furin, the MPRs and HCMV gB (Crump et al., 2003b; Scott et al., 2003b; Wan et al., 1998b). In addition, PACS-1 binds to an acidic cluster (that contains a phosphorylation site for casein kinase II) within the cytosolic domain of VZV gE (Wan et al., 1998b) and may mediate delivery of VZV gE to the TGN, though this function has not yet been proven. Considering the importance for the TGN localization of VZV glycoproteins in the final envelopment of VZV virions, PACS-

1 may play a critical role for the formation of VZV virions that bud from the TGN, as PACS-1 does for HCMV (Crump et al., 2003b).

A newer class of sorting motifs, the acidic-dileucine (DxxLL) motifs, are recognized by a family of monomeric adaptors consisting of GGA-1, -2 and -3 (Golgi-localized, γ -adaptin ear homology domain, ARF-binding protein 1-3, GGAs; Fig. 4; Bonifacino, 2004b). The GGAs are localized to the TGN where they cooperate with AP-1 to link membrane proteins with acidic-dileucine motifs directly to clathrin. This function concentrates several endogenous membrane proteins, including the MPRs, into clathrin-coated buds at the TGN and activates anterograde sorting of the MPRs to the early endosomes (Bonifacino, 2004b; Puertollano et al., 2001b). Like acidic cluster motifs, many acidic-dileucine motifs contain a serine/threonine residue that can be phosphorylated by casein kinase II (Doray et al., 2002a). Interestingly, the cytosolic domain of VZV gI contains a potential GGA binding site (ESDVML; not canonical, but highly similar to the GGA binding motif of the neuronal SorLA receptor), implicating GGAs in the sorting of VZV containing vesicles from the TGN to endosomes.

Two additional sorting molecules, TIP47 and the retromer complex, may also direct transport of membrane proteins such as MPRs, from endosomes to the TGN (Fig. 4). TIP47 binds to a diaromatic amino acid motif in the cytosolic domain of cargo proteins like the CD-MPR (FW) and HIV-gp160 (YW), mediating the late endosome to TGN transport of these proteins (Diaz and Pfeffer, 1998). This trafficking step has been shown to be essential for the incorporation of gp160 into HIV virions, however no VZV

glycoprotein contains a TIP47 binding motif. The mammalian retromer complex, which consists of five subunits (vps35, vps29, vps26, SNX1 and SNX2), was recently shown to localize to the tubular-vesicular profiles that emanate from either early endosomes or from intermediates in the maturation of early endosomes to late endosomes. From these endosomal compartments, retromer mediates the recycling of CI-MPR to the TGN (Seaman, 2004b). The cargo recognition motif for retromer is unknown and proposed to be conformational in nature.

The deenvelopment-reenvelopment model for acquisition of the final viral envelope proposed for herpesviruses suggests that mature viral glycoproteins must traffic to the TGN or to endosomal structures before being incorporated into the viral envelope (Gershon et al., 1994; Tooze et al., 1993). This scenario requires, at least in case of VZV, endocytosis of mature viral glycoproteins from the plasma membrane via a clathrin/AP-2/dynamin dependent process and delivery of these proteins to early endosomes. Endocytosed viral glycoproteins can reach the site of assembly, the TGN, either directly from early endosomes or indirectly from early endosomes via late endosomes. These retrograde transport pathways have been shown to be utilized not only by cellular and viral proteins like the MPRs, furin and HCMV gB, but also by bacterial toxins like Shiga toxin, which is internalized in clathrin-coated vesicles and traverses the early endosome-to-TGN pathway before reaching the ER (Mallard et al., 1998; Mallard et al., 2002; Sandvig and van Deurs, 2002). The final event in VZV assembly and egress is exocytosis at the cell surface (Fig. 5).

The failure in viral assembly in cells expressing either mutant VZV glycoproteins with trafficking defects or mutant VZV serine protein kinases with phosphorylation defects demonstrates the importance of these events for virus maturation (Heineman and Hall, 2002; Kenyon et al., 2002; Wang et al., 2001). In particular, the fact that a recombinant VZV genome containing only a single mutation, namely, the endocytosis motif within the gE gene, cannot replicate emphasizes the pivotal role of gE endocytosis in the life cycle of this alpha herpesvirus (Moffat et al., 2004; Maresova et al., 2004).

Acknowledgments

The authors thank all colleagues whose names appear on our cited articles from previous years. Research described in this chapter was supported by NIH grants AI 22795, DK 37274, AI 48585 and AI 49793.

Figure Legends

Figure 1. Amino acid sequences of the cytosolic domains of VZV glycoproteins gE, gH, gI and gB. The sequences are based on published VZV sequences (Davison and Scott, 1986; Grose et al., 2004). The amino terminal of gB has been recently realigned, so the enumeration of amino acids in the cytosolic domain differs from the earlier descriptions (Maresova et al., 2003). Both sets of numbers are given. The cytosolic domain of gH has been recently realigned also (Pasiaka et al., 2003). Domains discussed in the text are annotated.

Figure 2. Endocytosis assay. Endocytosis of the transfected VZV gE was gauged by a confocal microscopy assay. The assay was photographed at the following timepoints: 0 min (A), 5 min (B), 10 min (C), 15 min (D), 30 min (E) and 60 min (F). The characteristic profile of endocytosis includes multiple vesicles in the cytoplasm; see panels D, E and F. Endocytosis is more pronounced in assays of transfected cells than in VZV infected cells.

Figure 3. Identification of biotinylated VZV glycoproteins on infected cells and purified virions. (A) Cultured cells were infected and processed for the surface biotinylation assay as described in the text. The VZV glycoproteins were precipitated with monoclonal antibodies as designated at the bottom of each lane: gH (lanes 1, 9, 10 and 11); gB (lanes 2, 3 and 8); gE (lanes 5, 6 and 7) and gI (lane 4). Precipitated samples were resolved in an 8% gel under non-reducing conditions prior to Western blotting with Streptavidin-horse radish peroxidase. Closed circles indicate locations of some glycoproteins; in lane 4, closed circles also indicate the location of gE coprecipitated by antibody to gI. Lanes 1-6 and 7-11 represent two separate gels. The corresponding molecular mass markers (kilodaltons) are indicated on the right. (B) Virion band after ultracentrifugation in the second density gradient. The band was subsequently solubilized for immunoprecipitation (see panel C). (C). Biotinylated VZV gI in the virion band. As described in the text, biotinylated gI was immunoprecipitated from the virion band and stained by Western blotting with Streptavidin-horse radish peroxidase. Similar experiments for VZV gE, gH and gB are illustrated in the reference by Maresova et al. (2004).

Figure 4. Endosomal trafficking of the VZV glycoproteins. VZV glycoproteins (triangles) may follow several late secretory trafficking pathways to the TGN, where viral envelopment occurs. As reported for HCMV gB (Crump et al., 2003), retrograde transport from the early endosomes (EE) to the TGN may occur from early endosomes (EE) via PACS-1 and AP-1. In addition, transport through sorting pathways from intermediate endosomes (IE) via the retromer complex or from late endosomes (LE) via TIP47 may also occur. Anterograde transport from the TGN to early endosomes is mediated by GGA proteins and AP-1 or from the TGN to late endosomes by AP-3. VZV capsids (hexagons) bud into the TGN, forming a viral envelope of membranes enriched with viral glycoproteins. In turn, individual TGN-derived vesicles appear to form multi-vesicular organelles (vacuoles) containing several virions; these vacuoles fuse with the plasma membrane, exposing the virions on the surface of the cell. See figure 5 also.

Figure 5. Egress and exocytosis of virions from a cytosolic vacuole. This electron micrograph shows a cytosolic vacuole with four enveloped virions (arrow). The micrograph also shows one virion in the final stage of egress at the cell surface (arrowhead).

Table 1. Endocytosis motifs in herpesvirus gH homologs.

Note at bottom of Table: Underlined sequences indicate potential endocytosis motifs in the alphaherpesvirus gH homologs. Only the VZV gH endocytosis motif has been proven

to be functional. See reference by Pasiaka et al (2003) for greater dedomain and accession numbers. S=simian; F=feline; B=bovine; and E=equine herpesvirus

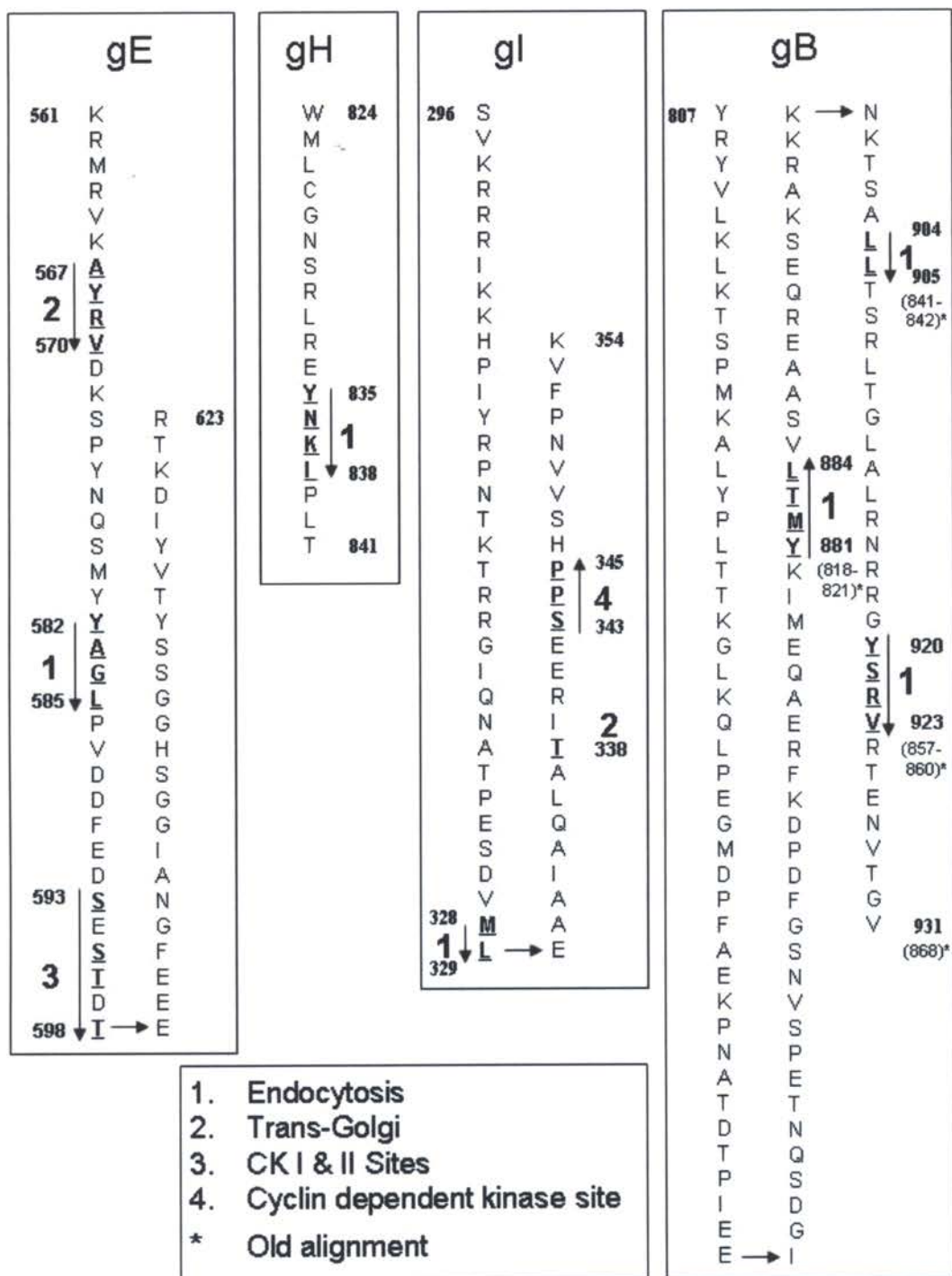


Figure 1

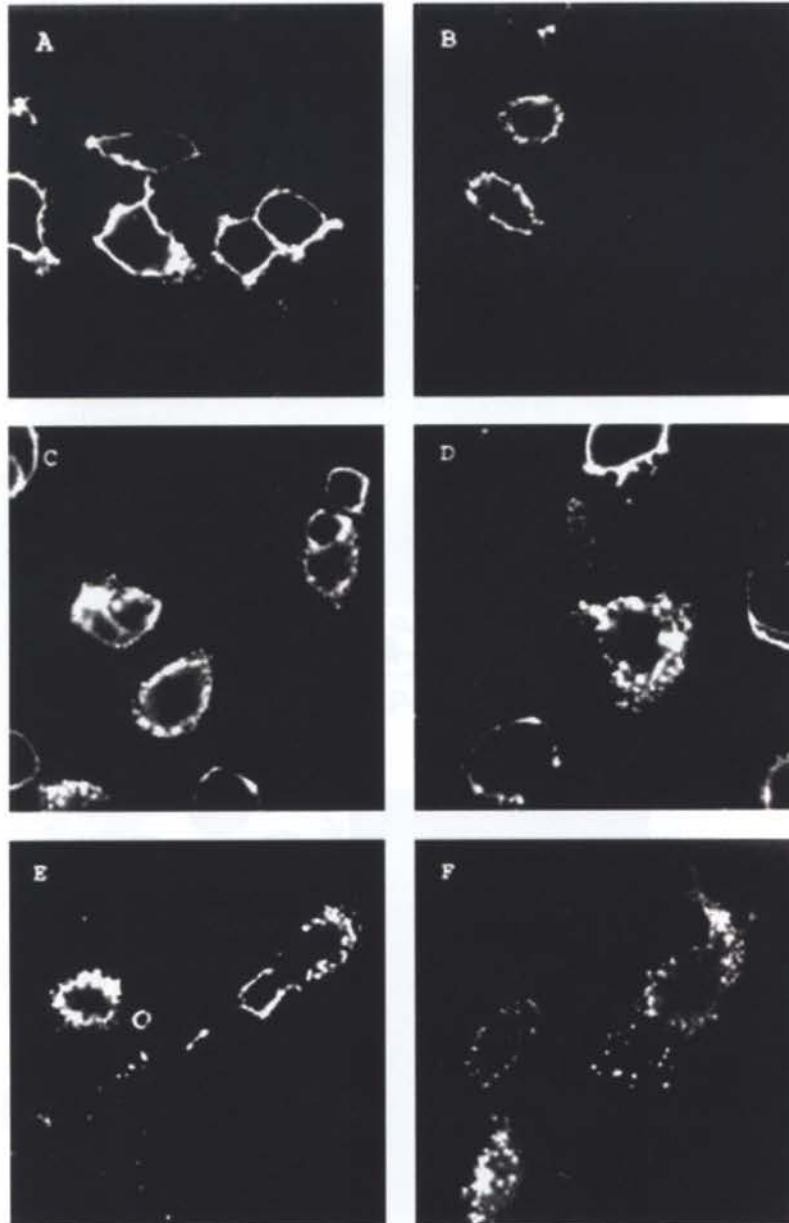


Figure 2

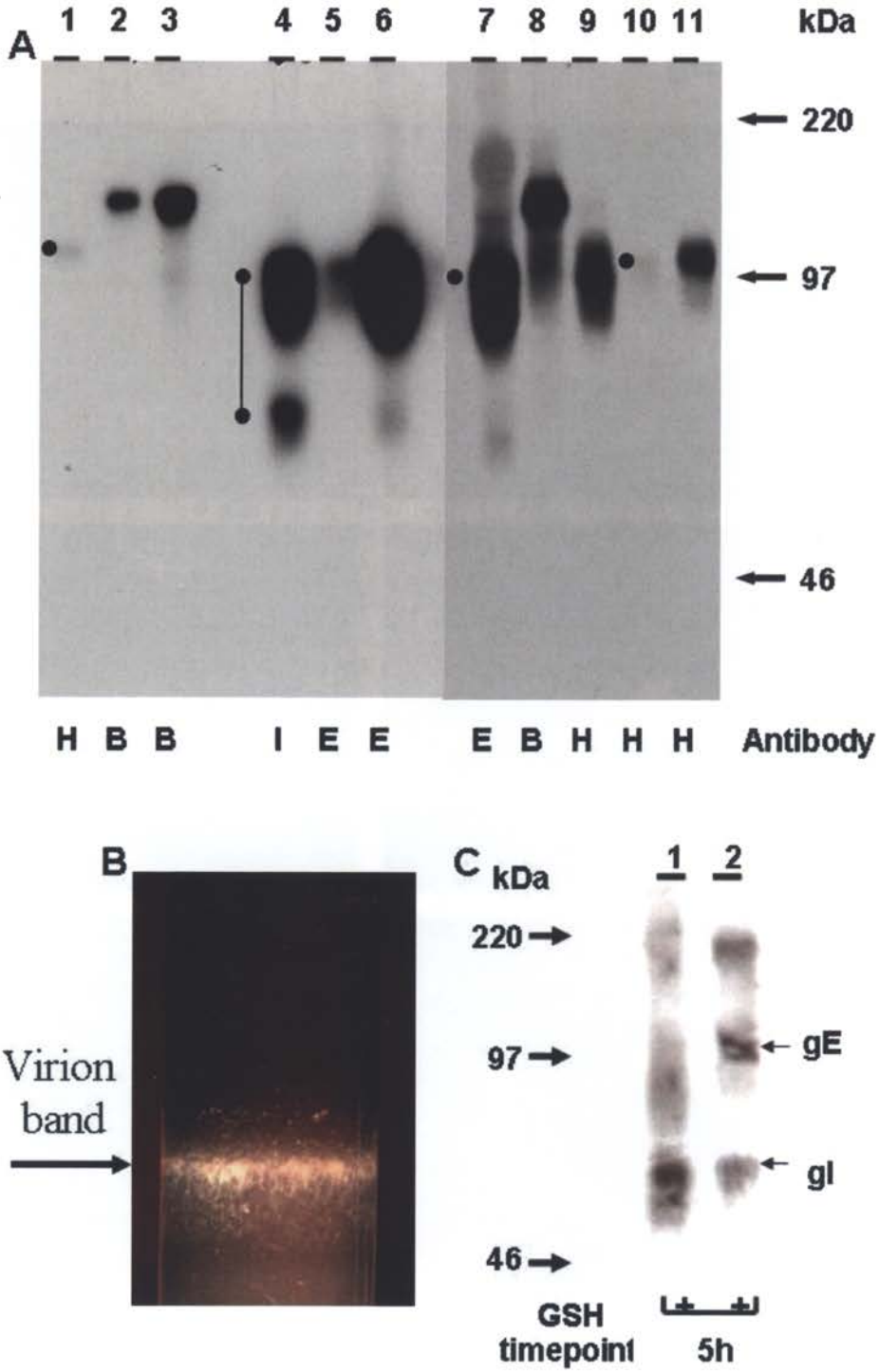


Figure 3

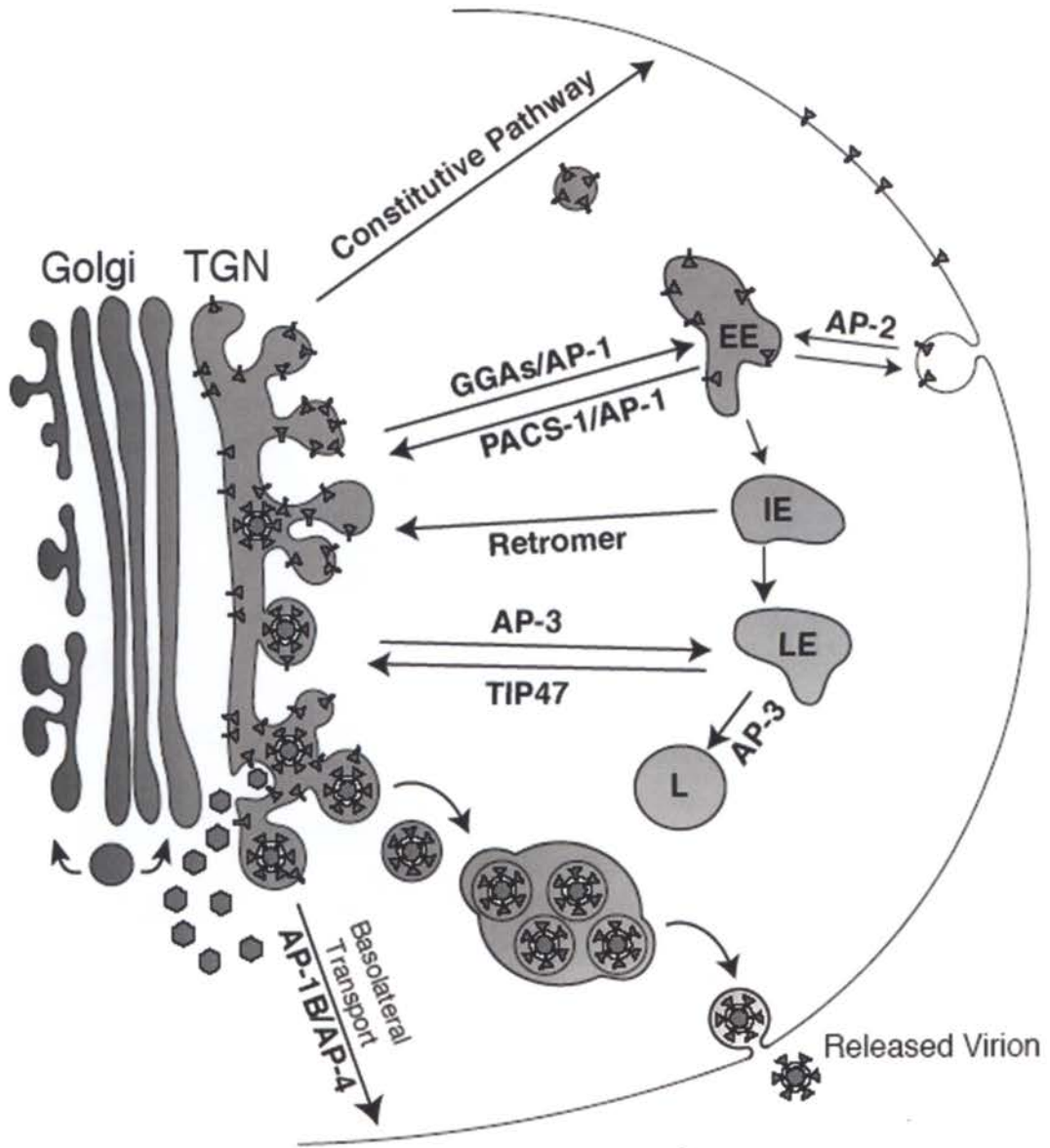


Figure 4



Figure 5

Table 1. Endocytosis motifs in herpesvirus gH homologs

Virus	Tail length	Motif in cytosolic tail
HSV-1	14	KVLRTSVPPFFWRRE (None predicted)
HSV-2	14	RVVRTCVPFLWRRE (None predicted)
VZV	18	WMLCGNSRLRE <u>YNKIPLT</u> (Realigned)
SVV	18	WMLCGSPRNIEY <u>TAVPLV</u> (Realigned)
PRV	19	KMLCSFSSE <u>GY</u> SRLINARS
FHV-1	17	KMLCSFTPDVRY <u>TLLNN</u>
BHV-1	19	KMLCSSVPLARGY <u>SSVPVF</u>
BHV-5	19	KMLCSSVPIARGY <u>SAVPAF</u>
EHV-1	19	KMLCGGVTNDGY <u>KLLLSYE</u>
EHV-4	19	KMLCGGVINNDY <u>SLLLNSE</u>

APPENDIX B

IDENTIFICATION OF A PH SENSOR IN THE FURIN PROPEPTIDE THAT REGULATES ENZYME ACTIVATION

Sylvain F. Feliciangeli², Laurel Thomas, Gregory K. Scott, Ezhilkani Subbian¹, Chien-Hui Hung, Sean S. Molloy, François Jean³, Ujwal Shinde¹ and Gary Thomas⁴

From the Vollum Institute, and ¹Department of Biochemistry and Molecular Biology, Oregon Health & Science University, Portland, OR 97239, USA, ²Institut de Pharmacologie Moleculaire et Cellulaire, Valbonne, France 06560, and ³Department of Microbiology and Immunology, University of British Columbia, Vancouver, BC, Canada V6T 1Z3

Running Title: Furin activation

⁴Address correspondence to: Dr. Gary Thomas, Vollum Institute, OHSU, 3181 SW Sam Jackson Park Road, Portland, OR 97239; tel. 503-494-6955; fax. 503-494-1218; Email: thomasg@ohsu.edu

In this appendix I performed the metabolic labeling experiments in Figure 5A, and I assisted in writing the manuscript.

Abstract

The folding and activation of furin occurs through two pH- and compartment-specific autoproteolytic steps. In the ER, profurin folds under the guidance of its prodomain and undergoes an autoproteolytic excision at the consensus furin site Arg-Thr-Lys-Arg₁₀₇[↓], generating an enzymatically masked furin•propeptide complex competent for transport to late secretory compartments. In the mildly acidic environment of the TGN/endosomal system, the bound propeptide is cleaved at the internal site His₆₉-Arg-Gly-Val-Thr-Lys-Arg₇₅[↓], unmasking active furin capable of cleaving substrates *in trans*. Here using cellular, biochemical, and modeling studies we demonstrate that the conserved His₆₉ is a pH sensor that regulates the compartment-specific cleavages of the propeptide. In the ER, unprotonated His₆₉ stabilizes a solvent-accessible hydrophobic pocket necessary for autoproteolytic excision at Arg₁₀₇. Profurin molecules unable to form the hydrophobic pocket, and hence, the furin•propeptide complex, are restricted to the ER by a PACS-2- and COPI-dependent mechanism. Once exposed to the acidic pH of the late secretory pathway, protonated His₆₉ disrupts the hydrophobic pocket, resulting in exposure and cleavage of the internal cleavage site at Arg₇₅ to unmask the enzyme. Together, our data explain the pH-regulated activation of furin, and how this His-dependent regulatory mechanism is a model for other proteins.

Introduction

The pH gradient formed by the various membranous compartments comprising the secretory and endocytic pathways has essential and manifold roles ranging from the regulation of protein traffic to the control of protein conformation and enzyme activities, including the processing of prohormones and proproteins by proprotein convertases (PCs). The PCs, a family of calcium-dependent serine endoproteases, cleave proproteins and prohormones at doublets or clusters of basic amino acids thus generating mature bioactive proteins as well as hormonal processing intermediates that require additional posttranslational modifications to gain full bioactivity (Steiner, 1998; Thomas 2002). The proteolytic maturation of prohormones by the neuroendocrine-specific PC1/3 and PC2 requires the acidic pH of maturing secretory granules (Rhodes et al., 1993; Zhou et al., 1999; Zhou and Lindberg, 1993), whereas the proteolytic activation of proprotein substrates by the ubiquitously expressed PC furin in the *trans*-Golgi network (TGN)/endosomal system is compartment- and hence, pH-specific (2,6). This compartment-specific processing by furin is mediated in part by the pH-dependent changes in the conformation of furin substrates as well as the utilization of pH-sensitive furin cleavage sites. Furin efficiently cleaves a number of proprotein substrates at the consensus site -Arg-X-Lys/Arg-Arg-[↓] (Thomas 2002). Kinetic studies show that the P1 and P4 Arg residues are required for the efficient processing of furin substrates whereas the P2 Arg has a modulatory role (Krysan et al., 1999; Rockwell et al., 2002). However, at acidic pH the absence of a P2 or P4 Arg can be compensated for by the presence of positively charged residues at P6 or possibly adjacent amino acids, demonstrating the

relevance of pH for furin-dependant processing (Bergeron et al., 2003; Degnin et al., 2004; Henrich et al., 2003; Rockwell et al., 2002; Rockwell and Thorner, 2004).

The pH-dependent processing of furin substrates by selective cleavage site utilization is exemplified by the autoproteolytic cleavages of its cognate prodomain. During transit from the pH neutral ER to the acidic TGN/endosomal system, the ordered and compartment-specific furin prodomain processing guides the folding of the inactive proenzyme to the mature, active endoprotease. Similar to the evolutionarily related bacterial subtilisins, the 83-amino acid furin prodomain is necessary to correctly fold the catalytic domain in the ER (Anderson et al., 2002; Zhou et al., 1995). The folded catalytic domain then rapidly ($t_{1/2} < 10$ min) excises the prodomain at the canonical P1/P4 Arg furin cleavage site -Arg-Thr-Lys-Arg₁₀₇[↓], generating a transport competent furin•propeptide complex. Inhibition of this excision step blocks transport of profurin molecules from the ER, suggesting that components of the cellular trafficking machinery detect formation of the furin•propeptide complex before directing their transit to late secretory pathway compartments (Anderson et al., 2002). However, the machinery that localizes profurin to the ER is unknown. We identified PACS-1, which is a cytosolic sorting protein that connects the CK2-phosphorylated furin cytosolic domain to AP-1, thereby localizing the endoprotease to the TGN (Crump et al., 2001; Wan et al., 1998). Recently, we discovered PACS-2, which localizes membrane cargo to the ER by connecting them to COPI (Kottgen et al., 2005). But whether PACS-2 binds to furin or mediates ER trafficking of profurin is unknown.

Despite formation of the catalytic center, the furin•propeptide complex remains inactive towards substrates *in trans* because the bound propeptide is a potent furin inhibitor ($K_{0.5} = 14$ nM (Anderson et al., 1997)). Release of the autoinhibitory propeptide from the enzyme requires trafficking of the furin•propeptide complex from the ER to the mildly acidic TGN/endosomal system (Anderson et al., 1997). There, the non-covalently associated propeptide undergoes a second, slow cleavage ($t_{1/2} \sim 90$ min) at the His-Arg-Gly-Val-Thr-Lys-Arg₇₅[↓] internal cleavage site, thus releasing the propeptide fragments and unmasking active furin capable of cleaving substrates *in trans* (Anderson et al., 2002; Anderson et al., 1997). This second-site cleavage is rate-limiting for activation of bacterial and human subtilisin-like proteases (Anderson et al., 2002; Subbian et al., 2005). *In vitro* studies of furin show that the internal propeptide cleavage occurs optimally at pH 6.0, the pH of the TGN, demonstrating the differential pH requirements of the two prodomain cleavage sites (Anderson et al., 2002; Anderson et al., 1997). Surprisingly, mutation of the P1/P6 Arg cleavage site to a canonical P1/P4 Arg furin site fails to yield mature, active furin but instead causes the accumulation of inactive profurin in the ER (Anderson et al., 2002). Together, these studies suggest that the ordered, compartment-specific cleavages of the furin propeptide are necessary to guide the folding and activation of the endoprotease and that this activation process could be controlled by a pH sensor.

The requirement for exposure of the furin•propeptide complex to pH 6 to complete enzyme activation suggests a role for one or more histidine residues to serve as a pH sensor controlling furin activation. Protonation of the histidine imidazole ring, which has

a pKa of 6.0, has profound effects on histidine chemistry under physiological conditions (Zamyatnin, 1984). While no pH sensor has been described for processing enzymes, such a role for histidine is well established for generating allosteric changes, including control of O₂/CO₂ exchange by hemoglobin, gating of electrogenic molecules, and the pH-dependent conformational changes within class II MHC molecules that promote ligand exchange (Baukrowitz et al., 1999; Jensen, 2004; Rotzschke et al., 2002; Wiebe et al., 2001).

Using mutants that mimic the protonation state of histidine and through molecular modeling analysis we report the role of His₆₉ in the folding and activation of furin. Our results demonstrate that the protonation state of His₆₉, which is located in a solvent-accessible hydrophobic pocket, plays a critical role in regulating the secondary propeptide cleavage. Mutations that interfere with the His₆₉ block propeptide excision, resulting in ER accumulation of profurin by a mechanism that requires the cytosolic sorting protein PACS-2 and COPI. Following propeptide excision, the furin•propeptide complex traffics to the mildly acidic TGN/endosomal system where protonation of His₆₉ disrupts the solvent-accessible hydrophobic pocket to expose the P1/P6 Arg internal cleavage site His-Arg-Gly-Val-Thr-Lys-Arg₇₅[↓], leading to release of the inhibitory propeptide and furin activation.

Experimental Procedures

Antibodies and reagents—Reagents were from Sigma except where stated. Antibodies against PACS-2 (Simmen et al., 2005), FLAG (M1 and M2; Sigma), HA (HA.11;

Covance) β -COP (Abcam), α -tubulin (Calbiochem), TGN46 (Serotec), PDI (R. Sitia), furin (PA-062, ABR), as well as Alexa (546 and 488)-conjugated secondary antibodies (Molecular Probes) and HRP-conjugated secondary antibodies (Southern Biotech) were described or provided as indicated.

Cell culture, DNA constructs, and virus construction—A7 and BSC-40 cells were cultured in minimal essential medium (MEM; Cellgro) containing 10% fetal bovine serum and 25 μ g/ml gentamycin as described (Anderson et al., 2002; Anderson et al., 1997). Vaccinia viruses (VV) expressing fur/f/ha, fur/f/ha Δ tc-k, and R75A:fur/f/ha Δ tc-k were generated as previously described (Anderson et al., 2002; Anderson et al., 1997). VV recombinants expressing H66L:fur/f/ha, H66L:fur/f/ha Δ tc-k, H69L:fur/f/ha, H69L:fur/f/ha Δ tc-k, H69K:fur/f/ha, and H69K:fur/f/ha Δ tc-k were generated using standard PCR methods and subcloned into pZVneo fur/f/ha and fur/f/ha Δ tc-k. Vaccinia virus recombinants were constructed using previously described methods (Anderson et al., 1997).

Pulse-chase analysis—Pulse-chase analysis was performed as described [5]. Briefly, BSC-40 cells grown in 35mm dishes were infected with the indicated VV recombinants (m.o.i.=5) for 3 hours (h), labeled with [3 H]-arginine and [3 H]-leucine (100 μ Ci each) in Arg/Leu-MEM (Gibco) for 30 min. The cells were then incubated at 37°C with complete MEM containing an excess of cold arginine and leucine for 20 min, harvested at the indicated time points in mRIPA buffer (150 mM NaCl, 50 mM Tris, pH 8.0, 1% deoxycholate, 1% NP-40) containing 1 mM CaCl₂. FLAG-tagged furin constructs were immunoprecipitated with mAb M1 (100 μ g/ml), captured with protein A sepharose, and

bound proteins were then separated by 15% Tris-Glycine SDS-PAGE and detected by autoradiography as described (Anderson et al., 1997).

Metabolic labeling—A7 cells were infected with VV expressing the indicated furin constructs (m.o.i. =3) for 12h, washed and incubated with phosphate-free MEM for 1h after which 0.5 mCi/ml $^{32}\text{P}_i$ (NEN) was added for 2h. The labeled cells were washed with PBS and lysed in mRIPA with 50 mM NaF, 0.1 μM orthovanadate, 10 μM Pepstatin-A, 10 μM leupeptin, 1 μM E64, 50 $\mu\text{g}/\text{ml}$ aprotinin, 500 μM PMSF and 1mM CaCl_2 . FLAG-tagged furin proteins were immunoprecipitated with mAb M2, separated by SDS-PAGE, transferred to nitrocellulose and analyzed by autoradiography and western blot.

Furin activity assays—To assay $\Delta\text{tc-k}$ constructs, high-speed cellular membrane preparations from BSC-40 cells infected with the indicated VV recombinants (m.o.i.=2) for 14h were prepared as described (Anderson et al., 1997). The membrane samples were incubated in activation buffer (10 mM Bis-Tris, 5 mM CaCl_2 , 1 mM 2-mercaptoethanol, 500 μM PMSF, 10 μM Pepstatin-A, 20 μM E64, 50 $\mu\text{g}/\text{ml}$ aprotinin, pH 6.0 or 7.5 as indicated) at 30°C either for 3h (at pH 6.0 and 7.5), or at pH 7.5 for 1h in the presence of trypsin (0.83 nM) followed by a 15 min incubation with soybean trypsin inhibitor (2.5 μM). Fluorometric assays of furin activity were performed with Abz-RVKRGLAY(NO_2)D-OH furin substrate (Bachem) using a FluoroMax-2 spectrofluorometer equipped with a 96-well plate reader (Anderson et al., 1997). To assay Fur/f/ha constructs, membrane preparations from BSC-40 cells expressing the indicated constructs were prepared and furin activity was assayed in 100 mM HEPES, pH

7.5, 1 mM CaCl₂ using the Abz-RVKRGLAY(NO₂)D-OH peptide as described (Anderson et al., 2002).

Fluorometric assays of internally quenched peptide substrates—Each fluorogenic peptide substrate was prepared, characterized, and assayed as described (Anderson et al., 2002). Briefly, each fluorogenic substrate was incubated with purified, soluble furin in 100 mM bis-Tris/100 mM sodium acetate (pH 6.0 or 7.5) with 1 mM CaCl₂. Incubations for the determination of kinetic constants were conducted with increasing concentrations of fluorogenic peptide substrate (corrected for peptide content) for up to 30 min. All assays were performed in duplicate and the average values are reported (relative error, <11%). Fluorescence measurements were made with a FluoroMax-2 spectrofluorometer equipped with a 96-well plate reader (Instrument SA) using an excitation wavelength set at 320 nm and an emission wavelength set at 425 nm. The values of K_m and V_{max} were determined using a computer-assisted algorithm (Enzfitter). Control studies showed no substrate inhibition for any of the fluorogenic peptides at concentrations 10-fold greater than their respective K_m values.

Immunoblotting—BSC-40 cells were infected with VV expressing the indicated furin constructs (m.o.i=2) for 14h, and harvested in mRIPA. The samples were separated by 8% Tris-Glycine SDS-PAGE, transferred to nitrocellulose, and analyzed by western blot. To detect the propeptide, crude membrane extracts were incubated in activation buffer at pH 6.0 or 7.5 for 3h at 30°C, separated by 15% Tris-Tricine SDS-PAGE, transferred to

nitrocellulose for 30 min at 36V and analyzed by western blot with mAb HA.11 as described (Anderson et al., 2002).

Immunofluorescence—BSC-40 cells were grown to 50-80% confluency on glass coverslips. After infection with the indicated VV recombinants (m.o.i.=5, 5h), cells were fixed with 4% paraformaldehyde and immunofluorescence analysis performed as described (Molloy et al., 1994). For the siRNA experiments, A7 cells were transfected with control (scr.), PACS-2 (24) or β -COP (CAACUCCAGAUGGGAGACU) siRNA as described (Simmen et al., 2005). After 48h, the cells were infected with recombinant VV for an additional 4 hr. The cells were fixed, permeabilized, and incubated with the indicated primary antisera followed by incubation with species- and subtype-specific fluorescently labeled secondary antisera. Images were then captured using a Zeiss axioplan 2 microscope with a 63X immersion objective and processed with the NIH image 1.62 program.

Sequence analysis and homology modeling—Multiple sequence alignments of the mammalian PC sequences obtained from the ExPasy server were aligned with ClustalW using default parameters. The alignments were then optimized manually using GeneDoc and the model of the furin propeptide was built using the alignment interface of SwissModel, which predicts structures reliably with a root mean square deviation (RMSD) $<2\text{\AA}$ for sequences with 50-60% identity (Schwede et al., 2003) and with the solution structure of the PC1 propeptide (1KN6) as a template. The modeled structure was minimized in the SwissPDB Viewer package using 10,000 steps of steepest descent

with the Gromos96 43B1 parameter set *in vacuo* and with a dielectric constant of 1. The model was further validated and manually checked for bad conformations and clashes by Whatcheck and ANOLEA software packages, and minimization procedures were repeated as necessary. The minimized model has an RMSD of 1 Å from that of the propeptide of PC1 (PDB ID:1KN6).

The furin propeptide was docked onto the crystal structure of the mouse furin catalytic domain ((Henrich et al., 2003) PDB ID:IP8J) using the homologous bacterial protease-propeptide (PDB ID:1SCJ) complex (Jain et al., 1998) as template. The x-ray structure of the bacterial homologue depicts a side-on interaction between the propeptide and protease domains that appears to be conserved throughout the subtilase family. Using this as a template the propeptide was docked onto the x-ray structure of furin. Side-chain clashes and deformations were then manually corrected using more favorable rotamers using InsightII. The docked structure was subsequently energy- minimized with CHARMM22 as the force-field, initially using 10,000 steps of steepest descent followed by 10,000 steps of the Newton Raphson's algorithm in the CHARMM module of InsightII.

Results

Analysis of the furin propeptide revealed two histidine residues adjacent to the internal cleavage site and which are either strictly (His₆₉) or partially (His₆₆) conserved within all PC family members (Fig. 1a). To ascertain whether one or both of these histidine residues may be spatially arranged to affect the pH-dependent activation of furin, we undertook a

structural analysis of the propeptide•furin complex using homology modeling (Schwede et al., 2003). The propeptide of furin was modeled using the solution structure of mouse PC1 propeptide (Tangrea et al., 2001), and docked onto the catalytic domain of furin using information from the structures of the propeptide•subtilisin E complex and prokumamolysin, a serine carboxyl protease containing a subtilisin-like fold (Fig. 1b and c; Comellas-Bigler et al., 2004; Jain et al., 1998). The correctness and accuracy of structures predicted using homology modeling is determined by the quality of the sequence alignment and the identity of the template, which as evident from Figure 1a, is high. The models were then refined and validated using approaches described earlier (Subbian et al., 2004). The internal cleavage site maps onto a loop between strands β 3 and α 3 and is part of a distinct hydrophobic pocket on the surface of the propeptide abutting the catalytic domain (Fig. 1c and d). Although the cleavage site lies in a surface loop, close examination revealed that the conserved P7 His₆₉ is buried at the center of a well-formed hydrophobic pocket. This pocket is lined by non-polar residues, Gly₅₃, Leu₅₅, and aromatic residues, Phe₅₄, Phe₆₇, and Trp₆₈ (Fig. 1d). By contrast, the P9 His₆₆ mapped to the interface between the propeptide and the mature enzyme. In the homologous bacterial subtilisins the interface between the propeptide and mature domains is dynamic with a relatively high average B factor (Jain et al., 1998) and increasing these dynamics can decrease rates of autoprocessing (Inouye et al., 2001). Further, studies have established that modulating the propeptide binding to this interface by varying solvent conditions prolongs its release and hence the activation of the mature protease suggesting that this interface would be solvent-accessible (Subbian et al., 2005). Therefore, our modeling analysis predicted that protonation of the His₆₉ located in a hydrophobic pocket

could have dramatic effects on the structure of the propeptide unlike protonation of the solvent accessible His₆₆.

To test the importance of the two histidine residues for the pH-dependent profurin activation step *in vitro* we measured the ability of profurin mutants containing a His₆₆→Leu or His₆₉→Leu substitution to undergo activation. We also tested a profurin variant His₆₉→Lys that mimics a constitutively protonated histidine residue which the modeling analysis predicted would block formation of the propeptide hydrophobic pocket (Fig. 1d). As a control, we expressed a profurin construct that contains an Arg₇₅→Ala substitution at the P1 position of the internal cleavage site, which blocks profurin activation but not propeptide excision or ER export of the furin•propeptide complex (Anderson et al., 2002). We assayed each variant using ER-localized profurin constructs in which the transmembrane and cytosolic domains were replaced by the luminal -Lys-Asp-Glu-Leu (KDEL) ER localization motif (Fig. 2a, referred to as Δtc-k constructs). The KDEL motif restricts the furin reporters to the neutral pH environment of the ER where they are able to undergo the first propeptide excision at Arg₁₀₇ to form a furin•propeptide complex, but are blocked from undergoing the second internal propeptide cleavage at Arg₇₅ (Anderson et al., 2002). To monitor propeptide excision at Arg₁₀₇, we inserted a FLAG epitope between the C-terminus of the propeptide and N-terminus of the catalytic domain. The FLAG epitope is recognized by the anti-FLAG mAb M2, which detects profurin and mature furin. Alternatively, mAb M1 requires exposure of the FLAG tag at the N-terminus and therefore only recognizes mature furin following autoproteolytic excision of the propeptide at Arg₁₀₇ (Fig. 2a). The constructs

also contain an HA epitope tag in the propeptide to monitor the fate of this domain. Insertion of these epitope tags has no effect on the activation, activity, or the trafficking of furin (Anderson et al., 1997; Molloy et al., 1994).

Western blot analysis of extracts from cells expressing each reporter construct revealed a prominent doublet of profurin (mAb M2 positive) and mature furin (mAbs M2 and M1 positive, Fig. 2b). Ratiometric comparison of the mAb M2-crossreactive bands showed that the Arg₇₅→Ala or His₆₆→Leu substitutions had no measurable effect on propeptide excision relative to the control (65% mature furin each). However, the His₆₉→Leu and His₆₉→Lys substitutions reduced the efficiency of propeptide excision (30% and 20% mature furin, respectively), suggesting that His₆₉ may be essential for folding, stability or activation of the mature enzyme. The presence of mature furin in each sample enabled us to test the ability of each ER-localized reporter to be activated *in vitro* following pre-incubation at pH 7.5 or 6.0 (Fig. 2c). In accordance with our previous studies (Anderson et al., 2002; Anderson et al., 1997), fur/f/haΔtc-k, which contains the native propeptide sequence (see Fig. 2a), showed no detectable furin activity above a control sample when assayed at pH 7.5 whereas pre-incubation at pH 6.0 triggered a robust increase in furin activity. This increased activity was coupled with the cleavage of the furin propeptide (Fig. 2d) and was blocked by the furin-specific inhibitor α₁-PDX (K_i = 0.6 nM (Anderson et al., 1993; Jean et al., 1998) and data not shown), demonstrating the pH-dependent autoproteolytic cleavage of the furin propeptide to unmask the active furin endoprotease. In addition, pretreatment of fur/f/haΔtc-k at pH 7.5 with trypsin to digest the bound inhibitory propeptide also activated furin, whereas the R75A:fur/f/haΔtc-k construct,

which cannot undergo propeptide cleavage at the internal site (Anderson et al., 2002), failed to be activated by pre-incubation at pH 6.0 but could be activated by trypsinolysis of the propeptide. This demonstrates that the Arg₇₅→Ala substitution had no effect on the folding of the catalytic domain but blocked sensitivity of the furin•propeptide complex to acid pH. Like the native propeptide sequence, we found that the His₆₆→Leu substitution had no effect on the pH-triggered activation and propeptide release or on the trypsin-mediated unmasking of furin, suggesting His₆₆ does not play an essential role in the pH-induced profurin activation (Fig. 2c and d). However, the His₆₉→Leu substitution at the P7 subsite completely blocked the ability of acid pH to trigger furin activation and propeptide cleavage but had no effect on the trypsin-mediated activation step, demonstrating that H69L:fur/f/haΔtc-k was correctly folded but unresponsive to an acidic environment (Fig. 2c and d). By contrast, H69K:fur/f/haΔtc-k failed to be activated by acidic pH or trypsinolysis (Fig. 2c). Together with the extremely inefficient formation of processed furin in cells expressing H69K:fur/f/haΔtc-k (Fig. 2b), our results suggest that the constitutively protonated His₆₉→Lys substitution affects correct folding and stabilization of the endoprotease in the ER.

The analysis of ER-localized profurin reporter constructs suggested that His₆₉ has an essential role in the pH-dependent activation of full-length furin in late secretory pathway compartments. To test this possibility, we expressed full-length epitope-tagged furin (fur/f/ha, see Fig. 2a) or furin mutants containing the His₆₉→Leu (H69L:fur/f/ha) or His₆₉→Lys (H69K:fur/f/ha) substitutions in cells. Western blot and enzyme activity assays of the profurin constructs showed marked differences in the efficiency of

propeptide excision and enzyme activation (Fig. 3a). Analysis of fur/f/ha revealed a prominent doublet of equal intensity composed of profurin (mAb M2 positive) and mature furin (mAb M2 and M1 positive, Fig. 3a), which correlated with a robust increase in furin enzyme activity (Fig. 3b). H69K:fur/f/ha exhibited dramatically reduced propeptide excision and, correspondingly, enzyme activity near background levels. The near absence of mAb M1-positive mature furin in cells expressing H69K:fur/f/ha did not appear to result from instability of the mature domain as pulse-chase analysis or treatment of cells with proteasome or lysosomal hydrolase inhibitors failed to result in the generation of increased amounts of mature furin (data not shown). Consistent with the corresponding Δ tc-k construct (Fig. 2), H69L:fur/f/ha underwent propeptide excision at Arg₁₀₇[↓] but did not produce active enzyme (Fig. 3a and 3b).

The block of propeptide excision in cells expressing H69K:fur/f/ha and the lack of active furin in cells expressing H69L:fur/f/ha despite correct propeptide excision, raised the possibility that the His₆₉ mutations altered trafficking of these furin variants. Immunofluorescence microscopy analysis demonstrated that both fur/f/ha and H69L:fur/f/ha were co-localized with the TGN marker TGN46 (Fig. 4a). By contrast, H69K:fur/f/ha remained at the ER, similar to profurin and other furin mutants unable to undergo propeptide excision (Anderson et al., 2002; Anderson et al., 1997). Our finding that the steady-state localization of H69L:fur/f/ha was at the TGN (Fig. 4a), but that this construct was enzymatically inactive (Fig. 3b), suggested that the inhibitory propeptide remained associated with furin. To test this possibility, we incubated cells expressing fur/f/ha or H69L:fur/f/ha with [³H]Arg and [³H]Leu to label the propeptide and then

harvested the cells at increasing chase times. Mature furin proteins were immunoprecipitated with mAb M1 and co-immunoprecipitated propeptide molecules were resolved by SDS-PAGE followed by fluorography (Fig. 4b). This analysis showed that the native propeptide released slowly from furin ($t_{1/2} = 105$ min) in agreement with earlier studies (Anderson et al., 1997). By contrast, the His₆₉→Leu mutant propeptide failed to dissociate from mature furin during the 4 hr course of this experiment. The inability for the His₆₉→Leu mutant propeptide to dissociate from mature furin in BSC-40 cells correlated with the absence of furin activity in extracts from cells expressing H69L:fur/f/ha (Fig. 3). As a control, we investigated the ability of H69L:fur/f/ha to internalize from the cell surface by mAb M1 uptake. Cells were incubated with mAb M1 to allow furin-dependent internalization of the antibody and then processed for immunofluorescence microscopy (Fig. 4c). We found that fur/f/ha and H69L:fur/f/ha internalized mAb M1 to the paranuclear region demonstrating that the His₆₉→Leu mutation had no obvious effect on the highly regulated trafficking itinerary of mature furin within the TGN/endosomal system.

Our determination that H69K:fur/f/ha, similar to profurin (13,25,33), fails to undergo efficient autoproteolytic propeptide excision (Fig. 3) and is restricted to the ER (Fig. 4), suggested that this furin construct would enable us to identify the sorting machinery that restricts profurin to the ER. One candidate profurin ER sorting protein is PACS-2, which combines with COPI to localize membrane proteins containing phosphorylated acidic cluster motifs—such as that present on the furin cytosolic domain—to the ER (Kottgen et al., 2005; Simmen et al., 2005). Therefore, we examined whether these molecules are

required to localize H69K:fur/f/ha to the ER. First, we used metabolic labeling studies with $^{32}\text{P}_i$ to show that, like furin, H69K:fur/f/ha is phosphorylated *in vivo* (Fig. 5a and reference 35). Second, protein-protein binding studies showed PACS-2 bound selectively to the phosphorylated furin cytosolic domain (Fig. 5b). Third, we depleted cells of PACS-2 and the β -COP subunit of COPI to determine whether these proteins are required for the ER localization of H69K:fur/f/ha. Treatment of A7 cells with PACS-2 or β -COP siRNA caused a marked reduction in their respective protein levels after 48 hr without causing cell toxicity (Fig. 5c and data not shown). In addition, depletion of either PACS2 or COPI caused H69K:fur/f/ha to redistribute from the ER to the Golgi/TGN without affecting the subcellular localization of the luminal ER chaperone protein disulfide isomerase (PDI) under the experimental conditions used (Fig. 5d). Our finding is consistent with other studies reporting that PDI is localized to the ER by a retention-based mechanism in addition to the canonical COPI-dependent retrieval based mechanism (Dorner et al., 1990). These results suggest that PACS-2 combines with COPI to mediate the ER localization of profurin and that propeptide excision releases the furin•propeptide complex from PACS-2, allowing the mature enzyme to traffic to the TGN/endosomal system. Moreover, these data support our model that protonation of His₆₉ disrupts the hydrophobic pocket in the propeptide, possibly by preventing correct folding of the enzyme and excision of the propeptide at Arg₁₀₇.

Our results suggest that one role for protonation of His₆₉ in the TGN/endosomal system is to disrupt the propeptide structure, thereby promoting cleavage of the internal propeptide cleavage site at Arg₇₅. However, recent studies suggest that protonation of a His residue

proximal to furin cleavage sites enhances proteolysis (Bergeron et al., 2003; Degrin et al., 2004). Therefore, to test whether protonation of His₆₉ increases the efficiency of the internal propeptide cleavage, we conducted a kinetic analysis using internally quenched fluorogenic peptide substrates. The peptide substrates were designed with either the native propeptide excision site at Arg₁₀₇[↓] (PS-1, Table 1), the propeptide internal cleavage site at Arg₇₅[↓] containing His₆₉ (PS-2), or the His₆₉→Leu (PS-2:H69L) or His₆₉→Lys (PS-2:H69K) substitutions. The PS-1 substrate exhibited a low K_m at both neutral and acidic pH ($K_m = 1.99\mu\text{M}$ and $1.62\mu\text{M}$, respectively). However, the PS-2 substrate revealed a preference for cleavage at pH 6.0 with a 3.6-fold lower K_m and increased cleavage efficiency. Unlike PS-2, PS-2:H69L exhibited a markedly high K_m and low cleavage efficiency irrespective of pH. By contrast, PS-2:H69K, which mimics a constitutively protonated P7 residue had a low K_m at both pH 7.5 and pH 6.0. Together, our data suggest that His₆₉ is a pH sensor that allows enzyme activation following transport of the furin•propeptide complex from the ER to the mildly acidic TGN/endosomal system and that protonated His₆₉ has a dual role—it disrupts the propeptide to expose the internal cleavage site and increases the efficiency of cleavage at Arg₇₅ to yield the active enzyme.

Discussion

We report the identification of His₆₉ in the furin prodomain as a pH sensor that guides the multi-step and compartment-specific autoproteolytic activation of furin. We used cellular and cell-free furin activation assays to show that a non-polar His₆₉→Leu substitution had no effect on propeptide excision at Arg₁₀₇ (Fig. 2), nor on the TGN localization or the endosomal trafficking of the furin•propeptide complex (Fig. 4). However, this

substitution blocked the acid pH-dependent cleavage of the furin propeptide at the internal Arg₇₅ site and the release of the propeptide from the furin•propeptide complex (Figs. 2 and 4). By contrast, a His₆₉→Lys substitution, which mimics constitutively protonated histidine blocked propeptide excision at Arg₁₀₇, trapping the profurin molecule in the ER by a mechanism requiring the sorting protein PACS-2 and COPI (Figs. 2, 4 and 5).

Our experimental studies and modeling analysis together demonstrate a possible mechanism for the His₆₉ protonation-dependent furin activation. In the neutral pH environment of the ER, unprotonated His₆₉ is buried in a solvent-accessible hydrophobic pocket, stabilized by nonpolar amino acids, including Gly₅₃, Leu₅₅, Phe₅₄, Phe₆₇ and Trp₆₈. This hydrophobic pocket may guide the correct folding of the catalytic domain while protecting the internal propeptide cleavage site. Once folded, the catalytic domain autoproteolytically excises the propeptide at Arg₁₀₇ to form a transport-competent furin•propeptide complex that transits to the mildly acidic TGN/endosomal system. Profurin molecules unable to efficiently fold and undergo autoproteolysis remain in the ER by a PACS-2- and COPI-dependent mechanism (Fig. 5). Upon exposure to the mildly acidic TGN/endosomal system, protonation of His₆₉ disrupts hydrophobic interactions, thereby resulting in the partial unfolding of the hydrophobic pocket. This puckering exposes the internal cleavage site, triggering cleavage at Arg₇₅ to release the propeptide and unmask the catalytic center for substrate cleavage *in trans*. Thus, the His₆₉→Leu mutation would stabilize the solvent-accessible hydrophobic pocket, permitting propeptide excision at Arg₁₀₇ and export of the furin•propeptide complex to the

TGN/endosomal system. However, this non-protonatable mimic prevents the pH-dependent cleavage of the propeptide at the internal site (Arg₇₅) and subsequent enzyme activation. Similarly, blocking internal propeptide cleavage by a P1 Arg₇₅→Ala mutation has no measurable effect on furin folding, propeptide excision, or the pH-dependent puckering of the solvent-accessible hydrophobic pocket, but blocks internal propeptide cleavage and enzyme activation (Fig. 2 and (Anderson et al., 2002)). Hence, trypsinization of the propeptide *in vitro* is sufficient to recover active enzyme. By contrast, the His₆₉→Lys mutation, which mimics constitutively protonated His, prevents stabilization of the hydrophobic pocket, blocking correct folding of the propeptide and propeptide excision at Arg₁₀₇, leading to the accumulation of the inactive profurin in the ER (Fig. 4). Similarly, a Val₇₂→Arg mutation, which converts the P1/P6 Arg internal propeptide cleavage site to a consensus P1/P4 Arg site, blocks profurin folding and ER export by also destabilizing the solvent-accessible hydrophobic pocket (Anderson et al., 2002).

NMR solution structures of the furin and PC1/3 propeptides suggest the molecular basis for the pH-dependent activation of the PCs. At neutral pH, the PC1/3 propeptide consists of four β -sheets and two α -helices in a β - α - β - β - α - β arrangement, with the internal cleavage site located in an extended loop between the β_3 and α_2 segments (Tangrea et al., 2002). Tangrea et al., proposed that His₆₆, which is present in furin but not PC1, serves as furin's pH sensor promoting dissociation of the pro- and catalytic-domains, whereas His₆₉, which is conserved in all PCs (Fig. 1a), would point away from the putative binding surface and therefore would not contribute to the pH dependent activation of

furin. In addition, a separate study found that the furin prodomain was in a molten-globule state at neutral pH with a measurable core and at acidic conditions undergoes unfolding largely in its C-terminal half that includes the internal cleavage site (Bhattacharjya et al., 2001). Our results suggest four key differences underlying the mechanism of profurin activation compared to these studies. First, we found that His₆₉ but not His₆₆ has an overriding role as the pH sensor controlling furin activation. Second, our modeling studies indicate that unprotonated His₆₉ is buried in a solvent-accessible hydrophobic pocket that guides the folding of the catalytic domain. This role for unprotonated His₆₉ in the ER explains why the His₆₉→Lys mutation blocks propeptide excision of profurin, leading to restriction of the misfolded proenzyme to the ER. Third, following transport of the furin•propeptide complex to the mildly acidic TGN/endosomal system, protonation of His₆₉ disrupts the hydrophobic interactions, thereby exposing the internal cleavage site to the catalytic center. Fourth, protonation of His₆₉ has an additional role in increasing the efficiency of propeptide cleavage (Table 1).

The utility of a protonatable His residue to regulate compartment-specificity of furin cleavage is not restricted to the furin propeptide but is also used to order the furin-dependent cleavages of pro-BMP-4 and pro- α 4 integrin in a compartment-specific manner (Bergeron et al., 2003; Degnin et al., 2004), underscoring the broad utility of the His pKa at physiological pH. In addition, *in vitro* activation of PC1, which contains the evolutionarily conserved His residue corresponding to furin's His₆₉, also requires an acidic pH for activation (our unpublished results). However, a recent study demonstrates that a His₆₉→Ala mutation had no effect on the ability of over-expressed furin to cleave

pro-von Willebrand factor in 293 cells (Bissonnette et al., 2004). This discrepancy between the His₆₉→Leu and His₆₉→Ala substitutions may be attributed to a larger Van der Waals volume of Leu, which may result in a more prominent effect on cleavage and activation due to stronger hydrophobic interactions, differences in the assays used to detect furin activity, or perhaps differences in the cell lines used (Bergeron et al., 2003; Deginin et al., 2004).

Our demonstration that localization of H69K:fur/f/ha to the ER requires PACS-2 and COPI (Fig. 5) identifies components of the cellular trafficking machinery that maintain profurin in the ER. We recently identified PACS-2 and reported that it localizes the ion channel polycystin-2 to the ER by linking the CK2 phosphorylated acidic cluster in the polycystin-2 cytosolic domain to COPI (Kottgen et al., 2005; Simmen et al., 2005). Here, we report that PACS-2 also binds to the CK2-phosphorylated furin cytosolic domain and, like furin and profurin, H69K:fur/f/ha is phosphorylated *in vivo* (Fig. 4 and (Jones et al., 1995)). Thus, dephosphorylation of the furin cytosolic domain by a furin phosphatase (Molloy et al., 1998) may be key for allowing ER export of the furin•propeptide complex. Alternatively, ER export of the furin•propeptide complex may occur if the PACS-2 binding site is masked, perhaps by furin dimerization (Wolins et al., 1997). Regardless, our studies identify new components of the cellular sorting machinery that cooperate with the His₆₉-based pH sensor to promote the stepwise-, compartment-specific activation of furin, and which may also control the activation of other PCs and secretory pathway proteins.

Acknowledgments

The authors thank E. Anderson for his effort in the early stages of this project, J. Larson for helpful discussions and R. Sitia for the PDI antiserum. This work was supported by NIH grants DK37274 and AI49793 (GT).

Figure Legends

Figure 1. Homology modeling of the furin propeptide. (A) Multiple Sequence Alignment between propeptides of the PC family. Predicted secondary structure of the furin propeptide and sequence conservation (black-highlight, 100% similarity; dark gray-highlight, >80% similarity, light gray-highlight, >50% similarity) between PCs is depicted. Propeptide residues are numbered in reference to the furin propeptide, which begins at Gln₂₅ (Anderson et al., 1997). (B) Ribbon representation of the furin propeptide structure obtained by homology modeling. His₆₆ and His₆₉ (blue) and Arg₇₅ (red) are highlighted. (C) Surface representation of the propeptide-furin complex. The modeled propeptide (yellow) is docked onto the active site of furin (green). The internal propeptide cleavage site (red) and His₆₉ (blue) are highlighted. (D) Surface representation of the secondary cleavage site illustrates His₆₉ (blue) buried in the solvent-accessible pocket formed by Gly₅₃, Phe₅₄, Leu₅₅, Phe₆₇, and Trp₆₈ hydrophobic residues (yellow).

Figure 2. His₆₉ controls the pH-sensitive furin propeptide cleavage and enzyme activation *in vitro*. (A) Schematic representation of the furin constructs used in this study. Shown is full-length profurin containing the N-terminal prodomain with the excision and internal cleavage sites (black bars), the catalytic domain (light gray segment), the transmembrane domain (TMD, dark gray segment), and the cytosolic domain, which is phosphorylated by CK2 (circled P) to promote binding to PACS proteins (Kottgen et al., 2005; Simmen et al., 2005; Wan et al., 1998). A FLAG epitope tag (horizontal bars) was inserted at the N-terminus of mature furin such that the FLAG N-terminus is exposed upon propeptide excision. mAb M2 recognizes either the blocked

(profurin) or N-terminally exposed (mature furin) FLAG tag whereas mAb M1 recognizes specifically the N-terminally exposed FLAG tag (mature furin). An HA epitope tag (vertical bars), which is recognized by mAb HA.11, was inserted at the N-terminus of the prodomain. The sequence of the prodomain is shown at the top with the signal peptidase cleavage site as well as the propeptide excision and internal cleavage sites highlighted by vertical arrows. The P1/P4 Arg residues of the excision site and the P1/P6 Arg residues of the internal cleavage site are in bold font. ER-localized, lumenally-restricted furin constructs (designated Δ tc-k) were generated by replacing the TMD and cytosolic domains with the Lys-Asp-Glu-Leu (KDEL) ER localization signal. **(B)** Cell extracts from BSC-40 cells expressing a control viral vector (WT) or the indicated - Δ tc-k ER-localized furin constructs were separated by SDS-PAGE and analyzed by western blot using mAbs M1 or M2. Open arrow, profurin. Filled arrow, mature furin. **(C)** Membrane preparations from cells used in **(B)** were tested for furin activity using the Abz-Arg-Val-Lys-Arg-Gly-Leu-Ala-Tyr(NO₂)-Asp-OH substrate, after incubation at pH 6.0 or 7.5 for 3h, or at pH 7.5 for 1h in the presence of trypsin followed by soybean trypsin inhibitor to block residual trypsin activity. Error bars represent the mean and SEM of three independent experiments. **(D)** Membranes preparations from **(C)** were analyzed by 15% Tris-Tricine SDS-PAGE followed by western blot using mAb HA.11. M_r values of the excised propeptide and the cleaved N-terminal propeptide fragment are indicated. Open arrowhead, intact propeptide. Filled arrowhead, cleaved propeptide.

Figure 3. The protonation state of His₆₉ controls propeptide excision and enzyme activation *in vivo*. **(A)** Cell extracts from BSC-40 cells expressing a control viral vector

(WT) or full-length epitope-tagged furin molecules containing the indicated mutations were separated by SDS-PAGE and analyzed by western blot with mAbs M1 and M2. Profurin (open arrow) and mature furin (filled arrow) are indicated. **(B)** Crude membrane preparations of cells used in (A) were tested for furin activity at pH 7.5 using the Abz-Arg-Val-Lys-Arg-Gly-Leu-Ala-Tyr(NO₂)-Asp-OH substrate peptide. Error bars represent the mean and SEM of three independent experiments.

Figure 4. The protonation state of His₆₉ affects the subcellular localization of furin.

(A) Immunofluorescence microscopy of BSC-40 cells expressing fur/f/ha, H69L:fur/f/ha or H69K:fur/f/ha. Cells were fixed and stained with anti-furin PA1-062 and anti-TGN46, then visualized with species-specific fluorescently labeled secondary antibodies. **(B)** BSC-40 cells expressing fur/f/ha or H69L:fur/f/ha were pulse-labeled for 30 min with 100 μ Ci each of [³H]Arg and [³H]Leu, then chased with excess unlabeled Arg and Leu at 37°C for the indicated times. Cell extracts were prepared, and mature furin molecules were immunoprecipitated with mAb M1, separated by 15% Tris-Tricine SDS-PAGE and co-precipitating propeptide molecules (open arrowhead) were detected by fluorography and quantified by densitometry. **(C)** Immunofluorescence microscopy of BSC-40 cells expressing fur/f/ha or H69L:fur/f/ha. Cells were incubated with mAb M1 in the culture medium (30 μ g/ml) for one hr and internalized mAb M1 was detected with a fluorescently labeled secondary antibody.

Figure 5. PACS-2 and COPI localize H69K:fur/f/ha to the ER. **(A)** A7 cells expressing fur/f/ha or H69K:fur/f/ha were metabolically labeled with ³²P_i, lysed,

immunoprecipitated with mAb M2, separated by SDS-PAGE and analyzed by autoradiography (upper panel) and western blot using anti-furin PA1-062 (lower panel). **(B)** GST or GST-Furin_{CD}, which contains the 56-amino acid furin cytosolic domain, was pre-incubated or not with CK2, then incubated with thioredoxin (Trx)-tagged PACS-2 FBR, which encodes the cargo binding region of PACS-2 (Kottgen et al., 2005; Simmen et al., 2005), separated by SDS-PAGE and analyzed by western blot using anti-Trx mAb. **(C)** A7 cells were treated with control (scr.) or siRNAs specific for PACS-2 or β -COP for 48 hr, lysed, separated by SDS-PAGE and analyzed by western blot using anti-PACS-2 and anti- β -COP antibodies. The blots were also incubated with anti-tubulin mAb to control for protein loading. **(D)** A7 cells were treated with the indicated siRNAs for 48 hr and then infected with virus expressing H69K:fur/f/ha for an additional 4 hr. The cells were then processed for immunofluorescence microscopy and stained with mAb HA.11 and anti-PDI followed by subtype-specific fluorescently labeled secondary antibodies.

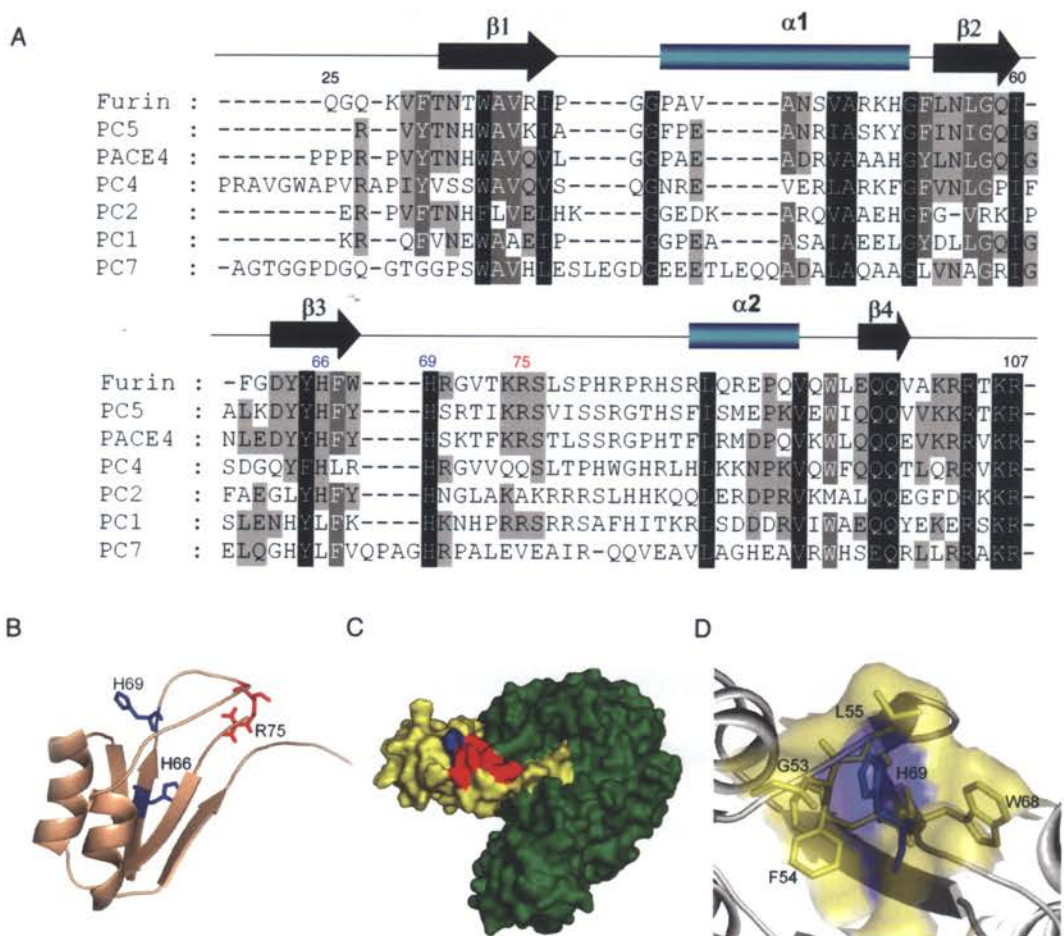


Figure 1

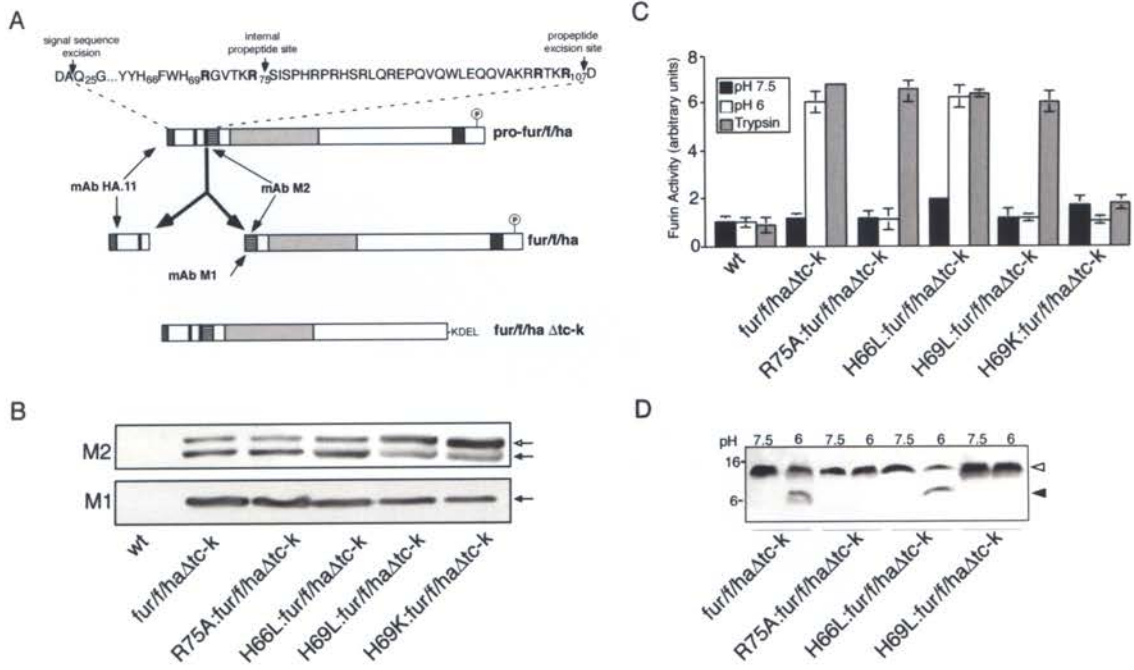


Figure 2

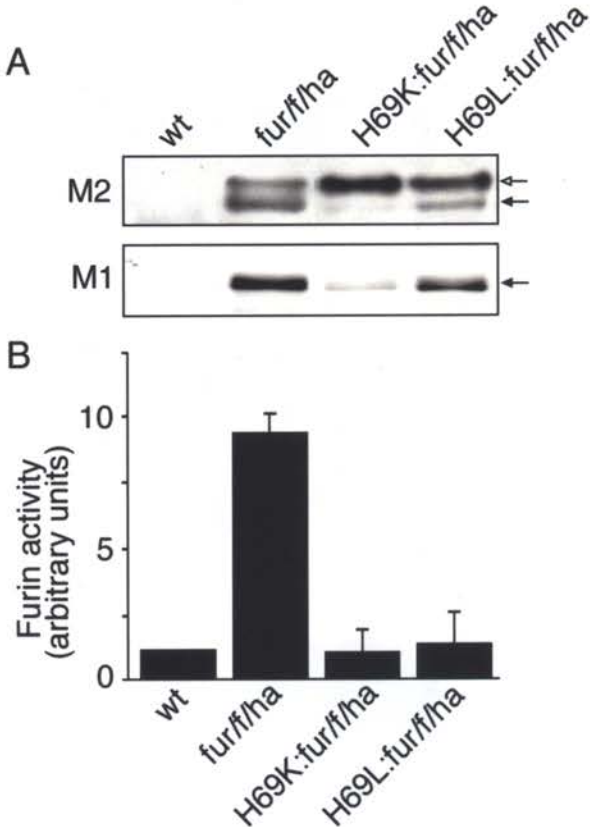


Figure 3

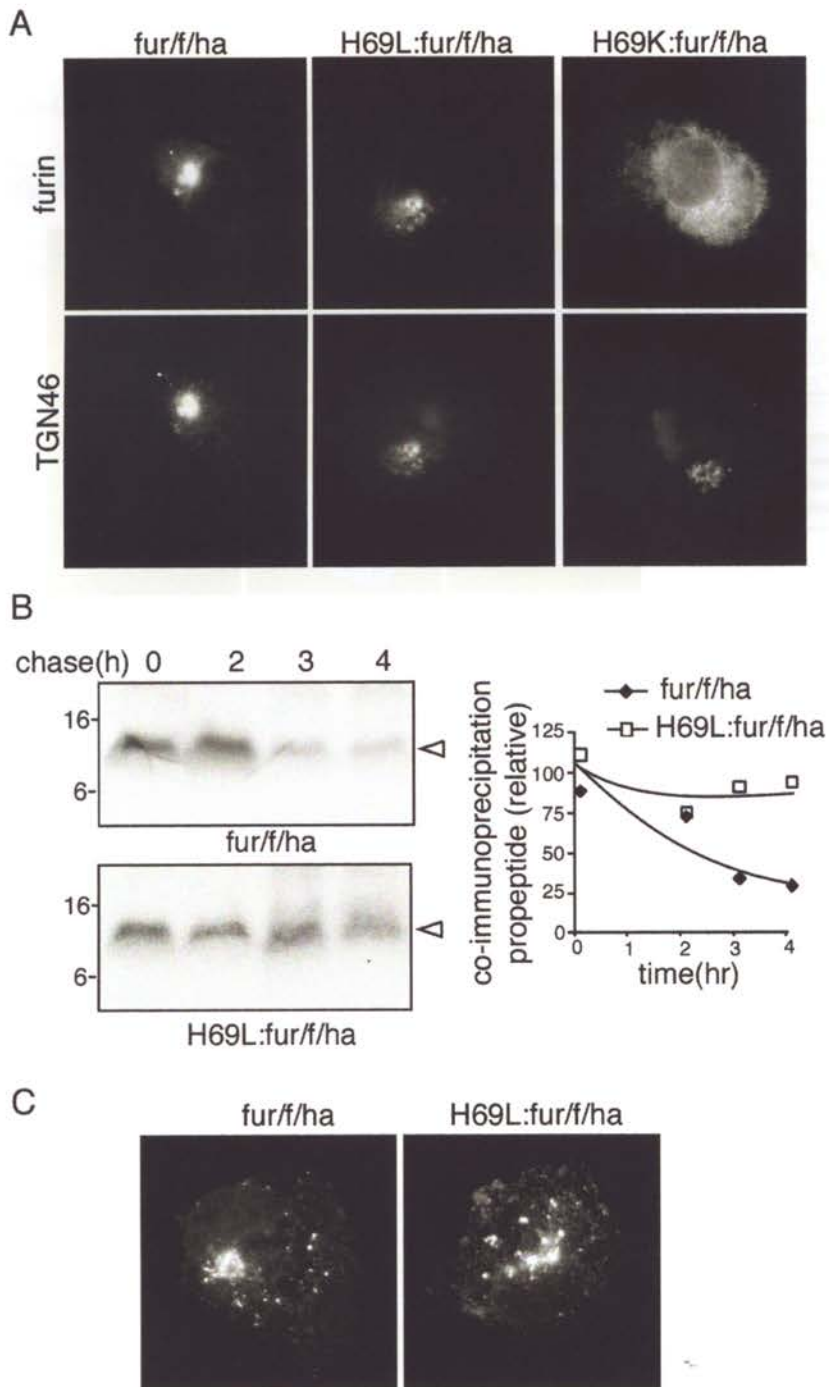


Figure 4

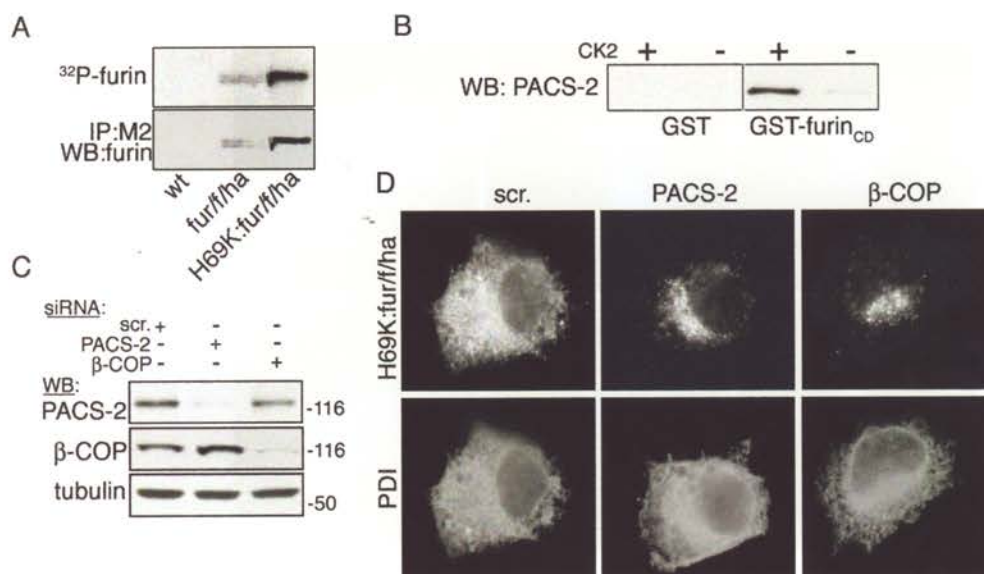


Figure 5

Table 1. Peptidyl substrates

PEPTIDE SEQUENCE		pH	K_m (μM)	k_{cat} (s^{-1})	k_{cat}/K_m ($s^{-1}M^{-1}$)	k_{cat}/K_m (<i>Rel.</i>)
PS-1*	Abz-Ala-Lys-Arg-Arg-Thr-Lys-Arg ₁₀₇ ↓ Asp-Val-Tyr(NO ₂)-Ala	7.5	1.99	1.90	9.58×10^5	1.000
		6.0	1.62	1.03	6.34×10^5	0.661
PS-2*	Abz- <u>His</u> -Arg-Gly-Val-Thr-Lys-Arg ₇₅ ↓ Ser-Leu-Tyr(NO ₂)-Ala	7.5	23.75	6.37	2.68×10^5	0.279
		6.0	6.59	2.92	4.43×10^5	0.458
PS-2: H69K	Abz- <u>Lys</u> -Arg-Gly-Val-Thr-Lys-Arg ₇₅ ↓ Ser-Leu-Tyr(NO ₂)-Ala	7.5	8.01	2.05	2.56×10^5	0.267
		6.0	11.95	1.61	1.35×10^5	0.141
PS-2: H69L	Abz- <u>Leu</u> -Arg-Gly-Val-Thr-Lys-Arg ₇₅ ↓ Ser-Leu-Tyr(NO ₂)-Ala	7.5	38.20	2.90	7.59×10^4	0.079
		6.0	45.93	2.66	5.79×10^4	0.060

*, from (Anderson et al., 2002).

APPENDIX C

Summary

This appendix records two preliminary results regarding 1) the activation of PACS-1, and 2) how PACS-1 is recruited to membranes. These are described in the legends to Figures 1 and 2 and discussed in Chapter 4.

Figure 1. PACS-1 forms an oligomer in cells. A7 cells expressing HA- or Myc-Tagged PACS-1, or both, were lysed in mRIPA+1mM DTT and COMPLETE protease inhibitor and HA-PACS-1 protein was immunoprecipitated with polyclonal HA antibody. The precipitated complexes were separated by SDS-PAGE, transferred to nitrocellulose and western blotted with anti-myc mAb 9E11. Control western blotting was done on cell lysate to confirm expression of PACS-1 proteins.

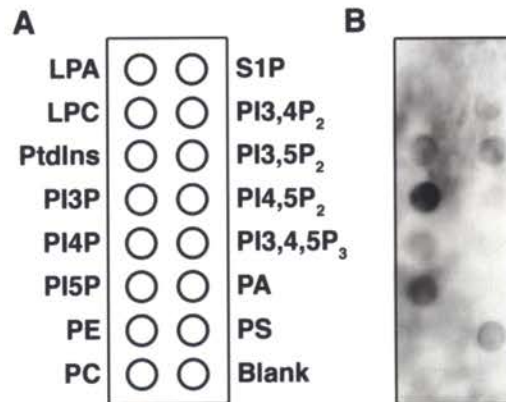
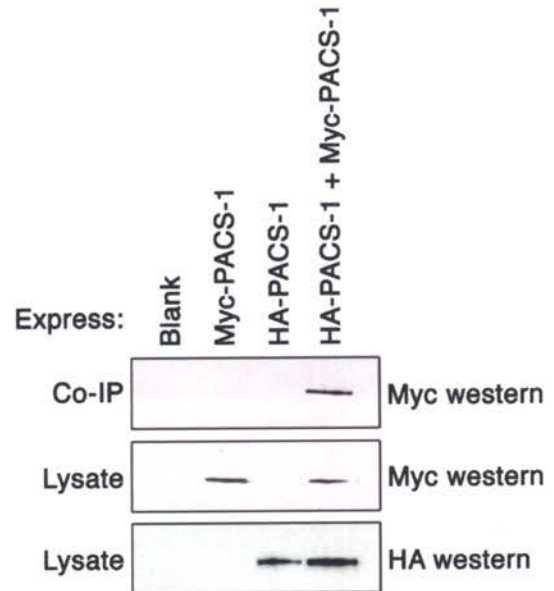


Figure 2. PACS-1 binds to PI3P. Full-length his-tagged PACS-1 expressed in baculovirus was overlaid onto a lipid-spotted membrane (Echelon Biosciences). The membrane was first blocked in TBST+3% fatty acid free BSA (faf-BSA, Sigma# A-7030) for one hour at room temperature. PACS-1 was overlaid at 0.5 μg/ml TBST+3% faf-BSA overnight at 4 C. The membrane was washed three times with TBST+3% faf-BSA for ten minutes each, and then probed with affinity purified PACS-1 antibody 601. The spotted lipids are Lysophosphatidic Acid (LPA), Lysophosphocholine (LPC), phosphatidylinositol (PtdIns), phosphatidylinositol-3-phosphate (PI3P), phosphatidylinositol-4-phosphate (PI4P), phosphatidylinositol-5-phosphate (PI5P), phosphatidylethanolamine (PE), phosphatidylcholine (PC), sphingosine-1-phosphate (S1P), phosphatidylinositol-3,4-bisphosphate (PI3,4P₂), phosphatidylinositol-3,5-bisphosphate (PI3,5P₂), phosphatidylinositol-3,4,5-bisphosphate(PI3,4,5P₃), phosphatidic acid (PA), and phosphatidylserine (PS).